

DISSERTATION

ANATOMIC PLASTICITY AND FUNCTIONAL IMPACTS OF NEURAL – IMMUNE AND
NEURAL – EPITHELIAL SIGNALING IN THE INTESTINE

Submitted by

Luke A. Schwerdtfeger

Department of Biomedical Sciences

In partial fulfillment of the requirements

For the Degree of Doctor of Philosophy

Colorado State University

Fort Collins, Colorado

Summer 2021

Doctoral Committee:

Advisor: Stuart A. Tobet

Adam Chicco

Brent Myers

Elizabeth Ryan

Copyright by Luke A. Schwerdtfeger 2021

All Rights Reserved

ABSTRACT

ANATOMIC PLASTICITY AND FUNCTIONAL IMPACTS OF NEURAL – IMMUNE AND NEURAL – EPITHELIAL SIGNALING IN THE INTESTINE

The intestinal wall is a multicompartmental barrier tissue composed of over 25 distinct cell types with integrated and complex signaling both within and between compartments. The gut wall is also a large endocrine organ comprised of cells capable of producing dozens of peptides used for hormonal and other signaling functions. However, the mechanistic roles that neural secretions play in regulating the gut epithelial barrier in health and disease are not well known. Additionally, frequently used models available for studying intestinal function outside of the body lack the complexity to investigate neural – epithelial and neural – immune signaling interactions. Using a bifurcated approach to method development, we created two culture systems for maintaining the full thickness of the intestinal wall *ex vivo*. One method allows for culture of mouse or human organotypic intestinal slices that maintain the gut wall for 6 or 4 days, respectively. This system does not however, maintain a true luminal – epithelial barrier as seen in the *in vivo* gut. The second method, a microfluidic organotypic device (MOD) enables maintenance of explanted mouse or pig intestinal tissue for up to 3 days *ex vivo*, with an intestinal barrier intact. These two methods allow for investigating and cross-validating of numerous biological questions now previously possible using traditional culture models.

Neuronal fiber proximity to gut epithelia has been shown, with goblet, tuft and enteroendocrine cells being closely opposed by fibers. Goblet cells secrete mucopolysaccharides, a first line of defense separating luminal microbiota from host tissue. I have recently shown that vasoactive intestinal peptide (VIP) can regulate goblet cell production in organotypic slices of mouse ileum. This peptide is also in close proximity to Paneth cells in

the base of the crypt, and enteric mast cells. There were sex differences in baseline mast cell neuronal proximity, quantities, and cell size in mouse ileum. Further, mast cells showed a sex difference in responses to lipopolysaccharide challenge. Further investigation of neurosecretory factor regulation of immune and epithelial function is needed, both in goblet cells and other secretory epithelia like anti-microbial producing Paneth cells, and in immune components like mast cells.

ACKNOWLEDGMENTS

I would like to take a moment to acknowledge and thank some of the people who made this dissertation possible. Stu, you have been an incredible mentor, teacher, scientific advisor, and friend throughout my years working in the lab, and I truly could not have done it without your unwavering support and insight. My parents, for whom this would not be possible either, thank you for everything you have done to support me, truly. Finally, my loving wife Kate, thank you for standing with me throughout this journey, I couldn't have made it without you darling.

TABLE OF CONTENTS

ABSTRACT.....	ii
ACKNOWLEDGMENTS.....	iv
Introduction.....	1
SECTION 1 - Specifications for Designing Gut Culture Systems.....	7
Chapter 1 – From organotypic culture to body-on-a-chip: A neuroendocrine perspective.....	7
Chapter 2 – Designing Multicellular Intestinal Systems.....	44
Chapter 3 – Powering <i>ex vivo</i> tissue models in microfluidic systems.....	66
SECTION 2 - Building Gut Explant Culture Systems.....	106
Chapter 4 – A microfluidic organotypic device for culture of mammalian intestines <i>ex vivo</i>	106
Chapter 5 – Human Colon Function Ex Vivo: Dependence on Oxygen and Sensitivity to Antibiotic.....	124
SECTION 3 - Gut Neural, Immune, and Epithelial Signaling in Mouse Ileum.....	152
Chapter 6 – Vasoactive Intestinal Peptide Regulates Ileal Goblet Cell Production in Mice.....	152
Chapter 7 - Sex Difference in Neuronal Mediation of Ileal Paneth Cell Response to Lipopolysaccharide.....	177
Chapter 8 – Sex Differences in Anatomic Plasticity of Gut Neuronal – Mast Cell Interactions.....	188
Discussion.....	208
APPENDIX.....	215

INTRODUCTION

Ancient History of Gut Study:

Investigations into how intestinal anatomy and tissue composition influences its ability to digest food, discard waste, and move contents along the length of the >25 foot long tube have been undergoing for centuries. Hippocrates is commonly attributed with saying “all disease begins in the gut,” however this is likely not something he ever wrote. That said, the collection of clinical notes, theories on humours and disease attributed to Hippocrates in the more than 70 works known as the “*Hippocratic Corpus*” go into intense detail about maladies afflicting the gut. These Hippocratic works laid the foundation for rudimentary treatment and diagnosis of gut pathologies such as dysentery among many others. The roman physician and philosopher Galen who waxed poetic about the “divine” nature of the stomach was among the first to describe functional portions of the gastrointestinal tract in the context of disease (Galen, c. 170 AD). Avicenna (Ibn Sina; c. 1025 AD) unknowingly described a function of the autonomic nervous system in his medical encyclopedia “*The Canon of Medicine*” stating that ‘mental excitement or emotion, vigorous exercise; these hinder digestion’. Perhaps the earliest descriptions of not only anatomy but anatomical structure influencing gut function can be attributed to renaissance anatomists. Leonardo Da Vinci described the anatomy of the entire peritoneal cavity in exquisite detail, and even proposed the idea of peristalsis, the rhythmic contractions of the gut wall that move food along its length, being regulated by pressure driven by the diaphragm (Da Vinci, c. 1508). Understanding of cellular functions of the gut was still hundreds of years away during da Vinci’s time. Only ~150 years later, Johan Peyer laid the foundation for gut immunology with his description of the clusters of immune cells in the distal intestinal tract that we know today as Peyer’s patches (Peyer JC, 1677). This history of anatomical study of the intestinal tract paved the way for fundamental investigations into biological function of the more than 25 cell types of the gut wall.

In the more modern world, an explosion of research into gut wall function occurred during the post WWII period. A notable shift in favored methodologies from whole organ focused to single cell layer focused has dominated the 20th and most of the 21st centuries. However, to understand organ function using in vitro systems, it is my belief that at least some of the organs cellular components must be studied together, in synchrony, as they are in the body. This ideology has driven much of the work contained in the pages below and served as a guide for the development of novel methodologies for culturing intestinal explants and organotypic slices outside of the mammalian body for multiple days.

Coming up with the right specs:

Prior to the turn of the 21st century, methods for studying the intestinal tract that allowed ready visualization and pharmacological perturbation were limited to monolayer cell cultures, Ussing chambers which clamped mucosa between two chambers of fluid, or whole organ perfusions that never gained widespread use (Schwerdtfeger & Tobet, 2019). A small number of investigations used explants of whole guts and sliced them on microtomes similar to the methods we use in our lab today. Unfortunately, these techniques were not well fleshed out, and maintenance of tissue health and subsequent analysis was lacking. During the 2000s and 2010s, the Groothuis lab in the Netherlands pioneered a new slicing technique that maintained mouse intestines for ~24 h ex vivo (de Graaf et al., 2010). The primary drawback of these slices was the inability to culture beyond 24 h, the first in what we have dubbed the 'specifications' for an ideal gut explant culture system. Creating a novel methodology for generating tissue slices of mouse gut seemed a top priority, however, discussions of the specifications required for such a system to be valuable to the scientific community were missing. In the first section of this dissertation, three manuscripts are included. Chapter 1 discusses the history of tissue cultures used to study neuroendocrinology and prescribes a host of areas in which these systems can

be improved in future iterations of methodologies. The second and third chapters focus more on explant cultures in devices, principally those that use microfluidics to flow media over gut tissues. In brief, the specifications for either tissue slice cultures or explant device cultures are much the same. Principally, to study the complex interactions between the myriad cell types of the gut wall, a culture system must maintain said cell types in an in vivo-like anatomical arrangement and chemical environment. Additionally, microbial components of the intestinal lumen would be maintained, ideally at oxygen concentrations consistent with the in vivo reality. A barrier separating the gut wall from the luminal contents is particularly critical when studying microbes and pathogens. These specifications, laid out in Section 1, guided the methodological design of both culture systems developed in our lab over the past years, and hopefully will serve to influence the design choices of the next generation of biomedical scientists and engineers looking to create novel and more refined methods for studying barrier tissues like the intestine outside of the body.

Gut Culture Systems:

Using the specifications laid out above and in Section 1, we designed two novel culture systems for maintaining mouse, pig, and human intestines ex vivo. Organotypic intestinal slices offer an improvement on the precision cut intestinal slices originally developed in the Netherlands, principally due to culturable time. Slices of mouse intestine, cut at 250 μm thick, can be maintained ex vivo for nearly a week (Schwerdtfeger et al., 2016). Applying the techniques used in mouse cultures allowed us to slice and maintain human colon biopsy slices ex vivo for up to 4 days (Schwerdtfeger et al., 2019), details of which are included in chapter 5 of this dissertation.

Organotypic slices were an improvement on other systems available for studying murine and human guts ex vivo, however, one key aspect of our outlined specifications was missing: the barrier. In vivo, microbes in the lumen are separated from the gut wall by a thick layer of

mucus, and a single cell layer of epithelia that prevent passive crossing of microbes into the gut wall proper. Addressing this, we used 3D printing to design a microfluidic organotypic device (MOD; Richardson et al., 2020) that can culture mouse intestines with an intact barrier for up to 3 days ex vivo. Details of the device and its validation for use with mouse intestinal explants are contained in Chapter 4 below.

Together, the two culture systems outlined in Section 2 offer two methods for maintaining mammalian intestines ex vivo, both offering advantages and disadvantages compared to the other. Descriptions of investigations into biological anatomic and functional pathways in the gut wall using organotypic slices are included in this dissertation, with future work planned using the MOD system.

Interrogating slices ex vivo:

The maintenance of numerous cell types in the intestinal wall, including neural, immune, and epithelial in organotypic slices allowed for investigation into the interactions between and amongst these cell populations. The gut barrier is composed not only of an epithelial monolayer, but a thick mucus layer secreted by a subset of epithelia known as goblet cells. Regulation of goblet cell mucus secretion and production of new goblet cells by neural elements is largely unknown. Section 3 of this dissertation includes three manuscripts, the first of which deals with neuronal regulation of goblet cell production in organotypic slices of mouse ileum. Within this manuscript, details about the anatomical relationships between neuronal fibers and goblet cells is described. Potential towards vasoactive intestinal peptide neuronal influence over goblet cell production is demonstrated in the latter portions of the manuscript.

Beneath the gut mucus and epithelial barrier sits a region of diverse cellular composition called the lamina propria. In this space can be found vasculature, neuronal and glial fibers, immune components (e.g., mast cells), monocyte derived cells, lymphatic drainage, and

interstitial tissue. Signaling among these components with the epithelial barrier is beginning to emerge rapidly throughout the field. Neural influence over immune components and vice versa, particularly pertaining to mast cells has been demonstrated. However, functional influence of neuronal peptides like vasoactive intestinal peptide (VIP) on lamina propria components in concert with epithelial barrier components is not well understood. Preliminary data in chapter 7 demonstrates a sex difference in a subset of epithelia known as Paneth cells which secrete antimicrobial compounds. Moving away from neural – epithelial anatomy, Chapter 8 begins to shed some light onto not only the anatomic pathways involved in neural – immune – epithelial signaling events, but also sex differences in the plasticity of these anatomic arrangements, including mast cell sex differences. Future work should focus on functional outcomes of perturbing VIP and its receptors on neural – immune – epithelial signaling in response to pathogen in a culture system that maintains a true gut wall barrier (e.g., MOD).

References:

- 1) Hippocrates, Polybus, & authors unknown. Hippocratic Corpus. c.400 BC, English translation by WHS Jones. 1959. Harvard University Press.
- 2) Galen. On the Natural Faculties. c.170 AD, English translation by AJ Brock, 1916. Loeb Classical Library.
- 3) Ibn Sina. The Canon of Medicine, Book 3. 1025.
- 4) Da Vinci. Anatomical Manuscripts B. c.1508
- 5) Peyer JC. Exercitatio Anatomico-Medica de Glandulis Intestinorum Earumque Usu & Affectionibus. Apud Henricum Wetstenium. 1677.
- 6) Schwerdtfeger LA, Tobet SA. From organotypic culture to body-on-a-chip: A neuroendocrine perspective. *J Neuroendocrinol.* 2019;31(3):e12650.
- 7) de Graaf IA, Olinga P, de Jager MH, Merema MT, de Kanter R, van de Kerkhof EG, Groothuis GM. Preparation and incubation of precision-cut liver and intestinal slices for application in drug metabolism and toxicity studies. *Nature protocols.* 2010;5(9):1540-51.
- 8) Schwerdtfeger LA, Ryan EP, Tobet SA. An organotypic slice model for ex vivo study of neural, immune, and microbial interactions of mouse intestine. *American journal of physiology Gastrointestinal and liver physiology.* 2016;310(4):G240-8.
- 9) Schwerdtfeger LA, Nealon NJ, Ryan EP, Tobet SA. Human colon function ex vivo: Dependence on oxygen and sensitivity to antibiotic. *PloS one.* 2019;14(5):e0217170.
- 10) Richardson A, Schwerdtfeger LA, Eaton D, McLean I, Henry CS, Tobet SA. A microfluidic organotypic device for culture of mammalian intestines ex vivo. *Analytical Methods.* 2020;12:297-303.

CHAPTER 1 – FROM ORGANOTYPIC CULTURE TO BODY-ON-A-CHIP: A NEUROENDOCRINE PERSPECTIVE¹

Overview:

Methods used to study neuroendocrinology have been as diverse as the discoveries to come out of the field. Maintaining live neurons outside of a body in vitro was important from the beginning, building on methods that dated back to at least the first decade of the 20th century. Neurosecretion defines an essential foundation of neuroendocrinology based on work that began in the 1920's and 1930's. Throughout the first half of the 20th century, many paradigms arose for studying everything from single neurons to whole organs in vitro. Two of these survived as preeminent systems for use throughout the second half of the century: cell cultures and explant systems. Slice cultures and explants that emerged as organotypic technologies included such neuroendocrine organs as brain, pituitary, adrenal, and intestine. The vast majority of these studies were carried out in static cultures for which media was changed on the time scale of days. Tissues were used for experimental techniques such as electrical recording of neuronal physiology in single cells and observation by live microscopy. Many of these systems, when maintained in vitro only partially capture the in vivo physiology of the organ system of interest, often due to a lack of cellular diversity (e.g., neuronal cultures lacking glia). Modern microfluidic methodologies show promise for organ systems ranging from reproductive to gastrointestinal to brain. Moving forward and striving to understand the mechanisms that drive neuroendocrine signaling centrally and peripherally, there will always be a need to consider the heterogeneous cellular compositions of organs in vivo.

Introduction:

¹ Schwerdtfeger LA & Tobet SA. From organotypic culture to body-on-a-chip: A neuroendocrine perspective. *Journal of Neuroendocrinology*. 2019;31(3):e12650.

Neuroendocrinology has a rich and colorful history. From groundbreaking discoveries to academic feuds, the field of neuroendocrinology in the mid 20th century shaped our knowledge of the brain and its interactions with peripheral organ systems. Methods used to study neuroendocrinology have been as diverse as the discoveries to come out of the field. Cell and tissue culture techniques were first developed for frog embryonic tissues beginning in the early 1900's¹. A pre- World War II period saw the development of methodologies for the study of organs in vitro before they could be thought of for neuroendocrinology since it was not yet a "field" of investigation. This pre-war era saw the advent of numerous in vitro 'culture' systems, however the end goal of many of these studies was simply to validate the methods themselves. Post World War II, the emerging field of neuroendocrinology was able to take advantage of earlier in vitro technologies. Modern day perfusion methods, which are microfluidic in that they pump small quantities (i.e., microliters) of media to bathe cells or tissues of choice, are providing for development of new miniaturized "organ-on-a-chip" cultures². Organ-on-a-chip cultures attempt to recapitulate an in vivo organ environment in vitro by harnessing microfluidics to mimic blood flow via continuously perfusing a chamber containing either cells or organ cultures with media. This allows more consistent clearance of cellular waste products and perfusion with nutrients³. This review focuses on a partial history of neuroendocrinology from the perspective of organotypic techniques developed and utilized over the last 100+ years including discoveries generated using these techniques. Incorporation of brain-centric methodologies into peripheral organ usage provides a foundation for new approaches to neuroendocrine questions. Currently evolving systems centered around the idea of "body-on-a-chip" provide newer ways to examine neuroendocrine links among the central nervous system and peripheral organs.

Central Nervous System Neuroendocrinology:

Historical Perspectives:

The origins of tissue culture can be traced back at least to the beginning of the 20th century with the development of the hanging drop method. Harvesting of regions of frog embryo ectoderm were plated onto coverslips coated with adult frog lymph¹. After the frog lymph clotted, the coverslips were immediately inverted and placed over a hollow slide before sealing with paraffin to prevent drying¹. This technique allowed the maintenance of tissues for weeks on end, culminating with a demonstration of neuronal projection growth dynamics for the first time in vitro⁴. Around the same time, Harrison's hanging drop method was modified for use with blood plasma, first in avian embryo⁵ and then adult mammalian⁶ tissue cultures, showing tissue maintenance in vitro for days at a time. Between 1910 and 1938 Carrel and associates went on to publish dozens of papers on tissue culture and organ perfusion methodologies⁷, ultimately culminating in a book describing the culture of organs⁸. The work received widespread coverage by the lay press (e.g., Time Magazine and the New York Times) leading to a number of popular fiction stories regarding "immortal cells"⁷. There were many intriguing promises and predictions for modern in vitro work made in those early days. However, issues with scientific replication and the likelihood that the most popularized culture work (a 34-year-old culture of heart cells) was likely misrepresented⁹, may have contributed to a delay in more widespread adoption of tissue culture.

In the early 1900's physiologists were actively engaged in characterizing molecules that influenced heart rate and blood pressure leading to connections to the vagus nerve¹⁰ and acetylcholine, among other interesting amines¹¹. Definitive evidence of neurosecretion and function followed in 1921 when whole frog hearts were cultured ex vivo in a saline bath with a portion of the vagus nerve intact¹². These cultures were maintained for hours at a time and used to demonstrate the vagal release of a chemical that decreased heart rate. Dubbed

“Vagusstoff” by Loewi, the mysterious vagally secreted chemical was later clarified as acetylcholine. The principle of neurosecretion was later noted in invertebrate central nervous system models in “gland-nerve cells”¹³. This work became fundamental to the creation of modern day neuroendocrinology, although it was principally performed in the realm of “cytophysiology”¹⁴.

Beyond the hanging drop method of Harrison (1907) another in vitro technique developed in the early 20th century was the Maximow technique that was used to culture connective tissues and mammalian embryos¹⁵. This technique involved placing tissues onto collagen coated coverslips bathed in culture media, and subsequently adding a second cover slip with a gap caused by drops of paraffin-petroleum jelly. Tissue in the Maximow assembly was stored in the laying drop position prior to imaging in which it was inverted to a hanging drop position to allow microscope access to the cover slip¹⁶. The Maximow assembly, while able to maintain tissue in vitro far longer than other methods of the day, was sparsely used by others until 1947 when human sympathetic ganglia explants were cultured and used to study neurite outgrowth and motility of ganglion cells which were observed migrating from the explant into media¹⁷. Another in vitro preparation was denervated muscle cultures that were used to discern the function of hypothesized neurotransmitters such as adrenaline and acetylcholine¹⁸. Neither the Maximow technique nor muscle cultures were used to address specific neuroendocrine questions until the latter part of the 20th century.

Although some actions of pituitary hormones were long known¹⁹, understanding the physiological mechanisms that control the pituitary gland was a key scientific problem throughout the 1940’s and 50’s. This included the innervation of the neurohypophysis²⁰ (posterior pituitary gland) and the structure and regenerative capacity of the hypophyseal portal vascular system²¹. The impacts of cutting the pituitary stalk or occluding the hypophyseal vasculature were observed for their influence on neuroendocrine functions, in particular their

critical role in regulating ovulation²¹. In vivo models were used to perform hypophyseal perturbations to test the hypothesis that a substance was secreted from the hypothalamus and humorally transmitted to the pituitary gland²². While this became well accepted by the 1970's, it was met with distinct skepticism in its day²³. The concepts of neurosecretion¹³ and secretory communication of brain to pituitary²² paved the way for cell/tissue culture and organotypic neuroendocrine studies that followed.

Organotypic Models in CNS Neuroendocrinology:

Theorizing that something secreted by the brain controls the pituitary, and then identifying the actual molecules performing this regulation were distinctly different and difficult endeavors. Organotypic explant systems played essential roles in the isolation of what were first postulated as hypothalamic "factors" and later identified as hormones (e.g., thyrotropin releasing hormone (TRH) or luteinizing hormone releasing hormone (LHRH) that was later renamed gonadotropin releasing hormone (GnRH)). Early attempts to culture pituitary glands on microscope slides using the hanging drop method failed. Not until a piece of hypothalamic tissue was added into the culture, was in vitro pituitary release of adrenocorticotrophic hormone (ACTH) possible^{24,25}. These experiments also affirmed the idea that some factor secreted by the hypothalamus must influence ACTH release from the pituitary. Although the releasing factor (corticotrophin releasing hormone) was not isolated until years later²⁶, the in vitro assay was established as an essential method for testing the functional activity of molecules in isolated chromatographic fractions in the process of hormone isolation. The discovery of the GnRH peptide would not have been possible without the original experiments involving the organotypic explant co-culture of pituitary gland and hypothalamic tissue^{24,25}.

Organotypic brain tissue culture methodologies reached a distinctive point in the 1960s with a method for maintaining complete rhesus monkey brains ex vivo. This was accomplished

by combining a series of fluid pumps, and donor monkeys for blood perfusion^{27,28}. Use of this organotypic brain perfusion system had scientific value in showing the conversion of 7- α [³H]androstenedione to [³H]estrone by the isolated monkey brain²⁹, but might be considered ethically challenging by today's standards. The work demonstrated the utility of fluidic systems for use in studying neuroendocrinology, albeit in an inefficient manner, requiring two monkeys per experiment.

A minimal medium culture technique, the Maximow slide assembly¹⁵ was finally used for central nervous system tissues from the 1960s through 1980s. The method was adapted for questions ranging from the investigation of myelin formation in the cerebellum³⁰ to the development of the hypothalamus^{31,32}. Using this technique, the brain regions of interest, be it cerebellum or hypothalamus, were maintained in vitro for weeks, or even months at a time. Two issues with the Maximow technique were apparent. First, dissection of anatomically discrete regions in developing brain is difficult¹⁶, a challenge shared by all organotypic slice methods where the anatomical orientation of tissue components is important. Second, the Maximow technique was used in conjunction with serum (often horse or fetal calf derived) to maintain healthy tissue. The use of serum for organotypic preparations has a long history, going back to 1912³³. Nonetheless, supplementing culture media with serum is seen more and more as problematic. Serum is a mixture of numerous factors (proteins, hormones, growth factors, etc.,) that have been shown to vary significantly from batch to batch, between seasons, and between regions of production³⁴. This creates obvious problems in reproducibility for various culture methods. Systems discussed within this review may use media comprised of as much as 10 – 50% serum.

Table 1. Exemplary neuroendocrine culture systems outlined in this review, grouped by organ.

	Brain/neurones	Pituitary	Adrenal	Intestine
Cell culture	Tixier-Vidal et al ³⁵ Scharrer ¹⁴ Dreifuss & Gahwiler ³⁶ Suter et al ⁶⁴	May et al ¹³³	Mulder et al ¹²⁸	Bohorquez et al ¹¹⁷
Organoid	Qian et al ⁴²			Bohorquez et al ¹¹⁸ In et al ³⁸
Explants	Guillemin & Rosenberg ²⁴ Saffran & Serially ²⁵ White et al ²⁷	Guillemin & Rosenberg ²⁴ Saffran & Serially ²⁵ Pelletier & Bornstein ⁷⁴	Manuelidis ⁸²	Dreyfus et al ¹⁰⁸ Autrup et al ⁹² Costa et al ¹⁰⁷ Senior et al ⁹¹ Finney et al ⁹⁴
Slices	Skrede & Westgaard ⁴⁵ Toran-Allerand ¹⁶ O'Rourke et al ⁵² Wray et al ⁵⁰ Tobet et al ⁷⁰	Guerineau et al ⁷⁸ Navratil et al ⁷⁹ Alim et al ⁸⁰	Barbara et al ⁸⁴ Petrovic et al ⁸³ DeNardi et al ⁸⁷	De Kanter et al ⁹⁹ De Graaf et al ¹⁰⁰ Li et al ¹⁰¹ Schwerdtfeger et al ⁹⁶
Organ-on-Chip	Queval et al ¹²⁵ Huang et al ¹²¹ Park et al ¹²⁴ Kilic et al ¹²⁰ Xu et al ¹²³	Loughlin et al ⁷⁶	Wydallis et al ⁸⁵ Tedjo et al ⁸⁶	Kim et al ¹¹⁴ Shah et al ¹¹⁵ Yissachar et al ¹²²
Body-on-chip	Vernetti et al ¹³¹			Van Midwoud et al ¹³⁰ Vernetti et al ¹³¹

A wide range of in vitro culture techniques (Table 1; Figure 1) were used throughout the mid part of the 20th century, ranging from organ explant cultures³², to cultures of dissociated cells^{35,36}. Dissociated cell cultures were useful due to their ease of access for electrophysiological analyses. Cell accessibility allowed for imaging of single neurons; however, these cell cultures lacked an organotypic organization that limits their physiological context, and thereby potential relevance. Organ explants cultured on Maximow slide assemblies were highly

organotypic in structure but proved difficult for use in single neuron electrophysiological studies³⁷.

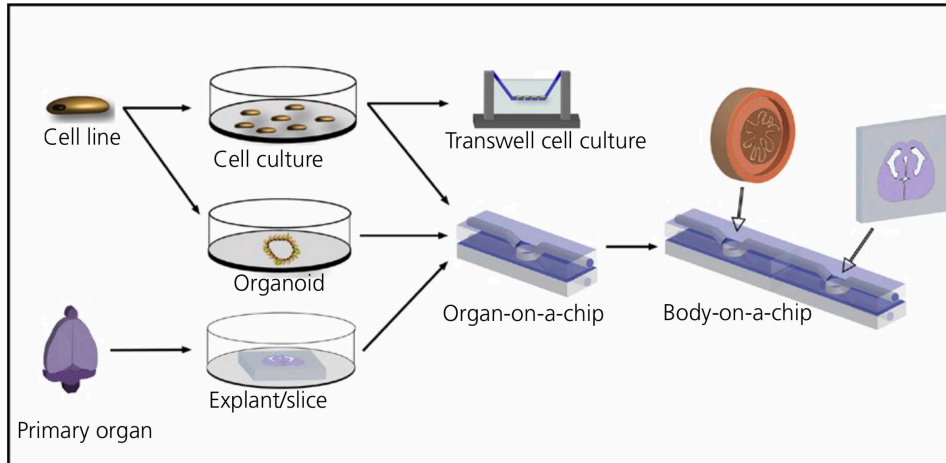


Figure 1. Schematic illustrating culture methods currently in use for neuroendocrine organs or cell lines.

Brain organoids are a recent mid-point between dissociated cells and organ explants. They elevate monolayer cultures to more complex, 3-dimensional models (Figure 1). These models use stem cells (induced pluripotent, embryonic, or endogenous adult progenitors) to generate patterned, 3-dimensional structures, and have been used to model a number of organs including intestine³⁸ and brain³⁹. Cerebral organoids have been used for study of neural development⁴⁰ and potential disease states⁴¹. Other brain-region-specific organoids have been developed for regions such as forebrain, midbrain and hypothalamus⁴². Their use in neuroendocrine studies has been limited to the demonstration of multiple peptidergic neuronal phenotypes. While brain organoids contain heterogeneous cellular elements⁴¹ that resemble neural tissue in a dish, their ability to organize into the complex cellular arrangements found within the mammalian brain is still limited. Brain organoids do not generate endothelial cells or oligodendrocytes, and are missing yolk-sac derived microglia, three cellular elements critical to physiological brain function.

Brain slicing emerged as an in vitro technology to the 1950's with attempts to "chop tissues"⁴³ for use in electrophysiological studies in the context of functional neuroanatomy⁴⁴. It was not long before there were many studies of slices of brain tissue performed by sectioning a brain region of interest with a guided razor blade that came to be known as a McIlwain Tissue Chopper. These slices were perfused with different salt-based physiological solutions, some with notably high oxygen levels climbing as high as 95%⁴⁵. The goal of the vast majority of these studies was not to maintain the tissue for longer than perhaps 4-18h. The focus of this review, on the other hand, is primarily on the generation of cultures that were maintained for days or longer. While the McIlwain tissue chopper provided a significant advance beyond free-hand dissections, the vibrating microtome offered a means to cut tissue with still more accurate section thickness and with less damage to the cut surfaces⁴⁶. This allowed sectioning brains thinner than the tissue chopper and with greater reliability, critical components for maintaining organotypic brain slices in culture for days at a time. The potential of brain slices for use in neuroendocrine investigations emerged in the 1970s as longer-term explant cultures of hypothalamus were used to study neuropharmacological agents impacts on the magnocellular secretion of vasopressin⁴⁷. Long-term cultures shifted towards short-term slice preparations of the hypothalamus to measure osmotic responsiveness by electrophysiology in magnocellular neurons of the supraoptic nucleus⁴⁸.

Roller tube cultures are designed to maintain an organotypic organization while offering better neuron accessibility⁴⁹. This system maintained supraoptic nucleus regions of the rat hypothalamus, co-cultured with a hypophyseal explant on a plasma clot, prior to the addition of 1 ml of serum containing medium. The assembly was rotated with a roller drum, causing tissue originally cut at 400 μ m thick to flatten over the course of the culture period⁴⁹. Thinning of tissue was advantageous, allowing imaging and/or electrophysiological study of tissues with organotypic cellular arrangements with cellular resolution. Roller cultures were used throughout

the 1980s and 1990s to characterize the hypothalamus and its cellular phenotypes, such as the suprachiasmatic nucleus, via immunohistochemistry⁵⁰. Investigation into GnRH neurons was performed using a roller system co-culture of preoptic area of the hypothalamus with brainstem and pituitary. The system demonstrated maintenance of anterior pituitary gonadotropes containing luteinizing hormone only in the presence of the hypothalamic co-cultures⁵¹.

Roller tube cultures have been employed for the study of neuronal migration in cerebral cortex using brain slices. In one study, slices from embryonic ferret cortex were injected with the indocarbocyanine dye, Dil, into the ventricular zone, allowing for fluorescent imaging of neurons during their migration through the intermediate zone of the cortex⁵². Despite these characterizations of the roller culture model, and its widespread use in studies of the hypothalamus among other brain regions, the model was not without its problems. Serum was widely used in the early roller culture experiments on hypothalamus (often 25% horse serum). This was a potential problem noted in GnRH neuronal cultures, where morphological differences were seen between neurons *in vivo* and those cultured *in vitro*, potentially caused by an unknown factor in the media⁵¹. Serum containing media continue to be the standard for organotypic culture systems well into the 21st century³⁴. The length of time that cultures have been maintained in roller tubes highlight the need to carefully consider the age of tissue being investigated in relation to how a developing or mature animal system works. The “aging” of brain slices *ex vivo* has been discussed elsewhere⁵³. The related issue of utilizing tissue from embryonic or neonatal sources to model adult disorders is also beyond the scope of the current review.

Other brain slice systems attempted to preserve the three-dimensional nature of tissue in culture by using a tissue support system such as agarose. Brain slice cultures generated using low melting point agarose for support, and cut on a vibrating microtome, were used for hypothalamic studies by generating 300 μm thick coronal slices of embryonic rat brain, and

subsequently labeling slices with Dil. This technique allowed for fluorescent visualization of migrating cells (assumed to be neurons based on morphology) in the preoptic area/anterior hypothalamus⁵⁴. As the method was transferred to mice it became clear that just a 50 μm difference to 250 μm was a significant improvement for sagittal sections of embryonic mouse heads to study the migration of GnRH neurons⁵⁵ indicating the importance of diffusion distances for oxygen, nutrients, or both. The slice technology was further adapted for use on membrane supports examining Dil labeled cell migration from developing striatum to cortex in mice with targeted mutations of *Dlx* genes⁵⁶. These early brain slice systems were useful in modeling complex neuronal migratory pathways in vitro and maintained an organotypic cellular arrangement which is critical in cellular interactions that guide motility.

Organotypic systems have been useful for investigating neuronal migration in neuroendocrine contexts. Explants of embryonic mouse nasal regions were one of the first organotypic methods used in GnRH work⁵⁷. This model maintained 20-50% of the GnRH neuronal population and utilized 25% horse serum in culture. Shortly thereafter, an organotypic slice model was developed using parasagittal slices of fetal mouse heads to study GnRH neuronal migration that used defined, serum free medium, and tissue sliced in an agarose gel, helping to support the tissue and maintain full slice thickness (250 μm) in vitro⁵⁵. This was important in visualizing the migratory paths of GnRH neurons as they cross from nasal to brain compartments^{55,58} and including the first live visualization of GnRH neuronal migration using video microscopy⁵⁹. Immortalized cell lines have been used to address some questions about cell motility⁶⁰, but explant and organotypic slice cultures provide information about the potential diversity of cells needed for GnRH neuron behaviors (e.g., neurons with GABA).

One of the most powerful tools to aid studies of live cell behaviors was the emergence of Green Fluorescent Protein^{61,62} (GFP) that could be genetically engineered for cell selective expression. Developmental neuroendocrinology was just one field ready to take advantage of

transgenic animal models. Using transgenic mice that express variants of GFP driven by neuronal specific promoters (e.g., Thy1 promoter driving – yellow fluorescent protein-YFP⁶³, murine brain slices were generated to study neuronal migration. Transgenic models offered more selective labeling of cell populations compared to previous fluorescent methods, such as Dil^{52,54}. The development of a transgenic mouse line in which GFP expression was driven by the GnRH promoter⁵⁷ provided for the study of live GnRH neurons in sagittal slices⁵⁹. Meanwhile, mice in which a neuron selective Thy-1 promoter drives YFP expression⁶³ have been used to study the development of several neuroendocrine hypothalamic regions. Using these and other approaches to mark neurons, investigations of neuronal migratory patterns in the preoptic area^{65,66}, ventromedial nucleus^{67,68}, and paraventricular nucleus^{69,70} were carried out using organotypic coronal slices⁷¹.

Using approaches that allow live assessments of neuronal function (e.g., calcium flux) add to a molecular tool box for organotypic studies. Genetically encoded calcium indicators in particular have helped advance the ability of investigators to view live cell functions in vitro without using dye-based methods. Regulatory immediate early genes such as *c-fos* provide an indirect assessment of neuronal activation⁷². Genetic indicators of cellular function are advantageous as they use native cellular elements to indicate activity and allow tracking of circuit-level functions in vitro⁷³. For neuroendocrine function, genetically regulated calcium indicators have been used to study transient intracellular calcium flux in GnRH neurons⁷⁴. This study demonstrated the requirement of an IP3-receptor dependent calcium release for transient calcium flux in GnRH neurons of mice, potentially pointing to the intracellular mechanism of GnRH neuronal episodic activity which is critical for regulating mammalian fertility. Use of genetic markers of neuronal function in the study of neuroendocrine questions has been sparse. Further utility for these methods remains to be seen moving forward, although some methods

(e.g., *c-fos*) are limited in their temporal resolution due to reliance on detection of transcriptional activation⁷².

Moving Peripherally:

Pituitary Culture Systems:

Since the initial use of hypothalamus – pituitary organotypic co-cultures^{24,25}, the pituitary has been used regularly in organotypic culture systems. Initial pituitary cultures were performed with fragments of the postnatal rat pituitary gland. These fragments were mounted in Maximow slide assemblies and maintained secretory competency for up to a week in vitro⁷⁵. Later work maintained similar pituitary explants in Maximow slides for up to 100 days; however, these cultures only had secretory granules for 3 weeks in vitro⁷⁶. The use of large amounts of human placental cord serum (33%) in these systems was a drawback due to the unknown and variable composition of serum. Perfused pituitary cell cultures marked one of the earliest methods to use flow to continually pass media over cells. These dissociated pituitary cultures were employed to investigate pulsatile GnRH treatment on LH secretion⁷⁷ as well as the influence of estrous cycle stage on pituitary release of LH⁷⁸. Roller culture techniques also proved efficacious for pituitary cultures from postnatal rats. As with hypothalamic roller cultures, rat anterior pituitary gland cultures were sliced at 400 µm and gradually flattened during the culture period, in this case, lasting up to 7 weeks⁷⁹. This model used 25 % horse serum to maintain tissue viability. Pituitary work also included organotypic slice models. GnRH mediated extensions of pituitary cell processes and apparent cellular repositioning were observed in 200µm thick slices⁸⁰. This organotypic slice model was extended to gonadotropes with the help of GFP selective cellular identification to demonstrate alterations in GnRH impacts on gonadotrope morphology during different female reproductive stages⁸¹.

Adrenal Gland Cultures:

A critical component of the mammalian stress response, the adrenal gland also has been used in organotypic conditions. Research into cells of the adrenal medulla has been conducted since the 1940s. Early experiments involved the blood perfusion of whole bovine adrenal glands using a complex vascular perfusion technique. This method was used for the study of adrenal conversion of 11-desoxycorticosterone to corticosterone⁸². Perinatal rat adrenal glands have been cultured for up to 3 weeks in vitro when supplemented with 33% horse serum⁸³. This model showed that treatment with dibutyryl cyclic AMP caused rough endoplasmic reticulum enlargement, leading to adrenal chromaffin cells exhibiting neuron-like morphologies. Adrenal glands offer a useful system for validating chemical release measurement technologies, as they release large amounts of catecholamines when appropriate stimuli is applied. This secretion was shown in an organotypic slice system, which used fast-scan cyclic voltammetry to measure catecholamine release⁸⁴. The model system used in this study was originally described as a method to study cholinergic innervation of chromaffin cells and maintained adrenal gland slices (200 – 300 μm thick) for 8 h in vitro⁸⁵. More recently organotypic adrenal slices have been used to test the validity of a high-density electrochemical microelectrode array for assessing spatial and temporal dynamics of catecholamine release^{86,87}. Independently, another group used tissue culture supernatants collected from 150 μm thick adrenal slices to measure changes in catecholamine secretion using high-performance liquid chromatography in response to acetylcholine, nicotine and hexamethonium⁸⁸. This study did not provide temporal resolution of secretion, as it only collected supernatants at one time point. The success of organotypic cultures of adrenal gland makes it an interesting organ of choice for testing neuroendocrine stimulated release of compounds in the context of multi-organ ex vivo systems; for example, coupled with cultures of hypothalamus and/or pituitary.

Gut Organotypic Approaches:

Mammalian intestines have been studied outside of the body since the 1930s. Isolated rabbit intestines were used to discern the physiological function of a then unknown 'depressor substance' later determined to be Substance P⁸⁹. Furthering the functional profile of vagus secretions originally established in 1921¹², whole dog intestines were arterially perfused with Locke's solution and used to examine effects of acetylcholine on contractions of the stomach⁹⁰. It was not until the 1960s that selective culture methodologies, as opposed to perfused whole organs, were used for studying intestinal physiology. A number of intestinal explant models were focused on characterizing and maintaining healthy tissue in vitro. Human colon explants were difficult to culture for longer than 72 h^{91,92} except for one study⁹³ in which human colonic epithelium was maintained for 20 days in vitro. Unfortunately, details of tissue health were minimal in the early colon studies, which also used serum (5-15% fetal calf serum). Other teams maintained organotypic culture systems from rodents to study epithelial proliferation rates in the colon⁹⁴, again with issues of tissue survival. Serum and antibiotics were also supplemented in the media, likely altering intestinal microbiota significantly. Later studies provided an additional indicator of health by incorporating the use of tritiated thymidine to study mitotic cells and their localization in vitro⁹⁵.

Antibiotic treatment, made possible in the 1940's, became common to a vast majority of in vitro studies, as well as in early explant cultures of intestine⁸³, which has been shown to significantly alter gut microbiota. Commensal bacteria that make up a large part of the gut microbiome play significant roles in regulating intestinal physiology. Antibiotics commonly used in culture (e.g. penicillin-streptomycin) alter gut bacterial abundance and diversity⁹⁶. They are known to influence tissue physiology and have been suggested to decrease intestinal motility⁹⁷, and regulate certain enteric neuronal subtypes⁹⁸.

Slicing intestines became a useful approach for metabolic and toxicological studies in the 2000's⁹⁹. Precision cut intestinal slices¹⁰⁰ (PCIS) were first used to study gut drug metabolism capabilities¹⁰¹, and subsequently characterize the intestinal response to toxins¹⁰². Better validation of tissue health in these PCIS studies, compared to the explant studies of the 70s and 80s, provides more confidence in the recapitulation of in vivo physiology, in vitro. Unfortunately, PCIS culture methods have been useful only in the first ~24 h of culture. A modified organotypic slice model, using a similar protocol to that previously used in brain⁷¹, was capable of maintaining 250 µm thick mouse intestinal slices in serum free media, without antibiotics, for up to 6 days ex vivo⁹⁷. The advances in culture technology over the past 40 years set the stage for organotypic intestinal culture systems to be used in the study of peripheral neuroendocrinology.

Gut Neuroendocrinology ex vivo:

The intestinal tract is a sizable endocrine organ, containing more than 30 genes encoding peptides that are used as hormones and for other signaling functions in the gut¹⁰³ and in the CNS. Endocrine regulation of the intestinal tract, and its subsequent influence on digestion and satiety among other things, is beyond the scope of this review. It is important to recognize, however, that both the enteroendocrine cellular network and secretory enteric nervous system found along the length of the gastrointestinal tract are extensive¹⁰⁴. It is a network capable of producing everything from somatostatin¹⁰³ to vasoactive intestinal peptide¹⁰⁵ (VIP) and immunoreactive GnRH (personal observation). Among the enteroendocrine cell products, serotonin (5-hydroxytryptamine, 5HT) could be argued to be particularly striking. Despite the attention to 5-HT in the brain, 90-95% of the 5-HT in the body is produced by enterochromaffin cells of the intestinal mucosa¹⁰⁶. Additionally, subsets of enteric neurons are serotonergic^{107,108}. An early gut organotypic system was used to culture guinea pig intestinal

musculature (including the enteric nervous system), 1-week after vagotomy in vivo. This system showed the capacity of enteric neurons to take up 5-HT, and how it was impacted by prior vagus nerve inputs¹⁰⁹.

Organotypic culture systems frequently have been employed to examine the intracellular response of guinea pig myenteric plexus neurons to perturbations such as enkephalin¹¹⁰. These studies used a pinned muscle layer of guinea pig ileum, that survived for less than 18 h. Improving upon traditional intracellular recording setups, organotypic cultures of guinea pig intestine have been used regularly to study the structural and functional characteristics of the myenteric plexus. Circular muscle layer motor neurons¹¹¹, and longitudinal muscular motor neurons¹¹² were both described using guinea pig organotypic culture systems that were maintained for up to 3 days ex vivo. Translation of the musculature organotypic model for use with human colon resected tissue showed that the majority of human colonic interneurons are either nitric oxide synthase (NOS) or choline acetyltransferase (ChAT) immunoreactive¹¹³. These systems were useful in describing the localization and phenotype of motor neurons; however, they may be partially confounded by the use of 10% fetal bovine serum, and the incubation of tissue with antibiotics that significantly alter intestinal microbiota.

The past 20 years has seen a significant resurgence in intestinal research, in part due to increases in the incidence of gastrointestinal disorders¹¹⁴ along with advances in gene sequencing and metabolomic technologies allowing for investigation of microbiome contributions to health and disorder. The need to understand drug pharmacodynamics and pharmacokinetics has also pushed intestinal research forward. While model systems for maintaining intestinal tissues in vitro have been used since the 1970s, the past 20+ years has also seen the adoption of simplistic cell culture systems that are easier to use for drug screening and permeability studies. Caco-2 cells are an immortalized colon cancer line that are frequently used to derive monolayers, and often cultured in microfluidic systems^{115,116}. Caco-2 cell cultures

differentiate into enterocyte-like populations; however, the phenotype of these cells is dependent on culture technique (e.g. microfluidic vs static, number of passages, etc.)¹¹⁷. Co-cultures of 2- or more intestinal cell types are occasionally used¹¹⁸. A variation on the theme is the expanding use of organoid culture systems³⁸. Organoids (or enteroids when just considering intestines) are based on an expanded population of progenitor cells isolated from healthy intestines. Co-culture systems have been used to show the presence of a neuroepithelial circuitry in intestinal cells, with enteroendocrine cells being directly innervated by enteric neurons¹¹⁸. Organoids demonstrated an enteroendocrine cell – enteric glial synapse¹¹⁹. While there is merit in all of these model systems, they fall short of delivering on the diversity of cells types that are normally found in natural tissue (e.g., including neurons, glia, and immune cells).

21st Century Neuroendocrinology:

Current Organs-on-a-chip

Organs-on-a-chip are engineered devices that maintain tissue, be it cell line monolayers, organoids, or even tissue explants (Figure 1) with microfluidic flow allowing continuous perfusion of media. Further development of organ-on-a-chip systems is required to transition from the realm of method development to that of using the novel methods to address physiological questions. Many organotypic culture systems have been ‘static’ in that they did not perfuse media through the preparations, and required media changes every 1-7 days^{71,93}. The “perfusion” systems (e.g., pituitary) may be the most common example of systems using some sort of flow. That said, fluid dynamics in those systems were difficult to regulate, shear stresses were not accounted for, and time ex vivo was limited. With the explosion of microfluidic technologies in the early 21st century, it is easier to find organotypic culture systems incorporating constantly perfused microfluidic delivery of media, generating organ-on-a-chip

systems¹²⁰. Varied device materials contribute to health of tissue on-chip, and have been reviewed recently¹²⁰. In the development of “organs-on-a-chip” most have utilized cultures of immortalized cell lines, often in monolayers^{115,121}. Continuously perfused media provides a more consistent delivery of oxygen and nutrients, and removal of cellular waste products¹²². An ideal device for culturing organs outside the body would offer this efficient and regular nutrient and oxygen delivery, coupled with access to microscopy and electrophysiological methods^{120,122}. Intestinal research has been at the forefront of recent developments for organ-on-a-chip systems. Early gut-on-a-chip devices were caco-2 monolayers cultured with continuous media flow¹¹⁵. Another model (HuMix) was developed to include a similar caco-2 monolayer that also maintained an oxygen gradient similar to that seen in the gut in vivo, with an exogenously added minimal bacterial population¹¹⁶. This system was used to show altered transcription in cultures maintained by themselves versus those maintained with small restricted bacterial populations. Intestinal explants have also been cultured on microfluidic platforms, being used to demonstrate a direct bacterial – immune – neuronal interaction ex vivo¹²³. Future advances are needed, since these microfluidic systems do not address the full thickness of the intestinal wall, and the latter used a culture system with 95% oxygen, thereby impacting the microbiome. The oxygen gradient across the intestinal wall creates a unique anaerobic – aerobic interface at the luminal surface of the gut epithelium. The ability of microfluidic systems to recapitulate this interface in vitro in cell monolayers¹¹⁶ is a key advantage of gut-on-chip systems. As engineered gut-on-chip technologies advance, one can envision an organotypic intestinal explant/slice inside a microfluidic device that recapitulates the anaerobic – aerobic interface, allowing for study of the complex bacterial – neural – immune interactions of the gut.

Various other systems outside of the intestinal tract have been cultured in organ-on-chip platforms. “Brain”¹²¹ and blood brain barrier¹²⁴, have both been cultured using microfluidic systems. These are composed of dissociated cells (e.g., neural progenitor cells for brain

models) that lack the physiological relevance of natural cell diversity. Recent papers describing “brain-on-a-chip” models illustrate interesting issues from the neuroendocrine perspective of identifying secretory cell(s). In one case, the cell line was a human teratocarcinoma differentiated to neuronal/astroglia phenotypes using retinoic acid¹²¹. In the other case, the cells were embryonic rat cortical cells that were at least partially characterized as neuronal¹²⁵. Both used serum free medium (Neurobasal medium with B-27 supplement^{121,125}. Looking toward the future, the heterogeneity of neuronal phenotypes in general and across brain regions will need to be better accounted for. A similar microfluidic device was designed to maintain an organotypic slice of hippocampal tissue inside a perfusion chamber¹²⁶. It had the tissue flattening and serum requirement drawbacks of roller tube culture, but the design of a brain-on-a-chip. This represents an interesting step towards a more physiological neural system maintained in an engineered culture device. These brain-on-a-chip systems are the first steps in advancing engineering technology for use in neural systems and will need to improve their physiological relevance in 3-D structure, cellular heterogeneity, and media composition moving forward before they can be relied on to provide heuristic answers to biological questions. Recapitulation of an in vivo biological event in vitro provides a useful test for organ-on-a-chip systems. This is getting closer to reality for multiple organ systems. It was recently accomplished to an extent with a model of human reproductive function in which mouse and human tissues were cultured for 4 weeks. Using a complex system of interconnected culture chambers, the ovary, uterus, fallopian tubes, and liver explants were cultured and able to mimic the human menstrual cycle¹²⁷. Production of 17 β -estradiol was observed in culture, and progesterone production was sensitive to treatment with human chorionic gonadotropin, representing on-chip follicular and luteal phases of a menstrual cycle. This multi-organ culture system represents a significant step forward in the field of organ-on-a-chip tissue engineering and paves the way for transitioning into more physiologically relevant body-on-a-chip systems.

Evolution to Body-on-a-chip:

Body-on-a-chip systems have been developed for investigation of organ-organ interactions; and may be an important direct way to view integrated neuroendocrine functions in feedback loops (e.g., hypothalamic-pituitary-adrenal axis). Engineering challenges remain to address validated physiological parameters needed for each organ and in the media and microfluidics that connect them. A principal need to advance body-on-chip methodologies, just as for organ-on-chip, is to include the cellular heterogeneity of the natural tissue in the body-on-chip platforms, thereby allowing for more general use of these systems in addressing biological questions¹²⁸. Interestingly, in vitro maintenance of multi-organ systems was done before World War II. Whole dog intestine, pancreas and spleen were all perfused with Locke's solution using the organs natural vasculature and used to show the function of vagus nerve secretions on the stomach⁹⁰. Approaches to showing multi-organ neuroendocrine function in vitro have been performed, with rat hypothalamus blocks and both pituitary and adrenal dissociated cells. Media was superfused from a culture well containing the hypothalamus block to a second well with dissociated pituitary cells and finally to a third well with dissociated adrenal cells¹²⁹. This technique was used to demonstrate that electrical stimulation of the hypothalamus led to pituitary release of corticotropin releasing factor (CRF), which subsequently caused production of corticosterone by the adrenal cortex.

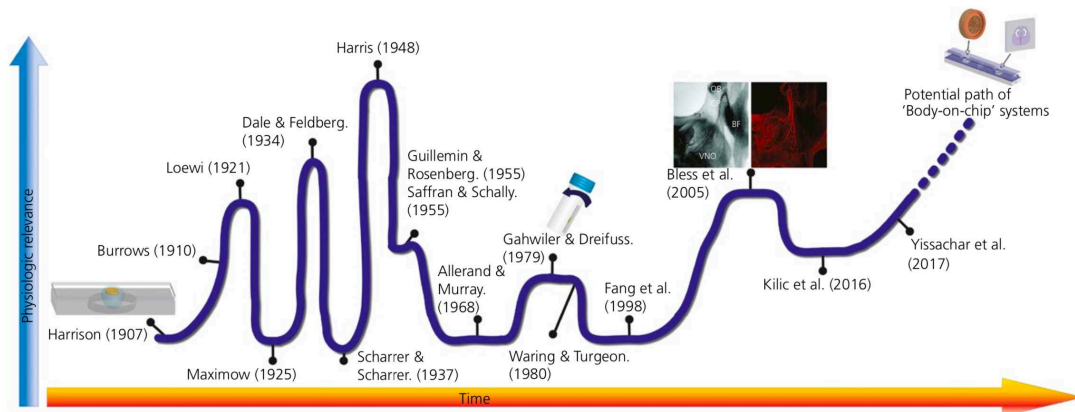


Figure 2. Schematic demonstrating the evolution of organotypic culture methodologies over time.

Movement to miniaturized Body-on-a-chip systems that require small amounts of tissue have garnered increased discussion¹³⁰, and attempts to recapitulate multi-organ systems in a single engineered in vitro culture model are becoming easier to find. One prime example of an early body-on-a-chip was the use of a sequentially perfused chamber to culture liver and intestine precision cut slices¹³¹. This system measured the influence of physiologic intestinal secretions on the metabolism of exogenous substrates (e.g., lidocaine) by the liver. Clear utility in analyzing organ – organ interactions, and the influence these interactions play on metabolism was apparent with this system. A step forward for multi-organ systems was taken with the coupling of intestine, liver, kidney, blood brain barrier, and muscle cultures in series¹³². This model was used to show the influence on multi-organ metabolism of trimethylamine and vitamin D3, and toxicity of terfenadine. While this multi-organ system represents a body-on-chip in the sense that numerous organs were ‘connected’ via shared media, it was conducted using cell line-based culture devices. Moving forward, use of more physiological organ tissues in this system would improve its power for translation efficacy for more accurate physiological outputs. Across the march of history, in vitro systems for study of mammalian physiology have vacillated between more physiologically organ related and more reductionist cell-oriented methods (Figure 2). As the pendulum swings back closer to “organ” techniques, attention to physiology will be

critical to hone new culture approaches. Microfluidic body-on-a-chip systems have yet to be harnessed for use in neuroendocrine studies. Movement from organotypic brain slices into brain-on-a-chip interfaces, and subsequent coupling to peripheral organs (e.g., pituitary, adrenal, intestine) will be a move likely to be seen in organ- and body- on-a-chip research in the future.

Neuroendocrinology sits at an interesting point, with divergent model systems available along reductionist versus physiological lines. One path uses cell lines-on-chip, offering high throughput systems that do not require additional animals. Cell lines, while useful for carefully crafted biochemical questions are inherently missing cellular interactions that emerge from the diversity of the normal cast of surrounding cells in the organs of interest. These systems can only go so far in providing a window on physiological realities. A second, perhaps more challenging path, couples the use of organotypic culture models with microfluidic engineering technology. Static cultures of brain, pituitary, gut and adrenal have proven useful for mechanistic study of various disease and neuro-endocrine secretory pathways. Coupling these organotypic cultures with more in vivo – like physiologic systems will be critical in increasing successful translation of ex vivo data into efficacious treatment modalities for neuroendocrine disorders.

References:

1. Harrison R. Observations on the Living Developing Nerve Fiber. *The Anatomical Record*. 1907;5:116-128.
2. Kimura H, Sakai Y, Fujii T. Organ/body-on-a-chip based on microfluidic technology for drug discovery. *Drug Metab Pharmacokinet*. 2018;33(1):43-48.
3. Kim L, Toh YC, Voldman J, Yu H. A practical guide to microfluidic perfusion culture of adherent mammalian cells. *Lab Chip*. 2007;7(6):681-694.
4. Harrison R. The outgrowth of the nerve fiber as a mode of protoplasmic movement. *J Exp Zool*. 1910;142(4):5-73.
5. Burrows M. The Cultivation of Tissues of the Chick-Embryo Outside the Body. *JAMA*. 1910;55(24):2057-2058.
6. Carrel A, Burrows M. Cultivation of Tissues in Vitro and Its Technique. *J. Exp Med*. 1911;13(3):387-396.
7. Hamilton D. *The First Transplant Surgeon. The Flawed Genius of Nobel Prize Winner, Alexis Carrel*. Singapore: World Scientific Publishing Co. Pte. Ltd; 2016. 450 p.
8. Carrel A, Lindbergh C. *The culture of organs*. Cornell University: Hoeber; 1938. 221 p.
9. Witkowski JA. Dr. Carrel's Immortal Cells*. *Medical History*. 1980;24:129-142.
10. Dale H, Laidlaw P, Symons C. A Reversed Action of the Vagus on the Mammalian Heart. *J Physiol*. 1910;XLI:1-18.
11. Dale H. The Action of Certain Esters and Ethers of Choline, and their Relation to Muscarine. *J Pharmacol Exp Ther*. 1914;147-190.
12. Loewi O. *Über humorale Übertragbarkeit der Herznervenwirkung*. *Pflugers Arch*. 1921;189:239-242.

13. Scharrer E, Scharrer B. Uber Drusen-Nervenzellen Und Neurosekretorische Organe Bei Wirbellosen Und Wirbeltieren. *Biological Reviews*. 1937;12:185-216.
14. Scharrer B. NEUROSECRETION: Beginnings and New Directions in Neuropeptide Research. *Ann Rev Neurosci*. 1987;10:1-17.
15. Maximow A. Tissue cultures of young mammalian embryos. In: *Embryol*. Vol 16. Carnegie Inst. of Wash. Publ.; 1925. 47 p.
16. Toran-Allerand C. Long-Term Organotypic Culture of Central Nervous System in Maximow Assemblies. In: *Methods in Neurosciences*. Vol 2. Massachusetts: Academic Press; 1990. 20 p.
17. Murray MR, Stout A. Adult human sympathetic ganglion cells cultivated in vitro. *Am J Anat*. 1947;80(2):225-273.
18. Dale H, Gaddum J. Reactions of Denervated Voluntary Muscle, and their Bearing on the Mode of Action of Parasympathetic and Related Nerves. *J Physiol*. 1930;70:109-144.
19. Dale H. The Action of Extracts of the Pituitary Body. *Biochem J*. 1909:427-447.
20. Harris GW. The Innervation and Actions of the Neurohypophysis - an Investigation Using the Method of Remote-Control Stimulation. *Philos Trans R Soc London., B*. 1947;232(590):385.
21. Harris G. Neural Control of the Pituitary Gland. *Physiol Rev*. 1948;28(2):139-179.
22. Harris GW. *Neural Control of the Pituitary Gland*. London: Edward Arnold Publishers Ltd; 1955. 298 p.
23. Zuckerman S. Control of Pituitary Function. *Nature*. 1956;178:442-443.
24. Guillemin R, Rosenberg B. Humoral hypothalamic control of anterior pituitary: a study with combined tissue cultures. *Endocrinology*. 1955;57(5):599-607.
25. Saffran M, Schally A. The Release of Corticotrophin by Anterior Pituitary Tissue In

- Vitro. *Can J Biochem Physiol.* 1955;33:408-415.
26. Vale W, Spiess J, Rivier C, Rivier J. Characterization of a 41-Residue Ovine Hypothalamic Peptide That Stimulates Secretion of Corticotropin and B-Endorphin. *Science.* 1981;213(4514):1394-1397.
 27. White R, Albin M, Verdura J. Isolation of the Monkey Brain: In vitro Preparation and Maintenance. *Science.* 1963;141(3585):1060-1061.
 28. White R, Albin M, Verdura J, Locke G. The Isolated Monkey Brain: Operative Preparation and Design of Support Systems. *J Neurosurg.* 1967;27(3):216-225.
 29. Flores F, Naftolin F, Ryan K, White R. Estrogen Formation by the Isolated Perfused Rhesus Monkey Brain. *Science.* 1973;180(4090):1074-1075.
 30. Allierand C, Murray M. Myelin formation in vitro: Endogenous Influences on Cultures of Newborn Mouse Cerebellum. *Arch Neurol.* 1968;19(3):292-301.
 31. Toran-Allierand C. Sex steroids and the development of the newborn mouse hypothalamus and preoptic area in vitro: implications for sexual differentiation. *Brain Res.* 1976;106(2):407-412.
 32. Toran-Allierand C. The luteinizing hormone-releasing hormone (LH-RH) neuron in cultures of the newborn mouse hypothalamus/preoptic area: ontogenetic aspects and responses to steroid. *Brain Res.* 1978;149:257-265.
 33. Ingebrigtsen R. The Influence of Heat on Different Sera as Culture Media for Growing Tissues.*. *J Exp Med.* 1912;15(4):397-403.
 34. van der Valk J, Brunner D, De Smet K, et al. Optimization of chemically defined cell culture media--replacing fetal bovine serum in mammalian in vitro methods. *Toxicol In Vitro.* 2010;24(4):1053-1063.
 35. Tixier-Vidal A, Nemerovski A, Faivre-Bauman A. Primary cultures of dispersed fetal hypothalamic cells. Paper presented at: Colloque international du CNRS, Biologie

- Cellulaire des processus neurosecretoires hypothalamiques; Paris.
36. Dreifuss J, Gahwiler B. Hypothalamic neurons in cultures I. A short review of the literature. *J Physiol.* 1979;75:15-21.
 37. Gahwiler B. Organotypic slice cultures: A model for interdisciplinary studies. *Model systems in Neurotoxicology: Alternative approaches to Animal Testing. Prog Clin Biol Res.* 1987;253:13-18.
 38. In JG, Foulke-Abel J, Estes MK, Zachos NC, Kovbasnjuk O, Donowitz M. Human mini-guts: new insights into intestinal physiology and host-pathogen interactions. *Nat Rev Gastroenterol Hepatol.* 2016;13(11):633-642.
 39. Lancaster MA, Renner M, Martin CA, Wenzel D, Bicknell LS, Hurles ME, Homfray T, Penninger JM, Jackson AP, Knoblich JA. Cerebral organoids model human brain development and microcephaly. *Nature.* 2013; 501(7467): 373-9.
 40. Lancaster MA, Knoblich JA. Generation of cerebral organoids from human pluripotent stem cells. *Nature Protoc.* 2014; 9(10): 2329-40.
 41. Di Lullo E, Kriegstein AR. The use of brain organoids to investigate neural development and disease. *Nature reviews Neuroscience.* 2017; 18(10): 573-84.
 42. Qian X, Nguyen HN, Song MM, Hadiono C, Ogden SC, Hammack C, Yao B, Hamersky GR, Jacob F, Zhong C, Yoon KJ, Jeang W, Lin L, Li Y, Thakor J, Berg DA, Zhang C, Kang E, Chickering M, Nauen D, Ho CY, Wen Z, Christian KM, Shi PY, Maher BJ, Wu H, Jin P, Tang H, Song H, Ming GL. Brain-Region-Specific Organoids Using Mini-bioreactors for Modeling ZIKV Exposure. *Cell.* 2016; 165(5): 1238-54.
 43. McIlwain H, Buddle H. *Techniques in Tissue Metabolism.* 1. A Mechanical Chopper. *Biochem J.* 1952;53(3):412-20.

44. Li C, McIlwain H. Maintenance of Resting Membrane Potentials in Slices of Mammalian Cerebral Cortex and other Tissues In Vitro. *J Physiol.* 1957; 139:178-190.
45. Skrede KK, Westgaard RH. The transverse hippocampal slice: a well-defined cortical structure maintained in vitro. *Brain Res.* 1971;35(2):589-593.
46. Arman AC, Sampath AP. Patch clamp recordings from mouse retinal neurons in a dark-adapted slice preparation. *J Vis Exp.* 2010(43).
47. Sakai K, Marks BH, George J, Koestner A. The Isolated Organ-Cultured Supraoptic Nucleus as a Neuropharmacological Test System. *J Pharmacol Exp Ther.* 1974;190(3):482-491.
48. Hatton G, Armstrong W, Gregory W. Spontaneous and Osmotically-Stimulated Activity in Slices of Rat Hypothalamus. *Brain Res Bull.* 1978;3:497-508.
49. Gahwiler B, Dreifuss J. Hypothalamic neurons in culture II. A progress report. *J Physiol.* 1979;75:23-26.
50. Wray S, Castel M, Gainer H. Characterization of the suprachiasmatic nucleus in organotypic slice explant cultures. *Microsc Res Tech.* 1993;25(1):46-60.
51. Wray S, Gahwiler BH, Gainer H. Slice cultures of LHRH neurons in the presence and absence of brainstem and pituitary. *Peptides.* 1988;9(5):1151-1175.
52. O'Rourke NA, Dailey ME, Smith SJ, McConnell SK. Diverse migratory pathways in the developing cerebral cortex. *Science.* 1992;258(5080):299-302.
53. Humpel C. Organotypic brain slice cultures: A review. *Neuroscience.* 2015; 30586-98.
54. Tobet S, Chickering T, Hanna I, Crandall J, Schwarting G. Can Gonadal Steroids Influence Cell Position in the Developing Brain? *Horm Behav.* 1994;28:320-327.
55. Tobet S, Hanna I, Schwarting GA. Migration of neurons containing gonadotropin

- releasing hormone (GnRH) in slices from embryonic nasal compartment and forebrain. *Dev Brain Res.* 1996;97(2):287-292.
56. Anderson S, Qiu M, Bulfone A, et al. Mutations of the Homeobox Genes Dlx-1 and Dlx-2 Disrupt the Striatal Subventricular Zone and Differentiation of Late Born Striatal Neurons. *Neuron.* 1997;19:27-37.
 57. Fueshko S, Wray S. LHRH cells migrate on peripherin fibers in embryonic olfactory explant cultures: an in vitro model for neurophilic neuronal migration. *Dev Biol.* 1994;166(1):331-348.
 58. Bless EP, Westaway AW, Schwarting GA, Tobet SA. Effects of γ -Aminobutyric AcidA Receptor Manipulation on Migrating Gonadotropin-Releasing Hormone Neurons through the Entire Migratory Route in Vivo and in Vitro*. *Endocrinology.* 2000;141(3):1254-1262.
 59. Bless EP, Walker HJ, Yu KW, et al. Live view of gonadotropin-releasing hormone containing neuron migration. *Endocrinology.* 2005;146(1):463-468.
 60. Fang ZQ, Xiong XY, James A, Gordon DF, Wierman ME. Identification of novel factors that regulate GnRH gene expression and neuronal migration. *Endocrinology.* 1998;139(8):3654-3657.
 61. Chalfie M, Tu Y, Euskirchen G, Ward WW, Prasher DC. Green Fluorescent Protein as a Marker for Gene-Expression. *Science.* 1994;263(5148):802-805.
 62. Tsien RY. The green fluorescent protein. *Annu Rev Biochem.* 1998;67:509-544.
 63. Feng G, Mellor R, Bernstein M, et al. Imaging Neuronal Subsets in Transgenic Mice Expressing Multiple Spectral Variants of GFP. *Neuron.* 2000;28(1):41-51.
 64. Suter KJ, Song WJ, Sampson TL, et al. Genetic targeting of green fluorescent protein to gonadotropin-releasing hormone neurons: characterization of whole-cell electrophysiological properties and morphology. *Endocrinology.* 2000;141(1):412-

- 419.
65. Henderson RG, Brown AE, Tobet SA. Sex Differences in Cell Migration in the Preoptic Area / Anterior Hypothalamus of Mice. *Dev Neurobiol.* 1999;41(2):252-266.
 66. Knoll JG, Wolfe CA, Tobet SA. Estrogen modulates neuronal movements within the developing preoptic area-anterior hypothalamus. *Eur J Neurosci.* 2007;26(5):1091-1099.
 67. Dellovade TL, Davis AM, Ferguson C, Sieghart W, Homanics GE, Tobet SA. GABA influences the development of the ventromedial nucleus of the hypothalamus. *J Neurobiol.* 2001;49(4):264-276.
 68. Davis AM, Henion TR, Tobet SA. Gamma-Aminobutyric Acid B Receptors and the Development of the Ventromedial Nucleus of the Hypothalamus. *J Comp Neurol.* 2002;449:270-280.
 69. McClellan KM, Calver AR, Tobet SA. GABAB receptors role in cell migration and positioning within the ventromedial nucleus of the hypothalamus. *Neuroscience.* 2008;151(4):1119-1131.
 70. Stratton MS, Staros M, Budefeld T, et al. Embryonic GABA(B) receptor blockade alters cell migration, adult hypothalamic structure, and anxiety- and depression-like behaviors sex specifically in mice. *PLoS one.* 2014;9(8):e106015.
 71. Tobet SA, Walker HJ, Seney ML, Yu KW. Viewing cell movements in the developing neuroendocrine brain. *Integr Comp Biol.* 2003;43(6):794-801.
 72. Hudson AE. Genetic Reporters of Neuronal Activity: c-Fos and G-CaMP6. *Methods Enzymol.* 2018; 603:197-220.
 73. Barth AL. Visualizing circuits and systems using transgenic reporters of neural activity. *Curr Opin Neurobiol.* 2007; 17(5): 567-71.

74. Jasoni CL, Todman MG, Strumia MM, Herbison AE. Cell type-specific expression of a genetically encoded calcium indicator reveals intrinsic calcium oscillations in adult gonadotropin-releasing hormone neurons. *J Neurosci.* 2007; 27(4): 860-7.
75. Pelletier G, Bornstein M. Effect of colchicine on rat anterior pituitary gland in tissue culture. *Exptl Cell Res.* 1971;70:221-223.
76. Bornstein M, Pelletier G, Stern J. A light and electron microscopic study of rat anterior pituitary in organotypic tissue culture. *Brain Res.* 1972;40(2):489-495.
77. Loughlin JS, Badger TM, Crowley WF. Perfused pituitary cultures : a model for LHRH regulation of LH secretion. *American Journal of Physiology Endocrinol Metab.* 1981;240:E591-E596.
78. Waring DW, Turgeon JL. Luteinizing Hormone-Releasing Hormone-Induced Luteinizing Hormone Secretion in Vitro: Cyclic Changes in Responsiveness and Self-Priming*. *Endocrinology.* 1980;106(5):1430-1436.
79. Guerineau NC, McKinney RA, Debanne D, Mollard P, Gahwiler BH. Organotypic cultures of the rat anterior pituitary: morphology, physiology and cell-to-cell communication. *J Neurosci Methods.* 1997;73(2):169-176.
80. Navratil AM, Knoll JG, Whitesell JD, Tobet SA, Clay CM. Neuroendocrine plasticity in the anterior pituitary: gonadotropin-releasing hormone-mediated movement in vitro and in vivo. *Endocrinology.* 2007;148(4):1736-1744.
81. Alim Z, Hartshorn C, Mai O, et al. Gonadotrope plasticity at cellular and population levels. *Endocrinology.* 2012;153(10):4729-4739.
82. Hechter O, Jacobsen R, Schenker V, Levy H, Jeanloz R, Marshall C, Pincus G. Chemical Transformation of Steroids by Adrenal Perfusion: Perfusion Methods. *Endocrinology.* 1953;52:679-91.
83. Manuelidis L. The effects of dbcAMP on adrenal chromaffin cells in organotypic

- culture. *J Neurocytol.* 1976;5:1-10.
84. Petrovic J, Walsh PL, Thornley KT, Miller CE, Wightman RM. Real-time monitoring of chemical transmission in slices of the murine adrenal gland. *Endocrinology.* 2010;151(4):1773-1783.
85. Barbara JG, Poncer JC, McKinney RA, Takeda K. An adrenal slice preparation for the study of chromaffin cells and their cholinergic innervation. *J Neurosci Methods.* 1998;80(2):181-189.
86. Wydallis JB, Feeny RM, Wilson W, et al. Spatiotemporal norepinephrine mapping using a high-density CMOS microelectrode array. *Lab Chip.* 2015;15(20):4075-4082.
87. Tedjo W, Nejad JE, Feeny R, et al. Electrochemical biosensor system using a CMOS microelectrode array provides high spatially and temporally resolved images. *Biosens Bioelectron.* 2018;114:78-88.
88. De Nardi F, Lefort C, Breard D, Richomme P, Legros C, Guerineau NC. Monitoring the Secretory Behavior of the Rat Adrenal Medulla by High-Performance Liquid Chromatography-Based Catecholamine Assay from Slice Supernatants. *Front Endocrinol (Lausanne).* 2017;8:248.
89. Euler Uv, Gaddum J. An Unidentified Depressor Substance in Certain Tissue Extracts. *J Physiol.* 1931;72(1):74-87.
90. Dale H, Feldberg W. The Chemical Transmitter of Vagus Effects to the Stomach. 1934:320-334.
91. Trier JS. Organ-culture methods in the study of gastrointestinal-mucosal function and development. *N Engl J Med.* 1976;295(3):150-155.
92. Senior PV PC, Sunter JP, Appleton DR, Watson AJ. Crypt regeneration in adult human colonic mucosa during prolonged organ culture. *J Anat.* 1982;134(3):459-469.

93. Autrup H, Barrett L, Jackson F, et al. Explant Culture of Human Colon. *Gastroenterology*. 1978;74:1248-1257.
94. Senior PV, Sunter JP, Appleton DR, Watson AJ. Morphological studies on the long-term organ culture of colonic mucosa from normal and dimethylhydrazine treated rats. *Br J Cancer*. 1984;49(3):281-290.
95. Finney K, Ince P, Appleton DR, Sunter JP, Watson A. A comparison of crypt-cell proliferation in rat colonic mucosa in vivo and in vitro. *J Anat*. 1986;149:177-188.
96. Garner CD, Antonopoulos DA, Wagner B, et al. Perturbation of the small intestine microbial ecology by streptomycin alters pathology in a *Salmonella enterica* serovar typhimurium murine model of infection. *Infect Immun*. 2009;77(7):2691-2702.
97. Schwerdtfeger LA, Ryan EP, Tobet SA. An organotypic slice model for ex vivo study of neural, immune, and microbial interactions of mouse intestine. *Am J Physiol Gastrointest Liver Physiol*. 2016;310(4):G240-248.
98. Khoshdel A, Verdu EF, Kunze W, McLean P, Bergonzelli G, Huizinga JD. *Bifidobacterium longum* NCC3001 inhibits AH neuron excitability. *Neurogastroenterol Motil*. 2013;25(7):478-484.
99. May S, Evans S, Parry L. Organoids, organs-on-chips and other systems, and microbiota. *Emerging Top Life Sci*. 2017;1(4):385-400.
100. de Kanter R, Tuin A, van de Kerkhof E, et al. A new technique for preparing precision-cut slices from small intestine and colon for drug biotransformation studies. *J Pharmacol Toxicol Methods*. 2005;51(1):65-72.
101. de Graaf IA, Olinga P, de Jager MH, et al. Preparation and incubation of precision-cut liver and intestinal slices for application in drug metabolism and toxicity studies. *Nat Protoc*. 2010;5(9):1540-1551.
102. Li M, de Graaf IA, Groothuis GM. Precision-cut intestinal slices: alternative model for

- drug transport, metabolism, and toxicology research. *Expert Opin Drug Metab Toxicol.* 2016;12(2):175-190.
103. Ahlman H, Nilsson O. The gut as the largest endocrine organ in the body. *Annals of Oncology.* 2001;12:S63-S68.
 104. Furness JB, Costa M. *The Enteric Nervous System.* Glasgow: Churchill Livingstone; 1987. 290 p.
 105. De Vadder F, Plessier F, Gautier-Stein A, Mithieux G. Vasoactive intestinal peptide is a local mediator in a gut-brain neural axis activating intestinal gluconeogenesis. *Neurogastroenterol Motil.* 2015;27(3):443-448.
 106. Gershon MD. 5-Hydroxytryptamine (serotonin) in the gastrointestinal tract. *Curr Opin Endocrinol Diabetes Obes.* 2013;20(1):14-21.
 107. Gershon MD, Sherman D, Dreyfus C. Effects of Indolic Neurotoxins on Enteric Serotonergic Neurons. *J Comp Neurol.* 1980;190:581-592.
 108. Costa M, Furness JB, Cuello AC, Verhofstad AJ, Steinbusch HWJ, Elde RP. Neurons with 5-Hydroxytryptamine-Like Immunoreactivity in the Enteric Nervous System: Their Visualization and Reactions to Drug Treatment. *Neuroscience.* 1982;7(2):351-363.
 109. Dreyfus CF, Sherman DL, Gershon MD. Uptake of serotonin by intrinsic neurons of the myenteric plexus grown in organotypic tissue culture. *Brain Res.* 1977;128(1):109-123.
 110. North RA, Williams JT. Enkephalin inhibits firing of myenteric neurones. *Nature.* 1976;264(5585):460-461.
 111. Brookes SJH, Costa M. Identification of Enteric Motor Neurons Which Innervate the Circular Muscle of the Guinea-Pig Small-Intestine. *Neurosci Lett.* 1990;118(2):227-230.

112. Brookes SJH, Song ZM, Steele PA, Costa M. Identification of Motor Neurons to the Longitudinal Muscle of the Guinea-Pig Ileum. *Gastroenterology*. 1992;103(3):961-973.
113. Porter AJ, Wattchow DA, Brookes SJH, Costa M. Cholinergic and nitrenergic interneurons in the myenteric plexus of the human colon. *Gut*. 2002;51(1):70-75.
114. Ng SC, Shi HY, Hamidi N, et al. Worldwide incidence and prevalence of inflammatory bowel disease in the 21st century: a systematic review of population-based studies. *The Lancet*. 2017;390(10114):2769-2778.
115. Kim HJ, Li H, Collins JJ, Ingber DE, Beebe DJ, Ismagilov RF. Contributions of microbiome and mechanical deformation to intestinal bacterial overgrowth and inflammation in a human gut-on-a-chip. *Proc Natl Acad Sci U S A*. 2015;113(1):E7-E15.
116. Shah P, Fritz JV, Glaab E, et al. A microfluidics-based in vitro model of the gastrointestinal human-microbe interface. *Nat Commun*. 2016;7:11535.
117. Sambuy Y, Angelis I, Ranaldi G, Scarino ML, Stammati A, Zucco F. The Caco-2 cell line as a model of the intestinal barrier: influence of cell and culture-related factors on Caco-2 cell functional characteristics. *Cell Biol Toxicol*. 2005; 21(1): 1-26.
118. Bohorquez DV, Shahid RA, Erdmann A, et al. Neuroepithelial circuit formed by innervation of sensory enteroendocrine cells. *J Clin Invest*. 2015;125(2):782-786.
119. Bohorquez DV, Samsa LA, Roholt A, Medicetty S, Chandra R, Liddle RA. An enteroendocrine cell-enteric glia connection revealed by 3D electron microscopy. *PloS one*. 2014;9(2):e89881.
120. McLean IC, Schwerdtfeger LA, Tobet SA, Henry CS. Powering ex vivo tissue models in microfluidic systems. *Lab Chip*. 2018;18(10):1399-1410.
121. Kilic O, Pamies D, Lavell E, et al. Brain-on-a-chip model enables analysis of human

- neuronal differentiation and chemotaxis. *Lab Chip*. 2016;16(21):4152-4162.
122. Huang Y, Williams JC, Johnson SM. Brain slice on a chip: opportunities and challenges of applying microfluidic technology to intact tissues. *Lab Chip*. 2012;12(12):2103-2117.
123. Yissachar N, Zhou Y, Ung L, et al. An Intestinal Organ Culture System Uncovers a Role for the Nervous System in Microbe-Immune Crosstalk. *Cell*. 2017;168(6):1135-1148 e1112.
124. Xu H, Li Z, Yu Y, et al. A dynamic in vivo-like organotypic blood-brain barrier model to probe metastatic brain tumors. *Sci Rep*. 2016;6:36670-36670.
125. Park J, Lee BK, Jeong GS, Hyun JK, Lee CJ, Lee SH. Three-dimensional brain-on-a-chip with an interstitial level of flow and its application as an in vitro model of Alzheimer's disease. *Lab Chip*. 2015;15(1):141-150.
126. Queval A, Ghattamaneni NR, Perrault CM, et al. Chamber and microfluidic probe for microperfusion of organotypic brain slices. *Lab Chip*. 2010;10(3):326-334.
127. Xiao S, Coppeta JR, Rogers HB, et al. A microfluidic culture model of the human reproductive tract and 28-day menstrual cycle. *Nat Commun*. 2017;8:14584.
128. Wang YI, Carmona C, Hickman JJ, Shuler ML. Multiorgan Microphysiological Systems for Drug Development: Strategies, Advances, and Challenges. *Adv Healthc Mater*. 2018;7(2):1-29.
129. Mulder G, Vermes I, Smelik P. A Combined Cell Column Superfusion Technique to Study Hypothalamus-Pituitary-Adrenal Interactions In Vitro. *Neurosci Lett*. 1976;2:73-78.
130. Shuler ML. Organ-, body- and disease-on-a-chip systems. *Lab Chip*. 2017;17(14):2345-2346.
131. van Midwoud PM, Merema MT, Verpoorte E, Groothuis GMM. A microfluidic

- approach for in vitro assessment of interorgan interactions in drug metabolism using intestinal and liver slices. *Lab Chip*. 2010;10(20):2778-2786.
132. Verneti L, Gough A, Baetz N, et al. Functional Coupling of Human Microphysiology Systems : Intestine , Liver , Kidney Proximal Tubule , Blood-Brain Barrier and Skeletal Muscle. *Sci Rep*. 2017;7:1-15.

CHAPTER 2 – DESIGNING MULTICELLULAR INTESITNAL SYSTEMS²

Overview:

The mammalian intestinal wall is one of the most complex organs in the body. A collection of heterogeneous cell types including immune, neural, and epithelial, among others, creates a complex physiology that is difficult to simulate outside of the body, *in vitro*. Methodologies for studying the intestinal wall *in vitro*, range from cultured monolayers of immortalized cells, to more complex co-cultures with multiple cell types and a third dimension, to those that use explants of actual gut tissues with more realistic three dimensions. The majority of current *in vitro* culture systems, fail to capture the richness of the physiology of the gut *in vivo*. However, cutting-edge engineering technologies open a window for novel approaches, using microfluidics to provide opportunities for new generations of organotypic methods with large potential. As intestinal disease rates rise globally, the need for reliable and heuristic methods for studying intestinal physiology outside of the body is apparent. This chapter presents current systems available for studying gut physiology *in vitro*, and then shifts to focus on physiological prescriptions for future needs of *ex vivo* gut cultures. A framework of biological specifications is provided, that may help engineer devices and culture systems, that more faithfully capture the *in vivo* physiology of the *ex vivo* gut wall.

Introduction:

Modern organotypic methods for maintaining human colon outside of the body, *in vitro*, emerged in the 1970s¹. A number of the early *in vitro* intestinal studies were performed using colon explants², enteric nervous system explants³, or gut musculature cultures⁴. Some of these early explant systems housed the full cellular diversity of the *in vivo* intestinal mucosa, however,

² Schwerdtfeger LA & Tobet SA. Multicellular *in vitro* organ systems. In Precision Medicine for Investigators, Practitioners and Providers, ed., J Faintuch and S Faintauch, Elsevier Publishing, Nov. 16th, 2019.

were rarely maintained beyond 72 h². While some studies cultured explants for 20 days or more¹, the details of tissue health were minimal. The use of large quantities of serum (e.g., fetal bovine serum) and antibiotics in culture media, is a persistent problem in intestinal *in vitro* systems, due to the variability of serum across sources, and the impacts of antibiotic treatment on the intestinal microbiome. Early explant systems are likely to have included some complement of microbiota, however, bacterial load or diversity were not analyzed.

Cancer cells:

Moving away from organotypic systems during the later part of the 20th century, immortalized cell lines (e.g., Caco-2 cells) became common, in studies of intestinal physiology. Caco-2 cells were originally derived from colorectal adenocarcinoma from a 72-year-old male⁵, and have been used to study a variety of topics, ranging from gut epithelial barrier permeability⁶ to applications in drug discovery⁷. Another line, HT-29 cells, was derived from colorectal adenocarcinoma from a 44-year-old female (ATCC). These cells display different characteristics, such as mucin secretory competence in a small portion of cells⁸. It is worth noting that a host of other immortalized cell lines, have been employed as models of mammalian intestines *in vitro*. However most of these cell lines, including Caco-2 and HT-29, suffer a problem of “passage number”, which is created when phenotypes change, based on the number of cell divisions and the development of subclones⁹.

Stem cells:

Development of organoid systems using induced pluripotent stem cells¹⁰, or patient isolated progenitors¹¹, has resulted in a powerful tool for studying intestinal epithelial cell biology, in a 3-D structured system not previously attainable with immortalized cell cultures. These systems, however, fail to capture the unique physiology of the intestinal wall *ex vivo*,

because the cells either de-differentiate at some point to less than normal function, or they lack sufficient cellular diversity even when they re-differentiate. The ability to answer questions regarding cell-cell interactions is limited by the absence of neural, immune and microbial components, relative to the original tissue.

Gut slices:

Organotypic slice models provide an alternative to cell cultures or organoids, for capturing the complex cellular heterogeneity and microbial presence of the *in vivo* gut wall, yet *in vitro*. Precision cut intestinal slices¹² (PCIS) represented an early use of an organotypic slice model, for study of the intestinal capacity for metabolizing drugs¹³. PCIS models were unfortunately only viable in the first ~24 h of culture. Longer maintenance of mouse intestinal tissues *ex vivo*, was achieved with a similar protocol to one used previously in brain¹⁴. This procedure allowed the maintenance of 250 µm thick slices, in serum and antibiotic free media, for up to 6 days *ex vivo*¹⁵, and provided for the study of antibiotic effects on intestinal segmental contraction rates.

While the rate of segmental contraction *ex vivo* was representative of *in vivo* behavior, maintenance of organotypic slices beyond 48 h required the use of calcium ion channel blockers (e.g., nifedipine), to prevent long-term muscular contractions that otherwise damaged epithelia¹⁵. Advances in organotypic slice technology provide for maintenance of epithelial populations, neuronal and glial cells, immune responses to pathogen, and a subset of the native microbiome *ex vivo*¹⁵. Although organotypic methods maintain more cellular diversity than many *in vitro* systems, there are other issues that would be helpful to address. Principally, there is a steep oxygen gradient across the intestinal wall¹⁶, one not reproduced in organotypic slice models, cell line cultures, or organoids. This gradient has a major impact on gut physiology, in the intestinal wall, and on luminal microbiome.

Gut Physiological Specifications:

General Considerations:

Evolution has provided a number of barrier tissues within mammals, that protect components of one compartment from the potential dangers of external environments. The function of such barriers is essential to maintaining healthy states, with an increasing number of gastrointestinal disorders attributed to barrier failures^{17,18}. Barrier tissues automatically define multiple environments, “external” and “internal” to epithelial monolayers, which also have multiple constituent components (Figure 3). This chapter focuses on mammalian intestines where the external space is the lumen, including microbial components, the epithelial lining includes multiple cell types and associated extended mucus layers, and the internal component is the tissue comprised of diverse cellular elements, that include neural and immune cells. There are cellular interactions within each compartment, and significant molecular signaling between compartments. Mechanistic understanding of the interplay between the diverse cell types that form such a multi-compartmental barrier structure is essential for developing treatments for barrier disorders. (Figure 3)

Reconstituting the complex physiology of the intestinal wall *ex vivo* is a tall order. With no fewer than 15 cell types, a complex microbiome, a functional nervous system, and the body’s largest immune system, the intestinal wall is one of the largest and most heterogeneous organs in any mammalian organism

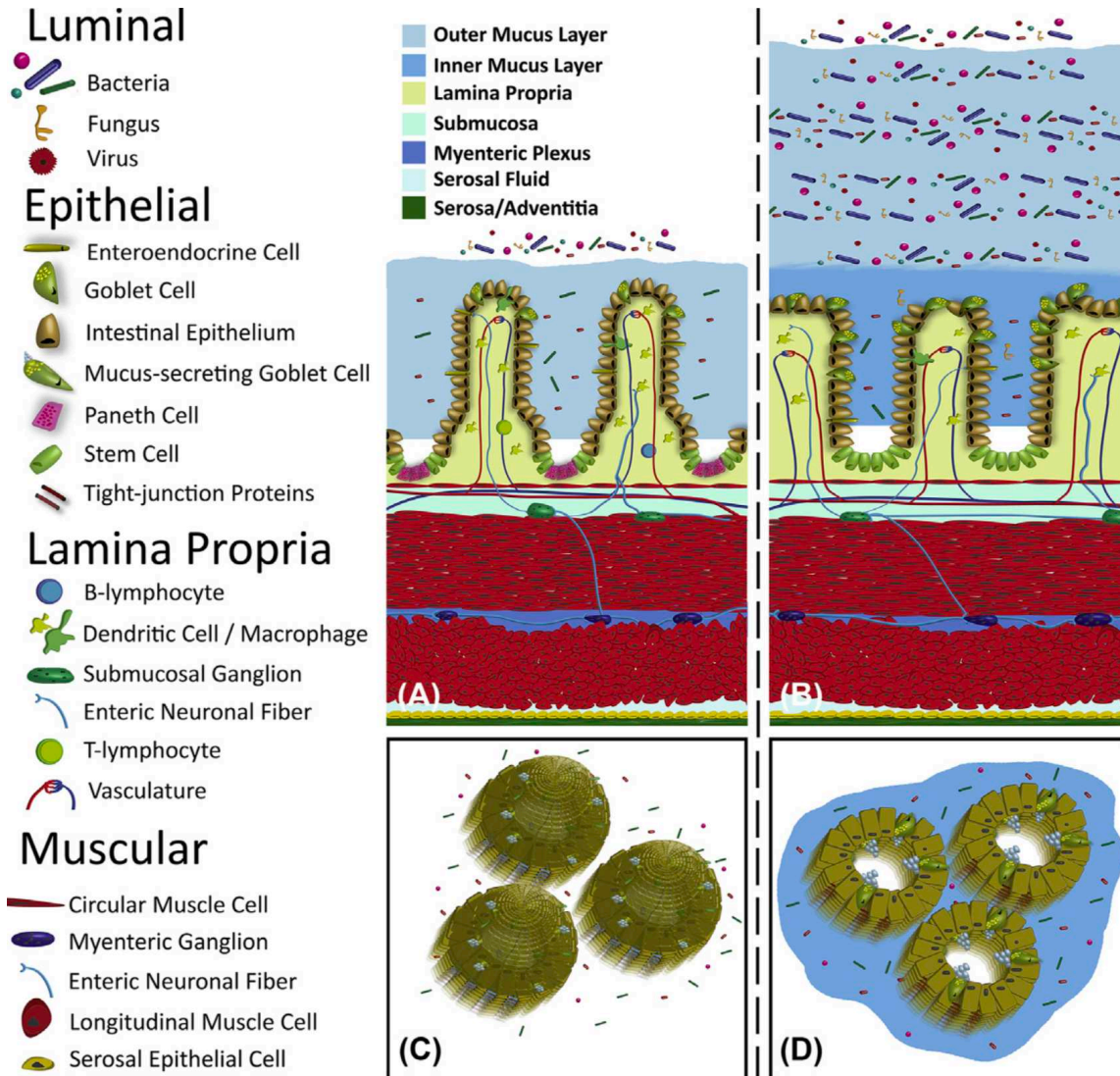


Figure 3: Schematic diagram illustrating the organization and complexity of the intestinal tripartite barrier system, with some of the extensive cellular heterogeneity. Luminal contents (e.g., microbiota) sit above and inside a mucus layer in the ileum (A), and in outer and inner mucus layers in the colon (B). Diverse epithelial elements comprise a barrier, between gut luminal microbiota and internal *lamina propria* contents. Organization of this barrier varies across the 10 anatomical regions of the gut tract (stomach, duodenum, jejunum, ileum, caecum, ascending colon, transverse colon, descending colon, sigmoid colon and rectum), however, a crypt-villus axis in the small intestine (e.g., ileum; A), and crypts in the colon (B) predominate. Internal to the *lamina propria*, two neuronal plexuses are visible. First, the submucosal plexus sits upon a circular smooth muscle layer. Second, the myenteric plexus is housed between circular and longitudinal smooth muscle layers. Finally, a layer of serosal fluid generated by serosal epithelium, is visualized between the longitudinal musculature and a layer of adventitia composed of connective tissue. Schematics of the view looking inward from the lumen of both the ileum (C) and colon (D), demonstrate the varied organization of the apical epithelium. Cellular representations are keyed on the left, organized by barrier compartment (e.g., luminal, epithelial, *lamina propria*, muscular), and color codes for each region are provided.

(Figure 3). *In vitro* systems frequently take one of two divergent paths, toward modeling *in vivo* physiology. One is to create reductionist systems, that allow the dissection of unique roles of individual component parts. The other is to recreate the complexity of the organ *in vitro*, allowing control of the system, with responses to perturbation being potentially more accurate indicators of *in vivo* function.

There are pros and cons to both paths. On the former, component parts function differently alone than when together. For the latter, *ex vivo* methods only offer an approximation of *in vivo* physiology. It is a premise of this chapter that the latter has been overlooked in much of intestinal research, and yet provides an important component with translational potential. Distilling the complex physiology of the intestinal wall into three ‘compartments’, namely luminal, epithelial, and tissue (Figure 3), with individualized specifications for each, aids in guiding the design of more physiologically relevant culture systems.

Luminal:

The contents of the intestinal lumen vary depending upon diet, gut segment, and local composition of microbiota. Home to thousands of species of bacteria, fungi, and archaea¹⁹, the gut lumen is a complex environment. Understanding the inter-species interactions, quorum signaling, and secretions from these microorganisms, is an ongoing investigation for microbiology. Secretory products from luminal microbiota influence tissue physiology, and a growing number of functional pathways have been recently shown, including direct metabolite – cell surface receptor signaling²⁰.

Many bacterial metabolite – host signaling pathways are still unknown. Environmental factors such as antibiotic treatment²¹ and oxygen culture condition²², influence the production of microbially derived metabolites. Designing culture methodologies that incorporate the native microbiome of the organism of interest, is an important target to advance understanding of

bacterial – host signaling mechanisms. Spiking monolayer cell cultures with specific bacteria to mimic a ‘microbiome’ , has been done in microfluidic devices^{23,24}. However, given that only a small percentage of the native gut flora can be cultured under the conditions of most microfluidic devices, it is difficult to consider these models reflective of microbiomes *in vivo*.

Culture methods that maintain explant tissues directly from donors, have potential to maintain larger subsets of the native microbiota, due to their presence in the lumen of the organ providing explants. Key design specifications for the luminal compartment can be thought of in two ways, that perhaps match the way the microbial community is naturally organized. From one perspective, a defined microbiome could be “selected”, as an engineered blend of anaerobic, facultative, and aerobic microbes. Alternatively, creating conditions that result in a specific metabolomic profile could influence microbial composition, as there are many ways to get to the same metabolic profile. In both cases, the *in vitro* luminal environment will be an end result of the initial conditions: source of microbial components and substrates for microbial energy utilization (e.g., glucose, oxygen, etc.), and bacterial survival skills (e.g., microbial interactions).

Epithelial:

Epithelial cells of the mammalian intestine constitute a critical barrier, between the luminal contents and gut tissue, and are an aspect of the intestine that has drawn significant attention for *in vitro* modeling. Separating the lumen from gut epithelia is a secreted layer of mucus that serves dual roles, as a pathogen barrier and as a source of nutrients for luminal microbiota. Goblet cells in the intestinal epithelial layer secrete large quantities of mucins, principally Muc2 in the intestine, with small quantities of other mucins (e.g., Muc5ac). These mucins provide protein cores for chains of O-linked glycans, that are comprised of varied

structures (e.g., galactose/galactosamine base, with variable inclusion of fucose or sialic acid) that also vary by gut region and across species²⁵.

Beneath this mucus layer, apical epithelia form a barrier that is interlinked with tight junction-associated proteins, such as ZO-1 (zona occludins) and claudins²⁶. Molecular regulation of tight junctions is complex and has been reviewed elsewhere²⁷. Interspersed among the epithelia are mucus secreting goblet cells, defensin secreting Paneth cells, and hormone producing enteroendocrine cells, among others, all derived from crypt Lgr5⁺ stem cell populations. These stem cells are supported by mesenchymal cells, and surrounded by soluble factors and extracellular matrix²⁸. Mesenchymal regulation of this stem cell niche may be important *in vivo*, or in response to tissue injury²⁹, however, it is not required to generate crypt-villus axes *in vitro*³⁰.

Communication between luminal contents (i.e., bacterial components) and epithelial cells has been demonstrated, often involving the toll-like receptor family members³¹. Apical surfaces of at least one type of barrier cell (i.e., tuft cells), have been shown to possess receptors, and bind specific microbial secreted metabolites³². Nonetheless, specific bacteria – metabolite – tissue receptor signaling mechanisms are still poorly understood. Epithelial cells also communicate directly with cells in the tissue compartment, via dendritic cell – epithelial interactions³³, enteric neurons via gut neuro-epithelial circuits³⁴, and enteric glia that lie beneath the epithelial layer³⁵.

Key design specifications for the barrier epithelial compartment, should not only account for the cellular diversity of the epithelial monolayer, with the extended mucus layer, but also for cells that regularly traffic in, out, or through the layer. Intraepithelial lymphocytes (IELs) are a subset of T-lymphocytes, that possess the unique ability to both present antigen and act as natural killer T-cells³⁶. IELs have been shown to move in and out of the epithelial layer in response to pathogens; a characteristic that was recently described as epithelial ‘flossing’³⁷.

While flossing between epithelial cells is not unique to IELs, as lamina propria dendritic cells act similarly³⁸, the speed of their movements (~6-7 μ m/min³⁹) is astounding. Additionally, phenotypically distinct IELs inhabit the small intestine compared to the colon, and can regulate colonic barrier integrity⁴⁰. Finally, design considerations for the epithelial compartment should also be able to account for relevant signaling molecules, that are secreted both cellularly and via mucus inhabiting microbiota.

Tissue:

Interspersed throughout the mucosa, the *lamina propria* is comprised of diverse immune cell populations, neuronal and glial cells and projections, significant extracellular matrix, and vascular and lymph networks (Figure 3). Due to the complex anatomical arrangement of *lamina propria*, which penetrates into the cores of small intestinal villi, and surrounds colonic crypts, engineering cellular components to mimic this unique epithelial – *lamina propria* arrangement is difficult, and may require different designs depending upon gut region of interest (e.g., small versus large intestine).

For example, gut associated lymphoid tissue is distributed differently in the ileum (Peyer's patches), versus the colon where they appear in smaller isolated lymphoid follicles. Interactions between barrier cells and tissue/lamina propria, via neural – epithelial signaling³⁴ are apparent. Tissue components also possess the ability to directly interact with the luminal contents. This is accomplished via multiple routes; first, as noted in the previous paragraph for both dendritic cells and IELs. Second, tuft cells can sense luminal metabolites such as succinate³², activating type 2 mucosal immune responses⁴¹. Additionally, invasive bacteria have been shown to directly signal, to sensory nerve endings in the *lamina propria*⁴².

Many intestinal models have focused on building systems, from the simplest state of mostly single cell type monolayers, and even those derived from Lgr5⁺ epithelial progenitors do

not include the diverse *lamina propria* and submucosal cell populations seen *in vivo* (e.g., neural, immune, vascular). Organotypic slice methods maintain the neural, immune and epithelial components of the tissue¹⁵. However, depending on the orientation of the slice preparation (e.g., perpendicular to the wall or other), there may be more or less potential to mimic the full “barrier function” of the intestinal wall. Key design specifications for the tissue compartment, should include as many of the diverse *lamina propria* and submucosal cell populations *in vitro* as possible.

Cell-cell and microorganism-cell signaling:

Signaling between intestinal neural components and microbial, epithelial, and immune cells are important areas for ongoing investigations. In the apical epithelium, direct synapses between a subset of enteroendocrine cells and neurons – both vagus and enteric in origin – have been shown anatomically³⁵ and functionally, with glutamate release from enteroendocrine cells stimulating nodose ganglion vagal afferents⁴³. Innervation of other epithelial cell types has been observed, with tuft cells directly contacting enteric sensory neurons⁴⁴. Moving inward from the apical epithelia, numerous components of the *lamina propria* and musculature regularly signal with enteric or vagal neurons.

Mast cells in the *lamina propria* have been shown to be in contact with both enteric and vagal neurons⁴⁵, and signal bi-directionally with these cells⁴⁶. In the intestinal muscle layers, *muscularis* macrophages are also in contact with vagal afferents⁴⁷, and are activated in response to enteric sympathetic neuron signaling during bacterial infection⁴⁸. *Lamina propria* dendritic cell and IEL interactions with vagal or enteric sensory neurons, is a yet unexplored area of investigation that will be necessary to fill in .

Compartmental environment problems:

In the case of oxygen concentration, the intestinal wall presents an extreme situation, in that it maintains a steep oxygen gradient *in vivo*⁴⁹. The gradient spans 0.1-1% in the luminal compartment, to 5-10% oxygen in the heavily vascularized submucosa and musculature layers⁵⁰. Without an ability to mimic the anaerobic-aerobic interface *in vitro*, the non-physiologic oxygen concentrations of many preparations, will likely lead to both cellular and microbial signaling among the components of the gut wall, that will fall short of modeling *in vivo* physiology.

Culturing organotypic slices in a static, fixed oxygen incubator, creates a non-physiologic oxygen environment that can influence tissue metabolism (Schwerdtfeger and Tobet, personal observation), and significantly impact the gut microbiome⁵¹. Similarly, nutrient provisions in the tissue compartment come from the arterial supply (e.g., glucose), whereas in the luminal compartment food consumption and metabolism play larger roles. Engineering a model that recreates differential environments will require differential flow across tissues, in a multi-channel microfluidic system.

Designing New Organotypic Systems:

Harnessing the power of advancing engineering technologies like microfluidics, allows for development of culture methods that incorporate media flow, making more accurate modeling of *in vivo* physiology possible. Current microfluidic systems provide a technical foundation for culturing intestinal cell lines and tissues, with continuously perfused media/nutrients, and clearance of waste products. Engineering advances of microfluidic culture systems have recently been reviewed^{52,53,54}. These technologies have been used for culture of liver⁵⁵ and intestine⁵⁶ among others. Their use in tissues like the intestine, however, need to better account for the compartmental requirements unique to barrier tissues.

Recently, microfluidic technology was used for culture of mouse intestinal explants, and was able to show a direct bacterial – immune – neuronal signaling event *ex vivo*⁵⁷, providing evidence of the importance of maintaining cellular heterogeneity of the intestinal wall *in vitro*. While this model advanced the microfluidic gut-on-chip paradigm, it required the use of 95% oxygen, which would have likely altered the explanted microbiome.

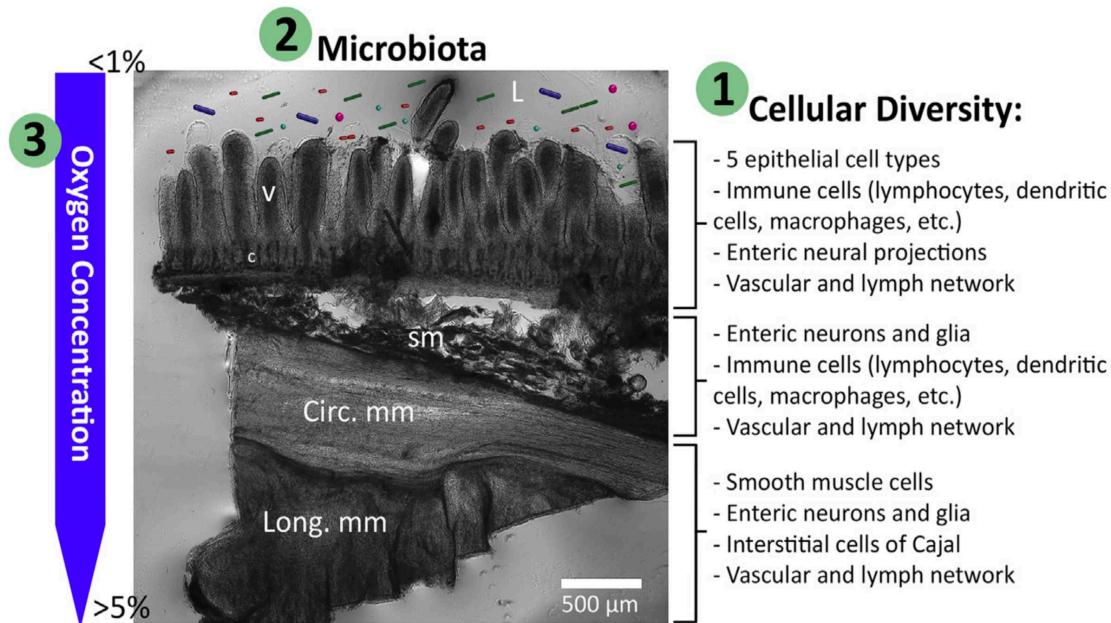


Figure 4: Graphical outline of three key components of intestinal tissues, superimposed on an image of a section of human gut wall (jejunum), that should be appreciated in designing next generation organotypic culture systems, to improve physiologic relevance. 'L' signifies lumen, 'V' a villus, 'c' a crypt, 'sm' submucosa, 'Circ. mm' the circular muscle layer, 'Long. mm' the longitudinal muscle layer. Scale bar is 500 μ m.

Furthermore, this method was only performed using juvenile (12-14 days old) mice, and had a limited survival time of 24 h. Given that the prepubertal gut wall is significantly different than after puberty, in terms of microbiome and immune system⁵⁸, there are many unanswered questions concerning the utility of this early system.

The thickness of the intestinal wall creates an inherent problem of nutrient and oxygen penetration. Human intestinal tissue is far thicker than cell monolayers and even organoids (Figure 4), increasing to ~3 mm in the small intestine (Figure 5), and significantly thicker in the

colon). Such tissue thicknesses require novel approaches to maintain tissue in a healthy state, due to oxygen and nutrient penetration into the gut wall.

Oxygen consumption by colonic epithelia, driven by oxidation of fatty acids such as butyrate, drives environmental oxygen down in the lumen, creating an ideal environment for anaerobic microbes⁵⁹. Given the influence of oxygen conditions on intestinal microbiome^{51,60}, bacterial metabolism⁶¹, and secretions²², recreating the anaerobic – aerobic interface in novel culture methods is of paramount importance, if the system is to faithfully mimic *in vivo* colonocyte metabolism. Many standard culture conditions (e.g., antibiotic use) alter the gut microbiome, which in turn alters microbially derived metabolites, that are key regulators

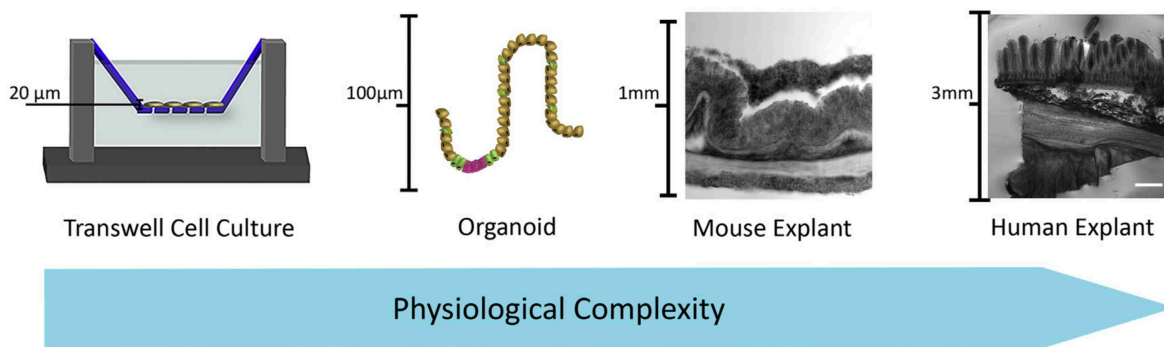


Figure 5: Schematic illustrating the progression in physiological complexity , across different intestinal culture systems.

of intestinal function. Additionally, the impact of the mode, rate, and volume of delivery of resources like oxygen and glucose are profound. Media flow rate has been shown to influence tissue metabolism⁶². (Figure 4, Figure 5)

Impact of antibiotics:

Antibiotic use is a standard tissue culture practice, to prevent “infection” of host cultures. Given that dense bacterial communities inhabit every barrier tissue of the mammalian body, understanding barrier function(s) requires understanding microbial-host relationships. For one, microbially derived metabolites are key regulators of intestinal function, and treatment with

antibiotics has been shown to alter the metabolome of rats²¹. Second, gut bacteria are a major source of antimicrobial compounds⁶³, and host cells such as Paneth cells produce large quantities of antimicrobial compounds⁶⁴. These considerations make it difficult to understand host-bacterial signaling when the investigator is adding extra antibiotics. Given the importance of the role of bacterial components in cell signaling and barrier function, exogenous antibiotic use *in vitro* should be either precise, in targeting particular microbial elements, or eliminated.

Conclusions:

The design specifications discussed throughout this chapter, offer a framework to guide development of novel intestinal – and barrier in general – culture methodologies, that faithfully recapitulate *in vivo* physiology. Optimizing design strategies, particularly concerning tissue health validation and microfluidic flow paradigms, is critical to moving forward. It will be beneficial for future model systems, to verify maintenance of components of tissue barriers, and validate their ability to mimic selected aspects of *in vivo* physiology.

References:

- 1) Autrup H, Barrett LA, Jackson FE, Jesudason ML, Stoner G, Phelps P, Trump BF, Harris CC. Explant Culture of Human Colon. *Gastroenterology*. 1978;74:1248-1257.
- 2) Senior PV, Pritchett CJ, Sunter JP, Appleton DR, Watson AJ. Crypt regeneration in adult human colonic mucosa during prolonged organ culture. *J Anat*. 1982;134:3:459-469.
- 3) Jessen KR, Saffrey MJ, Burnstock, G. The Enteric Nervous System in Tissue culture. I. Cell Types and Their Interactions in Explants of the Myenteric and Submucous Plexuses From Guinea Pig, Rabbit and Rat. *Brain Res*. 1983;262: 17-35.
- 4) Brookes SJH, Costa M. Identification of enteric motor neurons which innervate the circular muscle of the guinea pig small intestine. *Neurosci Lett*. 1990;118:227-230.
- 5) Fogh J, Fogh J, and Orfeo T. One hundred and twenty-seven cultured. human tumor cell lines producing tumors in nude mice. *J Natl Cancer Inst*. 1977;59:221-226.
- 6) Hidalgo IJ, Raub TJ, Borchardt RT. Characterization of the human colon carcinoma cell line (Caco-2) as a model system for intestinal epithelial permeability. *Gastroenterology*. 1989;96:736-749.
- 7) Peng Y, Yadava P, Heikkinen AT, Parrott N, Railkar A. Applications of the 7-day Caco-2 model in drug discovery and development. *Eur J Pharm Sci*. 2014;56:120-130.
- 8) Gagnon M, Zihler Berner A, Chervet N, Chassard C, and Lacroix C. Comparison of the Caco-2, HT-29 and the mucus-secreting HT29-MTX intestinal cell models to investigate Salmonella adhesion and invasion. *J Microbiol Methods*. 2013;94: 274-279.
- 9) Sambuy Y, De Angelis I, Ranaldi G, Scarino M, Stamatii A, and Zucco F. The Caco-2 cell line as a model of the intestinal barrier: influence of cell and culture-related factors on Caco-2 cell functional characteristics. *Cell Biol Toxicol*. 2005;21:1-26.
- 10) Rodansky ES, Johnson LA, Huang S, Spence JR, Higgins PDR. Intestinal organoids: A model of intestinal fibrosis for evaluating anti-fibrotic drugs. *Exp Mol Pathol*.

2015;98:346-351.

- 11) Kasendra M, Tovaglieri A, Sontheimer-Phelps A, Jalili-Firoozinezhad S, Bein A, Chalkiadaki A, Scholl W, Zhang C, Rickner H, Richmond CA, Li H, Breault DT, Ingber DE. Development of a primary human Small Intestine-on-a-Chip using biopsy-derived organoids. *Sci Rep*. 2018;8:2871.
- 12) De Kanter R, Tuin A, Van De Kerkhof E, Martignoni M, Draaisma AL, De Jager MH, De Graaf IAM, Meijer DKF, and Groothuis GMM. A new technique for preparing precision-cut slices from small intestine and colon for drug biotransformation studies. *J Pharmacol Toxicol Methods*. 2005;51:65-72.
- 13) De Graaf IAM, Olinga P, de Jager MH, Merema MT, de Kanter R, van de Kerkhof E, Groothuis GMM. Preparation and incubation of precision-cut liver and intestinal slices for application in drug metabolism and toxicity studies. *Nat Protoc*. 2010;5:9:1540-1551.
- 14) Tobet SA, Walker HJ, Seney ML, and Yu KW. Viewing cell movements in the developing neuroendocrine brain. *Integr Comp Biol*. 2003;43:794-801.
- 15) Schwerdtfeger LA, Ryan EP, Tobet SA. An organotypic slice model for ex vivo study of neural, immune, and microbial interactions of mouse intestine. *Am J Physiol Gastrointest Liver Physiol*. 2016;310:G240-G248.
- 16) Zheng L, Kelly CJ, and Colgan SP. Physiologic hypoxia and oxygen homeostasis in the healthy intestine. A Review in the Theme: Cellular Responses to Hypoxia. *Am J Physiol Cell Physiol*. 2015;309:C350-360.
- 17) Arik YB, van der Helm MW, Odijk M, Segerink LI, Passier R, van den Berg A, and van der Meer AD. Barriers-on-chips: Measurement of barrier function of tissues in organs-on-chips. *Biomicrofluidics*. 2018;12:042218.
- 18) Bischoff SC, Barbara G, Buurman W, Ockhuizen T, Schulzke J, Serino M, Tilg H, Watson A, and Wells J. Intestinal permeability - a new target for disease prevention and

- therapy. *BMC Gastroenterol.* 2014;13:25.
- 19) Sekirov I, Russell SL, Antunes LC, and Finlay BB. Gut microbiota in health and disease. *Physiol Rev.* 2010;90:859-904.
- 20) Schneider C, O'Leary CE, von Moltke J, Liang H, Ang QY, Turnbaugh PJ, Radhakrishnan S, Pellizzon M, Ma A, Locksley RM. A Metabolite-Triggered Tuft Cell-ILC2 Circuit Drives Small Intestinal Remodeling. *Cell.* 2018;174:271-284.
- 21) Sun J, Schnackenberg LK, Khare S, Yang X, Greenhaw J, Salminen W, Mendrick DL, Beger RD. Evaluating effects of penicillin treatment on the metabolome of rats. *J Chromatogr B.* 2013;932:134-143.
- 22) Schertzer JW, Brown SA, and Whiteley M. Oxygen levels rapidly modulate *Pseudomonas aeruginosa* social behaviours via substrate limitation of PqsH. *Mol Microbiol.* 2010;77:1527-1538.
- 23) Kim HJ, Li H, Collins JJ, Ingber DE, Beebe DJ, and Ismagilov RF. Contributions of microbiome and mechanical deformation to intestinal bacterial overgrowth and inflammation in a human gut-on-a-chip. *Proc Nat Acad Sci USA.* 2016;113(1):E7-E15.
- 24) Shah P, Fritz JV, Glaab E, Desai MS, Greenhalgh K, Frachet A, Niegowska M, Estes M, Jager C, Seguin-Devaux C, Zenhausem F, and Wilmes P. A microfluidics-based in vitro model of the gastrointestinal human-microbe interface. *Nat Commun.* 2016;7:11535.
- 25) Holmen Larsson JM, Thomsson KA, Rodriguez-Pineiro AM, Karlsson H, and Hansson GC. Studies of mucus in mouse stomach, small intestine, and colon. III. Gastrointestinal Muc5ac and Muc2 mucin O-glycan patterns reveal a regiospecific distribution. *Am J Physiol Gastrointest Liver Physiol.* 2013;305:G357-363.
- 26) Groschwitz KR and Hogan SP. Intestinal barrier function: molecular regulation and disease pathogenesis. *J Allergy Clin Immunol.* 2009;124:3-20.

- 27) Buckley A, Turner JR. Cell Biology of Tight Junction Barrier Regulation and Mucosal Disease. Cold Spring Harb Perspect Biol; 2018.
- 28) Pastula A, Marcinkiewicz J. Cellular Interactions in the Intestinal Stem Cell Niche. Archivum Immunologiae et Therapiae Experimentalis. 2018;Doi:10.1007/s00005-018-0524-8.
- 29) Miyoshi H, Ajima R, Luo CT, Yamaguchi TP, Stappenbeck TS. Wnt5a Potentiates TGF- β Signaling to Promote Colonic Crypt Regeneration After Tissue Injury. Science. 2012;338:108-113.
- 30) Sato T, Vries RG, Snippert HJ, van de Wetering M, Barker N, Stange DE, van Es JH, Abo A, Kujala P, Peters PJ, Clevers H. Single Lgr5 stem cells build crypt-villus structures in vitro without a mesenchymal niche. Nature Letters. 2009;459:262-265.
- 31) Carvalho FA, Aitken JD, Vijay-Kumar M, and Gewirtz AT. Toll-like receptor-gut microbiota interactions: perturb at your own risk! Annu Rev Physiol. 2012;74:177-198.
- 32) Nadjisombati MS, McGinty JW, Lyons-Cohen MR, Jaffe JB, DiPeso L, Schneider C, Miller CN, Pollack JL, Nagana Gowda GA, Fontana MF, Erle DJ, Anderson MS, Locksley RM, Raftery D, and von Moltke J. Detection of Succinate by Intestinal Tuft Cells Triggers a Type 2 Innate Immune Circuit. Immunity. 2018;49:33-41.
- 33) Jaensson E, Uronen-Hansson H, Pabst O, Eksteen B, Tian J, Coombes JL, Berg PL, Davidsson T, Powrie F, Johansson-Lindbom B, and Agace WW. Small intestinal CD103+ dendritic cells display unique functional properties that are conserved between mice and humans. J Exp Med. 2008;205:2139-2149.
- 34) Bohorquez DV, Samsa LA, Roholt A, Medicetty S, Chandra R, and Liddle RA. An enteroendocrine cell-enteric glia connection revealed by 3D electron microscopy. PloS One. 2014;9:e89881.
- 35) Bohorquez DV, Shahid RA, Erdmann A, Kreger AM, Wang Y, Calakos N, Wang F, and

- Liddle RA. Neuroepithelial circuit formed by innervation of sensory enteroendocrine cells. *J Clin Invest.* 2015;125:782-786.
- 36) Hu MD, Jia L, Edelblum KL. Policing the intestinal epithelial barrier: Innate immune functions of intraepithelial lymphocytes. *Curr Pathobiol Rep.* 2018;6(1):35-46.
- 37) Hoytema van Konijnenburg DP, Reis BS, Pedicord VA, Farache J, Victora GD, Mucida D. Intestinal Epithelial and Intraepithelial T Cell Crosstalk Mediates a Dynamic Response to Infection. *Cell.* 2017;171(4):783-794.
- 38) Niess J, Brand S, Gu X, Landsman L, Jung S, McCormick B, Vyas J, Ploegh H, Fox J, Littman D, and Reinecker H. CX3CR1-Mediated Dendritic Cell Access to the Intestinal Lumen and Bacterial Clearance. *Science.* 2005;307:254-258.
- 39) Edelblum KL, Shen L, Weber CR, Marchiando AM, Clay BS, Wang Y, Prinz I, Malissen B, Sperling AI, Turner JR. Dynamic migration of $\gamma\delta$ intraepithelial lymphocytes requires occluding. *Proc Natl Acad Sci.* 2012;109(18):7097-102.
- 40) Kuhn KA, Schulz HM, Regner EH, Severs EL, Hendrickson JD, Mehta G, Whitney AK, Ir D, Ohri N, Robertson CE, Frank DN, Campbell EL, Colgan SP. Bacteroidales recruit IL-6-producing intraepithelial lymphocytes in the colon to promote barrier integrity. *Mucosal Immunol.* 2017;11(2):357-368.
- 41) Gerbe F, Sidot E, Smyth DJ, Ohmoto M, Matsumoto I, Dardalhon V, Cesses P, Garnier L, Pouzolles M, Brulin B, Bruschi M, Harcus Y, Zimmermann VS, Taylor N, Maizels RM, Jay P. Intestinal epithelial tuft cells initiate type 2 mucosal immunity to helminth parasites. *Nature Letter.* 2016;529:226-230.
- 42) Pinho-Ribeiro FA, Baddal B, Haarsma R, O'Seaghdha M, Yang NJ, Blake KJ, Portley M, Verri WA, Dale JB, Wessels MR, and Chiu IM. Blocking Neuronal Signaling to Immune Cells Treats Streptococcal Invasive Infection. *Cell.* 2018;173:1083-1097.
- 43) Kaelberer MM, Buchanan KL, Klein ME, Barth BB, Montoya MM, Shen X, Bohorquez

- DV. A gut-brain neural circuit for nutrient sensory transduction. *Science*. 2018;361:1219.
- 44) Middelhoff M, Westphalen B, Hayakawa Y, Yan KS, Gershon MD, Wang TC, Quante M. Dclk1-expressing tuft cells: critical modulators of the intestinal niche? *Am J Physiol Gastrointest Liver Physiol*. 2017;313:G285-G299.
- 45) Sharkey KA, Kroese ABA. Consequences of Intestinal Inflammation on the Enteric Nervous System: Neuronal Activation Induced by Inflammatory Mediators. *The Anatomical Record*. 2001;262:79-90.
- 46) Sharkey KA, Mawe GM. Neuroimmune and epithelial interactions in intestinal inflammation. *Current Opinion in Pharmacology*. 2002;2:669-667.
- 47) Cailotto C, Gomez-Pinilla PJ, Costes LM, van der Vliet J, Giovangiulio MD, Nemethova A, Matteoli G, Boeckxstaens GE. Neuro-Anatomical Evidence Indicating Indirect Modulation of Macrophages by Vagal Efferents in the Intestine but Not in the Spleen. *PLoS One*. 2014;9(1)e87785.
- 48) Gabanyi I, Muller PA, Feighery L, Oliveira TY, Costa-Pinto FA, Mucida D. Neuro-immune Interactions Drive Tissue Programming in Intestinal Macrophages. *Cell*. 2016;164:378-391.
- 49) Kelly CJ and Colgan SP. Breathless in the Gut: Implications of Luminal O₂ for Microbial Pathogenicity. *Cell Host Microbe* 19: 2016;427-428.
- 50) Thermann M, Jostarndt L, Eberhard F, Richter H, Sass W. Oxygen supply of the human small intestine in mechanical ileus. *Langenbecks Arch Chir*. 1985;363:179-84.
- 51) Albenberg L, Esipova TV, Judge CP, Bittinger K, Chen J, Laughlin A, Grunberg S, Baldassano RN, Lewis JD, Li H, Thom SR, Bushman FD, Vinogradov SA, and Wu GD. Correlation between intraluminal oxygen gradient and radial partitioning of intestinal microbiota. *Gastroenterology*. 2014;147:1055-1063.
- 52) Bein A, Shin W, Jalili-Firoozinezhad S, Park MH, Sontheimer-Phelps A, Tovaglieri A,

- Chalkiadaki A, Kim HJ, and Ingber DE. Microfluidic Organ-on-a-Chip Models of Human Intestine. *Cell Mol Gastroenterol Hepatol*. 2018;5:659-668.
- 53) McLean IC, Schwerdtfeger LA, Tobet SA, and Henry CS. Powering ex vivo tissue models in microfluidic systems. *Lab Chip*. 2018;18:1399-1410.
- 54) van Duinen V, Trietsch SJ, Joore J, Vulto P, and Hankemeier T. Microfluidic 3D cell culture: From tools to tissue models. *Curr Opin Biotechnol*. 2015;35:118-126.
- 55) Prodanov L, Jindal R, Bale SS, Hegde M, William J, Golberg I, Bhushan A, Yarmush ML, and Usta OB. Long Term Maintenance of a Microfluidic 3-D Human Liver Sinusoid. *Biotechnol Bioeng*. 2016;113:241-246.
- 56) van Midwoud PM, Merema MT, Verpoorte E, and Groothuis GM. A microfluidic approach for in vitro assessment of interorgan interactions in drug metabolism using intestinal and liver slices. *Lab Chip*. 2010;10:2778-2786.
- 57) Yissachar N, Zhou Y, Ung L, Lai NY, Mohan JF, Ehrlicher A, Weitz DA, Kasper DL, Chiu IM, Mathis D, Benoist C. An Intestinal Organ Culture System Uncovers a Role for the Nervous System in Microbe-Immune Crosstalk. *Cell*. 2017;168:1135-1148.
- 58) Markle JGM, Frank DN, Mortin-Toth S, Robertson CE, Feazel LM, Rolle-Kampczyk U, von Bergen M, McCoy KD, Macpherson AJ, Danska JS. Sex Differences in the Gut Microbiome Drive Hormone-Dependent Regulation of Autoimmunity. *Science*. 2013;339:1084-1088.
- 59) Litvak Y, Byndloss MX, Baumler AJ. Colonocyte metabolism shapes the gut microbiota. *Science*. 2018;362:1017.
- 60) von Martels JZH, Sadaghian Sadabad M, Bourgonje AR, Blokzijl T, Dijkstra G, Faber KN, and Harmsen HJM. The role of gut microbiota in health and disease: In vitro modeling of host-microbe interactions at the aerobe-anaerobe interphase of the human

gut. *Anaerobe*. 2017;44:3-12.

61) Wessel AK, Arshad TA, Fitzpatrick M, Connell JL, Bonnecaze RT, Shear JB, and Whiteley M. Oxygen limitation within a bacterial aggregate. *mBio*. 2014;5:e00992.

62) Lee J, Choi JR, Ha SK, Choi I, Lee SH, Kim D, Choi N, and Sung JH. A microfluidic device for evaluating the dynamics of the metabolism-dependent antioxidant activity of nutrients. *Lab Chip*. 2014;14:2948-2957.

63) Garcia-Gutierrez E, Mayer MJ, Cotter PD, Narbad A. Gut microbiota as a source of novel antimicrobials. *Gut Microbes*. 2018;0(0):1-21.

64) Farin HF, Karthaus WR, Kujala P, Rakhshandehroo M, Schwank G, Vries RGJ, Kalkhoven E, Nieuwenhuis EES, Clevers H. Paneth cell extrusion and release of antimicrobial products is directly controlled by immune cell-derived IFN- γ . *The J of Exp Med*. 2014;211(7):1393-1405.

CHAPTER 3 – POWERING EX VIVO TISSUE MODELS IN MICROFLUIDIC SYSTEMS³

Overview:

This Frontiers review analyzes the rapidly growing microfluidic strategies that have been employed in attempts to create physiologically relevant ‘organ-on-chip’ models using primary tissue removed from a body (human or animal). Tissue harvested immediately from an organism, and cultured under artificial conditions is referred to as ex vivo tissue. The use of primary (organotypic) tissue offers unique benefits over traditional cell culture experiments, and microfluidic technology can be used to further exploit these advantages. Defining the utility of particular models, determining necessary constituents for acceptable modeling of in vivo physiology, and describing the role of microfluidic systems in tissue modeling processes is paramount to the future of organotypic models ex vivo. Virtually all tissues within the body are characterized by a large diversity of cellular composition, morphology, and blood supply (e.g., nutrient needs including oxygen). Microfluidic technology can provide a means to help maintain tissue in more physiologically relevant environments, for tissue relevant time-frames (e.g., matching the natural rates of cell turnover), and at in vivo oxygen tensions that can be controlled within modern microfluidic culture systems. Models for ex vivo tissues continue to emerge and grow in efficacy as mimics of in vivo physiology. This review addresses developments in microfluidic devices for the study of tissues ex vivo that can serve as an important bridge to translational value.

Introduction

³ McLean IC, Schwerdtfeger LA, Tobet SA, Henry CS. Powering ex vivo tissue models in microfluidic systems. *Lab on a Chip*. 2018;1399-1410.

Much biomedical research relies upon individualized cells in petri dishes (in vitro) or whole animals (in vivo) to address complex questions of health and disease.¹ In between these two extremes is a need to represent complex organs in vitro to enable more accurate understanding of the biological basis of disease as well as improving accuracy of drug screening. The varied needs of different cells in an organ complicate the development of a system to accurately reflect the function of that organ outside of the animal (ex vivo). The pursuit of more physiologically relevant ex vivo models drives the development of organotypic tissue approaches.² Blood flow is fundamental to all organs in vivo and microfluidics can provide an ex vivo source of fluid flow. Organotypic tissue models present difficulties, principally modulating appropriate local oxygen tensions, and using culture media compositions that are efficacious for a chosen organ system. While some of the challenges inherent in tissue culture are similar in nature to the challenges associated with dissociated cells in culture, they have added challenges related to the thickness and cellular heterogeneity of the specimens. Microfluidic technology offers a promising avenue for addressing many of the challenges related to numerous types of ex vivo approaches, from dissociated cells to more complicated organotypic systems.

Microfluidic approaches to media circulation address a number of issues with static organotypic tissue culture systems, and have been used to maintain numerous types of tissues, including, liver, intestine, retina, artery, lymphoid, tumor xenografts, and testis.^{3–10} Current technologies are evolving to address the heterogeneous, complex nature of mammalian tissues and provide more consistent and useful results. Nonetheless, microfluidic organ-on-chip systems must be assessed for tissue health using multiple endpoint measurements and validated for ex vivo function in the context of in vivo physiological functions.

Although tissue models cannot replace the high through-put potential of cell line studies, nor the importance of tests in live animals and people, organotypic models derived from organs in vivo can provide a critical bridge between the two levels. Tissue-based models have a strong potential to recapitulate complex physiological mechanisms that are missing from models built from one cell type at a time. This quality makes tissue models, and their developing microfluidic components, an important asset for research and development in the biomedical research enterprise. It is particularly notable in the final steps of therapeutic drug design, discovery, and safety analyses on the preclinical side to personalized medicine on the clinical side. Microfluidic technologies are a critical addition for tissue models to unlock this potential.

Cell and tissue models used with microfluidics:

Standard culture systems of the 20th century required that media be changed manually and regularly every 1–7 days, depending on the density and cell types being cultured.¹¹ The advent of microfluidic technology in the late 20th century, and explosion in popularity in the early 21st century removes this need.¹² What gets placed in vitro can vary greatly, ranging from dissociated cells (primary or immortalized), dissociated cells reconstructed in a device to form biological units (e.g., monolayers), organoids derived from stem cells, or tissue/organotypic explants or slices from explants. All of these in vitro model systems offer advantages and limitations. When comparing models comprised of cells to organotypic tissues, one principal advantage that sets tissue cultures apart is the diversity of cell types (depending on the target tissue) and biological structures that hold the tissue together (e.g., extracellular matrix) that are often not accounted for in dissociated cell cultures (e.g., glial cells when studying neurons). These factors enable organotypic tissue models to provide potential access to the cell–cell communication and mechanical signaling experienced in vivo.¹³

The drive towards the developing “organs-on-a-chip” has typically involved the culture of cell lines or stem cells, but the improved cellular diversity of organotypic tissue makes it attractive for certain applications and/or for bridging the in vitro/in vivo gap. This relevance is exemplified by examining intestine on-chip models. The simplest intestine on-chip systems, regardless of the microfluidic flow paradigms, involve culturing of Caco-2 epithelial progenitor cells, and allowing them to proliferate to mimic intestinal epithelium. These systems are sufficient to recapitulate the intestinal mucosa, a dense network of epithelial cell types constantly proliferating, dying off, and producing secretory factors.^{14–16} These models do not recreate the full cellular diversity of the in vivo intestinal mucosa. Intestinal organoids on a chip add a layer of diversity, better recapitulation of epithelial structure, and can include the formation of intestinal villi and crypts, something that Caco-2 systems only partially recapitulate.¹⁵ They still lack the diversity of cell types of the intestinal wall in vivo. Organoids lack representation of the enteric immune system (e.g. lymphocytes, dendritic cells and macrophages) and the vast enteric nervous system (e.g. neurons and glia). Communication between these neural-immune components is known to impact gut function in healthy and diseased states.¹⁷ Models that maintain cellular diversity have been achieved in static culture with varied temporal control, ranging from 24 h to 6 days ex vivo.^{18,19} When incorporation of organotypic tissues into microfluidic systems has been accomplished, tissue health analyses have been limited and validation of epithelial cell turnover incomplete.^{4,20}

Advantages and applications of microfluidic technology to ex vivo tissue culture:

Improve tissue viability and longevity:

The use of microfluidic technology to maintain mammalian tissue ex vivo has been shown to improve tissue viability when compared to traditional static systems that do not

incorporate continuous media exchange, particularly when long-term culture is necessary.^{21,22} Maintaining viable tissue is particularly challenging when using organotypic tissues with a thickness greater than 400 μm .¹⁹ In static cultures, tissue thicker than approximately 400 μm prevents adequate diffusion of oxygen and nutrients throughout the entirety of the tissue, and cytotoxic cellular waste products can rapidly build up within the media.¹⁹ This results in a direct correlation between tissue thickness and overall health in static culture.²³ Inadequate nutrient diffusion into the core of the tissue establishes limitations on the variety of tissue that can be effectively cultured and the length of time the tissue will remain healthy and viable ex vivo. Numerous non- microfluidic based techniques have been established to improve nutrient exchange to cells and tissues.²⁴ Culture dishes can be continuously shaken, rotated, or stirred to refresh the media within the diffusive boundary layer at the biological surface.²⁴ These techniques are useful for prolonging the viability of cultured tissue; however, these techniques result in microenvironments that are relatively under characterized and uncontrolled.^{25–27} A further complication is that the rates of diffusion and uptake of essential solutes vary based upon the preparation and the type of tissue being cultured.^{28,29}

A simplified mathematical model was developed to estimate the limits of oxygen diffusion through spherical tumor tissue ex- plants in static culture.³ The transport of oxygen within tissue can generally be modeled using Fick's second law:

$$\frac{\partial C}{\partial t} = D\nabla^2 C - q$$

where C represents the concentration of oxygen at time t and distance x; D is the diffusivity coefficient of oxygen; and the term q represents the volumetric consumption rate of oxygen by the tissue.³ Using this equation, two partial differential equations were derived to model the concentration of oxygen within the tissue and the surrounding culture media. By assuming a constant rate of oxygen consumption, infinite media surrounding a spherical explant, as well as a steady state system; the paired equations were solved, and a conservative estimate of the maximum depth of oxygen penetration (R_C) and critical spherical tissue diameter ($2R_C$) were determined as follows:³

$$2R_C = 2 \sqrt{\frac{6D_T D_M C_{\max}}{\rho Q (2D_T + D_M)}}$$

here, D_T and D_M are the diffusion coefficients of oxygen within tissue and culture medium, respectively; C_{\max} is the maximum possible concentration of oxygen in the media; and ρQ (cell density multiplied by average cellular oxygen consumption) is an estimate of oxygen consumption by the tissue. For the parameters associated with tumorous tissue in static culture, the critical diameter was calculated to be 424 μm .³ The theoretical critical diffusive diameter will vary depending on the shape and type of tissue being cultured.

Based on experimental evidence, diffusive limitations are mitigated in tissue that is maintained no thicker than 250 μm with a vibrating microtome.^{18,30} These organotypic slice models maintain their respective tissues in physiologically relevant environments for limited time frames (e.g., up to 6 days for murine intestine) and for many tissues, the 250 μm limit works reasonably for maintaining sufficient three- dimensional physical microenvironment.¹⁸ However,

due to the limited thickness of the slices, diffusion of natural chemicals and mechanical cues in differential physiological compartments that exist within tissues *in vivo* can be disrupted *ex vivo*. Gradients formed by oriented diffusion of critical signaling molecules guide cellular movement or growth and differentiation; and disruption of these gradients can alter cell interactions and tissue physiology.^{27,31,32} If the tissue of interest contains spatial boundaries, limited thicknesses may make it difficult to obtain slices with a full representation of cellular diversity. For example, mature ovarian follicles (from mice) are difficult to fit within 250 μm thick slices.³³ Microfluidic approaches automatically offer a potential method for combatting waste buildup, and nutrient deficiencies that might otherwise be problematic for experimental needs at longer time points.³⁴

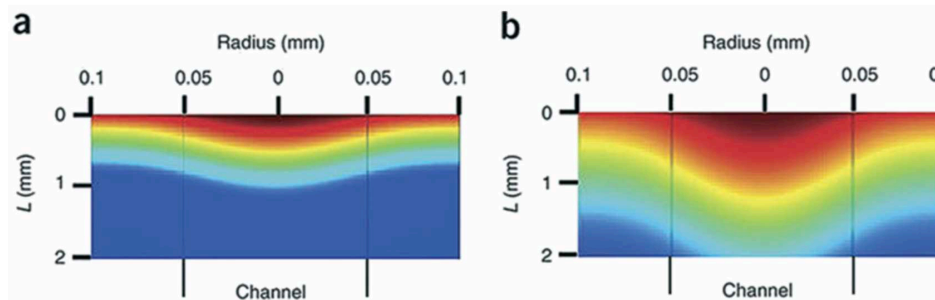


Fig. 6 Simulations of the steady state oxygen concentration (μM) profiles within a tissue compartment surrounding a 100 μm diameter channel under different flow conditions. The flow velocities of media are 490 $\mu\text{m s}^{-1}$ (panel a) and 1.35 mm s^{-1} (panel b). The depth of oxygen penetration (mm) is increased at higher flow velocities. Adapted with permissions from Macmillan Publishers Ltd: Nature Protocols (ref. 40), 2008.

The continuous perfusion of media across the surface(s) of an explant increases the efficiency of nutrient and waste transport to and from the tissue, respectively.^{15,35–38} This improvement in efficiency is equivalent to an increase in the media diffusion coefficient term (D_M) in the mathematical expression shown above in eqn (2).^{3,39} A larger media diffusion coefficient results in an increase in the maximum steady state depth of oxygen penetration (R_C) into the tissue. Finite element analysis was performed using FEMLAB 2.2 software to simulate oxygenated media perfusion through 100 μm diameter circular channels at low (490 $\mu\text{m s}^{-1}$) and high (1.35 mm s^{-1}) velocity.⁴⁰ The resulting concentration profiles of oxygen diffusing into the surrounding tissue compartment are shown in 6.

Controlled nutrient delivery:

Static culture systems use relatively large volumes of nutrient-rich media to keep the tissue alive. The culture media must be removed and replenished on a periodic basis to avoid the deleterious effects of insufficient nutrients and the buildup of cytotoxic metabolic waste products in the culture dish. This may result in inconsistent delivery of nutrients and removal of waste to the tissue.³⁴ The rate of delivery in vivo of nutrients, oxygen, and other soluble factors to cells is variable, and dependent upon a variety of environmental and physiological factors, such as stress, exercise, and diet.^{41,42} The rate of nutrient delivery fluctuates following the ingestion of meals.⁴³ Microfluidic perfusion offers the ability to control the rate of nutrient delivery and create a defined microenvironment.²⁵ The desired rate of delivery of soluble factors may be periodic, as in the case of modeling reproductive hormonal regulation, or constant, such as delivery of nutrients to cells.⁴⁴ For the latter cases, microfluidic technologies provide continuous media perfusion, ideally leading to a more consistent media composition, and thereby a more consistent delivery of nutrients and removal of waste from the tissue (Fig. 7).^{22,34}

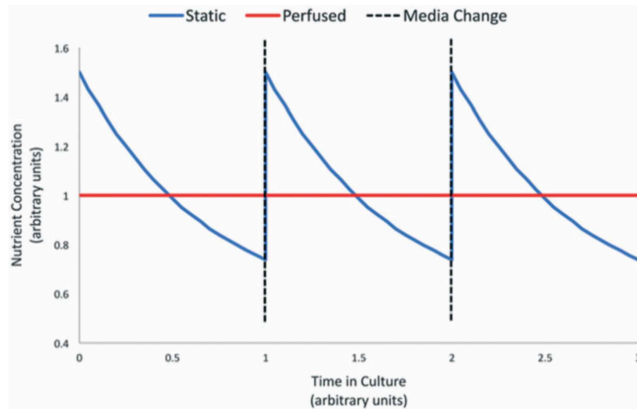


Fig. 7 Stylized representation of the varying nutrient concentration available to tissue or cells in static culture, compared to the constant media composition achievable through perfusion.

A recent example of the potential of microfluidic systems to enable analyses of a complex tissue construct was the demonstration of a model of human reproductive function.²¹ A combination of murine and human reproductive tissues were maintained *ex vivo* for 28 days, and effectively modeled the human menstrual cycle. The system consists of five culture chambers connected by microfluidic channels and electro- magnetically actuated micro-pumps to drive media flow and physiological hormones throughout connected chambers (Fig. 8). The microfluidic platform enabled the co-culture of ovary, fallopian tube, uterus, cervix and liver explant tissue in series, and allowed for hormonal and cellular communication to occur between the tissue chambers. Here, D_T and D_M are the diffusion coefficients of oxygen within tissue and culture medium, respectively; C_{MAX} is the maximum possible concentration of oxygen in the media; and ρQ (cell density multiplied by average cellular oxygen consumption) is an estimate of oxygen consumption by the tissue. For the parameters associated with tumorous tissue in static culture, the critical diameter was calculated to be $424 \mu\text{m}$.³ The theoretical critical diffusive diameter will vary depending on the shape and type of tissue being cultured.

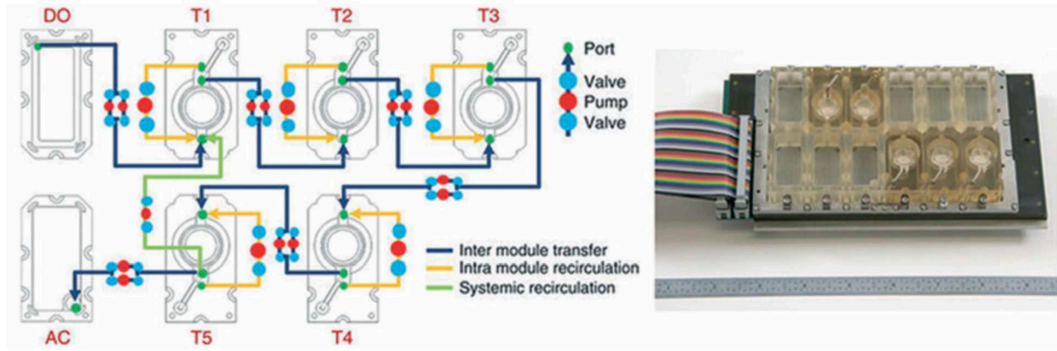


Fig. 8 Schematic representation and image of the five-tissue micro-fluidic culturing platform. The tissue modules (T1–T5) are fed fresh media from the donor module (DO) via electromagnetic micro-pumps. The tissue modules are connected fluidically to enable tissue-to-tissue communication. Adapted with permission from ref. 21, licensed under CC BY.

Based on experimental evidence, diffusive limitations are mitigated in tissue that is maintained no thicker than 250 μm with a vibrating microtome.^{18,30} These organotypic slice models maintain their respective tissues in physiologically relevant environments for limited time frames (e.g., up to 6 days for murine intestine) and for many tissues, the 250 μm limit works reasonably for maintaining sufficient three-dimensional physical microenvironment.¹⁸ However, due to the limited thickness of the slices, diffusion of natural chemicals and mechanical cues in differential physiological compartments that exist within tissues in vivo can be disrupted ex vivo. Gradients formed by oriented diffusion of critical signaling molecules guide cellular movement or growth and differentiation; and disruption of these gradients can alter cell interactions and tissue physiology.^{27,31,32} If the tissue of interest contains spatial boundaries, limited thicknesses may make it difficult to obtain slices with a full representation of cellular diversity. For example, mature ovarian follicles (from mice) are difficult to fit within 250 μm thick slices.³³ Microfluidic approaches automatically offer a potential method for combatting waste buildup, and nutrient deficiencies that might otherwise be problematic for experimental needs at longer time points.³⁴

The continuous perfusion of media across the surface(s) of an explant increases the efficiency of nutrient and waste transport to and from the tissue, respectively.^{15,35–38} This improvement in efficiency is equivalent to an increase in the media diffusion coefficient term (DM) in the mathematical expression shown above in eqn (2).^{3,39} A larger media diffusion coefficient results in an increase in the maximum steady state depth of oxygen penetration (R_C) into the tissue. Finite element analysis was performed using FEMLAB 2.2 software to simulate oxygenated media perfusion through 100 μm diameter circular channels at low ($490 \mu\text{m s}^{-1}$) and high (1.35 mm s^{-1}) velocity.⁴⁰ The resulting concentration profiles of oxygen diffusing into the surrounding tissue compartment are shown in Fig. 6.

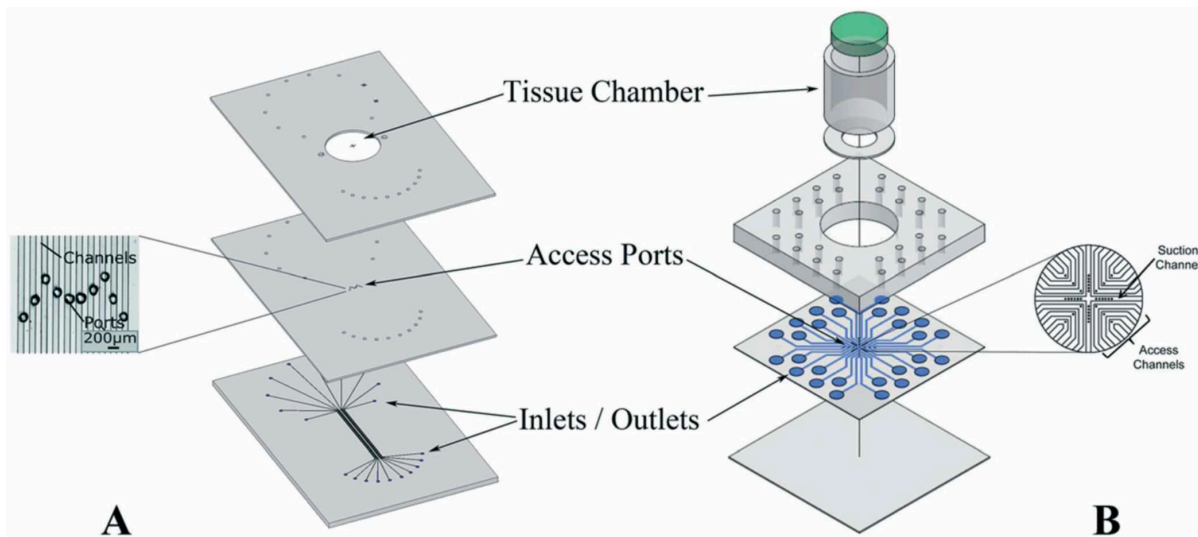


Fig. 9 Device designs for spatially resolved reagent delivery to lymph node (panel A) and retinal tissue (B). Panel A adapted from ref. 8 with permission from the Royal Society of Chemistry. Panel B adapted from ref. 5 with permission of Springer.

Spatially-controlled reagent delivery:

Microfluidic techniques have been used to study local cellular signaling within ex vivo tissue cultures. In a traditional static culture, drugs and reagents can be introduced in a global media

change or perhaps with the spatial precision of a local pipette application or even a slow release source placed in the dish. Microfluidic flow has the potential to provide spatially- controlled reagent administration and spatially-resolved sampling of tissue responses, making it easier to study local cellular mechanisms and responses. Development of these techniques can be particularly useful in understanding the physiology of tissues that are structured into discrete cellular units, defined by spatial boundaries. For example, lymph nodes are organized into distinct regions, with small B-cell zones in the periphery, surrounding larger, centralized T-cell zones; and infections, vaccinations and drug delivery are believed to elicit a differential immune response based on regional stimulation.^{8,45} To investigate response differences in lymph nodes with regional specificity, a microfluidic platform was recently developed to stimulate and monitor discrete zones of live lymphoid tissue.⁸ Murine lymph nodes were removed and sliced on a vibrating microtome to a thickness of 300 μm . Each slice was cultured in a multi-layered PDMS device with 80 μm ports spaced underneath the tissue slice (Fig. 9A). A fluorescently-labelled mock therapeutic glucose conjugated to bovine serum albumin was driven through microfluidic channels aligned to the ports, and glucose-facilitated uptake was monitored in real time. The small ports restricted the uptake of the fluorescent molecule to a 200–300 μm region of tissue, providing sufficient resolution to specifically target lymph node regions in future studies.

Microfluidic spatial control over reagent delivery has been used to observe microglia migration in live murine retinas.⁵ Excised retinas cultured in a tissue chamber were gently suctioned onto a thin PDMS layer containing molded microfluidic channels and regularly spaced 100 μm access ports (Fig. 9B). Small amounts of lipopolysaccharide, an inflammatory component of bacterial cell walls, delivered selectively through 100 μm ports was shown to induce microglia that were in the retinal slices to migrate to the microfluidic access points. The

local nature of the stimulation and the response demonstrates the ability to create microenvironments in discrete regions of ex vivo tissue, while simultaneously allowing for on-chip microscope detection of cell migration. The use of microfluidic ports could allow research teams to vary conditions (i.e. drug dosage) over spatially defined regions of a single explant, reducing the amount of tissue needed for experimental analysis.^{46,47} Development of this technique would be particularly useful for situations in which tissue samples are scarce, for example testing drugs on human biopsies. The utility of such techniques would depend on the rapidness of the tissue response and the immediacy of detection of the analyte of interest. For example, it would be reasonable to stimulate norepinephrine release across adrenal tissue in a spatially defined manner, and measure the biochemical concentration in real-time using an electrode array.⁴⁷ However, it might not be reasonable to compare endpoint cellular viability using this experimental design.

High throughput assays:

Static cell cultures win the day for high throughput. Robotic pipetting systems and uniformity of cells that can be handled in large batches provide expediency. The independence of sample handling provides shelter from cross contamination and the power of endless replicates. The win, however, comes at the price of cellular complexity and model validity. This limits the translation of cell culture into an accurate use for drug screening in the pharmaceutical and diagnostic industries. For the single cell based approaches, microfluidics may not provide a meaningful advantage because for each of 1 million wells with cells you would need 2 lines of fluid flow (in and out) and they might not provide appreciably more information. Additional value is provided when you consider cell-based systems that are multi-cellular.

Ex vivo organotypic tissue will not replace cell culture for mass screening of toxicity and drug interactions. The smaller number of matching tissue samples that can be processed comes with the opportunity to gather a richer pipeline of data provided by more complex cellular interactions. Microfluidic systems augment the value of organotypic tissue because it provides for temporal resolution of physiological changes. In this respect, the capability to culture multiple tissue samples in parallel is still important. Implicit in this complexity is a large number of biological variables; many that vary from tissue source to tissue source. With a sufficient number of replicates, otherwise subtle biological differences can be uncovered.

The supply of healthy (or diseased) tissue is a limiting factor for the number of replicate samples that can be cultured for any given experiment. Acquiring viable excised human tissue often requires proximity and access to major healthcare centers and for tissue only from 1 patient at a time. For animal tissues the labor-intensive process required to culture may limit the number of animals in any one preparation period. To maximize data efficiency microfluidic techniques should be applied to multiple simultaneous experiments on separate small tissue sections, thereby multiplexing the assay, maximizing the number of replicates given a finite tissue supply, and minimizing the labor required.⁴⁸

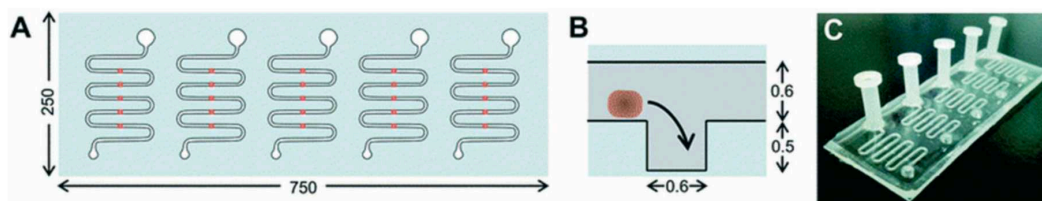


Fig. 10 High-throughput microfluidic platform for the analysis of microdissected tumor biopsy tissue. The platform consists of five microfluidic channels (panel A), each lined with five rectangular biopsy traps (panel B). This enables simultaneous experimentation on 25 primary tumor sections under 5 different conditions (panel C). Reproduced from ref. 3 with permission from The Royal Society of Chemistry.

Microfluidic multiplexing strategies have been developed for cultures involving human tumor

tissue. A recently developed culture system allowed for the parallel culture and chemosensitivity testing of multiple microdissected tumor biopsies (approximately 400 μm diameter).³ The microfluidic platform included 5 separate fluidic channels. Rectangular wells on the bottom of each channel were used to capture and culture individual biopsy tissue sections (Fig. 10). The authors estimated that 300 microdissected tissue sections could be prepared and loaded onto the microfluidic platform in less than 6 hours. Validation of the viability of the cells in tumor explants was achieved by labeling dead cells with the DNA binding dye propidium iodide, and labeling apoptotic cells with Annexin V and 7AAD dyes (PE Annexin V Apoptosis Detection Kit I, BD Biosciences). On-chip microscopy allowed for real-time tracking of cell death within the tissue. The multiplexed capabilities of the platform make it appealing for personalized medicine and for clinical screening of chemotherapeutics.

The standardization of loading tissues into microfluidic devices can also improve the throughput of ex vivo tissue culture. A multi organ chip (MOC) was developed to simultaneously culture, in series, human juvenile prepuce skin and single hair follicular units obtained from human skin samples.²² The MOC contains two tissue compartments linked by microfluidic channels, and connected to an on-chip micro-pump that simulates peristaltic blood flow. A key advantage of the MOC design is that standard Transwell® inserts were loaded with tissue samples, and then rapidly inserted into the microfluidic chip. The ease of use and flexibility associated with the operation of this culture model system expedites the culturing of multiple tissue replicates simultaneously, and may facilitate wider utility. Standardization of inserts for microfluidic culture systems could also make automated readout systems more accessible. Plate readers for conventional 96-wellplate cultures allow for convenient multiplexed detection of a variety of assays that could readily mesh “lab on a chip” with microfluidic culture systems. Due to the decreased diffusional distances associated with microfluidic culture, the results of

chemical assays can be obtained more rapidly than in a conventional culture.⁴⁹ For instance, a biomarker detection device for human cancerous tissue slices decreased immunohistochemical development from 120 minutes in conventional system to 3.5 minutes in a microfluidic device.⁴⁹

Present considerations and future challenges:

Choosing the right material:

Choosing a proper material for microfluidic device fabrication is critical when designing for live tissue. Ideally, fabrication should be easy and cost effective, and the chip material should be biocompatible with the chosen tissue and support the most physiologically relevant environment possible. The contributions of material properties upon live tissue physiology and possibly even media composition are hard to define and quantify, but understanding these properties is crucial to obtain repeatable and translatable results.

Novel fabrication techniques, from 3D printing to laser ablation, have resulted in a significant increase in the material options available for microfluidic systems.⁵⁰ This includes devices fabricated out of thermoplastics such as cyclic olefin co-polymer, polycarbonate, and polystyrene, collagen based three dimensional-models, and glass devices, among others.^{16,51–53} The most commonly used material to fabricate microfluidic devices in academic laboratories is polydimethylsiloxane (PDMS).⁵⁴ PDMS is an attractive material due to the low overhead cost involved, the ease of fabrication, and the elastomeric properties of PDMS that simplify chip bonding and “world-to-chip” interfaces. The emergence of soft lithography techniques in conjunction with PDMS molding is considered one of the most important developments to help launch the microfluidic revolution.¹² However, there is evidence that PDMS may not be suitable for certain in vitro culture applications.^{55,56}

PDMS is widely considered a biocompatible plastic; however, biocompatibility can mean a wide range of things related to cell health, functionality, and absorption of media components. Past studies have shown that there are no differences in cell death rates for immortalized cell lines cultured on PDMS versus polystyrene (a common laboratory plastic). Other studies, however, have observed changes in gene expression and differentiation of cells cultured on PDMS.^{56–58} When attempting to model complex biological processes, physiological measures other than cell death may be needed. A recent study investigated cellular adhesion and migratory properties of cells on PDMS compared to a glass and conventional lab plastic substrate (Thermanox®).⁵⁹ Chick embryonic brain and liver explants cultured on the PDMS substrate exhibited less cell migration and increased cell adhesion compared to the other substrates.⁵⁹ Such considerations may significantly impact design characteristics of cell or tissue culture experiments to investigate cell migration or membrane dynamics.

Another important consideration in chip design is the diffusivity of the material to molecules within the culture solution. One significant advantage of using PDMS for cell and tissue culture systems is that the material readily allows for diffusion of gas, thus simplifying the process of oxygenating and buffering the culture media.³⁴ On the other hand, the permeability of PDMS to water vapor can lead to evaporation of small amounts of media out of the system, potentially leading to altered concentrations of media solutes.⁵⁵ In some cases where regulation of oxygen tensions is desired the porosity of PDMS may create problems in the other direction. PDMS is a porous hydrophobic material that has been shown to rapidly absorb small molecules and adsorb proteins from contacting fluids.^{60,61} This can pose a major issue when culturing tissue on a microfluidic platform as alterations in bio- molecule concentrations in media/tissue due to adherence to the devices material could alter the tissue physiology or

response to perturbations such as therapeutic screenings. Plasma and UV treatment of PDMS has been shown to decrease the hydrophobicity of the material, but these techniques may not be appropriate for long-term tissue culture, as the plastic may return to the original hydrophobic state one week after treatment.³⁴

Cyclic olefin copolymer (COC) has emerged as a promising alternative to PDMS for the fabrication of microfluidic culture systems. COC has a high resistance to chemicals, low permeability to air, and minimal adsorption of small hydrophobic molecules.⁵⁸ The optical properties of COC give it low autofluorescence and high transparency.⁶² Difficulties and expenses associated with COC chip fabrication have discouraged widespread use of COC in the academic laboratory.⁶² However, novel and inexpensive techniques to prepare master molds for COC chips have recently been reported.⁶² A combination of micromilling and hot embossing was used to create a COC device for the culture of oocytes. A mid-level micromilling machine, Protomat S63 (LPKF Laser & Electronics, Garbsen, Germany), was capable of producing 50 μm features. Nonetheless, it is important to note that PDMS is advantageous for many applications. The ease of fabrication, the ability to incorporate on-chip valves and micropumps, and the precision and resolution of PDMS chips are currently unmatched in the academic laboratory.⁶³ Fig. 11 provides a qualitative assessment of the advantages and disadvantages of a selection of materials that can be used to fabricate tissue culture microfluidic systems.⁶³

As the complexity of the biological systems being modeled increases, so does the importance of material choice in microfluidic design. For instance, a microfluidic model of hormonal regulation may be problematic for physiological relevance if a relevant proportion of steroids are being absorbed out of solution and into the microfluidic device. Recent requests

for applications from the National Institutes of Health (RFA's) have expressed reservation about the use of PDMS in microphysiological systems (e.g., RFA-TR-16-017). The material used for microfluidic chip fabrication should be chosen with care based upon the type of tissues cultured and the intended experimental results. A full analysis of the material's impact on the physiological function of the cultured tissue and cells should be taken into account.

Design considerations:

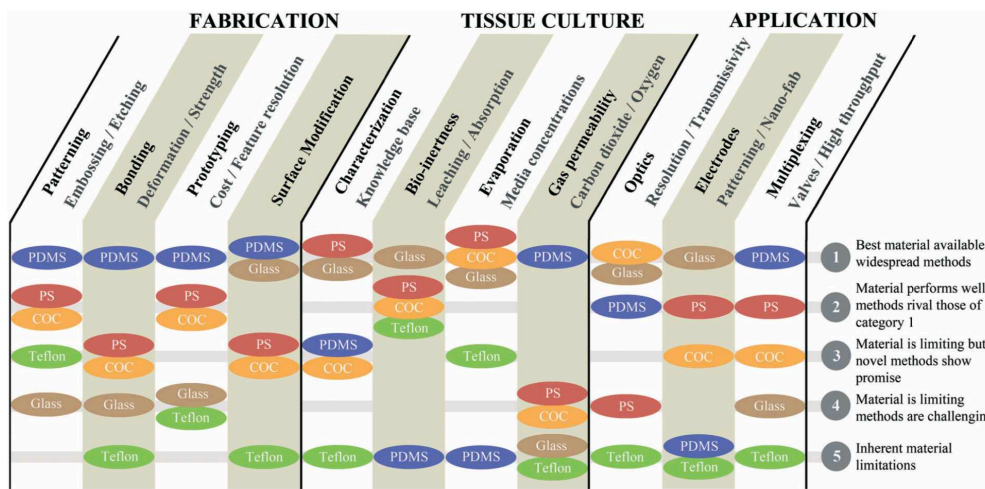


Fig. 11 Qualitative comparison of the strengths and weaknesses of common materials used to fabricate microfluidic culture systems. Each color denotes a particular material. Reproduced from ref. 63 with permission from The Royal Society of Chemistry.

The principles developed for the design of microfluidic cell-line culture platforms can be translated to tissue culture applications. Similar methods can be used for channel design, chip-to-world connections, and the fabrication of tissue culture microfluidic platforms. Quality reviews are available that detail these techniques.^{25,64} However, the size and three dimensionality of tissue samples creates unique design challenges associated with loading samples. In cell-line derived cultures, cells can be loaded into a microfluidic device by injecting a cell suspension through a perfusion inlet.²⁵ This method allows the fluidic system to be primed prior to loading

the cells. A similar technique has been used to load tissue samples, but only when the tissue sections are smaller than the perfusion channel.³ For larger tissue slices and explants, this is not a viable strategy. One alternative is to load tissue sections onto an insert lined with a semi-porous membrane (for example a modified Transwell® insert).²² The insert can then be integrated into the microfluidic chip via a threaded port to form a fluid-tight seal between the insert and the microfluidic chip.⁶⁵

Special considerations are required when attempting to model the function of barrier tissues. To expose two sides of the tissue sample to two different environments, the tissue must form a seal between two distinct fluids. This has been accomplished through uncomplicated techniques, such as using petroleum jelly to form a seal around the tissue, or suturing intestinal tissue to a fluidic port.^{4,20} Alternatively, sub-atmospheric pressure has been applied through micro-channels to conform outer surfaces of resected arteries to perfusion channel, and thereby selectively perfuse the lumen of the vessel.⁹ In certain applications, for example when targeting spatially-defined regions of a tissue, it is particularly important that tissue samples remain stationary during culture. Negative pressure, applied by a weak vacuum through micro-suction channels, has been used to hold excised retinas in place without damaging the tissue.⁵ Alternatively, collagen overlays work to hold tissue in place in other systems.^{18,30}

There are considerations that are selectively important when designing the geometry of a tissue perfusion chamber. Cell-lines are often cultured in straight microfluidic channels; in which each cell positioned transverse to the channel experiences the same laminar flow and mass transport.⁶⁴ For tissues in culture this is often not possible, and the perfusion chamber must be designed to fit the three-dimensional shape of the tissue. A small microfluidic channel entering a large perfusion chamber may result in unequal flow. The mass transport at the outer

edges of a large circular chamber can be significantly less than the transport near the center of the chamber. This could affect the health and function of the tissue. Computational flow dynamics can be used to predict the extent of mass transport deviations.

Choosing the right media:

From the advent of tissue culture techniques to the present, determining appropriate media for mammalian tissue culture always has been a challenge. It is important to use culture media that is optimized for amino acids, fatty acids, sugars, ions, cofactors, and vitamins to keep tissues viable.⁶⁶ Different cell types can have different nutritional requirements, and that makes finding a universal media more difficult.⁶⁷ It particularly complicates the choice of media for the culture of heterogeneous cell populations. For this reason, animal serum is often added to basic tissue culture media. Serum can be derived from a variety of animal sources, but most often is taken from bovine fetuses (FBS).⁶⁷ FBS contains a host of undefined hormones, growth factors, and proteins that can help many cell and tissue types thrive in vitro.⁶⁸

The use of serum in cell and tissue culture systems is controversial.⁶⁸ The properties of commercial serum are inconsistent from animal to animal, and from lot to lot, and can influence the phenotype of cells maintained in the media.⁶⁸ Furthermore, the exact composition of serum is typically undefined or undisclosed, which runs contrary to the desire to maintain control over experimental reagents.⁶⁹ Due to these shortcomings, much effort has been expended on developing defined serum-free medias for the culture of a variety of different cell and tissue types.⁶⁷ Ideally, each medium would deliver the same nutrients and small molecules that the particular tissue experiences in vivo. This is difficult to achieve when culturing multiple tissue types in series. There is potential for the development of a relatively “universal” serum free

medium that can be used to culture a wide range of tissue types. To this point, neurobasal media (Gibco, Invitrogen) with B27 supplement has been used to maintain tissue viability by one group without serum for murine brain, pituitary, ovary, adrenal and gastrointestinal tissues.^{18,30,33,47,70,71} It has also been used with human intestinal tissue.⁷²

Tissue response to shear stress:

At increasing perfusion velocities, a greater depth of oxygen diffusion can be achieved; although care must be taken to avoid high flow rates in which cell-damaging shear stress can develop.^{25,73} Within the healthy human circulatory system in vivo, endothelial cells that line the blood vessels experience shear stresses ranging from approximately 1 to 6 dyne per cm² in the venous system to 10–70 dyne per cm² in the arterial system.⁷⁴ Laminar shear stress within this physiological range has been found to promote certain cytoprotective re-modeling processes in vascular endothelial cells cultured in vitro.⁷⁵ However, with the exception of certain epithelial-lined organ systems, such as the gastrointestinal tract, lung, and kidneys, non-endothelial lined tissues in vivo are only subjected to extremely low interstitial shear forces (<0.1 dyne per cm²).⁷⁶ For tissues that do not normally experience significant shear stresses, fluidic shear stress greater than 2.5 dyne per cm² can influence cell permeability.⁷⁷ Therefore, tissues cultured ex vivo should be perfused at a flow rate that maximizes the efficiency of nutrient delivery while minimizing the detrimental effects of shear stress. The introduction of flow at an appropriate velocity can help prevent nutrient and oxygen deprivation within the core of cultured tissue, and enable explants with thicknesses greater than 250 μm to remain viable for longer periods of time in culture. Greater detail on determining the proper perfusion rate are available.⁶⁴

Oxygen control:

Oxygen availability *in vivo* varies significantly depending on the tissue of interest, and is a concern for generating physiologically relevant *in vitro* models. In addition, oxygen tensions can vary within single organs, such as in the intestines⁷⁸. Many static culture systems of the past 50+ years used either ~20% (150 mm Hg) or 95% oxygen (720 mm Hg) concentration media.⁷⁹ Similar dissolved oxygen concentrations in media are observed within microfluidic culture systems, and while these systems often maintain cells alive and functional, they may provide an incomplete view of cell functions *in vivo*.¹⁵ Mimicking oxygen tensions seen *in vivo* is important as tissue immune responses depend on them; as do cellular signaling mechanisms, cell proliferation, and health of the tissue.^{80–82}

Where oxygen gradients exist across tissues such as for barrier tissues (e.g. intestine, uterus), the recreation of oxygen gradients *in vitro* can be challenging. In the intestines, as you move from the luminal to serosal aspects of the gut wall, the pO₂ varies between ~10 (physiological hypoxia) and ~35 mm Hg (~5% O₂) respectively.⁸³ A microfluidic platform developed to investigate microbial–intestinal interactions modeled this oxygen gradient across a Caco-2 cell monolayer.¹⁶ Oxygen was precisely measured in real-time on both sides of a cell layer via optical spot sensors (PreSens). A near anoxic environment of less than 6 mm Hg pO₂ was maintained on the apical side of the cell layer by continuously bubbling N₂ gas through the circulating media, and a near physiological pO₂ of 41 mmHg was achieved on the basolateral side by the simultaneous perfusion of oxygenated media.¹⁶ The relevance of establishing *in vivo*-like oxygen environments is highlighted when trying to incorporate bacteria into tissue models. Non-physiological concentrations of oxygen may kill some bacteria depending on their metabolic demands and alter the function and metabolism of facultative and obligate anaerobes

alike, possibly leading to confounding results.⁸⁴ It is important to note that while near-physiological oxygen conditions were established on the two sides of the cell layer, the oxygen tension experienced by the cells would still have differed from physiological conditions.¹⁶ In vivo, the oxygen gradient from lumen to serosa would occur over the full thickness of the tissue comprised of many cell layers thick, rather than a single cell layer.

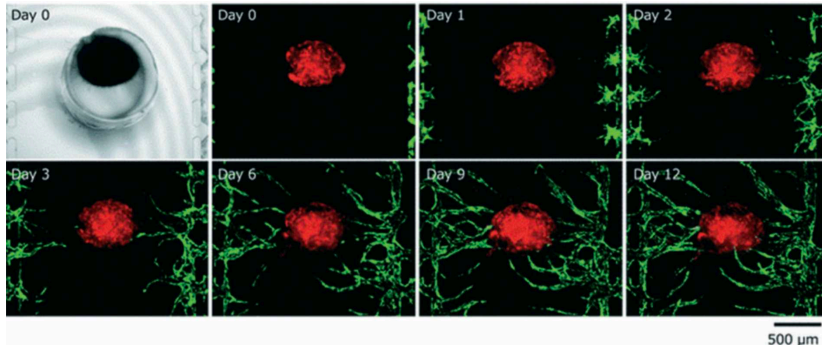


Fig. 12 Time series of micrographs demonstrating the sprouting of HUVECs cultured in adjacent microfluidic channels (green fluorescence). At day 9, engineered microvessels had anastomosed with HUVEC derived vessel-like structures within the organoid (red fluorescence). Reproduced from ref. 85 with permission from The Royal Society of Chemistry.

Vascularization of organotypic tissue:

One solution to mimic in vivo oxygen tensions would be to perfuse native vasculature within tissue, ex vivo. This has not been accomplished using primary tissues, but there is emerging research in the field of tissue engineering that demonstrates that microfluidic technology may make vascular perfusion ex vivo possible in the future.^{85,86} In a recent study immortalized fibroblasts and human dermal microvascular endothelial cells (HDMECs) were seeded into channels located underneath a media reservoir to culture cancerous spheroids.⁸⁶ The media reservoir was connected to the fibroblast and HDMEC channels by micropores 200 μm in diameter. After 5 days of culture, the HDMECs sprouted and formed a microvessel

network. The network of microvessels formed tight walls, and could be perfused with media selectively, potentially allowing for a more physiologically accurate perfusion of the spheroid.

It may be possible to connect an engineered microvessel network to existing vasculature within primary tissue. A microfluidic chip, similar in design and concept to the one mentioned above, was used to engineer a network of perfuseable microvessels adjacent to a culturing spheroid composed of human lung fibroblasts (HLF) and human umbilical vein endothelial cells (HUVECs).⁸⁵ After 9 days in culture, the group observed angiogenic sprouts from the engineered microvessels with connections to vessel-like structures within spheroids (Fig. 12). Chip-based perfuseable networks may one day allow for more physiological perfusion of tissue *ex vivo*. However, further development must be done to determine how connections can be made from an engineered microvascular network to mature vasculature within tissues. Functionality of native vasculature in tissues *ex vivo* needs to be determined. Capillary-like structures have been maintained in brain slices for up to 14 days in culture, but the results have not indicated whether the capillary-like structures remain viable.⁸⁷

In mammals, oxygen is carried through the body attached to hemoglobin. Hemoglobin effectively increases the solubility of oxygen within blood and improves the efficiency of oxygen exchange from the lungs to other tissues.⁸² Oxygen carrier molecules, however, are absent from the media in microfluidic and conventional tissue model systems.⁸² Oxygen delivery to cells is instead accomplished through simple diffusion from the media through the tissue, which is not physiologically accurate. More work is needed to develop artificial oxygen carriers that mimic the function of hemoglobin *in vitro*. This would be particularly useful in thicker tissue culture systems when oxygen transport is needed over multiple cell layers. Realization of such technology would allow microfluidic culture systems to better mimic *in vivo* oxygen transport.

Other means of measuring and controlling oxygen have been developed. A recent in-depth review offers a detailed look at the strategies used and challenges in implementing oxygen control in microfluidic devices.⁸²

On-chip tissue validation:

As microfluidic models become more common in the laboratory, developing proper standardized on-chip validation of tissue health and functionality are important for characterizing and comparing biological results. This is particularly true for microfluidic models involving the culture of human tissue *ex vivo*, in which tissue injury and/or suboptimal timing during processing may occur. In one study, less than 1% of total gene expression had changed in excised prostate tissue one hour after surgery.⁸⁸ However, more pronounced physiological changes have been noted post-surgery in excised human tissue, and validation strategies should account for this possibility.⁸⁹ There is no single validation method that fits all tissue types or microfluidic designs, making standardization of validation methodologies difficult. Validation strategies are needed based upon the applicable parameters for each tissue of choice. For instance, quantifying epithelial cell proliferation rates is an accepted and commonly used methodology for measuring intestinal tissue health.^{18,90,91} This same measure may be less sensitive when looking at brain-on-a-chip models, because cell turnover is spatially and temporally more complex compared to intestinal tissue. Quantifying cell death on the other hand, in brain-on-chip models provides a more universal indicator for assessing tissue health.⁹² If a system maintains the 3D structure of the tissue in question, the anatomical context may help determine if the observed chemical markers and rates are consistent with *in vivo* physiology.^{8,18}

Measures of tissue function need to be validated, depending on the physiological process that is being modeled. For example, if a system is designed to model and quantify transport across barrier tissues, it becomes important to verify the integrity of tight junctions that comprise the barrier. There are several ways to approach the question. One approach could be assessing tight junction viability through the quantification of tight-junction protein expression.¹⁶ Measuring the transepithelial resistance (TEER) across a tissue barrier is another acceptable option for evaluation in real-time.⁹³ Another might be monitoring the passage of a labeled compound (e.g., by fluorescence or a radiolabeled tracer such as mannitol). These measures would be less useful in non-barrier tissues illustrating the need to validate tissue functions that are relevant to the experimental model.

Tissue validation should include comparisons to an appropriate baseline as well as appropriate controls. The answer to the question of ‘what constitutes functional and viable tissue?’ may not be simple, and depends on the tissue being studied and the context of the experiment. Simple measures of cell health that only quantify cell death and proliferation may be insufficient. These measures, by themselves, are not robust indicators of biological validity or physiological relevance, particularly when the aim of the model is to represent a complex organ system. Additionally, markers of tissue integrity are often compared to past in vitro studies. While this may have some value, in vitro markers of viability ideally should be compared to rates derived from in vivo observation. Creating controls may be as simple as including parallel microfluidic devices during studies when sufficient tissue is available but may also require more creative methods with tissue supplies are limited. The value of all ex vivo systems will be in their predictive validity for events that occur in vivo.

Conclusions:

Collaboration between engineers and biologists will be key moving forward to design microfluidic devices of the future. Such devices will maintain physiologically relevant environments, while still offering cost effective and time-efficient device generation. The accuracy of models for in vivo physiology is important for designing organ-on-chip microfluidic devices with heuristic value. For commercialization, it would be helpful for models to be scalable and offer high throughput results. Scalability for organotypic systems presents a challenge, but one that can be overcome with advances in device technologies, and further understanding of the physiological demands for tissue-on-chip.

Further utilization of microfluidic technologies and optimization of organ/tissue physiology ex vivo will no doubt yield more relevant tissue models than static culture systems. Controlling for the myriad variables in tissue viability, cell-cell interactions, and extracellular matrix and signaling molecules will be an important challenge. The microfluidic designs of the future will likely improve the efficacy of microfluidic models for applications such as drug development and personalized medicine.

A recent survey shows that approximately 90% of all drugs entering clinical trials are not approved.⁹⁴ Estimates for the cost of bringing a drug to market have risen to \$2.6 billion dollars.⁹⁴ A significant portion of this cost is attributed to the high rate of rejection for drugs that were identified as viable candidates through high-throughput cell culture screening and in vivo animal research. Rejection is often due to unforeseen toxicity, unintended interactions, or lack of efficacy. It has become evident that the current methodologies for pre-clinical research is insufficient and do not accurately capture the complexity of heterogeneous cellular interactions that occur within the human body. Cell-line based assays and in vivo animal testing will continue to serve an essential role in drug development. Ex vivo tissue culture systems can provide supplementary techniques for intermediate test-beds between preclinical and clinical testing.

Adapting microfluidic technology to tissue culture systems will make them more accurate, useful, and attractive for the testing of mechanisms and translation to the pharmaceutical industry and clinical settings.

References:

- 1) Pampaloni F, Reynaud EG, Stelzer EHK. The third dimension bridges the gap between cell culture and live tissue. *Nat. Rev. Mol. Cell Biol.* 2007;8:839.
- 2) Shamir ER and Ewald AJ. Three-dimensional organotypic culture: experimental models of mammalian biology and disease. *Nat. Rev. Mol. Cell Biol.* 2014;15:647.
- 3) Astolfi M, Péant B, Lateef MA, Rousset N, Kendall-Dupont J, Carmona E, Monet F, Saad F, Provencher D, Mes-Masson A-M, Gervais T. Micro-dissected tumor tissues on chip: an ex vivo method for drug testing and personalized therapy. *Lab on a chip.* 2015; 16:312-25.
- 4) Dawson A, Dyer C, Macfie J, Davies J, Karsai L, Greenman J, Jacobsen M. A microfluidic chip based model for the study of full thickness human intestinal tissue using dual flow. *Biomicrofluidics.* 2016; 10.
- 5) Dodson KH, Echevarria FD, Li D, Sappington RM, Edd JF. Retina-on-a-chip: a microfluidic platform for point access signaling studies. *Biomedical microdevices.* 2015; 17:114.
- 6) Komeya M, Kimura H, Nakamura H, Yokonishi T, Sato T, Kojima K, Hayashi K, Katagiri K, Yamanaka H, Sanjo H, Yao M, Kamimura S, Inoue K, Ogonuki N, Ogura A, Fujii T, Ogawa T. Long-term ex vivo maintenance of testis tissues producing fertile sperm in a microfluidic device. *Scientific reports.* 2016; 6:21472.
- 7) Prodanov L, Jindal R, Bale SS, Hegde M, Mccarty WJ, Golberg I, Bhushan A, Yarmush ML, Usta OB. Long-term maintenance of a microfluidic 3D human liver sinusoid. *Biotechnology and Bioengineering.* 2016;113:241-6.
- 8) Ross AE, Belanger MC, Woodroof JF, Pompano RR. Spatially resolved microfluidic stimulation of lymphoid tissue ex vivo. *Analyst.* 2016.

- 9) Yasotharan S, Pinto S, Sled JG, Bolz S-S, Günther A. Artery-on-a-chip platform for automated, multimodal assessment of cerebral blood vessel structure and function. *Lab on a chip*. 2015; 15:2660-9.
- 10) van Midwoud PM, Groothuis GMM, Merema MT, Verpoorte E. Microfluidic biochip for the perfusion of precision-cut rat liver slices for metabolism and toxicology studies. *Biotechnol. Bioeng*. 2010;105:184–194.
- 11) Masters JR and Stacey GN. Changing medium and passaging cell lines. *Nat. Protoc*. 2007;2:2276–2284.
- 12) Whitesides GM. The origins and the future of microfluidics. *Nature*. 2006; 442:368-73.
- 13) van Duinen V, Trietsch SJ, Joore J, Vulto P, Hankemeier T. Microfluidic 3D cell culture: From tools to tissue models. *Current Opinion in Biotechnology*. 2015; 35:118-26.
- 14) Chen Y, Lin Y, Davis KM, Wang Q, Rnjak-Kovacina J, Li C, Isberg RR, Kumamoto Ca, Meccas J, Kaplan DL. Robust bioengineered 3D functional human intestinal epithelium. *Scientific Reports*. 2015; 5:13708.
- 15) Kim HJ, Li H, Collins JJ, Ingber DE, Beebe DJ, Ismagilov RF. Contributions of microbiome and mechanical deformation to intestinal bacterial overgrowth and inflammation in a human gut-on-a-chip. *Pnas*. 2015; 113(1): E7-E15.
- 16) Shah P, Fritz JV, Glaab E, Desai MS, Greenhalgh K, Frchet A, Niegowska M, Estes M, Jager C, Seguin-Devaux C, Zenhausern F, Wilmes P. A microfluidics-based in vitro model of the gastrointestinal human-microbe interface. *Nature communications*. 2016; 7:11535.
- 17) O'Malley D. Neuroimmune Cross Talk in the Gut. Neuroendocrine and neuroimmune pathways contribute to the pathophysiology of irritable bowel syndrome. *Am. J. Physiol*. 2016;311:G934–G941.
- 18) Schwerdtfeger LA, Ryan EP, Tobet SA. An organotypic slice model for ex vivo study of

neural, immune, and microbial interactions of mouse intestine. *Am J Physiol Gastrointest Liver Physiol.* 2016;310(4):G240-248.

- 19) Li M, de Graaf IA, Groothuis GM. Precision-cut intestinal slices: alternative model for drug transport, metabolism, and toxicology research. *Expert Opin Drug Metab Toxicol.* 2016; 12(2): 175-90.
- 20) Yissachar N, Zhou Y, Ung L, Chiu IM, Mathis D, Benoist C, Yissachar N, Zhou Y, Ung L, Lai NY, Mohan JF, Ehrlicher A, Weitz DA. An Intestinal Organ Culture System Uncovers a Role for the Nervous System in Microbe-Immune Crosstalk. *Cell.* 2017; 168(6): 1135-48.e12.
- 21) Xiao S, Coppeta JR, Rogers HB, Isenberg BC, Zhu J, Olalekan SA, McKinnon KE, Dokic D, Rashedi AS, Haisenleder DJ, Malpani SS, Arnold-Murray CA, Chen K, Jiang M, Bai L, Nguyen CT, Zhang J, Laronda MM, Hope TJ, Maniar KP, Pavone ME, Avram MJ, Sefton EC, Getsios S, Burdette JE, Kim JJ, Borenstein JT, Woodruff TK. A microfluidic culture model of the human reproductive tract and 28-day menstrual cycle. *Nature communications.* 2017; 8:14584.
- 22) Atac B, Wagner I, Horland R, Lauster R, Marx W, Tonevitsky AG, Azar RP, Lindner G. Skin and hair on-a-chip: in vitro skin models versus ex vivo tissue maintenance with dynamic perfusion. *Lab Chip.* 2013;13:3555–3561.
- 23) Guy T, Rupert AE, Sandberg M, Weber SG. A simple method for measuring organotypic tissue slice culture thickness. *J. Neurosci. Methods,* 2011, 199:78–81.
- 24) Swim HE. Microbiological Aspects of Tissue Culture. *Annu. Rev. Microbiol.* 1959;13:141–176.
- 25) Kim L, Toh YC, Voldman J, Yu H. A practical guide to microfluidic perfusion culture of adherent mammalian cells. *Lab on a chip.* 2007; 7(6): 681-94.

- 26) Azuaje-Hualde E, García-Hernando M, Etxebarria- Elezgarai J, De Pancorbo MM, Benito-Lopez F, Basabe-Desmouts L. Microtechnologies for Cell Microenvironment Control and Monitoring. *Micromachines*. 2017;8:166.
- 27) Keenan TM and Folch A. Biomolecular Gradients in Cell Culture Systems. *Lab Chip*. 2008;8:34–57.
- 28) Longmuir IS and A. Bourke A. The measurement of the diffusion of oxygen through respiring tissue. *Biochem J*. 1960;76:225–229.
- 29) de Kanter R, Monshouwer M, Draaisma AL, De Jager MH, de Graaf IA, Proost JH, Meijer DK, Groothuis GM. Prediction of whole-body metabolic clearance of drugs through the combined use of slices from rat liver, lung, kidney, small intestine and colon. *Xenobiotica*. 2004;34:229–241.
- 30) Tobet SA, Walker HJ, Seney ML, Yu KW. Viewing cell movements in developing neuroendocrine brain. *Integr Comp Biol*. 2003(43): 794-801.
- 31) Wu J, Mao Z, Tan H, Han L, Ren T, Gao C. Gradient biomaterials and their influences on cell migration. *Interface Focus*. 2012;2:337–355.
- 32) Khan AA, Suits JMT, Kandel RA, Waldman SD. The effect of continuous culture on the growth and structure of tissue-engineered cartilage. *Biotechnol. Prog.* 2009; 25:508–515.
- 33) Frahm KA, Clay CM, Tobet SA. Characterization of an ovarian slice model in vitro to view ovulation (Abstract). *Biol Reprod*. 2010(83): 66.
- 34) Halldorsson S, Lucumi E, Gómez-Sjöberg R, Fleming RMT. Advantages and challenges of microfluidic cell culture in polydimethylsiloxane devices. *Biosens. Bioelectron*. 2014; 63:218–231.
- 35) Finelli CM, Helmuth BST, Pentcheff ND, Wetthey DS. Water flow influences oxygen transport and photosynthetic efficiency in corals. *Coral Reefs*. 2005;25:47-57.

- 36) De Beer D, Stoodley P, Lewandowski Z. Liquid flow and mass transport in heterogeneous biofilms. *Water Res.* 1996;30:2761–2765.
- 37) Hidalgo IJ, Hillgren KM, Grass GM, Borchardt RT. Characterization of the unstirred water layer in Caco-2 cell monolayers using a novel diffusion apparatus. *Pharm. Res.* 1991;8:222-227
- 38) Fröhlich M, Grayson WL, Marolt D, Gimble JM, Kregar-Velikonja N, Vunjak-Novakovic G. Bone Grafts Engineered from Human Adipose-Derived Stem Cells in Perfusion Bioreactor Culture. *Tissue Eng Part A.* 2010;16:179–189.
- 39) Dusny C and Schmid A. Microfluidic single-cell analysis links boundary environments and individual microbial phenotypes. *Environ. Microbiol.* 2015;17:1839–1856.
- 40) Radisic M, Marsano A, Maidhof R, Wang Y, Vunjak- Novakovic G. Cardiac tissue engineering using perfusion bioreactor systems. *Nat. Protoc.* 2008;3,719.
- 41) Moore MC, Coate KC, Winnick JJ, An Z, Cherrington AD. Regulation of Hepatic Glucose Uptake and Storage In Vivo. *Adv. Nutr.* 2012;3:286–294.
- 42) Lomax MA and Baird GD. Blood flow and nutrient exchange across the liver and gut of the dairy cow. *Br. J. Nutr.* 1983;49:481–496.
- 43) Freckmann G, Hagenlocher S, Baumstark A, Jendrike N, Gillen RC, Rössner K, Haug C. Continuous glucose profiles in healthy subjects under everyday life conditions and after different meals. *J Diabetes Sci Technol.* 2007;1(5):695–703.
- 44) Antoni D, Burckel H, Josset E, Noel G. Three-dimensional cell culture: a breakthrough in vivo. *Int. J. Mol. Sci.* 2015;16:5517–5527.
- 45) Willard-Mack CL. Normal structure, function, and histology of lymph nodes. *Toxicologic pathology.* 2006; 34:409-24.

- 46) Sung KE, Yang N, Pehlke C, Keely PJ, Eliceiri KW, Friedl A, Beebe DJ. Transition to invasion in breast cancer: a microfluidic in vitro model enables examination of spatial and temporal effects. *Integr. Biol.* 2011;3:439–450.
- 47) Wydallis JB, Feeny RM, Wilson W, Kern T, Chen T, Tobet S, Reynolds MM, Henry CS. Spatiotemporal norepinephrine mapping using a high-density CMOS microelectrode array. *Lab on a chip.* 2015; 15(20):4075-82.
- 48) Wevers NR, van Vught R, Wilschut KJ, Nicolas A, Chiang C, Lanz HL, Trietsch SJ, Joore J, Vulto P. High-throughput compound evaluation on 3D networks of neurons and glia in a microfluidic platform. *Sci Rep.* 2016; 6:38856.
- 49) Ciftlik AT, Lehr H-A, Gijs MAM . Microfluidic processor allows rapid HER2 immunohistochemistry of breast carcinomas and significantly reduces ambiguous (2+) read-outs. *Proc Natl Acad Sci USA.* 2013;110:5363–5368.
- 50) Hou X, Zhang YS, Trujillo-de Santiago G, Alvarez MM, Ribas J, Jonas SJ, Weiss PS, Andrews AM, Aizenberg J, Khademhosseini A. Interplay between materials and microfluidics. *Nat. Rev. Mater.* 2017;2(5):17016.
- 51) Kim JA, Kim HN, Im SK, Chung S, Kang JY, Choi N. Collagen-based brain microvasculature model in vitro using three-dimensional printed template. *Biomicrofluidics.* 2015;9(2):024115.
- 52) Satoh T, Narazaki G, Sugita R, Kobayashi H, Sugiura S, Kanamori T. A pneumatic pressure-driven multi-throughput microfluidic circulation culture system SUPP. *Lab on a chip.* 2016;16:2339-48.
- 53) Wang X, Yi L, Roper MG. Microfluidic device for the measurement of amino acid secretion dynamics from murine and human islets of Langerhans. *Analytical Chemistry.* 2016;88: 3369-3375

- 54) Shirure VS and George SC. Design considerations to minimize the impact of drug absorption in polymer-based organ-on-a-chip platforms. *Lab on a Chip*. 2017;17:681–690.
- 55) Chen T, Gomez-escoda B, Munoz-garcia J, Babic J, Griscom L, Wu P-yJ, Coudreuse D, Wu P-yJ. A drug-compatible and temperature- controlled microfluidic device for live-cell imaging. *Open Biology*. 2016; 6:160156.
- 56) Futrega K, Yu J, Jones JW, Kane MA, Lott WB, Atkinson K, Doran MR. Polydimethylsiloxane (PDMS) modulates CD38 expression, absorbs retinoic acid and may perturb retinoid signalling. *Lab on a Chip — Miniaturisation for Chemistry and Biology*. 2016;16(8):1473-1483.
- 57) Lopacinska JM, Emneus J, Dufva M. Poly(Dimethylsiloxane) (PDMS) Affects Gene Expression in PC12 Cells Differentiating into Neuronal-Like Cells. *PloS One*. 2013;8:e53107.
- 58) van Midwoud PM, Janse A, Merema MT, Groothuis GM, Verpoorte E. Comparison of biocompatibility and adsorption properties of different plastics for advanced microfluidic cell and tissue culture models. *Anal Chem*. 2012; 84:3938-44.
- 59) Leclerc E, Duval JL, Egles C, Ihida S, Toshiyoshi H, Tixier-Mita As. In vitro cytobiocompatibility study of thin-film transistors substrates using an organotypic culture method. *Journal of Materials Science: Materials in Medicine*. 2017; 28:0-1.
- 60) Toepke MW, Beebe DJ. PDMS absorption of small molecules and consequences in microfluidic applications. *Lab on a chip*. 2006; 6:1484-6.
- 61) van Meer BJ, de Vries H, Firth KSA, van Weerd J, Tertoolen LGJ, Karperien HBJ, Jonkheijm P, Denning C, Ijzerman AP, Mummery CL. Small molecule absorption by PDMS in the context of drug response bioassays. *Biochemical and biophysical research communications*. 2017; 482:323-8.

- 62) Berenguel-Alonso M, Sabés-Alsina M, Morató R, Ymbern O, Rodríguez-Vázquez L, Talló-Parra O, Alonso-Chamarro J, Puyol M, López-Béjar M. Rapid Prototyping of a Cyclic Olefin Copolymer Microfluidic Device for Automated Oocyte Culturing. *SLAS TECHNOLOGY: Translating Life Sciences Innovation*. 2017;47.
- 63) Berthier E, Young EW, Beebe D. Engineers are from PDMS-land, Biologists are from Polystyrenia. *Lab on a chip*. 2012; 121224-37.
- 64) Young EWK and Beebe DJ. Fundamentals of microfluidic cell culture in controlled microenvironments. *Chem. Soc. Rev.* 2010;39:1036–1048.
- 65) Wagner I, Materne EM, Brincker S, Sussbier U, Fradrich C, Busek M, Sonntag F, Sakharov DA, Trushkin EV, Tonevitsky AG, Lauster R, Marx U. A dynamic multi-organ-chip for long-term cultivation and substance testing proven by 3D human liver and skin tissue co-culture. *Lab Chip*. 2013;13:3538–3547.
- 66) Mather JP and Roberts PE. *Introduction to Cell and Tissue Culture*, Springer, US, 1998.
- 67) Van der Valk J, Brunner D, De Smet K, Fex Svenningsen A, Honegger P, Knudsen LE, Lindl T, Noraberg J, Price A, Scarino ML, Gstraunthaler G. Optimization of chemically defined cell culture media—replacing fetal bovine serum in mammalian in vitro methods. *Toxicology in vitro : an international journal published in association with BIBRA*. 2010; 24(4): 1053-63.
- 68) Martin BM. *Tissue Culture Techniques*, Birkhäuser Basel, 1 edn, 1994.
- 69) Drakou K and Georgiades P. A serum-free and defined medium for the culture of mammalian postimplantation embryos. *Biochem. Biophys. Res. Commun.* 2015;468:813–819.
- 70) Navratil AM, Knoll JG, Whitesell JD, Tobet SA, Clay CM. Neuroendocrine plasticity in the anterior pituitary: gonadotropin-releasing hormone-mediated movement in vitro and in vivo. *Endocrinology*. 2007; 148(4): 1736-44.

- 71) Brewer GJ, Torricelli JR, Evege EK, Price PJ. Optimized survival of hippocampal neurons in B27-supplemented neurobasal, a new serum-free medium combination. *J Neurosci Res.* 1993;35:567–576.
- 72) Schwerdtfeger LA, Nealon NJ, Ryan EP, Tobet SA. Human colon function ex vivo: Dependence on oxygen and sensitivity to antibiotic. *PloS one.* 2019; 14(5): e0217170.
- 73) Rashidi H, Alhaque S, Szkolnicka D, Flint O. and Hay DC. Fluid shear stress modulation of hepatocyte-like cell function. *Arch Toxicol.* 2016;90:1757–1761
- 74) Chiu JJ and Chien S. Effects of Disturbed Flow on Vascular Endothelium: Pathophysiological Basis and Clinical Perspectives. *Physiol. Rev.* 2011;91:327–387.
- 75) Liu J, Bi X, Chen T, Zhang Q, Wang SX, Chiu JJ, Liu GS, Zhang Y, Bu P, Jiang F. Shear stress regulates endothelial cell autophagy via redox regulation and Sirt1 expression. *Cell Death Dis.* 2015;6:e1827.
- 76) Kim KM, Choi YJ, Hwang JH, Kim AR, Cho HJ, Hwang ES, Park JY, Lee SH, Hong JH. Shear stress induced by an interstitial level of slow flow increases the osteogenic differentiation of mesenchymal stem cells through TAZ activation. *PloS One.* 2014;9:e92427.
- 77) Sun YS. Comparison of Chip Inlet Geometry in Microfluidic Devices for Cell Studies. *Molecules.* 2016;21:778.
- 78) Kelly CJ, Colgan SP. Breathless in the Gut: Implications of Luminal O₂ for Microbial Pathogenicity. *Cell Host Microbe.* 2016; 19(4): 427-8.
- 79) Carreau A, El Hafny-Rahbi B, Matejuk A, Grillon C, Kieda C. Why is the partial oxygen pressure of human tissues a crucial parameter? Small molecules and hypoxia. *J Cell Mol Med.* 2011; 15(6): 1239-53.
- 80) Sitkovsky M and Lukashev D. Regulation of immune cells by local-tissue oxygen tension: HIF1 alpha and adenosine receptors. *Nat. Rev. Immunol.* 2005;5:712–721

- 81) Rios C, D'Ippolito G, Curtis KM, Delcroix GJR, Gomez LA, El Hokayem J, Rieger M, Parrondo R, de Las Pozas A, Perez-Stable C, Howard GA, Schiller PC. Low Oxygen Modulates Multiple Signaling Pathways, Increasing Self-Renewal, While Decreasing Differentiation, Senescence, and Apoptosis in Stromal MIAMI Cells. *Stem Cells Dev.* 2016;25:848–860.
- 82) Oomen PE, Skolimowski M, Verpoorte S. Implementing Oxygen Control in Chip-Based Cell and Tissue Culture Systems. *Lab on a chip.* 2016; 163394-414.
- 83) Zheng L, Kelly CJ, Colgan SP. Physiologic hypoxia and oxygen homeostasis in the healthy intestine. A Review in the Theme: Cellular Responses to Hypoxia. *American journal of physiology Cell physiology.* 2015; 309(6): C350-60.
- 84) Albenberg L, Esipova TV, Judge CP, Bittinger K, Chen J, Laughlin A, Grunberg S, Baldassano RN, Lewis JD, Li H, Thom SR, Bushman FD, Vinogradov SA, Wu GD. Correlation between intraluminal oxygen gradient and radial partitioning of intestinal microbiota. *Gastroenterology.* 2014; 147(5): 1055-63 e8.
- 85) Nashimoto Y, Hayashi T, Kunita I, Nakamasu A, Torisawa Y, Nakayama M, Takigawa-Imamura H, Kotera H, Nishiyama K, Miura T, Yokokawa R. Integrating perfusable vascular networks with a three-dimensional tissue in a microfluidic device. *Integr. Biol.* 2017;9:506–518
- 86) Oh S, Ryu H, Tahk D, Ko J, Chung Y, Lee HK, Lee TR, Jeon NL. “Open-top” microfluidic device for in vitro three-dimensional capillary beds. *Lab Chip.* 2017;17:3405–3414.
- 87) K. V. Moser, R. Schmidt-Kastner, H. Hinterhuber and C. Humpel, Brain capillaries and cholinergic neurons persist in organotypic brain slices in the absence of blood flow. *Eur J Neurosci*, 18 (2003), pp. 85-94.

- 88) Dash A, Maine IP, Varambally S, Shen R, Chinnaiyan AM, Rubin MA. Changes in differential gene expression because of warm ischemia time of radical prostatectomy specimens. *Am J Pathol.* 2002;161:1743–1748.
- 89) Grizzle WE, Bell WC, Sexton KC. Issues in collecting, processing and storing human tissues and associated information to support biomedical research. *Cancer Biomark.* 2011;9:531–49.
- 90) Senior PV, Pritchett CJ, Sunter JP, Appleton DR, Watson aJ. Crypt regeneration in adult human colonic mucosa during prolonged organ culture. *Journal of anatomy.* 1982; 134459-69.
- 91) Asano M, Yamamoto T, Tsuruta T, Nishimura N, Sonoyama K. Dual labeling with 5-bromo-2'-deoxyuridine and 5-ethynyl-2'-deoxyuridine for estimation of cell migration rate in the small intestinal epithelium. *Development, growth & differentiation.* 2015; 57(1): 68-73.
- 92) Ahlgren H, Henjum K, Ottersen OP, Rundén-Pran E. Validation of organotypical hippocampal slice cultures as an ex vivo model of brain ischemia: Different roles of NMDA receptors in cell death signalling after exposure to NMDA or oxygen and glucose deprivation. *Cell and tissue research.* 2011; 345329-41.
- 93) Srinivasan B, Kolli AR, Esch MB, Abaci HE, Shuler ML, Hickman JJ. TEER measurement techniques for in vitro barrier model systems. *J Lab Autom.* 2015;20: 107-126.
- 94) Langley GR, Adcock IM, Busquet F, Crofton KM, Csernok E, Giese C, Heinonen T, Herrmann K, Hofmann-Apitius M, Landesmann B, Marshall LJ, Mclvor E, Muotri AR, Noor F, Schutte K, Seidle T, van de Stolpe A, Van Esch H, Willett C, Woszczek G. Towards a 21st-century roadmap for biomedical research and drug discovery: consensus report and recommendations. *Drug Discov Today.* 2017; 22(2): 327-39.

CHAPTER 4 – A MICROFLUIDIC ORGANOTYPIC DEVICE FOR CULTURE OF MAMMALIAN INTESTINES EX VIVO⁴

Overview:

The physiological characteristics of the gastrointestinal (GI) tract are diverse and include rapid rates of epithelial turnover, complex nervous and immune systems, a thick mucus layer, and a large microbial population. Most GI models in vitro rely upon cell lines or organoids and consequently lack the diversity of cells and microorganisms present in vivo. In vivo studies retain function and cellular diversity but are more difficult to control. Microfluidic tissue-on-a-chip devices provide powerful alternatives for modeling physiological systems. Such devices show promise for use in GI research; however, most models use non-physiologic culture environments with higher than in vivo oxygen levels and insufficient gut microbiota. Our goal is to create a bridge between in vitro and in vivo using microfluidic devices by incorporating ex vivo tissue explants in physiologically relevant environments. Here, we report a microfluidic organotypic device (MOD) that enables media flow with differential oxygen concentrations across luminal and muscular surfaces of gut tissue ex vivo. Tissue was shown to be viable for 72 h and lowering oxygen concentration to a more physiologic level impacted bacterial populations.

Introduction:

Intestinal tissue is composed of a complex network of epithelial, neural, immune, muscular, and vascular components.¹ Bacteria that inhabit the intestinal lumen are major contributors to maintaining intestinal homeostasis. An imbalance in microbial communities (dysbiosis) is associated with a variety of local tissue diseases such as inflammatory bowel

⁴ Richardson A, Schwerdtfeger LA, Eaton D, McLean I, Henry CS, Tobet SA. A microfluidic organotypic device for culture of mammalian intestines ex vivo. *Analytical Methods*. 2020;12,297-303.

(IBD) and celiac disease.^{2,3} More globally, dysbiosis influences disorders ranging from cardiovascular disease to brain function.^{4,5} For *in vitro* and *ex vivo* intestinal models, cellular diversity and recapitulation of the *in vivo* environment is paramount to better understanding the relationship between dysbiosis and disease. For instance, bacterial cell products can activate intestinal neurons, leading to the release of inflammatory cytokines associated with IBD.⁶ Traditional *in vitro* cell culture can recapitulate some aspects of intestinal physiology and is useful for high throughput screening, but these models often rely upon cell monolayers to represent the intestinal barrier. Cell monolayers lack the *in vivo* cellular diversity from both a mammalian host and bacterial perspective and do not accurately represent the three-dimensional architecture of the intestinal wall.^{7,8} Three-dimensional intestinal organoids overcome some of these limitations by integrating multiple epithelial cell subtypes and exhibiting villus/crypt organization, but they are generally missing the neural, immune, and muscular components of the gut wall.^{8,9}

Improving upon static transwell models, 'gut-on-a-chip' microfluidic devices have been developed that allow media to be continuously perfused across opposing sides of a cell-seeded porous membrane representing the intestinal epithelial barrier.¹⁰⁻¹³ The incorporation of microfluidics in these devices improves cellular viability and longevity, constantly removes toxic cellular waste, and allows for controlled nutrient delivery.¹⁴ Recently, microbes have been incorporated into some *in vitro* microfluidic intestinal models by generating an oxygen gradient between microfluidic channels.¹⁵⁻¹⁹

Organotypic intestinal culture models are an attractive middle ground between *in vitro* and *in vivo* systems because they include the three-dimensional architecture of the gut wall while still providing easily controllable experimental parameters.²⁰ *Ex vivo* models of various tissues have been successfully used in microfluidic devices previously.²¹⁻²⁵ *Ex vivo* models, however, are generally low-throughput compared to cell-monolayer cultures and many have

limited long-term tissue viability.^{8,26} The Ussing chamber is a well-established *ex vivo* model for studying trans-epithelial drug, nutrient, and ion transport. While the Ussing chamber is valuable for pharmacokinetic/pharmacodynamic studies, viable epithelial tissue can only be maintained for several hours,^{27,28} making these models inappropriate for long-term host tissue-microbiome interaction studies.²⁹ In this report, we describe the design and testing of a microfluidic organotypic device (MOD) for use with mammalian intestinal explants *ex vivo*. The MOD houses full-thickness mouse intestinal tissue, including muscular, neural, immune, and epithelial components. The MOD system was used to maintain mouse intestinal explants for 72 h and showed differential bacterial growth as a function of oxygen concentration.

Methods:

Device prototypes were designed in SolidWorks (Dassault Systemes, Waltham, MA) and 3D printed with a Form 2 SLA printer (Formlabs, Somerville, MA). Once a final device design was established, the MOD was manufactured via injection molding (Applied Medical, Rancho Santa Margarita, CA) using cyclic olefin copolymer (COC; TOPAS Grade 8007) as material. All devices used during tissue testing were injection molded. Injection molding was chosen over other microfluidic device manufacturing methods because of its reproducibility and potential for large-scale manufacturing.³⁰ COC was chosen because of its biocompatibility, high chemical resistance, low oxygen permeability, and excellent optical properties.³¹⁻³³

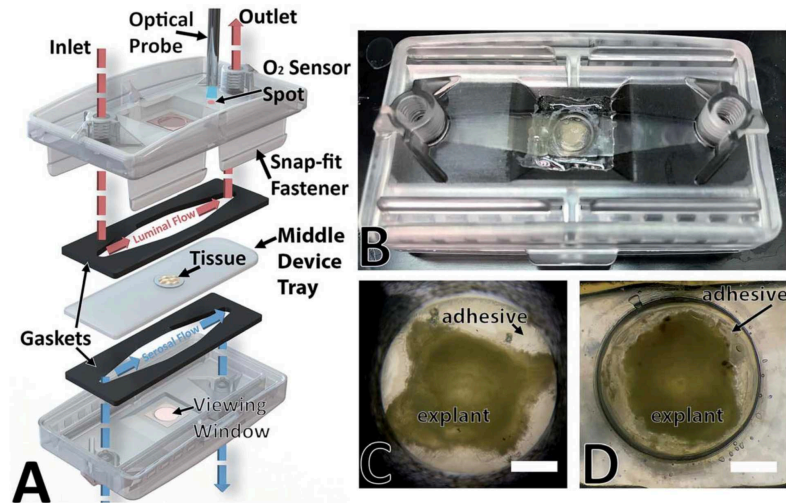


Figure 13. Schematic illustration of the MOD design and maintenance of tissue explants *ex vivo*. (A) an exploded model of the MOD system showing luminal (red) and serosal (blue) flow paths. (B) image of mouse colon explant inside the MOD. (C) image of colon explant tissue at 0h *ex vivo* through the viewing window. (D) image of different colon explant tissue at 72 h *ex vivo* through viewing window. Scale bars in C and D are 2 mm.

The MOD (Figure 13A) consists of three COC layers separated by polyurethane gaskets (PORON® AquaPro™, Rogers Corporation, Chandler, AZ); the gaskets define independent fluidic channels (10 mm wide, 1.1 mm deep, ~ 50 mm long, ~ 450 μ L). Intestinal tissue is housed in the middle layer such that the mucosa and serosa face independent channels. The edge of the tissue is supported by a thin lip molded into the middle layer, eliminating the need for a porous membrane. The top layer was designed with integrated snap-fit fasteners for rapid, reversible assembly (Video S1), which is crucial to minimizing the time tissue explants are without media. Unlike other fasteners, snap-fit fasteners can be injection molded and enable consistent assembly regardless of the user. Both the top and bottom layers contain threaded inlet and outlet ports that connect to 10-32 PEEK finger-tight fittings (IDEX Health & Science, LLC, Oak Harbor, WA). Rubber O-rings were installed at the base of each port to ensure airtight leakproof connections (IDEX Health & Science, LLC, Oak Harbor, WA). Glass coverslips (VWR,

Radnor, PA) were fixed on the top and bottom layers using cyanoacrylate glue (Krazy Glue, Elmers Products, High Point, NC) directly above the tissue to enable on-chip imaging and tissue visualization (VWR, Radnor, PA). Quick setting epoxy was applied around the edges of the coverslips to further prevent leakage and the top and bottom layers were placed in a 65° C oven for 15 min.

As a first step in instrumenting the device, oxygen sensor spots (OptiEnz, Fort Collins, CO) were adhered to the inner surface of the top layer downstream of the tissue chamber. The sensor's response was measured at two dissolved oxygen concentrations (DOC) using an external fiber optic probe (OptiEnz, Fort Collins, CO) to allow for the estimation of real-time DOC using the Stern-Volmer relationship:

$$\frac{\tau_0}{\tau} = 1 + K_{SV}[O_2] \quad , \quad (1)$$

where τ_0 is the luminescent decay time in the absence of oxygen, τ is the luminescent decay time in the presence of oxygen, K_{SV} is the Stern-Volmer constant, and $[O_2]$ is the oxygen concentration. Fluorescence of an oxygen-sensitive compound on the sensor spot is quenched in the presence of oxygen, leading to a reduction in luminescent decay time.³⁴

After assembly, each device was tested for failure modes, sterilized, and placed in a sterile environment until use. All fittings, ferrules, and tubing were submerged in diluted (1:10) bleach for 10 min, rinsed thoroughly with DI water, placed in a soapy water bath and vigorously scrubbed. After a second DI water rinse, the components and devices were submerged in a 70% ethanol solution containing 0.1% benzalkonium chloride for 30 min and rinsed with sterile water. Lastly, all other components including the gaskets and collection tubes were autoclaved at 120°C for 25 min. The devices could not be autoclaved due to COC's glass transition temperature of 78°C. Culture media was composed of CTS Neurobasal-A Medium (Thermo Fisher Scientific, Waltham, MA), 5% (v/v) 1M HEPES Buffer (Sigma Aldrich, St. Louis, MO), 2%

(v/v) B-27 Supplement (Thermo Fisher Scientific, Waltham, WA) and supplemented with 10 μM Nicardipine (Sigma Aldrich, St. Louis, MO), an L-type calcium ion channel blocker, that has previously been shown to block intestinal contractions *ex vivo*, a necessity when culturing intestinal tissue slices beyond 48 h.³⁵ For each device, two syringes were filled with media (one containing 99.3 μM fluorescein), connected to NE-300 syringe pumps (New Era Pump Systems Inc., Farmingdale, NY) and equilibrated in a 37°C incubator prior to experiments to remove any air bubbles formed by the expansion of dissolved gasses in the media. Mouse tissue was prepared as previously described³⁵ from mice approved under the Colorado State University IACUC protocol 17-720(A). Briefly, adult mice were sacrificed and the intestines were removed and placed in 4° C 1X Krebs buffer (in mM: 126 NaCl, 2.5 KCl, 2.5 CaCl₂, 1.2 NaH₂PO₄, 1.2 MgCl₂), and cut longitudinally along the mesenteric border to open the intestinal lumen and form a flat sheet of tissue. Tissue was free-hand dissected to form slices with a diameter of ~5 mm and placed in the center of the middle device layer. Cyanoacrylate glue was applied around the perimeter of the tissue to fill gaps between the tissue and plastic. While cyanoacrylate glue has been reported to be cytotoxic,³⁶ we only observed higher than expected levels of cell death where the glue directly contacted the tissue. After securing the tissue in the middle device layer, the device was quickly assembled by stacking successive layers separated by the gaskets and snapping them together. The devices were placed in a 37° C incubator, connected to syringes, and purged with media at a flow rate of 2.5 mL/hr. Media containing fluorescein was perfused through the luminal channel while media without fluorescein was perfused through the serosa facing channel. Once effluent media reached the collection tubes, the flow rate was reduced to 250 $\mu\text{L/hr}$ for the remainder of the experiments to provide low shear stress across the tissue. Collection tubes were changed every 10 h and immediately stored at -80°C. At the conclusion of experiments, tissue explants were removed from the devices and placed in media containing Ethidium Homodimer III (EtHD; Biotium, Hayward, CA) at a concentration of 2.5 μM

to evaluate cell death. After 30 min of incubation with EtHD, tissue explants were washed three times with culture media and fixed in 4% formaldehyde for a minimum of 8 h. Fixed tissue was washed with, and stored in, cold 0.05 M PBS until further analysis.

Fixed explants were sectioned at 50 μm thick on a vibrating microtome (VT1000s, Leica Microsystems, Wetzlar, Germany) before mounting on glass microscope slides. Imaging was performed on a Nikon TE2000-U inverted microscope (20x Plan-Apo objective) with a UniBlitz shutter system (Vincent Associates, Rochester, NY) and an Orca-flash 4.0 LT camera (Hamamatsu, Hamamatsu City, Shizuoka Prefecture, Japan).

Fluorescein quantities contained in culture media effluents were analyzed using an Epoch Gen5 Microplate Spectrophotometer (BioTek, Winooski, VT) with a wavelength of 488 nm. Absorbance was quantified in effluent media from both channels in 10 h increments, with hour 0 representing initial placement of explants into devices. Background signal from phenol red, a component of CTS Neurobasal Medium, was removed.

Results and Discussion:

Mouse colon explants were cultured in the MOD for up to 72 h *ex vivo* (in both low and ambient mucosal DOC) maintaining healthy, intact tissue, as marked by patterned rows of colonic crypts, with interspersed lamina propria and stereotypic arrangement of intestinal submucosal and muscular layers (Figure 14A, B, C). Minimal cell death was shown across 0h – 72h *ex vivo* (Figure 14D, E, F), indicated by labelling with EtHD. As expected, some EtHD was observed at the apical most epithelium, but not at the base of colonic crypts. Stem/progenitor cells at the base of colonic crypts proliferate and progeny migrate along the length of the crypt, towards the luminal aspect, before undergoing apoptosis and sloughing off into the intestinal lumen.³⁷ This cycle is continuously repeated to regenerate a new epithelium every 2-3 days in the mouse.³⁸ Minimal cell death observed throughout our explants during *ex vivo* culture,

coupled with the EtHD signal at the apical most aspect of the crypt, points towards healthy tissue undergoing normal epithelial turnover. While others have maintained mammalian intestines in microfluidic devices for up to 72 h,³⁹ evidence of tissue health was minimal. Another concern in many systems^{15, 39-41} is that serum-containing media with supplemented antibiotics was used to culture the tissue. A key advantage of the MOD is that we have maintained tissue in serum-free media, without antibiotics, and enables controlled substance delivery to the tissue as well as studying the role of bacteria on tissue health and physiology.

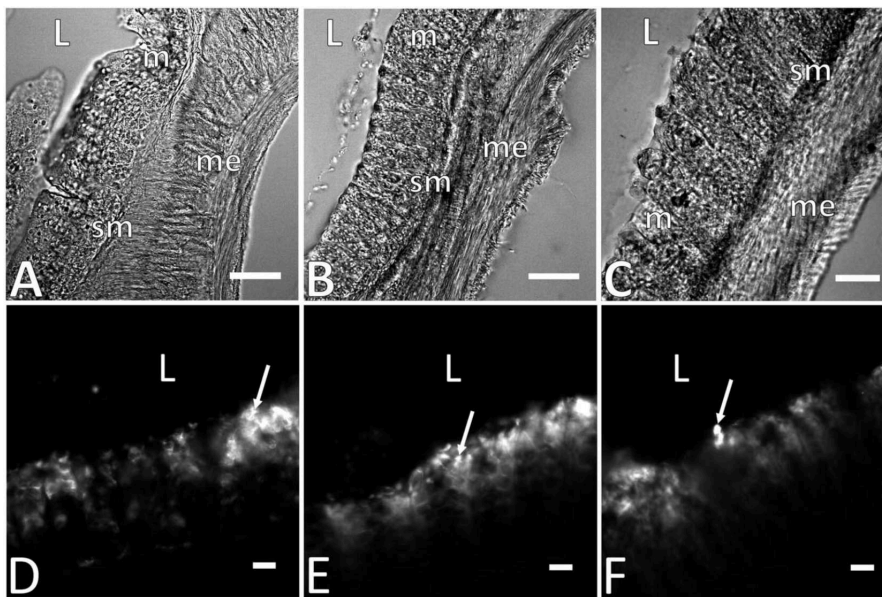


Figure 14. Tissue health was maintained for 72 h *ex vivo* in MOD in both ambient and low oxygen conditions. Brightfield images in A-C demonstrate patterned rows of colonic crypts, and stereotypic anatomical arrangement of gut wall musculature and submucosa at 0h (A), 72 h in ambient oxygen (B) and 72 h in low oxygen (C). Fluorescent images in D-F demonstrate EtHD labelling in colonic explants, with stereotypic signal observed at apical most aspect of colonic crypts (arrows) at 0h (D), 72 h in ambient oxygen (E) and 72h in low oxygen (F). 'L' denotes intestinal lumen, 'm' indicates mucosa, 'sm' submucosa, and 'me' muscularis externa. Scale bars in A and B are 100 μm , scale bar in C is 50 μm , and scale bars in D-F are 25 μm .

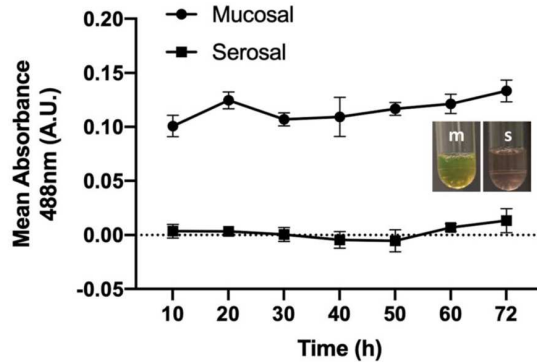


Figure 15. Media was separated across channels as marked by fluorescein absorbance in effluent media. Mean absorbance (A.U.) at 488 nm wavelength demonstrates significantly more fluorescein presence in mucosal (circular points) effluents compared to serosal (square points) ($P < 0.001$). No significant differences were observed across time in either the mucosal ($P > 0.20$) or serosal ($P > 0.45$) effluents. All statistical analyses were performed using a one-way ANOVA with $\alpha = .05$. Representative images show visible green color from fluorescein in mucosal (m) effluent compared to serosal (s) effluent.

In addition to maintaining viable tissue for 72 h, media was separated in independent microfluidic channels facing the mucosal and serosal sides of the tissue. Mean (+/- standard deviation) absorbance across all time points for luminal effluents was 0.11 ± 0.03 and 0.00 ± 0.02 for serosal effluents, indicating that media did not cross channels throughout the duration of the experiments (Figure 15). One potential concern is that fluorescein leakage could be diluted by the fluid flow, under the spectrophotometer's detection limit. Since fluorescein and fluorescein-isothiocyanate are commonly used to assess barrier permeability *in vivo*⁴² and *in vitro*,⁴³ any leakage below the detection limit is not biologically significant as an indication of barrier disruption. If media had crossed through the tissue, absorbance values would have increased substantially in the serosal effluent due to transfer or leakage of fluorescein across the tissue. The verification of media separation is a critical indicator that the gut wall tissue retained one of its most essential features *ex vivo*, that of a physical barrier with tight junctions

between cells. This helps ensure that pathogens, pharmaceuticals, and other compounds of interest for study *ex vivo* can only access tissue physiology by going through normal cellular processes (e.g., active transport, diffusion, cellular transfer). By comparison, in most organ-on-a-chip devices, a barrier is formed by a confluent cell monolayer without the underlying cellular diversity needed to understand intestinal physiology.

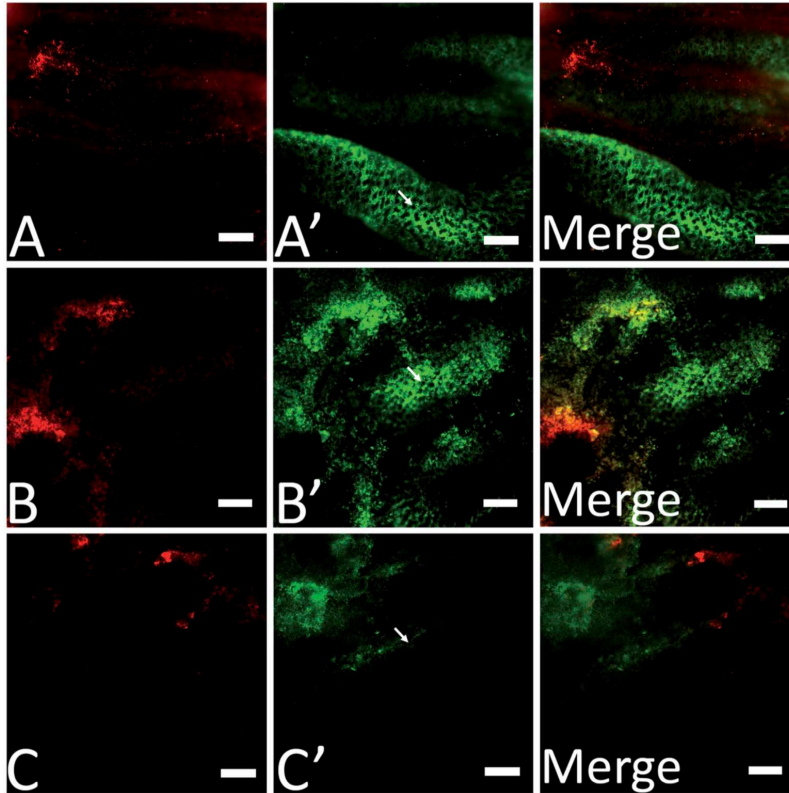


Figure 16. Microbiota were maintained in MOD, and more bacteria were visible in an explant cultured in lower oxygen conditions. Baseline bacterial levels are shown at 0h *ex vivo* via hexidium iodide (7.05 μM) fluorescence in red (A), signifying Gram-positive bacteria, and SYTO9 (5.01 μM) fluorescence in green (A'), signifying Gram-negative bacteria. Gram stain fluorescence was noticeably higher in tissue cultured in lowered oxygen conditions (B-B'; 3 mmHg) when compared to tissue cultured in ambient oxygen (C-C'; 100 mmHg) containing media. Arrows in A', B' and C' denote a single colonic crypt. Scale bars in all panels are 100

The MOD enabled recapitulation of the *in vivo* oxygen gradient across the epithelial layer. DOC in the luminal channel were maintained at 3.0 \pm 0.38 mmHg for 48 h using 0.5 M

sodium sulfite. *In vivo* intraluminal oxygen concentrations at the mucosal interface are nearly anoxic.⁴⁴ Perfusion of low oxygen-containing media within the luminal microfluidic channel increased bacterial presence on the tissue's mucosal surface compared to tissue perfused with media at ambient oxygen levels (~ 100 mmHg), as marked by fluorescent gram stain³⁵ (Figure 16A-F). Increases were most notable for gram-negative bacteria. Increased bacterial presence in a low oxygen environment was expected since many bacteria in the colon are anaerobic.⁴⁵ Therefore, recapitulation of the *in vivo* oxygen gradient is vital to studying host tissue interactions with a more diverse, physiologically relevant bacterial community. It is also important to note that these experiments are proof-of-principle. Quantifying specific bacteria and overall bacteria concentrations will be the focus of future reports.

Microfluidics provide a mechanism of tissue perfusion *ex vivo* that should allow for healthier tissue over longer periods.¹⁴ Previous *ex vivo* systems such as intestinal organotypic slices maintained tissue for 6 days, but without a true luminal barrier.³⁵ Other methods such as Ussing chambers maintain full thickness tissues with an intact barrier, but with limited viability over a few hours.²⁷ Using dual flow microfluidics, the MOD allows for the culture of full thickness explants with an intact barrier over an extended length of culture (3 days).

Future extensions to the MOD will include developing and integrating optical and/or electrochemical sensors for analytes relevant to the intestinal environment (i.e. glucose, lactate). Electrodes can be added to assess transepithelial electrical resistance, which has been a useful measure of barrier integrity in other systems.^{15,46,47} Ultimately, the MOD will be implemented in long-term microbiome studies to elucidate the relationship among microbial, epithelial, neuro and immune components of the gut wall in health and disease.

Conclusion:

In conclusion, a novel *ex vivo* microfluidic organotypic device was designed and tested. This system maintains viable polarized murine intestinal explants for 72 h *ex vivo* and enables a physiological oxygen gradient to be established between independent microfluidic channels rendering luminal and vascular compartments. The MOD bridges a substantial gap in current approaches to modeling barrier tissue as it overcomes several limitations associated with both *in vitro* and *in vivo* models. Due to the culture of full thickness explants, the MOD more closely recapitulates the *in vivo* physiology of the gut wall, as tissue explants include the complex cellular diversity and native tissue structural relationships of the gut wall. The MOD system offers a novel approach to culturing intestinal tissues with intact luminal barriers.

References:

- 1) Wells JM, Rossi O, Meijerink M, van Baarlen P. Epithelial crosstalk at the microbiota-mucosal interface. *Proc. Natl. Acad. Sci.* 2010; 108:4607–4614.
- 2) Ghaisas, S., Maher, J. & Kanthasamy, A. Gut microbiome in health and disease: Linking the microbiome–gut–brain axis and environmental factors in the pathogenesis of systemic and neurodegenerative diseases. *Pharmacol. Ther.* 2016;158:52–62.
- 3) Carding S, Verbeke K, Vipond DT, Corfe BM, Owen LJ. Dysbiosis of the gut microbiota in disease. *Microb Ecol Health Dis.* 2015; 26: 26191.
- 4) Shreiner AB, Kao JY, Young VB. The gut microbiome in health and disease. *Curr Opin Gastroenterol.* 2015;31:69–75.
- 5) Jiang H, Ling Z, Zhang Y, Mao H, Ma Z, Yin Y, Wang W, Tang W, Tan Z, Shi J. Altered fecal microbiota composition in patients with major depressive disorder. *Brain Behav. Immun.* 2015;48:186–194.
- 6) Bernardazzi C, Pêgo B, De Souza HSP. Neuroimmunomodulation in the Gut: Focus on Inflammatory Bowel Disease. *Mediators Inflamm.* 2016;1363818.
- 7) Lea T, in *The Impact of Food Bioactives on Health*, 2015, pp. 103–111.
- 8) Bein A, Shin W, Jalili-Firoozinezhad S, Park MH, Sontheimer-Phelps A, Tovaglieri A, Chalkiadaki A, Kim HJ, Ingber DE. Microfluidic Organ-on-a-Chip Models of Human Intestine. *Cell Mol Gastroenterol Hepatol.* 2018; 5(4): 659-68.
- 9) Schwerdtfeger LA, Tobet SA. From organotypic culture to body-on-a-chip: A neuroendocrine perspective. *J Neuroendocrinol.* 2019; 31(3): e12650.

- 10) Kim HJ, Ingber DE. Gut-on-a-Chip microenvironment induces human intestinal cells to undergo villus differentiation. *Integrative biology : quantitative biosciences from nano to macro*. 2013; 5(9): 1130-40.
- 11) Shim KY, Lee D, Han J, Nguyen NT, Park S, Sung JH. Microfluidic gut-on-a-chip with three-dimensional villi structure. *Biomed. Microdevices*. 2017;19:37.
- 12) Shin W, Kim HJ. Intestinal barrier dysfunction orchestrates the onset of inflammatory host-microbiome cross-talk in a human gut inflammation-on-a-chip. *Proc. Natl. Acad. Sci*. 2018;115:E10539-E10547.
- 13) Esch MB, Sung JH, Yang J, Yu C, Yu J, March JC, Shuler ML. On chip porous polymer membranes for integration of gastrointestinal tract epithelium with microfluidic 'body-on-a-chip' devices. *Biomed. Microdevices*. 2012;14:895-906.
- 14) McLean IC, Schwerdtfeger LA, Tobet SA, Henry CS. Powering ex vivo tissue models in microfluidic systems. *Lab on a chip*. 2018; 18(10): 1399-410.
- 15) Shah P, Fritz JV, Glaab E, Desai MS, Greenhalgh K, Frachet A, Niegowska M, Estes M, Jager C, Seguin-Devaux C, Zenhausern F, Wilmes P. A microfluidics-based in vitro model of the gastrointestinal human-microbe interface. *Nature communications*. 2016; 7:11535.
- 16) Marzorati M, Vanhoecke B, De Ryck T, Sadaghian Sadabad M, Pinheiro I, Possemiers S, Van den Abbeele P, Derycke L, Bracke M, Pieters J, Hennebel T, Harmsen HJ, Verstraete W, Van de Wiele T. The HMI™ module: A new tool to study the host-microbiota interaction in the human gastrointestinal tract in vitro. *BMC Microbiol*. 2014;14:133.
- 17) Kim HJ, Li H, Collins JJ, Ingber DE, Beebe DJ, Ismagilov RF. Contributions of microbiome and mechanical deformation to intestinal bacterial overgrowth and inflammation in a human gut-on-a-chip. *Pnas*. 2015; 113(1): E7-E15.

- 18) Shin W, Wu A, Massidda MW, Foster C, Thomas N, Lee DW, Koh H, Ju Y, Kim J, Kim HJ. A Robust Longitudinal Co-culture of Obligate Anaerobic Gut Microbiome With Human Intestinal Epithelium in an Anoxic-Oxic Interface-on-a-Chip. *Front. Bioeng. Biotechnol.* 2019;7:1–13.
- 19) Jalili-Firoozinezhad S, Gazzaniga FS, Calamari EL, Camacho DM, Fadel CW, Bein A, Swenor B, Nestor B, Cronce MJ, Tovaglieri A, Levy O, Gregory KE, Breault DT, Cabral JMS, Kasper DL, Novak R, Ingber DE. *Nat. Biomed. Eng.* 2019;3.
- 20) R. Nunes, C. Silva and L. Chaves, in *Concepts and Models for Drug Permeability Studies: Cell and Tissue Based in Vitro Culture Models*, 2016, pp. 203-236.
- 21) Xiao S, Coppeta JR, Rogers HB, Isenberg BC, Zhu J, Olalekan SA, McKinnon KE, Dokic D, Rashedi AS, Haisenleder DJ, Malpani SS, Arnold-Murray CA, Chen K, Jiang M, Bai L, Nguyen CT, Zhang J, Laronda MM, Hope TJ, Maniar KP, Pavone ME, Avram MJ, Sefton EC, Getsios S, Burdette JE, Kim JJ, Borenstein JT, Woodruff TK. A microfluidic culture model of the human reproductive tract and 28-day menstrual cycle. *Nature communications.* 2017; 8:14584.
- 22) Ross AE, Belanger MC, Woodroof JF, Pompano RR. Spatially resolved microfluidic stimulation of lymphoid tissue ex vivo. *Analyst.* 2016.
- 23) Dodson KH, Echevarria FD, Li D, Sappington RM, Edd JF. Retina-on-a-chip: a microfluidic platform for point access signaling studies. *Biomedical microdevices.* 2015; 17:114.
- 24) Atac B, Wagner I, Horland R, Lauster R, Marx W, Tonevitsky AG, Azar RP, Lindner G. Skin and hair on-a-chip: in vitro skin models versus ex vivo tissue maintenance with dynamic perfusion. *Lab Chip.* 2013;13:3555–3561.

- 25)Yasotharan S, Pinto S, Sled JG, Bolz S-S, Günther A. Artery-on-a-chip platform for automated, multimodal assessment of cerebral blood vessel structure and function. *Lab on a chip*. 2015; 15:2660-9.
- 26)Pearce SC, Coia HG, Karl JP, Pantoja-Feliciano IG, Zachos NC, Racicot K. Front Physiol. 2018;9:1584
- 27)Clarke LL. A guide to Ussing chamber studies of mouse intestine. *Am J Physiol Gastrointest Liver Physiol*. 2009; 296:1151–1166.
- 28)Kisser B, Mangelsen E, Wingolf C, Partecke LI, Heidecke CD, Tannergren C, Oswald S, Keiser M. The ussing chamber assay to study drug metabolism and transport in the human intestine. *Curr. Protoc. Pharmacol*. 2017;77(1):7–19.
- 29)May S, Evans S, Parry L. Organoids, organs-on-chips and other systems, and microbiota. *Emerging Topics in Life Sciences*. 2017; 1(4): 385-400.
- 30)Fiorini GS, Chiu DT. Disposable microfluidic devices: fabrication, function, and application. *Biotechniques*. 2005;38:429–446.
- 31)Berenguel-Alonso M, Sabés-Alsina M, Morató R, Ymbern O, Rodríguez-Vázquez L, Talló-Parra O, Alonso-Chamarro J, Puyol M, López-Béjar M. Rapid Prototyping of a Cyclic Olefin Copolymer Microfluidic Device for Automated Oocyte Culturing. *SLAS TECHNOLOGY: Translating Life Sciences Innovation*. 2017;47.
- 32)van Midwoud PM, Janse A, Merema MT, Groothuis GM, Verpoorte E. Comparison of biocompatibility and adsorption properties of different plastics for advanced microfluidic cell and tissue culture models. *Anal Chem*. 2012; 84:3938-44.
- 33)Ochs CJ, Kasuya J, Pavesi A, Kamm RD. Oxygen levels in thermoplastic microfluidic devices during cell culture. *Lab on a Chip*. 2014;14:459–462.

- 34) Wang XD, Wolfbeis OS. Optical methods for sensing and imaging oxygen: materials, spectroscopies and applications. *Chem. Soc. Rev.* 2014;43:3666–3761.
- 35) Schwerdtfeger LA, Ryan EP, Tobet SA. An organotypic slice model for ex vivo study of neural, immune, and microbial interactions of mouse intestine. *Am J Physiol Gastrointest Liver Physiol.* 2016;310(4):G240-248.
- 36) Leggat PA, Kedjarune U, Smith DR. Toxicity of cyanoacrylate adhesives and their occupational impacts for dental staff. *Ind. Health.* 2004;42:207–211.
- 37) Allaire JM, Crowley SM, Law HT, Chang SY, Ko HJ, Vallance BA. The intestinal epithelium: central coordinator of mucosal immunity. *Trends Immunol.* 2018;39: 677–696.
- 38) Chong H, Bjerknes M. Cell production in mouse intestinal epithelium measured by stathmokinetic flow cytometry and Coulter particle counting. *Anat Rec.* 1983;207:423-434
- 39) Dawson A, Dyer C, Macfie J, Davies J, Karsai L, Greenman J, Jacobsen M. A microfluidic chip based model for the study of full thickness human intestinal tissue using dual flow. *Biomechanics.* 2016; 10.
- 40) Oh S, Ryu H, Tahk D, Ko J, Chung Y, Lee HK, Lee TR, Jeon NL. “Open-top” microfluidic device for in vitro three-dimensional capillary beds. *Lab Chip.* 2017;17:3405–3414.
- 41) Astolfi M, Péant B, Lateef MA, Rousset N, Kendall-Dupont J, Carmona E, Monet F, Saad F, Provencher D, Mes-Masson A-M, Gervais T. Micro-dissected tumor tissues on chip: an ex vivo method for drug testing and personalized therapy. *Lab on a chip.* 2015; 16:312-25.
- 42) Vicuna EA, Kuttappan VA, Galarza-Seeber R, Latorre JD, Faulkner OB, Hargis BM, Tellez G, Bielke LR. Effect of dexamethasone in feed on intestinal permeability, differential white blood cell counts, and immune organs in broiler chicks. *Poult Sci.* 2015; 94(9): 2075-80.

- 43) Zhang L, Song J, Bai T, Qian W, Hou XH. Stress induces more serious barrier dysfunction in follicle-associated epithelium than villus epithelium involving mast cells and protease-activated receptor-2. *Sci Rep.* 2017; 7(1): 4950.
- 44) Albenberg L, Esipova TV, Judge CP, Bittinger K, Chen J, Laughlin A, Grunberg S, Baldassano RN, Lewis JD, Li H, Thom SR, Bushman FD, Vinogradov SA, Wu GD. Correlation between intraluminal oxygen gradient and radial partitioning of intestinal microbiota. *Gastroenterology.* 2014; 147(5): 1055-63 e8.
- 45) Henry OYF, Villenave R, Cronce MJ, Leineweber WD, Benz MA, Ingber DE. Organs-on-chips with integrated electrodes for trans-epithelial electrical resistance (TEER) measurements of human epithelial barrier function. *Lab on a Chip.* 2017;17:2264–2271.
- 46) Srinivasan B, Kolli AR, Esch MB, Abaci HE, Shuler ML, Hickman JJ. TEER measurement techniques for in vitro barrier model systems. *J Lab Autom.* 2015;20: 107-126.

CHAPTER 5 – HUMAN COLON FUNCTION EX VIVO: DEPENDENCE ON OXYGEN AND SENSITIVITY TO ANTIBIOTIC⁵

Overview:

Background: Human intestines contain a heterogeneous collection of cells that include immune, neural and epithelial elements interacting in a highly complex physiology that is challenging to maintain ex vivo. There is an extreme oxygen gradient across the intestinal wall due in part to microbiota in the lumen and close to the gut wall, which complicates the design of tissue culture systems. The current study established the use of an organotypic slice model of human intestinal tissue derived from colonoscopy biopsies to study host-microbial interactions after antibiotic treatment, and the influence of oxygen concentration on gut wall function.

Methods: Organotypic slices from human colon biopsies collected during routine colonoscopy provided three-dimensional environments that maintained cellular morphology ex vivo. Biopsy slices were used to study impacts of oxygen concentrations and antibiotic treatments on epithelial proliferation rates, and metabolites from tissue culture supernatants.

Results: Immune function was validated via demonstration of a T lymphocyte response to *Salmonella enterica* serovar Typhimurium. Following 24 h of *Salmonella* exposure there was a significant increase in CD3⁺ T-lymphocytes in biopsy slices. Metabolite profiling of tissue culture supernatants validated the influence of antibiotic treatment under varied oxygen culture conditions on both host and microbiome-mediated metabolism. Epithelial health was influenced by oxygen and antibiotic. Increased epithelial proliferation was measured in lowered oxygen conditions (1% = 5.9 mmHg) compared to atmospheric conditions standard at 5000 feet above sea level in Colorado (~17% = 100 mmHg). Antibiotic treatment reduced epithelial proliferation only in 5.9 mmHg oxygen cultured slices. Conclusions: A human colon organotypic slice model

⁵ Schwerdtfeger LA, Nealon NJ, Ryan EP, Tobet SA. Human Colon Function Ex Vivo: Dependence on Oxygen and Sensitivity to Antibiotic. *PLoS One*. 2019;14(5):e0217170.

was established for applications ranging from gut epithelial proliferation to enteric pathogen influence on mucosal immune functions *ex vivo*. The results further support the need to account for oxygen concentration in primary tissue cultures, and that antibiotic use impacts gut-microbe-immune interactions.

Introduction:

Gastrointestinal issues send over 70 million Americans a year to a physician, often due to complex inflammatory diseases such as ulcerative colitis and Crohn's disease [1]. Physiological mechanisms underlying these diseases are poorly understood [2]. Teasing apart the etiology of intestinal pathologies in humans requires the use of *in vitro* model systems to mimic *in vivo* gut physiology. Methods for culturing human colon explants go back over 40 years [3], however there were issues of tissue degradation over time. Difficulties with maintaining intestinal tissues *ex vivo* are due in part to the unique physiology of the human colon, including the oxygen gradient seen across the intestinal wall.

The gastrointestinal tract is a complex multicellular tube with varied cellular composition based on not only region (e.g. ileum vs ascending colon) but also location within each gut region. The cellular heterogeneity of the intestine contributes to immunological functions including pathogen surveillance, antigen presentation, and secretion of pro- and/or anti-inflammatory cytokines. Lamina propria also contains dense enteric neural cell populations comprised of enteric glial cells and neuronal fibers [4] with the former having been implicated in issues ranging from barrier maintenance [5] to Crohn's disease and ulcerative colitis [6,7].

Adding to the complexity of the colonic wall, the colonic mucosa sits in close proximity to the microbial communities of the gut. Composed of thousands of distinct species, these organisms, and in particular the metabolites they produce, play key roles in regulating intestinal

physiology and homeostasis [8]. Microbial metabolism in the colon is responsible for production of a wide array of metabolites, offering a measure of the functional output of the microbiome [9]. Short chain fatty acids (e.g., acetate) are among the most common, and are thought to play key roles in inhibiting pro-inflammatory cytokine production [10]. How microbial derived metabolites regulate tissue physiology in protective and detrimental manners is an active area of investigation [11].

While the microbiome is normally commensal, pathogenic bacterial species such as *Salmonella enterica* can invade the intestinal mucosa and cause infection [12]. Once inside the gut wall, *Salmonella* can cause immune responses through a number of mechanisms, including Toll-like and NOD receptor signaling. Such signaling leads to activation and expansion of mucosal T lymphocyte populations [13,14]. In the present study, this *Salmonella* response was used to validate the competence of biopsy slices to elicit an immune response in vitro.

A steep oxygen gradient is present across the intestinal wall [15]. The apical mucosa closest to the lumen maintains in vivo oxygen concentrations of 0.1 – 1% oxygen (~1 – 6 mmHg). Climbing rapidly across the intestinal wall, the oxygen concentration is ~6% (~42 mmHg) in the vascularized submucosa. The colonic muscle wall is the most well oxygenated region, with 7-10% (42 – 71 mmHg) oxygen concentrations [16]. Alterations in this oxygen gradient can lead to impacts on the composition of the gut microbiome both in vivo [17] and in vitro [18]. Commensal bacteria can impact mouse intestinal contractions [19] and expression of genes associated with inflammation and antigen presentation [20]. In addition to oxygen culture condition, antibiotic exposure (e.g. penicillin-streptomycin) can substantially alter microbiome composition [21,22] and microbial derived metabolites such as phenyllactate [23].

Several methods that have been employed to maintain human colon tissue in vitro regularly use explants or immortalized cell culture monolayers (e.g. caco-2) at ambient oxygen (~120 – 145 mmHg) [24,25,26] or higher (675 mmHg) [5,27] concentrations, in the presence of

antibiotics. One system recapitulated an oxygen gradient across a caco-2 monolayer culture in a gut-on-a-chip system using only a subset of bacterial strains instead of native human microbiome [28]. Influences of varied oxygen culture conditions and antibiotic exposures on microbially derived metabolites impacting gut immunity and general tissue physiology are unknown. The current study presents a human colon tissue model system with a heterogeneous mucosal cellular population at physiologic oxygen tensions, and without antibiotics. The model maintains epithelial structure, components of the immune system in the form of T-lymphocytes, and a metabolically active microbiome for up to 3 days ex vivo. The results demonstrate impacts of oxygen concentration and antibiotic exposure on biopsy slice epithelial structure, cell turnover rates, and metabolome composition.

Methods:

Biopsy collection:

Healthy adult participants were recruited prior to a routinely scheduled colonoscopy at Harmony Surgery Center or Poudre Valley Hospital (Fort Collins, CO). For each participant, colon biopsies of ~5mm diameter were collected from both the right (ascending) and left (descending) colon using standard biopsy forceps (Figure 17A'), and subsequent slicing (Figure 17A''). In total, biopsies were collected from 31 participants (21 female and 10 male), with between 10 – 30 slices being generated per biopsy. Mean age of participants was 56.1 +/- 2.8 years for females, and 56.2 +/- 2.3 years for males. Body mass index (BMI) was similar between sexes, with male mean BMI 28.8 +/- 1.3, and female 27.3 +/- 1.5. Biopsies were harvested from mucosal tissue, composed of colonic crypts and lamina propria, and did not penetrate the muscle wall. De-identified biopsies were immediately placed into 1X Krebs buffer (in mM: NaCl, 126; KCl, 2.5; CaCl₂, 2.5; NaH₂PO₄, 1.2; MgCl₂, 1.2) and maintained on ice for transport to Colorado State University. For all participants, colon tissue samples had less than

30 min transit time between collection and processing in the research lab. This project was approved by the University of Colorado Health Institutional Review Board under IRB #15-6051, and Colorado State University IRB registration number 00010144.

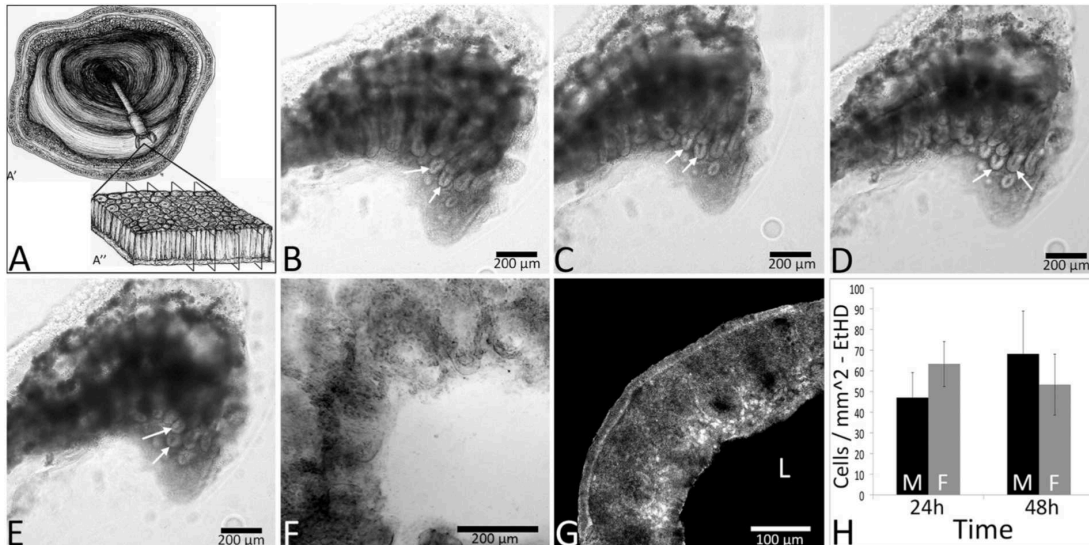


Figure 17. Structural integrity of organotypic colon biopsy slices (schematic in A) was maintained for up to 3 days ex vivo. Bright-field images of one organotypic biopsy slice at 0 (B), 24 (C), 48 (D) and 72h (E) ex vivo show intact colonic crypts and lamina propria. Crypt enterocytes were organized at the luminal surface (arrows). A representative slice is shown at 96h ex vivo with tissue degradation that rendered crypt patterning difficult to identify (F). A representative image shows minimal cell death (EtHD label; RFP; G) at 48h ex vivo. No differences were seen in EtHD label between 24 and 48h of culture regardless of sex (H). Data in panel H are +/- SEM, n = 3 male and 3 female participants per time point. Black bars in panel H represent males (M), and gray bars females (F). 'L' represents the luminal aspect.

Organotypic slice preparation:

Slice preparation was similar to that previously described in [19]. Biopsies were placed in 4°C 1X Krebs buffer and dissected free of any connective structure. The entire tissue was submerged in 8% agarose (Agarose LM; Gold Biotechnology, St. Louis, MO) for a total of 7 min: 5 min on a room temperature shaker, and 2 min in 4°C to polymerize. Tissues were cut on a vibrating microtome (VT1000S; Leica Microsystems, Wetzlar, Germany) at a thickness of 250 µm. Slices from both right and left colon biopsies were pooled. Slices were collected in 4°C 1X Krebs buffer, and immediately transferred into a 60 mm plastic-bottom dish (Corning, Corning,

NY) containing 5 ml of Hibernate media (Life Technologies, Grand Island, NY) and either zero (nPS) or 1.3% penicillin-streptomycin (PS; HyClone Laboratories, Logan, UT). Slices spent at least 15 min in Hibernate media (Gibco, Grand Island, NY) at 4°C before being transferred to 5 ml of Adult Neurobasal Media (ANB; Life Technologies) containing 5% B-27 supplement (B-27; Life Technologies). For slices treated with antibiotic, PS was added to the media (final concentration of 1.3%). Next, slices were transferred to a 37°C incubator for 35 min. Samples were then plated on 35 mm diameter plastic bottom dishes (Corning). Slices were allowed to adhere to the dish for 10 min at 37°C before being overlaid with a bovine collagen solution [vol/vol: 10.4% 10X MEM (Minimal Essential Medium, Sigma-Aldrich, St. Louis, MO), +/- 1.9% PS, 4.2% sodium bicarbonate, and 83.5% collagen (PureCol; Inamed, Fremond, CA)]. The collagen solution was allowed to polymerize in 37°C for 20 min before a final 1 ml addition of ANB with B-27 and +/- PS that was pre-incubated in either a standard 37°C, 5% CO₂, ambient oxygen incubator (100 mmHg), or a three gas incubator set for 37°C, 5% CO₂, and 5.9 mmHg oxygen as modulated by nitrogen injection (Panasonic MCO-5M-PA; Panasonic Healthcare, Tokyo, Japan). Finally, slices were left at 37°C in either ambient or 5.9 mmHg oxygen until visualization or experiments as described below. All slices generated from a given biopsy were used for experimentation, however when a rare slice (< 5% of slices) had large amounts of cell debris in the luminal aspect and un-patterned crypts with an undefined tissue edge, it was discarded. Experiments were performed on slices after at least 24 h of culture, and no longer than 72 h of culture. This ensured that slices were able to recover fully after cutting procedures prior to experimentation (24 h), and also that slices were not undergoing tissue degradation prior to experiments concluding (72 h).

Live slice imaging:

Slices were imaged on one of two microscopes: a Nikon TE2000-U inverted microscope (4X, 10X Plan-Fluor and 20X Plan-Apo objectives) with a UniBlitz shutter system (Vincent Associates, Rochester, NY) and an Orca-flash 4.0 LT camera (Hamamatsu, Hamamatsu City, Shizuoka Prefecture, Japan), or a Zeiss LSM 800 confocal microscope with an Axiocam 503 mono camera (Carl Zeiss, Inc., Thornton, NY).

Salmonella inoculation:

Organotypic colon biopsy slices were challenged with Green Fluorescent Protein (GFP) tagged *Salmonella enterica* serovar Typhimurium (*S. ser. Typhimurium*-GFP; strain 14028s) which was generously donated by Dr. Andres Vazquez-Torres (University of Colorado) and prepared as previously described [29]. Briefly, *S. ser. Typhimurium*-GFP was brought up in Luria Bertani Broth (Mo Bio Laboratory, Carlsbad, CA) to 1×10^8 colony forming units (CFU's) per 1 ml. 1 μ l of *S. ser. Typhimurium*-GFP or vehicle (sterile Luria Bertani broth) was added adjacent to the luminal aspect of nPS biopsy slices under 100 mmHg oxygen conditions, due to the strict aerobic nature of this strain. Invasion into the colonic epithelium was visualized using a Nikon inverted microscope setup for time-lapse video microscopy with a 488 nm excitation wavelength. Time-lapse video microscopy was performed at 0 h post inoculation and again at 4 h, for 10 min each with 30 s between exposures. After 4 h, any non-tissue adherent *S. ser. Typhimurium*-GFP was washed away with 3x media (ANB + B27) washes, and allowed to incubate for an additional 20 h prior to fixation followed by immunohistochemistry for CD3⁺ T-lymphocytes.

Whole-mount immunohistochemistry (IHC):

Following live culture, slices were immersion fixed in 4% formaldehyde (Polysciences, Inc. Warrington, PA) for 15 minutes and washed three times in 0.05 M PBS, pH 7.5.

Immunohistochemical studies were performed similar to those previously described [19]. Post-fixing and PBS washes, slices were incubated at 4°C for 2 h in 1% sodium borohydride in PBS. Slices were then washed two times in PBS for 5 minutes and subsequently incubated in a blocking solution composed of PBS, 5% normal goat serum (NGS; Lampire Biological, Pipersville, PA), 3% hydrogen peroxide and 0.3% Triton-X (Tx) for 1 h before a change into fresh solution for subsequent 1 h. Slices were then placed into affinity purified polyclonal anti-CD3 (cell surface marker for T lymphocytes; Dako Denmark, Glostrup, Denmark), affinity purified polyclonal anti-ZO-1 (tight junction protein; Invitrogen, Eugene, OR), polyclonal anti-peripherin (peripheral neuronal marker; EMD Millipore, Billerica, MA), or monoclonal anti-S100 β (glial cell marker; Abcam, Cambridge, MA), composed of PBS with 5% NGS and 0.3% Tx for 4 days. Anti-CD3 was used at a concentration of 2 μ g/ml, anti-ZO-1 at 2 μ g/ml, anti-peripherin diluted 1:300, and anti-S100 β at 2.4 μ g/ml. Samples without primary antibody were used as control. After 4 days of incubation with primary antibody, slices were washed at 4°C with PBS containing 1% NGS and 0.02% Tx for 2 h with 4 changes. Next, biotinylated secondary anti-serum (anti-rabbit, 1:2500 for ZO-1, peripherin, S100 β , and anti-mouse, 1:1000 for CD3; Jackson ImmunoResearch, West Grove, PA), specific to the species of the primary antibody, was made up in PBS with 1% NGS and 0.32% Tx and added overnight. Lastly, tissue was washed 4 times at room temperature in PBS with 0.02% Tx before being placed into solution containing the conjugated fluorophore (Cy-3 Streptavidin) for 3 h before being washed in PBS for 2 h and subsequently mounted on slides and cover slipped with an aqueous mounting medium (Aqua-Poly/Mount, Polysciences, Warrington, Pa). Following the IHC protocol, tissue was imaged on either a Nikon TE2000 inverted microscope, or a Zeiss LSM 800 confocal microscope (Carl Zeiss, Inc., Thornton, NY). A researcher blinded to treatment group counted cells using the ImageJ analysis software 'analyze particles' toolset.

Metabolite profile analysis of supernatants:

Data processing and metabolite identification:

Metabolomics was performed by Metabolon Inc (Durham, NC, USA). Tissue culture supernatants from ex vivo tissue slices (4 females, 4 males) were collected in triplicate and stored at -80° C until processing. Supernatants were garnered from slices that were not treated with *S. ser. Typhimurium*-GFP. Processing of supernatants was performed with an 80% methanol extraction and metabolite detection via ultra-high-performance liquid chromatography-tandem mass spectrometry. Raw data was processed by Metabolon Inc as described previously [30], where it was extracted from the mass spectrometer, quality-controlled, and raw peaks and retention times were aligned across individual samples. With the aligned data, compound identifies were confirmed within an internal Metabolon library containing over 3,300 purified standards by comparing retention times and mass/charge ratios to those of purified standards. Retention time indices had to match within a narrow window, their mass to charge ratios had to include a mass within +/- 10 parts per million of a library entry, and their mass spectral profiles had to contain forward and reverse match scores that fell between the experimental data and spectral profiles from the Metabolon database. For each metabolite, total ion current area under the curve quantitation was used to generate metabolite raw abundances. These raw abundances were log₂-transformed and median-scaled by dividing the metabolite's raw abundance by the median raw abundance of that metabolite across the entire data set. For any sample missing a metabolite, the minimum median scaled abundance was input. For each metabolite, fold differences were determined between pairs of treatments by dividing the average median scaled abundance of a metabolite across one treatment group by another. Pairs of treatments used to calculate fold differences included: 100 mmHg O₂,

antibiotic; 100 mmHg O₂, no antibiotic; 5.9 mmHg O₂, antibiotic; 5.9 mmHg O₂, no antibiotic.

Pathway enrichment score calculations:

Following annotation, metabolites were grouped into pathways based on their biological/biochemical functions. Pathway enrichment scores (PES) were calculated to assess the overall contribution of a pathway to explaining treatment differences between 100 mmHg and 5.9 mmHg oxygen in both the presence and absence of antibiotics. PES were calculated using the following equation:

$$\frac{\binom{k}{m}}{\binom{n}{N}}$$

Where “k” represents the number of statistically-significant metabolites in the pathway, “m” is the total number of metabolites in the pathway, “n” is the number of statistically-significant metabolites across all pathways, and “N” is the total number of detected metabolites. PES greater than one are considered major contributors to treatment differences. GraphPad Prism Version 7.0 (San Diego, CA, USA) was used to visualize all PES.

Cell proliferation analysis:

Incorporation of the thymidine analog 5-ethynyl-2'-deoxyuridine (EdU; Invitrogen) was used to label cells undergoing DNA synthesis. After slices were plated, they were incubated at ambient oxygen, 5% CO₂ or in an incubator with 5.9 mmHg oxygen, 5% CO₂ for 24 h before the addition of EdU at a final molarity of 4 μM. Half of slices were subjected to PS treatment for the entirety of their time ex vivo and experimental process while the other half did not receive antibiotic. All slices were fixed at 48 h ex vivo in 4% formaldehyde prior to processing for visualization. Slices were washed 3 times in phosphate-buffered saline (0.05M PBS), followed

by 30 min in glycine (Fisher Scientific, Pittsburgh, PA) at 4°C, and again washed with PBS for 10 min with 1 change. Slices were then blocked in 3% bovine serum albumin buffer (BSA; Lampire Biological, Pipersville, PA) and 0.5% Tx for 2 h. Post blocking, tissue was washed twice with 3% BSA before addition of Click-IT cocktail (1X click-It Reaction Buffer, CuSO₄, Alexa-Fluor azide, 1X reaction buffer additive; Invitrogen) for 2 h at room temperature. Finally, slices were washed 3 times in 3% BSA with 0.02% Tx for 30 min each, and left in a final wash of 3% BSA prior to imaging. Analysis of EdU incorporation was performed using ImageJ Image Processing and Analysis software (NIH; Version 1.49) to determine the percentage of area labeled, with the whole biopsy slice as the region of interest. EdU incorporation was determined to be cellularly localized based on the cell size and anatomical localization in the colonic crypts. Using ImageJ, regions of interest (ROIs) were chosen based on crypt anatomy, with 'Crypt' ROIs encompassing one crypt region in that plane, and 'nCrypt' ROIs being similarly sized regions not containing any portion of a crypt. Optical density was used to set image thresholds, and small objects were eroded to remove spurious signals, and measured using the 'analyze particles' tool. A researcher blinded to treatment condition counted cells contained within ROIs.

Cell death analysis:

The incidence of cell death was measured using Ethidium Homodimer (EtHD; Biotium, Hayward, CA), a membrane impermeable, red fluorescent (RFP), DNA marker. EtHD was added to slice dishes containing three slices each, ex vivo, for 45 minutes, at a volume of 1 µl of 2.5 mM stock EtHD per 1 ml of media (ANB + B-27 ± PS). This resulted in a final concentration of 2.5 µM of EtHD, before the unbound material was washed out. EtHD labeling was analyzed using ImageJ (NIH; Version 1.49). One image per slice, totaling three images per biopsy were taken prior to thresholding according to optical density. Subsequently, objects smaller than 10 µm² were deemed too small to be cells and were eroded to remove spurious signals. Finally,

images were measured using the 'analyze particles' tool to garner cells counts. All data were collected by a researcher blinded to treatment condition.

Statistics:

All slices were generated from two biopsies from the same colon as biological replicates, and slices were used in triplicate to generate technical replicates, prior to statistical analyses being performed with the number of patients = n for analysis. T- lymphocyte data were analyzed by repeated measures ANOVA that accounted for pathogen exposure and sex of the tissue donor. For all metabolite analyses, statistics were performed by Metabolon Inc using Array Studio (Omicsoft, Cary, NC, USA). Briefly, a 2-way ANOVA was applied across all metabolite abundances over the treatment groups described above with a Welch's post-hoc test. To account for multiple comparisons, a false discovery rate (q-value) was calculated for each metabolite across each contrast. Given the small number of samples and the large number of metabolites, there was insufficient power to generate statistically reliable sex differences. The metabolite data presented is combined for males and females. Cell proliferation data were analyzed by repeated measures ANOVA that accounted for oxygen condition, sex of tissue donor and antibiotic treatment, with antibiotic treatment as a repeated measure. Finally, cell death data were analyzed by 2-way ANOVA that accounted for sex of tissue donor and time point as a repeated measure. A p-value < 0.05 was considered as statistically significant in all analyses.

Results:

Tissue integrity was maintained for 72 h (3 days).

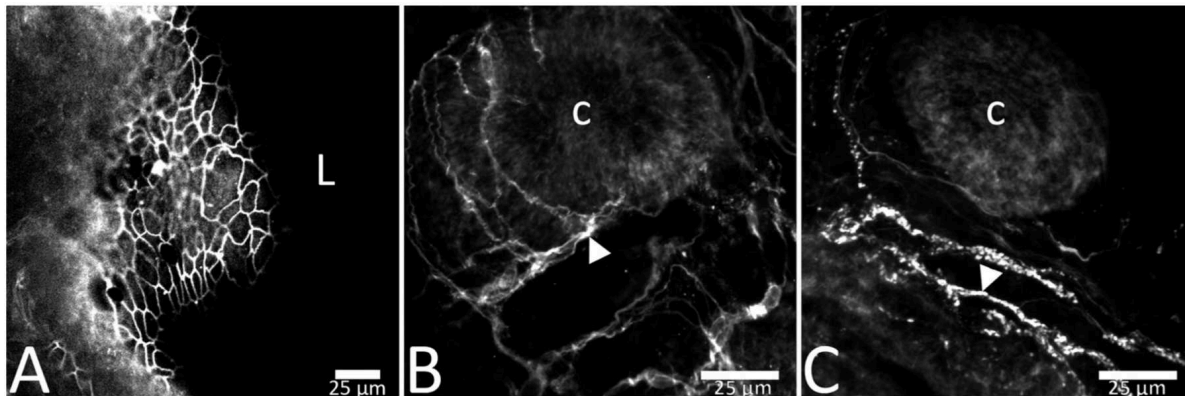


Figure 18. Barrier integrity was intact at 24 hours ex vivo, as assessed by the presence of tight junction protein ZO-1 at the apical mucosal surface (A). Neural components of lamina propria were present at 24h ex vivo. Representative images show S100 β -immunoreactivity at 24h ex vivo indicating enteric glial cells (B) and peripherin immunoreactivity indicating neuronal fibers ex vivo (C). Scale bars in panels A – C are 25 μ m. 'L' represents the luminal aspect and 'c' represents a colonic crypt. Arrowheads in panels B and C represent fibers with stereotypic immunoreactivity.

There was strong evidence of morphological preservation from freshly collected biopsy tissue in the form of patterned rows of crypts with minimal cell debris and a defined tissue edge. Cell turnover was also observed in organotypic slices for up to 3 days *ex vivo*. In 250 μ m slices at 24, 48, and 72 h, colonic crypts were intact and patterned in rows and columns, and showed organized tissue at the crypt surface (Figure 17 B-E). At 96 h *ex vivo*, there was degradation of observable patterned rows of crypts in many slices (Figure 17F) indicating a decline in tissue viability. The apical epithelia were organized with tight junction protein ZO-1 present between epithelial cells at 24h (Figure 18A). Immunohistochemistry for enteric glial marker S100 β and the neuronal intermediate filament protein peripherin show presence of neural components of the colonic mucosa at 24h *ex vivo* (Fig 18B-C). Intestinal function was further confirmed by measures of epithelial cell turnover using indicators of death (EtHD) and proliferation (EdU incorporation). Cells in slices died at a mean rate of 60 +/- 11.9 cells/mm² across 24 h and 48 h *ex vivo* (less than 5% of tissue area; Figure 17H) consistent with the rate of cell turnover seen in the human colon *in vivo* [31].

T – Lymphocytes increase in response to S. Typhimurium infection

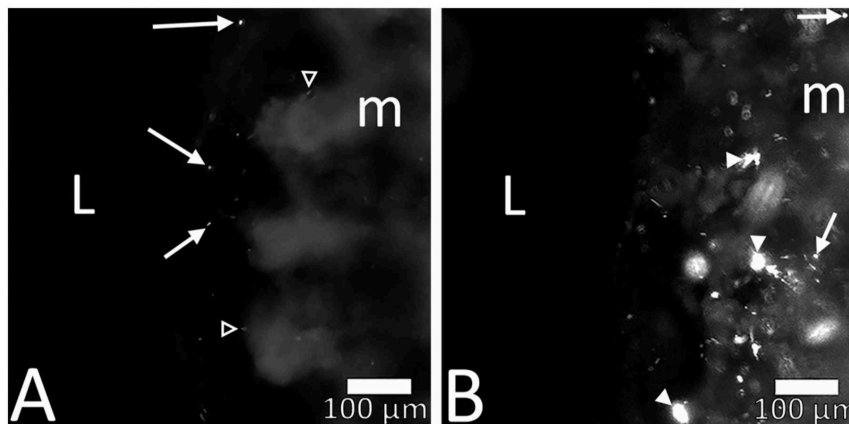


Figure 19. *S. ser. Typhimurium-GFP* infiltrated colon mucosa within 24 h of culture. At 4 h ex vivo (A) *S. ser. Typhimurium-GFP* were seen approaching the luminal aspect of the colonic mucosa (arrows) with minimal mucosal binding observed (open arrow heads in A). *S. ser. Typhimurium-GFP* appeared in colonic mucosa at 24 h post inoculation (B), and were often clustered together (arrowheads in B). Scale bar in both panels is 100 μm .

T-lymphocyte counts increased in biopsy slices after a 24 h challenge with *S. ser. Typhimurium-GFP*. After 4 h, fluorescence was visible in the apical most regions of colonic mucosa (Figure 19A), primarily as scattered individual fluorescent particles. At 24 h post inoculation, there were notably more *Salmonella* seen throughout the colonic mucosa, particularly in clusters (Figure 19B, arrow heads), but with some bacteria still independently bound to the mucosa (arrows). After slice fixation and subsequent IHC for CD3, biopsy slices showed CD3⁺ cells localized closely with tissue adherent *S. ser. Typhimurium-GFP* (Figure 19C). Figure 20A presents a visualization of the ROIs used for generating CD3-IR data. After biopsy slices were challenged with *S. ser. Typhimurium-GFP*, immunoreactive (IR) T-lymphocytes were increased in slices from both males (Figure 20B, control; 2.8C, treatment)

and females (Figure 20D, control; 2.8E treatment) 24h later (48h ex vivo; Figure 20F).

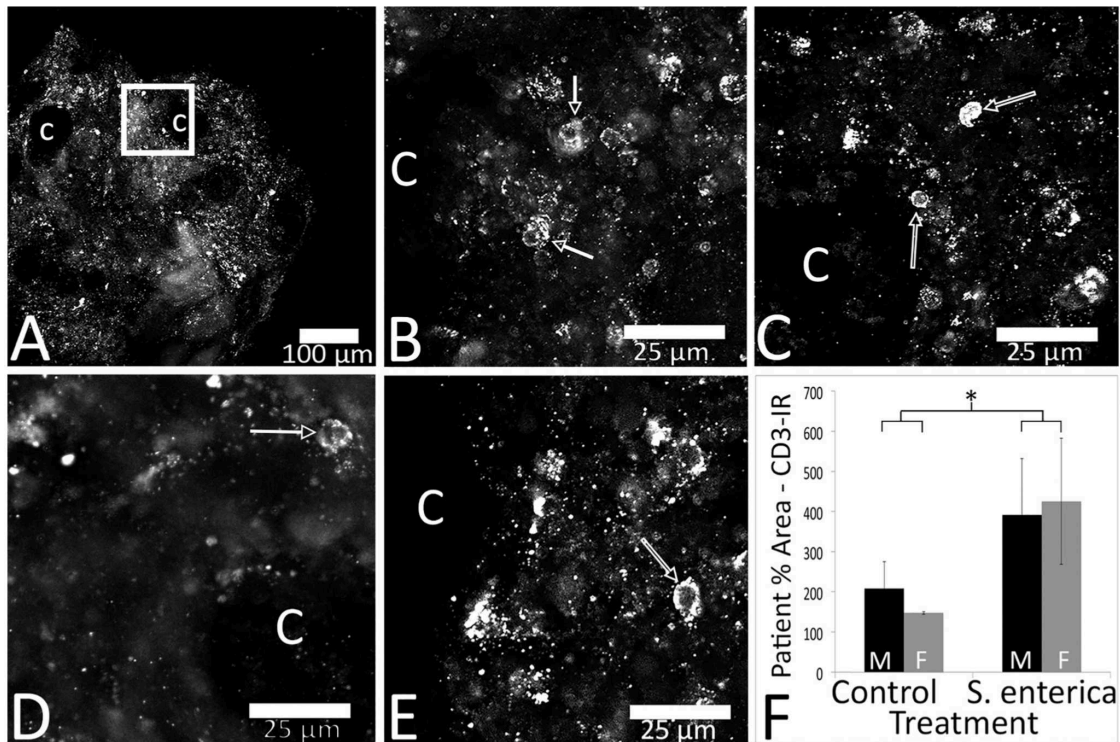


Figure 20. Challenge with *S. ser. Typhimurium-GFP* lead to an up-regulation of CD3⁺ T-lymphocytes after 24 h, regardless of sex. Images of CD3-IR (RFP in A-E) were captured from a region of lamina propria close to a colonic crypt. An example region of interest where higher magnification images were acquired is represented with a white square in (A) that applies conceptually to B-E. Representative images of CD3-IR in slices show less immunoreactivity in control (B, male; D, female) versus *S. ser. Typhimurium-GFP* treated slices (C, male; E female). There was a significant impact of treatment on CD3-IR, regardless of sex (F). Black bars represent males (M) and grey bars females (F). L = lumen, m = mucosa, C = colonic crypt. Arrows point to individual bacterium. Open arrows point towards cells with stereotypic CD3-IR. * Signifies $p < 0.05$. Data in panel I are \pm SEM, $n = 4$ male and 3 female participants.

There was a significant increase in T-lymphocytes following pathogen challenge, independent of sex [$F(1,5) = 7.480$; $p < 0.05$].

Metabolites and metabolic pathways were impacted by oxygen concentration and antibiotic presence

Table 2. Number of identified metabolites from tissue culture supernatants across oxygen and antibiotic treatments, organized by chemical class.

Chemical Class	100 mmHG Oxygen, Antibiotic	100 mmHG Oxygen, No Antibiotic	5.9 mmHg Oxygen, Antibiotic	5.9 mmHg Oxygen, No Antibiotic
Amino acids	116	118	110	118
Peptides	3	3	3	2
Carbohydrates	12	13	12	12
Energy/Tricarboxylic Acid Cycle	8	9	9	8
Lipids	46	46	39	45
Nucleotides	22	24	21	24
Cofactors/Vitamins	20	20	19	20
Xenobiotics	22	20	18	22
Total number of identified metabolites	249	253	231	251

There were 258 metabolites identified in the tissue culture supernatants maintained for 48 h ex vivo from 31 colon slices obtained from 8 participants. Table 2 provides an overview of the number of metabolites in each of the chemical classes detected, including: amino acid (119), peptide (3), carbohydrate (13), energy/tri-carboxylic acid cycle (9), lipid (46), nucleotide (24), cofactors and vitamins (20), and xenobiotics (24). Statistically significant [$p < 0.05$] changes were identified based on the concentration of oxygen in the tissue culture incubator (5.9 mmHg oxygen versus 100 mmHg oxygen) as well as due to the presence or absence of antibiotic in the tissue culture media. Across oxygen concentrations, independent of antibiotic status, there were 41 metabolites that were significantly different (Table 2). When comparing antibiotic treatments, independent of oxygen concentration, 198 metabolites differed (Table 2). In addition, there was an interaction between antibiotic and oxygen status for 28 metabolites (Table 2). A complete list of identified metabolites, including those that were statistically different when accounting for oxygen concentration, antibiotic presence, and for oxygen*antibiotic are provided in the supporting information (S1 Table).

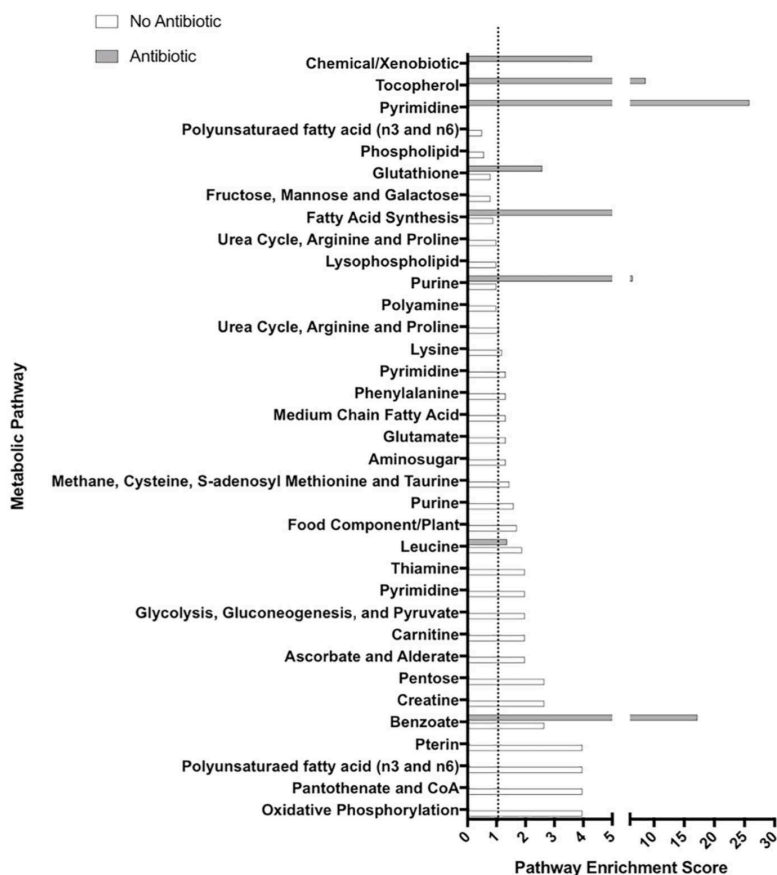


Figure 21. Pathway enrichment scores were calculated for 100 mmHg versus 5.9 mmHg oxygen in both the presence of antibiotic (grey) and absence of antibiotic (white). Bars that extend past the dotted line (at a score of 1) were considered the primary pathways contributing to treatment differences. Lack of a white or grey line for any pathway indicates that no metabolites were statistically-different between treatments ($p < 0.05$) within that pathway.

The analysis of tissue culture supernatants indicates the presence of microbially derived metabolites, including lipids, amino acids, and carbohydrates. These metabolites included trimethylamine N-oxide (TMAO), indole-containing metabolites (e.g. indolacetate), and phenyllactate, amongst others. Additionally, these three metabolites were decreased in response to antibiotic treatment (S1 Table). Pathway enrichment scores were calculated to identify pathways that had highest contributions to the treatment differences. In each pathway, a score greater than or equal to 1 was defined as a major contributing pathway [32]. Pathway

enrichment scores are displayed for 100 mmHg versus 5.9 mmHg oxygen in the presence and absence of antibiotic (Figure 21). In the presence of antibiotic, 8 pathways distinguished 100 mmHg oxygen from 5.9 mmHg oxygen treatments, while in the absence of antibiotic, 25 pathways distinguished 100 mmHg oxygen from 5.9 mmHg oxygen treatments (Figure 21).

Antibiotic and oxygen impact epithelial proliferation

Following the finding that antibiotics and oxygen impacted microbial metabolites, mucosal epithelial proliferation was assessed by EdU incorporation in response to antibiotic treatment and oxygen concentration. After 48h ex vivo, slices maintained at 5.9 mmHg oxygen showed significantly more EdU labeling compared to ambient oxygen slices [Figure 22G-H; $F(1,14) = 41.1$, $p < 0.01$], regardless of sex [$p > 0.5$]. Interestingly, antibiotic treatment impacted EdU incorporation in slices maintained at 5.9 mmHg oxygen (Figure 22C-D), but not 100 mmHg (Figure 22E-F). There was a statistically significant interaction between antibiotic and oxygen conditions [$F(1,14) = 10.4$, $p < 0.01$] that was due to the enhanced impact of antibiotic on EdU incorporation at 5.9 mmHg oxygen (Figure 22G-H). Mean cell counts within regions of interest (ROIs; circle in Fig 6A) inside colonic crypts were compared to ROIs outside colonic crypts. Significantly more cells incorporated EdU in Crypt regions compared to nCrypt regions, independent of sex [Figure 22B; $F(1,12) = 102.9$, $p < 0.01$] and consistent with DNA synthesis being localized primarily to epithelial cells in the crypt proliferative regions.

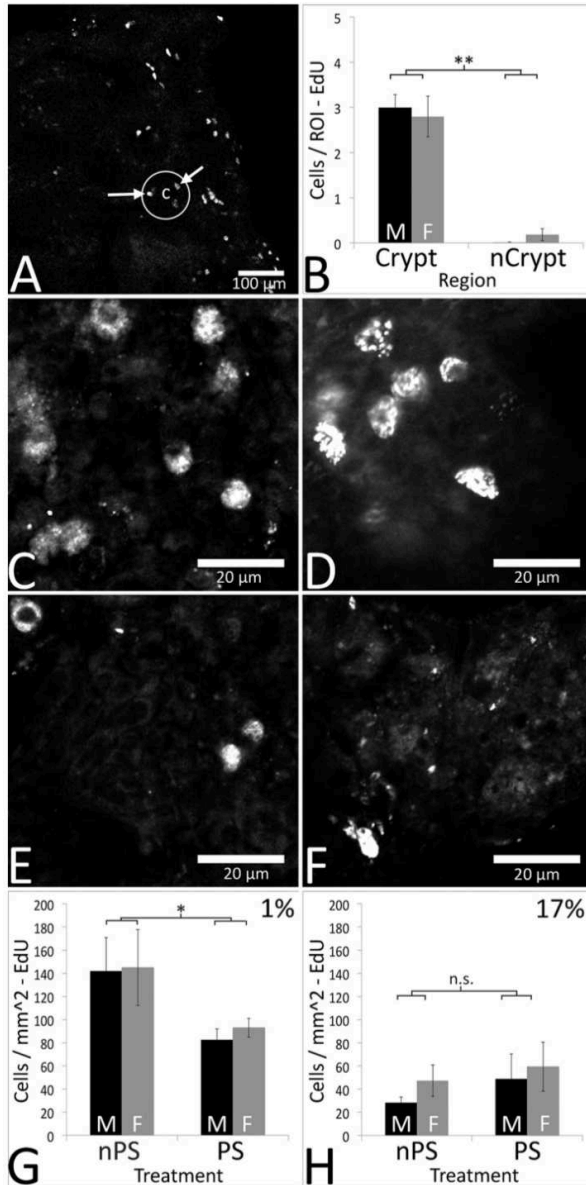


Figure 22. Incorporation of Ethynyl deoxyuridine (EdU) as indicative of DNA synthesis was observed in all oxygen and +/- PS treatments and across all time points (0 – 72h ex vivo). EdU was localized to cells in the colonic crypts (A). This localization was quantified (B), with significantly more EdU⁺ cells per ROI observed in the crypts compared to non-Crypt (nCrypt) regions, regardless of sex ($p < 0.05$). Representative images of cells in slices from a male participants biopsy show increased EdU⁺ cells in 1% nPS (C) compared to 1% PS (D), both of which are have higher cell counts than 17% nPS (E) and 17% PS (F). Antibiotic had a significant impact on EdU incorporation in slices incubated at 1% oxygen independent of sex (G), with more cells / mm² of tissue seen in nPS slices compared to PS slices. Additionally, oxygen concentration significantly impacted EdU incorporation, with more cells / mm² in 1% slices compared to 17% oxygen cultured slices (G and H). There was no significant impact of PS treatment on slices cultured in 17% oxygen, regardless of sex (H). In B, G and H, black bars are males (M), and grey bars are females (F). Arrows in A point toward stereotypic EdU⁺ cells. “c” represents a colonic crypt, and the circle is encapsulating one crypt. ** Signifies $p < 0.01$, * signifies $p < 0.05$, and n.s. = not significant. Data in B, G and H are +/- SEM, $n = 5$ female, 4 male participants for all EdU experiments except Crypt vs nCrypt analysis, in which $n = 3$ female, 3 male participants.

Discussion:

The current study validates an organotypic slice model for the study of human intestinal physiology *ex vivo*. Three-dimensional tissue integrity was maintained by embedding the tissue in a solid agarose support that allowed the culture of the diverse cells of the intestine in a physiologically appropriate arrangement. Tissues were maintained for up to 3 days *ex vivo*, preserving crypt structure, normal cell proliferation and death rates, enteric glia and neuronal fibers, and an immune response to pathogen. Tissue culture supernatants contained known microbial metabolites [9] indicating the maintenance of functional microbiota. These metabolites were sensitive to treatment with antibiotic (PS), demonstrating the influence of antibiotic on microbial populations and/or their metabolite secretory competence. The model further demonstrated a difference in human colonic epithelial health in response to oxygen condition and antibiotic exposure, both known to alter gut microbial diversity [21]. Of paramount importance was that the influence of antibiotic on epithelial proliferation was dependent on oxygen culture condition, further implicating microbes as key influencers of mucosal epithelial biology. These findings highlight the need for better definition of the microbial composition (or the functional metabolite profile output) in *ex vivo* systems moving forward.

The efficacy of the organotypic model in the present study to elicit a functional immune response *ex vivo* was validated via a demonstrated T-lymphocyte response to challenge with *S. ser. Typhimurium*-GFP. T-lymphocytes in colon biopsy slices showed a more than 2-fold increase in response to pathogen when compared to vehicle (no pathogen, Figure 20F). The increased T lymphocyte count was similar to that seen in mice [33,34], and chickens [13] where T-lymphocytes were up-regulated after dosing with *S. Typhimurium*. This immune response to pathogen *ex vivo* supports the utility of this model for future studies investigating host pathogen defense and gut mucosal protection in human intestines.

Analysis of colon tissue culture supernatants revealed the presence of a number of microbial metabolites [23] including phenyl containing organic acids (e.g., phenyllactate), the choline/carnitine bacterial breakdown product TMAO, and indole containing metabolites involved in the bacterial metabolism of tryptophan. The substantial impact of both oxygen concentration and antibiotics on the production of metabolites was notable for lipids and amino acids spanning diverse metabolic pathways (Table 2). Interestingly, differences in the influence of oxygen on metabolites were only visible in antibiotic free tissue supernatants. Treatment with penicillin has been shown to decrease bacterial sequence counts and microbial diversity in the cecum of chickens [35], potentially due to antibiotic treatment (PS) resulting in a decrease in select PS-sensitive microbiota, allowing PS-resistant bacteria to flourish. Penicillin treatment has also been shown to directly decrease the microbially derived metabolite phenyllactate, a change also observed in the present study (S1 Table). Similarly, as intermittent hypoxia has been shown to alter gut microbial diversity of mice [36] it is likely that lower oxygen concentrations facilitate the growth of some facultative and anaerobic bacteria, but perhaps decrease the growth rates of aerobic bacteria. A determination of bacterial species that contribute to these metabolic changes will require future metagenomics analyses.

Maintenance of tissue in ambient oxygen conditions has been standard in mammalian cell and tissue culture for decades [37]. While gut cell cultures can survive under these conditions, they do not represent physiologically relevant oxygen concentrations. Oxygen concentrations in the colonic mucosa range from roughly 1% (~6 mmHg) near the lumen, to between 5-10% (~25 – 70 mmHg) near the vascularized submucosa or deeper muscle layers [38]. The gut oxygen gradient is important for regulating the transcription factor hypoxia inducible factor-1 alpha (HIF-1 α) that helps control numerous metabolic and physiologic pathways, including creatine metabolism [39] and intestinal angiogenesis [40]. Recapitulating this oxygen gradient *ex vivo* is a difficult task, and one that was not attempted in the current

study. The present study mimicked the in vivo oxygen concentration seen in the apical colonic mucosa (approximately 1%, ~6 mmHg), ex vivo. Under 5.9 mmHg oxygen conditions, significantly more crypt cells underwent DNA synthesis, marked by EdU incorporation, when compared to slices cultured in ambient (100 mmHg) oxygen. In addition, the exclusion of penicillin-streptomycin treatment, and subsequent culture in 5.9 mmHg oxygen lead to a further significant increase in EdU incorporation compared to tissue cultured without PS. The amount of EdU incorporation observed at 5.9 mmHg oxygen without PS is consistent with the rates of another thymidine analog, 5-bromo-2'-deoxyuridine, incorporation seen in numerous in vivo human colonic mucosal proliferation studies [31,41]. The statistical interaction between oxygen and PS conditions pointed towards the importance of oxygen tension for antibiotics to have an effect on DNA synthesis in colonic mucosal crypts ex vivo. Altered oxygen availability can lead to varied bacterial metabolism [42] and secretion of products such as virulence factors [43]. The lowered oxygen concentration in the current study could thus influence microbial metabolism, potentially rendering bacteria more susceptible to antibiotic treatment. Further investigation into the interaction between oxygen concentration in culture and antibiotics influence on microbial metabolites is warranted.

Conclusions:

This report provides an organotypic slice model for human intestinal tissues ex vivo that optimizes cellular diversity and 3-dimensional integrity. This model can be used to tease apart complex multi – system – gut interactions with translational potential, including enteric pathogen interactions and intestinal immune responses to host - microbiome interactions. Importantly, cell proliferation in this model was impacted by two factors that influence microbial diversity and function: oxygen tension and antibiotic exposure. The physiological relevance of these factors may be missed under standard culture conditions with higher oxygen tension and exogenous

antibiotic added, especially in the context of how commensal microbial interactions impact tissue function. The current findings set the stage for use of the present organotypic slice model for studies of the complex roles of commensal microbiota and microbially-derived metabolite secretions in regulating human gut health. There is significant cell diversity in the colon along with unique physiologic oxygen tensions that are coupled with the presence of differentially active tissue and microbial metabolism. The system described in the current study offers important similarities to the intestinal wall *ex vivo*. It provides for live microscopic imaging of fluorescently tagged bacteria interacting with the native human gut environment, setting the stage for unravelling specific microbial – host cell interactions. For example, the complexity of local immune cell responses to pathogen will be more accessible *in vitro* as in the T-cell proliferation observed in the current study. Particular microbial metabolites may be manipulated to discern potential cellular mechanisms that may be disturbed in different disease states or tested for potential therapeutic value.

References:

- 1) National Institutes of Health, U.S. Department of Health and Human Services. Opportunities and Challenges in Digestive Diseases Research: Recommendations of the National Commission on Digestive Diseases. Bethesda, MD: National Institutes of Health; 2009. NIH Publication 08–6514.
- 2) Adams SM, Bornemann PH. Ulcerative Colitis. *Am Fam Physician*. 2013;87: 699-705.
- 3) Autrup H, Barrett LA, Jackson FE, Jesudason ML, Stoner G, Phelps P, Trump BF, Harris CC. Explant culture of human colon. *Gastroenterology*. 1978;74:1248-1257.
- 4) Liu YA, Chung YC, Pan ST, Shen MY, Hou YC, Peng SJ, et al. 3-D imaging, illustration, and quantitation of enteric glial network in transparent human colon mucosa. *Neurogastroenterol Motil*. 2013;25:e324-e338.
- 5) Yu YB, Li YQ. Enteric glial cells and their role in the intestinal epithelial barrier. *World J Gastroenterol*. 2014;20:11273-11280.
- 6) Sharkey KA. Emerging roles for enteric glia in gastrointestinal disorders. *J Clin Invest*. 2015;125:918-925.
- 7) Pochard C, Coquenlorge S, Freyssinet M, Naveilhan P, Bourreille A, Neunlist M, et al. The multiple faces of inflammatory enteric glial cells: is Crohn's disease a gliopathy? *Am J Physiol Gastrointest Liver Physiol*. 2018; doi:10.1152/ajpgi.00016.
- 8) Lee W, Hase K. Gut microbiota-generated metabolites in animal health and disease. *Nat Chem Biol*. 2014;10:416-424.
- 9) Brown JM, Hazen SL. Targeting of microbe-derived metabolites to improve human health: The next frontier for drug discovery. *J. Biol. Chem*. 2017;292:8560-8568.
- 10) Louis P, Hold GL, Flint HJ. The gut microbiota, bacterial metabolites and colorectal cancer. *Nature Reviews Microbiology*; 2014; doi:10.1038/nrmicro3344.

- 11) Berdy J. Bioactive Microbial Metabolites. *J. Antibiot.* 2005;58:1-26.
- 12) Jepson MA CM. The role of M cells in Salmonella infection. *Microbes Infect.* 2001;3:1183-90.
- 13) Bai SP, Huang Y, Luo YH, Wang LL, Ding XM, Wang JP, et al. Alteration in lymphocytes responses, cytokine and chemokine profiles in laying hens infected with Salmonella Typhimurium. *Vet Immunol Immunopathol.* 2014;160:235-243.
- 14) Lopez-Medina M, Carrillo-Martin I, Leyva-Rangel J, Alpuche-Aranda C, and Ortiz-Navarrete V. Salmonella impairs CD8 T cell response through PD-1: PD-L axis. *Immunobiology.* 2015;220:1369-1380.
- 15) Kelly CJ, Colgan SP. Breathless in the Gut: Implications of Luminal O₂ for Microbial Pathogenicity. *Cell Host Microbe.* 2016;19:427-428.
- 16) Thermann M, Jostarndt L, Eberhard F, Richter H, Sass W. Oxygen supply of the human small intestine in mechanical ileus. *Langenbecks Arch Chir.* 1985;363:179-84.
- 17) Albenberg L, Esipova TV, Judge CP, Bittinger K, Chen J, Laughlin A, et al. Correlation Between Intraluminal Oxygen Gradient and Radial Partitioning of Intestinal Microbiota. *Gastroenterology.* 2014;147:1055-1063.
- 18) von Martels JZH, Sadabad MS, Bourgonje AR, Blokzijl T, Dijkstra G, Faber KN, et al. The role of gut microbiota in health and disease: In vitro modeling of host-microbe interactions at the aerobe-anaerobe interphase of the human gut. *Anaerobe.* 2017;44:3-12.
- 19) Schwerdtfeger LA, Ryan EP, and Tobet SA. An organotypic slice model for ex vivo study of neural, immune, and microbial interactions of mouse intestine. *Am J Physiol Gastrointest Liver Physiol.* 2016;310:G240-248.
- 20) Chowdhury SR, King DE, Willing BP, Band MR, Beever JE, Lane AB, et al. Transcriptome profiling of the small intestinal epithelium in germfree versus conventional piglets. *BMC Genomics* 2007;8:215.

- 21) Tulstrup MV, Christensen EG, Carvalho V, Linninge C, Ahrne S, Hojberg O, et al. Antibiotic Treatment Affects Intestinal Permeability and Gut Microbial Composition in Wistar Rats Dependent on Antibiotic Class. *PLoS One*. 2015;10: e0144854.
- 22) Garner CD, Antonopoulos DA, Wagner B, Duhamel GE, Keresztes I, Ross DA, et al. Perturbation of the small intestine microbial ecology by streptomycin alters pathology in a *Salmonella enterica* serovar typhimurium murine model of infection. *Infect Immun*. 2009;77:2691-2702.
- 23) Sun J, Schnackenberg LK, Khare S, Yang X, Greenhaw J, Salminen W, et al. Evaluating effects of penicillin treatment on the metabolome of rats. *J Chromatogr B*. 2013;932:134-143.
- 24) Gustafsson JK, Ermund A, Johansson ME, Schutte A, Hansson GC, and Sjoval H. An ex vivo method for studying mucus formation, properties, and thickness in human colonic biopsies and mouse small and large intestinal explants. *Am J Physiol Gastrointest Liver Physiol*. 2012;302:G430-438.
- 25) Mapes B, Chase M, Hong E, Ludvik A, Ceryes K, Huang Y, et al. Ex vivo culture of primary human colonic tissue for studying transcriptional responses to 1 α ,25(OH) $_2$ and 25(OH) vitamin D. *Physiol Genomics*. 2014;46:302-308.
- 26) Drew JE, Farquharson AJ, Vase H, Carey FA, Steele RJ, Ross RA, et al. Molecular Profiling of Multiplexed Gene Markers to Assess Viability of Ex Vivo Human Colon Explant Cultures. *Biores Open Access*. 2015;4:425-430.
- 27) Yissachar N, Zhou Y, Ung L, Lai NY, Mohan JF, Ehrlicher A, et al. An Intestinal Organ Culture System Uncovers a Role for the Nervous System in Microbe-Immune Crosstalk. *Cell*. 2017;168:1135-1148.
- 28) Shah P, Fritz JV, Glaab E, Desai MS, Greenhalgh K, Frachet A, et al. A microfluidics-based in vitro model of the gastrointestinal human-microbe interface. *Nat Commun*. 2016;7:

11535.

- 29) Kumar A HA, Forster GM, Goodyear AW, Weir TL, Leach JE, Dow SW, et al. Dietary rice bran promotes resistance to *Salmonella enterica* serovar Typhimurium colonization in mice. *BMC Microbiol.* 2012;12:71-80.
- 30) Nealon NJ, Yuan L, Yang X, Ryan EP. Rice Bran and Probiotics Alter the Porcine Large Intestine and Serum Metabolites for Protection against Human Rotavirus Diarrhea. *Front Microbiol.* 2017;8:653.
- 31) Potten CS KM, Roberts SA, Rew DA, Wilson GD. Measurement of in vivo proliferation in human colorectal mucosa using bromodeoxyuridine. *Gut.* 1992;33:71-78.
- 32) Nealon NJ, Worcester CR, and Ryan EP. *Lactobacillus paracasei* metabolism of rice bran reveals metabolome associated with *Salmonella Typhimurium* growth reduction. *J Appl Microbiol.* 2017;122:1639-1656.
- 33) Li X, Yao Y, Wang X, Zhen Y, Thacker PA, Wang L, et al. Chicken egg yolk antibodies (IgY) modulate the intestinal mucosal immune response in a mouse model of *Salmonella typhimurium* infection. *Int Immunopharmacol.* 2016;36:305-314.
- 34) Rydstrom A & Wick MJ. Monocyte Recruitment, Activation, and Function in the Gut-Associated Lymphoid Tissue during Oral *Salmonella* Infection. *J Immunol.* 2007;178:5789-5801.
- 35) Singh P, Karimi A, Devendra K, Waldroup PW, Cho KK, Kwon YM. Influence of penicillin on microbial diversity of the cecal microbiota in broiler chickens. *Poult Sci.* 2013;92:272-276.
- 36) Moreno-Indias I, Torres M, Montserrat JM, Sanchez-Alcoholado L, Cardona F, Tinahones FJ, et al. Intermittent hypoxia alters gut microbiota diversity in a mouse model of sleep apnoea. *Eur Respir J.* 2015;45:1055-1065.
- 37) Rodriguez-Hernandez CO MA, Gonzalez FJA, Guerrero-Barrera AL. Cell culture: History, Development and Prospects. *Int J Curr Res Aca Rev.* 2014;2:188-200.

- 38) Zheng L, Kelly CJ, and Colgan SP. Physiologic hypoxia and oxygen homeostasis in the healthy intestine. A Review in the Theme: Cellular Responses to Hypoxia. *American J Physiol Cell Physiol*. 2015;309:C350-360.
- 39) Glover LE, Bowers BE, Saeedi B, Ehrentraut SF, Campbell EL, Bayless AJ, et al. Control of creatine metabolism by HIF is an endogenous mechanism of barrier regulation in colitis. *Proc Natl Acad Sci U S A*. 2013;110:19820-19825.
- 40) Bakirtzi K, West G, Fiocchi C, Law IKM, Iliopoulos D, Pothoulakis C. The Neurotensin-HIF- 1α -VEGF α Axis Orchestrates Hypoxia, Colonic Inflammation, and Intestinal Angiogenesis. *Am J Pathol*. 2014;184:3405-3414.
- 41) Khan S, Raza A, Petrelli N, Mittleman A. In Vivo Determinations of Labelling Index of Metastatic Colorectal Carcinoma and Normal Colonic Mucosa Using Intravenous Infusions of Bromodeoxyuridine. *J Surg Oncol*. 1988;39:114-118.
- 42) Wessel AK, Arshad TA, Fitzpatrick M, Connell JL, Bonnecaze RT, Shear JB, et al. Oxygen Limitation within a Bacterial Aggregate. *mBio*. 2014;5:e00992-14.
- 43) Schertzer JW, Brown SA, Whiteley M. Oxygen levels rapidly modulate *Pseudomonas aeruginosa* social behaviors via substrate limitation of PqsH. *Mol Microbiol*. 2010;77(6):1527-1538.

CHAPTER 6 – VASOACTIVE INTESTINAL PEPTIDE REGULATES ILEAL GOBLET CELL PRODUCTION IN MICE⁶

Overview:

Innervation of the intestinal mucosa has gained more attention with demonstrations of tuft and enteroendocrine cell innervation. However, the role(s) these fibers play in maintaining the epithelial and mucus barriers are still poorly understood. The present study therefore examines the proximity of mouse ileal goblet cells to neuronal fibers, and the regulation of goblet cell production by vasoactive intestinal peptide (VIP). An organotypic intestinal slice model that maintains the cellular diversity of the intestinal wall *ex vivo* was used. An *ex vivo* copper-free click-reaction to label glycosaminoglycans was used to identify goblet cells. Pharmacological treatment of slices was used to assess the influence of VIP receptor antagonism on goblet cell production and neuronal fiber proximity. Goblet cells were counted and shown to have at least one peripherin immunoreactive fiber within 3 μm of the cell, 51% of the time. Treatment with a VIP receptor type I and II antagonist (VPACa) resulted in an increase in the percentage of goblet cells with peripherin fibers. Pharmacological treatments altered goblet cell counts in intestinal crypts and villi, with tetrodotoxin and VPACa substantially decreasing goblet cell counts. When cultured with 5-Ethynyl-2'-deoxyuridine (EdU) as an indicator of cell proliferation, colocalization of labeled goblet cells and EdU in ileal crypts was decreased by 77% when treated with VPACa. The present study demonstrates a close relationship of intestinal goblet cells to neuronal fibers. By using organotypic slices from mouse ileum, vasoactive intestinal peptide receptor regulation of gut wall goblet cell production was revealed.

⁶ Schwerdtfeger LA, Tobet SA. Vasoactive intestinal peptide regulates ileal goblet cell production in mice. *Physiol Rep.* 2020;8:e14363.

Introduction:

Gut luminal microbiota are separated from the small intestinal epithelial barrier by an a non-adherent mucus layer in the small intestine (26). Goblet cells in the intestinal wall secrete large quantities of mucus, composed of mucins – principally Muc2 in intestine – which are comprised of a protein core, connected to chains of O-linked glycans, usually in the form of glucosamino- or glycosamino- glycans (21). How the gut mucus layer and epithelial barrier are regulated in health and disease is poorly understood. This is partially due to investigations using monolayer epithelial culture models that until recently did not contain a mucus layer (50). While this is an advance, epithelial culture systems miss the cellular diversity of the gut wall, a critical aspect of in vivo physiologic function (33, 44). Understanding intestinal wall function ultimately requires parsing the interactions of the diverse cellular elements. The current study addresses the impact of neural regulation on gut wall goblet cells in an organotypic model of gut physiology that maintains numerous cell types ex vivo, including goblet cells and neurons.

There have been several recent demonstrations of neural influence(s) on gut epithelial components, principally on secretory epithelial cell types (49). One line of study focused on glial – enteroendocrine cell (EEC) interactions (6) and more recently, direct innervation of EECs via vagal afferents (26). Another line of study focused on tuft cells and show close proximity to neuronal fibers, with more connections observed in the proximal small intestine (11). There are peptidergic neuronal fibers throughout the intestinal mucosa (19) in close proximity to the apical enterocytes in the sub-epithelial plexus (16, 28). Whether, and which, peptides/factors regulate goblet cell function is unclear. Corticotropin releasing hormone (CRH) has been shown to stimulate mucus secretion in the colon of rats (40), and blocking neuronal firing with tetrodotoxin has been shown to inhibit goblet cell secretion normally evoked by electrical field stimulation (38). Vasoactive intestinal polypeptide (VIP) has been shown to cause goblet cell secretion (14,

30), but other reports have not found influences of VIP on intestinal goblet cell mucus secretion (20, 34). Given the critical role goblet cells play in maintaining the gut mucus layer (1) and in direct interactions with microbiota (5, 22, 31), the current study was conducted to further delineate the peptide regulation of goblet cell function.

VIP is a 28 amino acid peptide secreted by enteric neurons (17, 46), and has known roles in gut smooth muscle contractility/relaxation (27), and ion secretion (13). While VIP shares high sequence homology with pituitary adenylate cyclase-activating polypeptide (PACAP), both peptides bind the same receptors, VPAC1 and VPAC2, however at slightly different affinities (47). Both receptors can be antagonized by [D-p-CI-Phe⁶,Leu¹⁷]-VIP (37) which will be referred to as “VPACa”. Given the large distribution of VIP receptors throughout the gut wall (23), it is reasonable to consider the potential for a neuronal regulation of goblet cell quantities, production of mucus, and/or secretion, at baseline and potentially in response to bacterial infiltration.

The current study uses organotypic intestinal slices (42, 43) as a platform for investigating neural – goblet cell interactions in mouse ileum ex vivo. This intestinal slice method allowed for use of three pharmacological tools for altering goblet cell function ex vivo in a cellularly heterogenous tissue. Lipopolysaccharide (LPS), which causes intestinal goblet cells to secrete mucus in the mouse colon, but not ileum (5). The sodium ion channel blocker tetrodotoxin (TTX), which blocks large amounts of enteric neuronal signaling (36), and finally VPACa, an antagonist for both VIP receptors (37). These ex vivo pharmacological treatments were coupled with molecular visualization tools to reveal an anatomical bases for neuronal fiber signaling with ileal goblet cells. Further, this study suggests a specific role for neuronal fibers containing VIP to play in regulating intestinal goblet cell production.

Materials and Methods:

Animals:

Male and female adult mice aged between 8-16 wk old, of the C57BL/6 background were used for all experiments. Mice were housed at Colorado State University, under the care of Laboratory Animal Resources, and kept in cages with aspen bedding (autoclaved Sani-chips; Harlan Teklad, Madison, WI). Mice were housed under a 14:10-h light-dark cycle, with ad libitum access to water and food (no. 8649; Harlan Teklad). Intestinal slices were generated from a transgenic strain where animals expressed yellow fluorescent protein (YFP) driven by a neuronally selective Thy-1 promoter (15) (Thy-1 YFP). Animal studies were approved by the Colorado State University IACUC under protocol #17-7270a. Intestines from at least 3 animals were used for all experiments and matched by sex where possible.

Organotypic slice preparation:

Preparation of intestinal slices was similar to that previously described (43). Briefly, mice were deeply anesthetized with isoflurane and subsequently killed via decapitation, to ensure severing of vagal fibers. The entire small intestine was removed from the pylorus-duodenal junction, to the ileo-cecal junction. Tissue was immediately placed into 4°C 1X Krebs buffer and the ileum was separated from the remainder of the intestine based off tissue anatomy. Remnant mesenteric fat and connective tissue was dissected away, and tissue was cut into pieces roughly 2-4-mm in length. Tissue was blocked in low melting point, 8% agarose (Gold Biotechnology, St. Louis, MO) and spent 5 min on a room temperature shaker and 2 min in 4°C to ensure gelation. Slices were cut at 250 µm thick on a vibrating microtome (VT1000S; Leica Microsystems, Wetzlar, Germany) and collected into ice cold 1X Krebs buffer, before transfer into a 60 mm plastic-bottom dish (Corning, Corning, NY) containing 5 ml of Hibernate Media (Life Technologies, Grand Island, NY). Slices spent 15 min at 4°C in Hibernate media

prior to being transferred into 5 ml of CTS Neurobasal-A Media (ANB; Life Technologies) with 5% B-27 supplement (B-27; Life Technologies, Carlsbad, CA) where they spent 35 min at 37°C. Samples were plated on 35 mm plastic bottom dishes (MatTek, Ashland, MA) with excess media being siphoned from the dish, and incubated at 37°C for 10 min. Next, slices were covered by a thin layer of collagen solution [vol/vol: 10.4% 10X MEM (Minimal Essential Medium, Sigma-Aldrich, St. Louis, MO), 4.2% sodium bicarbonate, and 83.5% collagen (PureCol; Inamed, Fremond, CA)] which was allowed to polymerize for 15 min prior to final addition of 1 ml of ANB + B-27. Tissue was left in a 37°C, 5% CO₂, and 1% O₂ incubator until experiments were performed.

Glycosaminoglycan Visualization and Drug Dosing:

Slices were created as above and cultured in ANB with B-27 for 24 h prior to the addition of an azido-modified galactosamine, Tetraacetylated N-Azidoacetylgalactosamine (GalNAz; 12.5 µM; Fisher Scientific, Pittsburgh, PA). GalNAz was allowed to incubate in the slice dishes for 24 h prior to development. Concurrently with GalNAz treatment, slices were dosed with one of four compounds at 24 h ex vivo: vehicle (10 µl Milli-Q Water), TLR grade lipopolysaccharide derived from *E. coli* Serotype EH100 (10 µg/ml; Enzo Life Sciences, Inc. Farmingdale, NY), the sodium ion channel blocker tetrodotoxin (10 µM; Abcam, Cambridge, MA) or the vasoactive intestinal peptide receptor antagonist [D-p-CI-Phe⁶,Leu¹⁷]-VIP (10 µM, Bio-Techne Corporation, Minneapolis, MN). After 24 h of incubation, the fluorophore-tagged alkyne, Dibenzocyclooctyne-Cy3 (DBCO-Cy3; 2 µM; Sigma-Aldrich, St. Louis, MO) was added to visualize GalNAz. This copper-free click reaction was allowed to proceed in the dark for 15 minutes at 37°C, 5% CO₂, 1% O₂. Finally, culture supernatant was removed, and slices were fixed in 4% formaldehyde prior to re-sectioning.

Re-sectioning of Slices:

After 48h of culture, ileum slices were fixed for 10 min in 4% formaldehyde. Tissue was then placed in a 4% agarose solution (w/v; Fisher Scientific, Pittsburgh, PA) and subsequently put in a 4°C fridge for 4 min to ensure agarose gelation. Ileum slices were then sectioned on a vibrating microtome (VT1000S; Leica Microsystems, Wetzlar, Germany) at 50 µm thick (Figure 1C) before being processed for immunohistochemistry.

Immunohistochemistry:

After re-sectioning, 50 µm sections were washed in PBS for at least 10 min prior to receiving 0.1M glycine made in 0.05M PBS for 30 min. Tissue was subsequently washed three times in PBS for 5 min each wash. Next, sections received 0.5% sodium borohydride in PBS for 15 min. Sections were then washed twice for 5 min in PBS before blocking in 5% NGS, 0.5% Tx, and 1% H₂O₂ in PBS for 30 min. After blocking, sections received one of three primary antisera for two days: a monoclonal anti-peripherin (1:300; Chemicon International, Temecula, CA), a polyclonal anti-VIP (1:8000; Immunostar, Inc. Hudson, WI), or a polyclonal anti-MUC2 (3 µg/mL; Novus Biologicals, Centennial, CO). After primary, sections were washed with 1% NGS in PBS four times for 15 min each wash. Next, secondary antibody was added for 2 h at room temperature and consisted of 1% NGS and 0.5% Tx in PBS with a biotinylated goat anti-rabbit secondary antibody (1:2500; Jackson ImmunoResearch Inc. West Grove, PA). Secondary antibody was washed out with four 15 min washes composed of 0.02% Tx in PBS. Sections were next incubated with an Alexa Fluor 488 conjugated to streptavidin (1:500; Invitrogen, Carlsbad, CA) in 0.32% Tx in PBS for 1 h. Finally, sections received three PBS washes prior to mounting and imaging.

Tissue Imaging and Analysis:

Slices and re-sectioned tissue were imaged on either a Nikon TE2000-U inverted microscope (10X Plan-Fluor and 20X Plan-Apo objectives) with a UniBlitz shutter system (Vincent Associates, Rochester, NY) and an Orca-flash 4.0 LT camera (Hamamatsu, Hamamatsu City, Shizuoka Prefecture, Japan), or a Zeiss LSM 880 confocal microscope with an Axiocam 503 mono camera (Carl Zeiss, Inc., Thornton, NY). Data in GalNAz-DBCO-Cy3 fluorescent cell counting and the EdU / GalNAz colocalization experiments were gathered via confocal Z-stack with 30- 1 μ m planes being captured through the center of the tissue. A max intensity Z-projection was performed using FIJI (ImageJ, v1.0; NIH) and cells were manually counted by a researcher blinded to treatment. Data for GalNAz-DBCO-Cy3 fluorescent cell proximity to peripherin immunoreactive fibers was performed by a researcher blinded to treatment who randomly sampled 3- Z-planes throughout the tissue section based on GalNAz-DBCO-Cy3 fluorescence only. Analysis was performed in FIJI using a 3 μ m dilation around all GalNAz-DBCO-Cy3 fluorescent cells before using the analyze particles tool to quantify peripherin immunoreactive fibers within the 3 μ m dilations.

Statistics:

All statistical analysis was performed using Prism 8 (Graphpad, San Diego, CA). For all GalNAz cell count analysis and peripherin-GalNAz analysis, a two-way ANOVA was performed by treatment and region. A Sidak's multiple comparisons post-hoc test was performed for comparison of individual group means. For the GalNAz – EdU colocalization experiment, data was analyzed using a one-way ANOVA by treatment, with a Tukey's multiple comparisons post-hoc test. All data is presented as means +/- standard error of the mean (SEM).

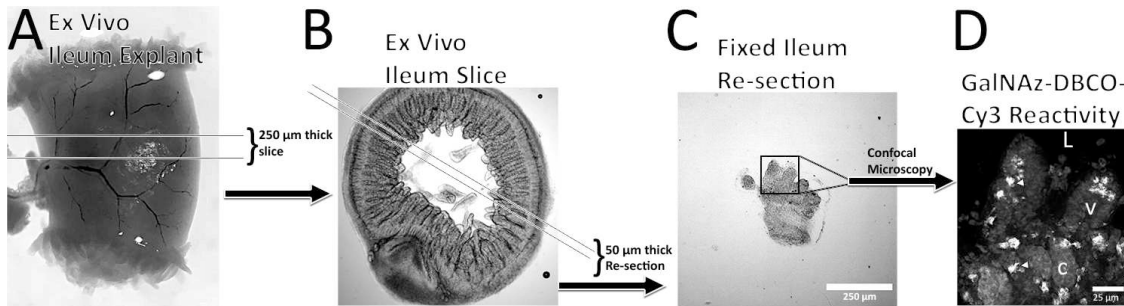


Figure 23. Schematic representation of culture protocol path from a ~2cm long ileum explant (A) to a 250 μm thick ex vivo ileum slice (B) to a 50 μm thick re-sectioned piece of fixed ileum (C), and a representative confocal photomicrograph of GalNAz-DBCO-Cy3 reactivity (D). In D, arrow heads point to stereotypic GalNAz-DBCO-Cy3 labeled cells, and 'L' represents the lumen, 'v' a villus, and 'c' a crypt. Scale bars are 250 μm in C, and 25 μm in D.

Results:

Intestinal slices maintain goblet cells ex vivo

Organotypic intestinal slices from mouse ileum (Figure 23A-B) maintained glycosaminoglycan producing goblet cells ex vivo for at least 48 h. Labeling of glycosaminoglycans was

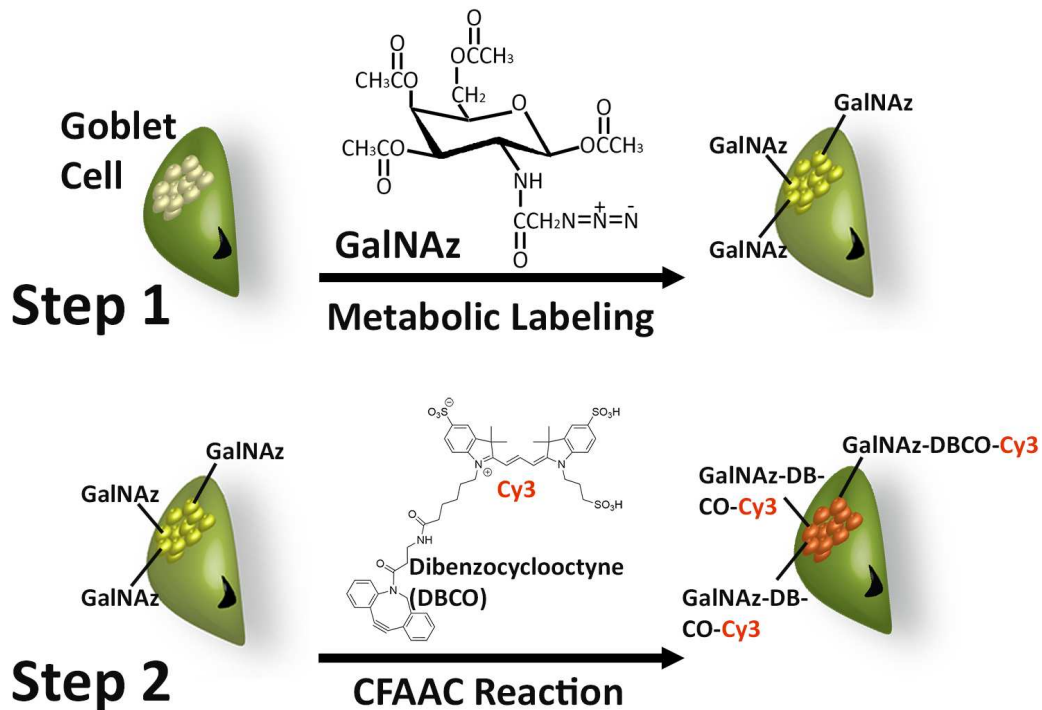


Figure 24. Schematic representation of both the metabolic incorporation of GalNAz into goblet cell glycosaminoglycans (Step 1), and the copper free azide-alkyne cycloaddition (CFAAC) of DBCO-Cy3 onto GalNAz (Step 2). GalNAz-DBCO-Cy3 labeled cells are indicated with orange/red granules.

accomplished using a copper free azide-alkyne cycloaddition (CFAAC; Figure 24) click reaction. Incorporation of Tetraacetylated N-Azidoacetylglactosamine (GalNAz) into goblet cell glycosaminoglycans was visualized with dibenzocyclooctyne-Cy3 (DBCO-Cy3) and thereby labeled glycosaminoglycan producing goblet cells ex vivo (Figure 23C-D). For preliminary experiments, slices of mouse colon from 4 animals per treatment were cultured in either atmospheric oxygen conditions at 5000 feet above sea level in Colorado (~17% = 100 mmHg) or low oxygen (1% = 5.9 mmHg) incubators. The percentage of area labeled in regions of interest drawn around the colonic mucosa with GalNAz-DBCO-Cy3 fluorescence were measured. GalNAz-DBCO-Cy3 label was 2-fold higher in 1% cultured slices compared to 17% oxygen cultured tissue, with slices cultured in 1% oxygen showing a mean of 20.16 +/- 2.3 percentage area labeled, while 17% oxygen slices had 10.55 +/- 1.9 percent area labeled ([t =

3.23, df = 33] $p < 0.01$). Area analyzed was similar for both conditions and incorporated dozens of crypts per treatment. Mean area analyzed was $409.8 \pm 43.3 \text{ mm}^2$ for 17% oxygen slices, and $306.5 \pm 56.7 \text{ mm}^2$ for 1% oxygen slices ([$t = 1.436$, df = 33] $p = 0.16$). All subsequent experiments were conducted in the low oxygen environment. Organotypic intestinal slices from mouse ileum housed GalNAz-DBCO-Cy3 labeled cells along the length of the crypt-villus axis. Post-hoc immunohistochemistry showed regular colocalization of MUC2 immunoreactivity with GalNAz-DBCO-Cy3 fluorescence (Figure 25A-B). Across all treatments in mouse ileal slices, GalNAz-DBCO-Cy3 fluorescent cells were colocalized with immunoreactive MUC2 62% of the time.

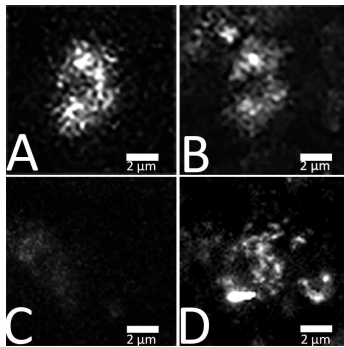


Figure 25. GalNAz reliably labels intestinal goblet cells. (A) shows GalNAz-DBCO-Cy3 reactivity in a single goblet cell. (B) shows MUC-2 immunoreactivity in the same goblet cell as panel A. C and D show a representative goblet cell that has MUC-2 immunoreactivity (D) but no GalNAz-DBCO-Cy3 reactivity (C). Scale bars in all panels are 2 μm .

Neural fibers densely innervate ileal mucosa

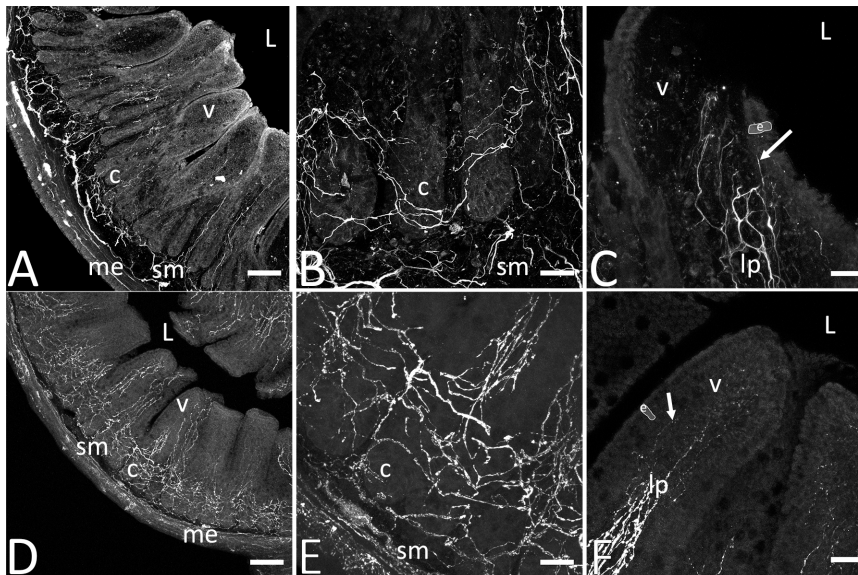


Figure 26. Representative z-projected confocal images of peripherin (A-C) and VIP (D-F) immunoreactivity in 50 μm sections of mouse ileum. Panels A and D show patterns of fiber distribution throughout the mucosa. Panels B and E show dense ileal crypt innervation patterns, and panels C and F show neuronal fibers in the villi, with arrows pointing to fibers of the sub-epithelial plexus running beneath the apical-most epithelial layer. Outlined and highlighted areas labeled with 'e' in panels C and F represent apical enterocytes. High magnification images in panels B and C are not directly taken from the same section as the low-magnification image in panel A. In all panels, 'L' represents the lumen, 'v' a villus, 'c' a crypt, 'sm' submucosa, 'me' muscularis externa, and 'lp' lamina propria. Scale bars 100 μm in A and D, and 25 μm in B,C,E,F.

An extensive network of enteric neuronal fibers infiltrated the gut mucosa. Fibers containing immunoreactive peripherin densely wrapped around intestinal crypts weaving throughout the lamina propria towards the intestinal lumen (Figure 26A-B). In these same sections peripherin immunoreactive fibers were projected to the apical most enterocytes (outlined and highlighted in Figure 26 C and F) that form the gut epithelial barrier (arrow, Figure 2C). VIP – immunoreactive fibers were also observed densely wrapping intestinal crypts (Figure 26D-E) and throughout the villus lamina propria and extended to the villus apex (arrows,

Figure 26F). These fibers were detected projecting directly to the apical-most enterocytes in the ileal villi, as with peripherin fibers.

Peripherin fibers project to ileal goblet cells

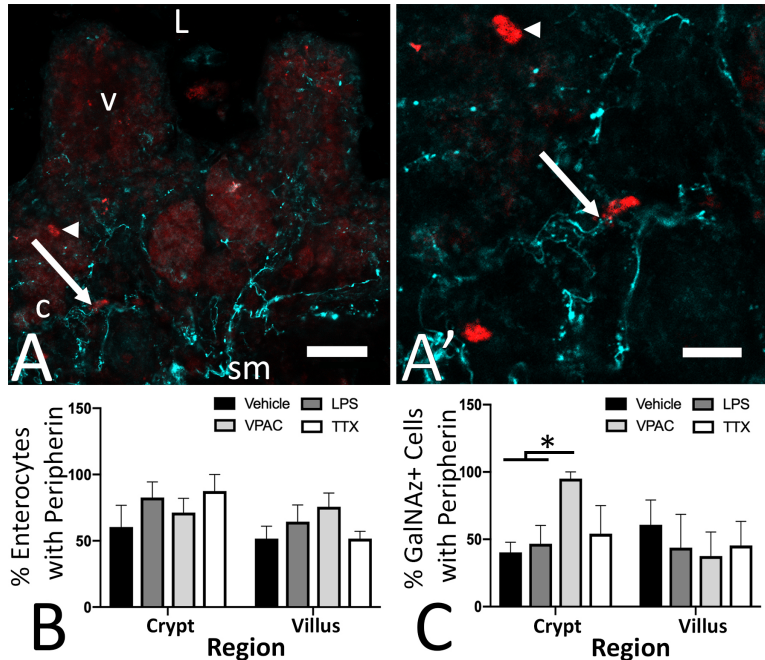


Figure 27. Percentage of GalNAz+ cells with peripherin fibers within 3µm is increased in VPACa treatment in ileal crypts. Representative photomicrograph (A) shows GalNAz-DBCO-Cy3 reactive cells in red (arrow and arrow head) with peripherin-immunoreactive fibers in cyan throughout the mucosa. (A') is a magnified view of (A) showing numerous fibers projecting towards a GalNAz-DBCO-Cy3 reactive cell (arrow), and a second cell without any fibers (arrow head). (B) quantification of the percentage of non-GalNAz reactive enterocytes peripherin fibers. (C) quantification of the percentage of GalNAz-DBCO-Cy3 reactive cells with peripherin fibers. 'L' represents the lumen, 'v' a villus, 'c' a crypt. The * in panel B denotes $p < 0.05$. Scale bars are 25 µm in A and 10 µm in A'. Data from $n = 4$ animals (2 males, 2 females). Values are means +/- SEM.

Neuronal fibers were in close proximity (within 3 µm) to GalNAz-DBCO-Cy3 reactive goblet cells throughout the mucosa (Figure 27A-A'; arrow). Neuronal fibers containing immunoreactive peripherin were denser in the submucosal and crypt regions of ileal tissue

(Figure 27A) than in the villi. This was consistent with both peripherin- and VIP-immunoreactivity patterns in fixed 50 μm sections of ileum (Figure 26A-C). Numerous fibers were found in close proximity to GalNAz-DBCO-Cy3 fluorescent goblet cells (e.g., arrow in Figure 27A-A'). There were also many goblet cells that did not have closely apposed peripherin fibers (arrow head in Figure 27A-A'). In addition, when looking at enterocytes directly adjacent to GalNAz labelled cells, there was no change in percentage of these enterocytes with proximal peripherin fibers, regardless of region ($[F(1,24) = 3.18]$; $p = 0.09$) or treatment (Figure 27B; $[F(3,24) = 1.02]$; $p = 0.4$). When analyzing GalNAz-DBCO-Cy3 reactive cells, vehicle treated slices had 53.9 \pm 9.2 percent of goblet cells with at least one peripherin fiber. LPS treated slices showed 44.7 \pm 12.4 percent with a fiber, while VPACa and TTX had 56.7 \pm 11.7 and 48.4 \pm 10.4 percent of cells with a fiber, respectively.

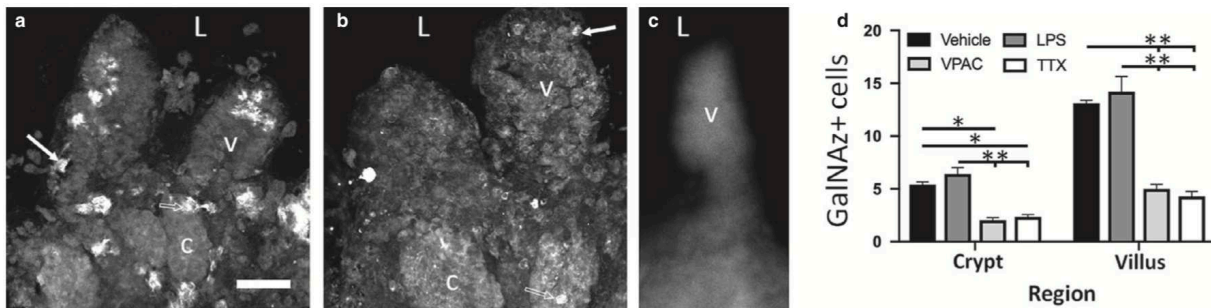


Figure 28. Dosing with VPACa or TTX substantially decreases the quantity of GalNAz+ cells per crypt, and per villus compared to vehicle and/or LPS. (A) a representative photomicrograph of a vehicle treated slice showing large quantities of GalNAz-DBCO-Cy3 reactive cells in both the crypts 'c' and the villi 'v'. (B) a representative photomicrograph of DBCO-Cy3 reactive cells in a VPACa treated slice. Arrows in both A and B point to a stereotypic DBCO-Cy3 labelled cell in the villus, while hollow arrows point to a stereotypic cell in the crypt. (C) Representative negative control image showing a lack of clearly labeled goblet cells. (D) quantification of the GalNAz+ cell counts throughout the crypt and villi. 'L' represents the lumen. In panel C, * denotes $p < 0.05$, and ** denotes $p < 0.01$. Scale bars in A – C are 25 μm . Data from $n = 6$ animals (3 males, 3 females). Values are means \pm SEM.

No differences were observed across these treatments ($[F(3,44) = 0.24]$; $p = 0.86$). When separated by anatomic region, no differences were observed in the percentage of GalNAz-DBCO-Cy3 reactive cells with closely apposed peripherin fibers across all treatments ($[F(3,24) =$

0.59]; $p = 0.62$) or by region (i.e. crypt vs villus; $[F(1,24) = 1.03]$; $p = 0.32$) except for slices treated with VPACa. Slices treated with VPACa for 24 h showed an increase in the percentage of GalNAz-DBCO-Cy3 fluorescent cells with peripherin fibers in the crypt (95 +/- 5 percent) compared to vehicle (40.3 +/- 7.5) and LPS (46.7 +/- 13.7; Figure 27C $[F(3,11) = 6.07]$; $p = 0.01$).

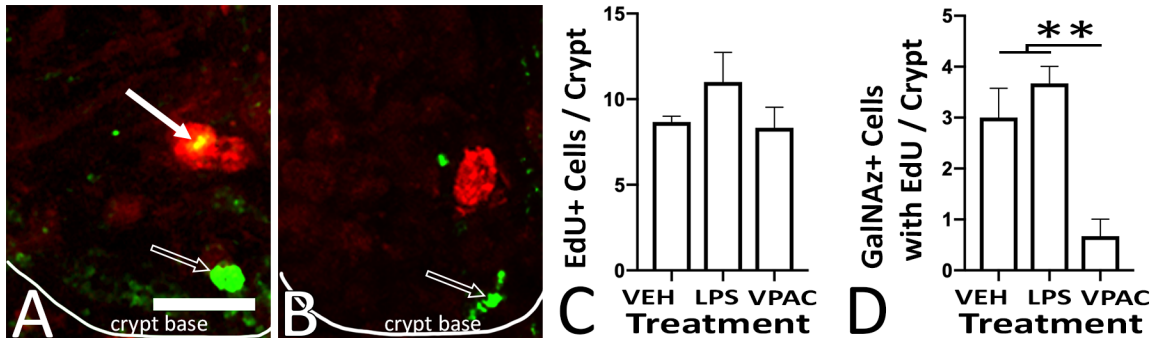


Figure 29. Dosing with VPACa decreased the number of GalNAz+ cells with EdU colocalization. (A) shows the base of a single crypt in a vehicle treated slice, with a GalNAz-DBCO-Cy3 reactive cell (red) colocalized with EdU (green). In A there is an EdU reactive cell (hollow arrow) and a colocalized cell (arrow). (B) shows the base of a single crypt in a VPACa treated slice, and an EdU reactive cell (hollow arrow), and a GalNAz-DBCO-Cy3 reactive cell (red) without any EdU colocalization are visible. White line denotes the crypt base in A-B. (C) quantification of total EdU cell counts per crypt. (D) quantification of GalNAz – EdU colocalization. Scale bar in A is 5 μ m. Scale in B is the same as A. Data from $n = 3$ animals (2 males, 1 female). Values are means +/- SEM.

VPAC receptors regulate goblet cell count and production

GalNAz-DBCO-Cy3 fluorescent goblet cell count and proliferation were altered by ex vivo pharmacological treatment with VPACa. There was a 50% decrease in GalNAz+ cell counts in the crypts and villi compared to vehicle and/or LPS (Figure 28) that can be seen in a representative image of a vehicle treated slice (Figure 28A) compared to a VPACa treated slice (Figure 28B). When separated by region, more GalNAz-DBCO-Cy3 reactive cells were observed in the ileal villi compared to crypts across treatments (Figure 28A-D; $[F(3,32) = 131.4]$; $p < 0.0001$). This effect was also observed between vehicle and VPACa, as well as vehicle and TTX (Figure 28D; $[F(3,32) = 68.9]$; $p < 0.0001$). Negative controls were performed for the

CFAAC reaction, showing no fluorescently labeled goblet cells when mouse ileal slices were cultured with DBCO-Cy3 alone, without GalNAz (Figure 28C). When vehicle (Figure 29A) and VPACa (Figure 29B) treated slices were given the thymidine analog 5-Ethynyl-2'-deoxyuridine (EdU) ex vivo, incorporation of EdU was detected in 9.3 +/- 1.09 cells / crypt across all treatments. No differences were observed in EdU cell counts per crypt between treatments (Figure 29C). Slices treated with EdU and GalNAz-DBCO-Cy3 ex vivo showed colocalization in ~30% of all EdU cells in ileal crypts in vehicle treated slices (Figure 29A,D). When treated with LPS, there was no difference compared to control. However, treatment with VPACa (Figure 29B) resulted in a 77% decrease in the number of GalNAz-DBCO-Cy3 reactive cells that were colocalized with EdU (Figure 29D; [F(2,6) = 13.4]; p < 0.01).

Discussion:

The intestinal wall functions as an ensemble of cellular constituents that provide for nutrient absorption on one hand and protection from the outside world on the other. From the luminal space to the outside of the wall, the constituents include microbiota, mucus, and then epithelial, immune, neural, and muscle cells. Communication among these elements is extensive, but poorly defined in many places. The present study provides an anatomical basis for neural signaling to enteric goblet cells of the epithelial layer and shows the selective impact of VIP receptors on goblet cell production. There have been demonstrations of neural – epithelial signaling in the intestine via enteroendocrine cells (6, 7), and cholinergic regulation of goblet cells in the eye conjunctiva (18). Peptidergic regulation of goblet cells in the intestine has been suggested, but potential sources have been vague. The close proximity of enteric neuronal fibers to a subset of goblet cells labeled for live mucus synthesis in the current study provides an anatomical linkage for potential functional signaling between these cells. Goblet

cells with live glycosaminoglycan labeling in the crypts were more likely to be in close proximity to peripherin immunoreactive neuronal fibers when slices were treated *ex vivo* with a VIP antagonist (VPACa) compared to control, an inhibitor of synaptic signaling through sodium channels (tetrodotoxin), or an immune system stimulant (LPS). Thus, VIP of local origin may be a key modulator of goblet cell function in the intestinal wall.

The current study adapted a powerful technique to label goblet cells and mucus *in vivo* (25) to label *ex vivo* and ultimately will make it possible to examine *live*. Copper-catalyzed azide-alkyne additions have been used but are traditionally thought to be cytotoxic to living cells and tissues (3). Copper-free azide-alkyne cycloadditions (CFAACs) have gained some prominence due to their biocompatibility and have been used to label intestinal goblet cells in fixed tissue (41). CFAACs have not previously been used *ex vivo* to label goblet cells in cellularly heterogeneous tissues. The present study verified that a CFAAC method labeled live glycosaminoglycan producing intestinal goblet cells *ex vivo*. GalNAz incorporation and subsequent label via CFAAC with a fluorophore had a consistent colocalization with Muc2-immunoreactivity in ~62% of cells. This colocalization matched a previous study that labeled mouse colonic goblet cells *in vivo* with GalNAz and subsequently labeled with Muc2 via immunohistochemistry (25). These data indicate that the percent incorporation of GalNAz into a Muc-2 immunoreactive goblet cells in ileum is similar *ex vivo* as *in vivo* removing the concern of tissue toxicity due to copper while retaining the labeling efficiency. Whether the percent of goblet cells labeled for glycosaminoglycan synthesis being less than the total indicates unique attributes of the cells such as synthesis of sugars other than galactosamines, or is due to limitations of the technique as suggested previously (24) remains to be determined.

The presence of a subepithelial plexus of neural fibers in intestinal villi was first observed by Ramon y Cajal, among others, in the late 1800s (9, 16). However, in-depth phenotyping of

these fibers along the length of the gastrointestinal tract is still incomplete. Neuronal fibers carrying immunoreactive VIP have been shown to travel in close proximity to enterocytes in the intestinal crypts (51), however, the role these fibers play in regulating goblet cells (production and/or function) is unclear. In the present study, VIP receptor antagonism affected neuronal fiber localization close to goblet cells in the ileal crypts, but not villi. Therefore, VIP's role may be spatially limited, and other transmitters may be involved in goblet cell signaling as they ascend the length of the villi. There are a large number of neuronally secreted peptides in the intestine that may play roles in modulating goblet cell secretion (16), including corticotropin releasing hormone (10), substance P (48), somatostatin (48), and calcitonin gene related peptide (39), among others. Additionally, bi-directional neuroimmune signaling between enteric neuronal fibers and mast cells (8) can regulate mucus secretion (10) among a host of other cellular responses (4). Therefore, VIP produced in neurons is not the only pathway for peptidergic regulation of goblet cell functions, and further fleshing out of the molecular signaling mechanisms between enteric neuronal projections, mast cells, and goblet cells will be important.

Enteric neurons express a large variety of receptors, produce numerous different peptides and transmitters, and vary in their excitatory state dependent upon region (35). TTX blocks voltage gated sodium channels, of which there are numerous types in the intestine, with differential expression based on neuron type (2). Inhibition of sodium channels via TTX dosing served as a more global, non-specific, neuronal inhibition for pharmacological studies in which the specific receptor antagonist, VPACa, was used. Observations in the present study showed similar influences of TTX and VPACa on the counts of goblet cells incorporating GalNaz ex vivo in both crypts and villi. This points toward a neural (TTX) influence on goblet cells, and a potentially more specific pathway via VIP receptors (VPACa). Further work is needed to

explicitly define the peptide receptor expression on enteric goblet cells, with a focus on crypt and villi cell populations as a distinct variable.

Goblet cell function in the intestinal tract is likely regulated by neural factors, however, there is a large intestinal immune component that holds influence over epithelial function. The pathways involved in goblet cell signaling with neurons, immune cells, or both, remain poorly understood. Treatment with the bacterial cell wall component LPS has been shown to increase mast-cell activation (12). While mast cells have been observed to be involved in enteric neuro-immune signaling (8), and are known to have VIP-receptors (29), there was no direct influence of LPS on the counts of goblet cells incorporating GalNaz *ex vivo* in any of the present experiments. This suggests that there may not be a direct immune signaling altering glycosaminoglycan synthesis in goblet cells or their proximity to neuronal fibers. Given the influence of VPACa dosing on neuronal fiber localization and goblet cell counts, VIP may be a key regulator of goblet cells in the ileal mucosa. However, given the likely role of neural – immune signaling in host-pathogen interactions (45), further work is needed to flesh out more obscure influences of the immune system on enteric goblet cell regulation.

The results of the current study are consistent with the hypothesis that epithelial cell functions (e.g., goblet cell production) in the small intestine are modulated by peptides normally produced in neurons, such as VIP. There is a dense network of neuronal fibers wrapping around intestinal crypts (16). The mechanisms of signaling between neural fibers and crypt epithelia remains unclear. Incorporation of the thymidine analog EdU into DNA has previously been used to quantify the rate of epithelial cell production in mouse small intestine both *in vivo* (32) and *ex vivo* (43). In the current study, the number of glycan synthesizing goblet cells that were also undergoing DNA synthesis as marked by EdU was substantially decreased in slices treated with the VIP receptor antagonist VPACa. This indicates potential ongoing VIP regulation

of goblet cell production. Further investigation is required to determine whether this was a direct impact on goblet cell proliferation from a progenitor, or a later influence on differentiation into a goblet cell fate.

In conclusion, the present study provides an anatomical foundation for neural influences on goblet cell function in the mouse ileum. Further, these interactions are seemingly important for regulation of the extent of the proximity of neural fibers to goblet cells, and the production of new goblet cells in the ileal crypt. The experiments in this study lay a foundation for analyzing goblet cell – neuronal interactions in the mouse ileum. Future investigation will be needed to tease apart the role of other neuropeptides in mediating neural interactions with goblet cells along the length of the intestinal crypt-villus axis.

References:

- 1) Allaire JM, Morampudi V, Crowley SM, Stahl M, Yu H, Bhullar K, Knodler LA, Bressler B, Jacobson K, Vallance BA. Frontline defenders: goblet cell mediators dictate host-microbe interactions in the intestinal tract during health and disease. *American journal of physiology Gastrointestinal and liver physiology*. 2018; 314(3): G360-G77.
- 2) Bartoo AC, Sprunger LK, Schneider DA. Expression and distribution of TTX-sensitive sodium channel alpha subunits in the enteric nervous system. *The Journal of comparative neurology*. 2005; 486(2): 117-31.
- 3) Baskin JM, Prescher JA, Laughlin ST, Agard NJ, Chang PV, Miller IA, Lo A, Codelli JA, Bertozzi CR. Copper-free click chemistry for dynamic in vivo imaging. *Proc Natl Acad Sci U S A*. 2007; 104(43): 16793-7.
- 4) Bednarska O, Walter SA, Casado-Bedmar M, Strom M, Salvo-Romero E, Vicario M, Mayer EA, Keita AV. Vasoactive Intestinal Polypeptide and Mast Cells Regulate Increased Passage of Colonic Bacteria in Patients With Irritable Bowel Syndrome. *Gastroenterology*. 2017; 153(4): 948-60 e3.
- 5) Birchenough GM, Nystrom EE, Johansson ME, Hansson GC. A sentinel goblet cell guards the colonic crypt by triggering Nlrp6-dependent Muc2 secretion. *Science*. 2016; 352(6293): 1535-42.
- 6) Bohorquez DV, Samsa LA, Roholt A, Medicetty S, Chandra R, Liddle RA. An enteroendocrine cell-enteric glia connection revealed by 3D electron microscopy. *PloS one*. 2014; 9(2): e89881.
- 7) Bohorquez DV, Shahid RA, Erdmann A, Kreger AM, Wang Y, Calakos N, Wang F, Liddle RA. Neuroepithelial circuit formed by innervation of sensory enteroendocrine cells. *The Journal of clinical investigation*. 2015; 125(2): 782-6.

- 8) Buhner S, Barki N, Greiter W, Giesbertz P, Demir IE, Ceyhan GO, Zeller F, Daniel H, Schemann M. Calcium Imaging of Nerve-Mast Cell Signaling in the Human Intestine. *Front Physiol.* 2017; 8971.
- 9) Cajal SR. *Les Nouvelles Idees Sur la Structure du Systeme nerveux Chez L'Homme et Chez les Vertebres* Paris: C. Reinwald & Cie, Libraires-Editeurs, 1894.
- 10) Castagliuolo I, Lamont JT, Qiu B, Fleming SM, Bhaskar KR, Nikulasson ST, Kornetsky C, Pothoulakis C. Acute stress causes mucin release from rat colon: role of corticotropin releasing factor and mast cells. *Am J Physiol.* 1996; 271(5 Pt 1): G884-92.
- 11) Cheng X, Voss U, Ekblad E. Tuft cells: Distribution and connections with nerves and endocrine cells in mouse intestine. *Experimental cell research.* 2018; 369(1): 105-11.
- 12) Cho KA, Park M, Kim YH, Choo HP, Lee KH. Benzoxazole derivatives suppress lipopolysaccharide-induced mast cell activation. *Mol Med Rep.* 2018; 17(5): 6723-30.
- 13) Cooke HJ. Neuroimmune signaling in regulation of intestinal ion transport. *Am J Physiol.* 1994; 266(2 Pt 1): G167-78.
- 14) Dartt DA, Kessler TL, Chung EH, Zieske JD. Vasoactive intestinal peptide-stimulated glycoconjugate secretion from conjunctival goblet cells. *Exp Eye Res.* 1996; 63(1): 27-34.
- 15) Feng G, Mellor RH, Bernstein M, Keller-Peck C, Nguyen QT, Wallace M, Nerbonne JM, Lichtman JW, Sanes JR. Imaging neuronal subsets in transgenic mice expressing multiple spectral variants of GFP. *Neuron.* 2000; 28(1): 41-51.
- 16) Furness JB, Costa M. Projections of Intestinal Neurons Showing Immunoreactivity for Vasoactive Intestinal Polypeptide Are Consistent with These Neurons Being the Enteric Inhibitory Neurons. *Neuroscience Letters.* 1979; 15(2-3): 199-204.
- 17) Furness JB, Costa M. *The Enteric Nervous System* New York: Churchill Livingstone, 1987.

- 18) Garcia-Posadas L, Hodges RR, Li D, Shatos MA, Storr-Paulsen T, Diebold Y, Dartt DA. Interaction of IFN-gamma with cholinergic agonists to modulate rat and human goblet cell function. *Mucosal immunology*. 2016; 9(1): 206-17.
- 19) Goyal RK, Hirano I. The enteric nervous system. *N Engl J Med*. 1996; 334(17): 1106-15.
- 20) Halm DR, Halm ST. Secretagogue response of goblet cells and columnar cells in human colonic crypts. *American journal of physiology Cell physiology*. 2000; 278(1): C212-33.
- 21) Holmen Larsson JM, Thomsson KA, Rodriguez-Pineiro AM, Karlsson H, Hansson GC. Studies of mucus in mouse stomach, small intestine, and colon. III. Gastrointestinal Muc5ac and Muc2 mucin O-glycan patterns reveal a regiospecific distribution. *American journal of physiology Gastrointestinal and liver physiology*. 2013; 305(5): G357-63.
- 22) Jakobsson HE, Rodriguez-Pineiro AM, Schutte A, Ermund A, Boysen P, Bemark M, Sommer F, Backhed F, Hansson GC, Johansson ME. The composition of the gut microbiota shapes the colon mucus barrier. *EMBO Rep*. 2015; 16(2): 164-77.
- 23) Jayawardena D, Guzman G, Gill RK, Alrefai WA, Onyuksel H, Dudeja PK. Expression and localization of VPAC1, the major receptor of vasoactive intestinal peptide along the length of the intestine. *American journal of physiology Gastrointestinal and liver physiology*. 2017; 313(1): G16-G25.
- 24) Johansson ME. Fast renewal of the distal colonic mucus layers by the surface goblet cells as measured by in vivo labeling of mucin glycoproteins. *PloS one*. 2012; 7(7): e41009.
- 25) Johansson ME, Larsson JM, Hansson GC. The two mucus layers of colon are organized by the MUC2 mucin, whereas the outer layer is a legislator of host-microbial interactions. *Proc Natl Acad Sci U S A*. 2011; 108 Suppl 14659-65.
- 26) Kaelberer MM, Buchanan KL, Klein ME, Barth BB, Montoya MM, Shen X, Bohorquez DV. A gut-brain neural circuit for nutrient sensory transduction. *Science*. 2018; 361(6408).

- 27) Katsoulis S, Clemens A, Schworer H, Creutzfeldt W, Schmidt WE. Pacap Is a Stimulator of Neurogenic Contraction in Guinea-Pig Ileum. *American Journal of Physiology*. 1993; 265(2): G295-G302.
- 28) Keast JR, Furness JB, Costa M. Distribution of Certain Peptide-Containing Nerve Fibers and Endocrine Cells in the Gastrointestinal Mucosa in Five Mammalian Species. *The Journal of comparative neurology*. 1985; 236:403-22.
- 29) Keita AV, Carlsson AH, Cigehm M, Ericson AC, McKay DM, Soderholm JD. Vasoactive intestinal polypeptide regulates barrier function via mast cells in human intestinal follicle-associated epithelium and during stress in rats. *Neurogastroenterology and motility : the official journal of the European Gastrointestinal Motility Society*. 2013; 25(6): e406-17.
- 30) Kirkegaard P, Lundberg JM, Poulsen SS, Olsen PS, Fahrenkrug J, Hokfelt T, Christiansen J. Vasoactive intestinal polypeptidergic nerves and Brunner's gland secretion in the rat. *Gastroenterology*. 1981; 81(5): 872-8.
- 31) Knoop KA, McDonald KG, McCrate S, McDole JR, Newberry RD. Microbial sensing by goblet cells controls immune surveillance of luminal antigens in the colon. *Mucosal immunology*. 2015; 8(1): 198-210.
- 32) Krndija D, Marjou F, Buirao B, Richon S, Leroy O, Bellaiche Y, Hannezo E, Vignjevic DM. Active cell migration is critical for steady-state epithelial turnover in th gut. *Science*. 2019; 365:705-10.
- 33) McLean IC, Schwerdtfeger LA, Tobet SA, Henry CS. Powering ex vivo tissue models in microfluidic systems. *Lab on a chip*. 2018; 18(10): 1399-410.
- 34) Neutra MR, O'Malley LJ, Specian RD. Regulation of intestinal goblet cell secretion. II. A survey of potential secretagogues. *Am J Physiol*. 1982; 242(4): G380-7.

- 35) Nurgali K. Plasticity and ambiguity of the electrophysiological phenotypes of enteric neurons. *Neurogastroenterology and motility : the official journal of the European Gastrointestinal Motility Society*. 2009; 21(9): 903-13.
- 36) Osorio N, Korogod S, Delmas P. Specialized functions of Nav1.5 and Nav1.9 channels in electrogenesis of myenteric neurons in intact mouse ganglia. *The Journal of neuroscience : the official journal of the Society for Neuroscience*. 2014; 34(15): 5233-44.
- 37) Pandol SJ, Dharmasathaphorn K, Schoeffield MS, Vale W, Rivier J. Vasoactive intestinal peptide receptor antagonist [4Cl-D-Phe6, Leu17] VIP. *Am J Physiol*. 1986; 250(4 Pt 1): G553-7.
- 38) Phillips TE, Phillips TH, Neutra MR. Regulation of intestinal goblet cell secretion. III. Isolated intestinal epithelium. *Am J Physiol*. 1984; 247(6 Pt 1): G674-81.
- 39) Plaisancie P, Barcelo A, Moro F, Claustre J, Chayvialle JA, Cuber JC. Effects of neurotransmitters, gut hormones, and inflammatory mediators on mucus discharge in rat colon. *Am J Physiol*. 1998; 275(5): G1073-84.
- 40) Pothoulakis C, Castagliuolo I, Leeman SE. Neuroimmune mechanisms of intestinal responses to stress - Role of corticotropin-releasing factor and neurotensin. *Neuroimmunomodulation*. 1998; 840635-48.
- 41) Schneider H, Pelaseyed T, Svensson F, Johansson MEV. Study of mucin turnover in the small intestine by in vivo labeling. *Sci Rep*. 2018; 8(1): 5760.
- 42) Schwerdtfeger LA, Nealon NJ, Ryan EP, Tobet SA. Human colon function ex vivo: Dependence on oxygen and sensitivity to antibiotic. *PloS one*. 2019; 14(5): e0217170.
- 43) Schwerdtfeger LA, Ryan EP, Tobet SA. An organotypic slice model for ex vivo study of neural, immune, and microbial interactions of mouse intestine. *American journal of physiology Gastrointestinal and liver physiology*. 2016; 310(4): G240-8.

- 44) Schwerdtfeger LA, Tobet SA. From organotypic culture to body-on-a-chip: A neuroendocrine perspective. *J Neuroendocrinol.* 2019; 31(3): e12650.
- 45) Sharkey KA, Beck PL, McKay DM. Neuroimmunophysiology of the gut: advances and emerging concepts focusing on the epithelium. *Nature reviews Gastroenterology & hepatology.* 2018; 15(12): 765-84.
- 46) Sikora LKJ, Buchan AMJ, Levy JG, McIntosh CHS, Brown JC. VIP-Innervation of Rat Intestine: A Developmental Study with Monoclonal Antibodies. *Peptides.* 1984; 5:231-7.
- 47) Vaudry D, Falluel-Morel A, Bourgault S, Basille M, Burel D, Wurtz O, Fournier A, Chow BK, Hashimoto H, Galas L, Vaudry H. Pituitary adenylate cyclase-activating polypeptide and its receptors: 20 years after the discovery. *Pharmacological reviews.* 2009; 61(3): 283-357.
- 48) Wagner U, Fehmann HC, Bredenkroter D, Yu F, Barth PJ, von Wichert P. Galanin and somatostatin inhibition of substance P-induced airway mucus secretion in the rat. *Neuropeptides.* 1995; 28(1): 59-64.
- 49) Walsh KT, Zemper AE. The Enteric Nervous System for Epithelial Researchers: Basic Anatomy, Techniques, and Interactions With the Epithelium. *Cell Mol Gastroenterol Hepatol.* 2019; 8(3): 369-78.
- 50) Wang Y, Kim R, Sims CE, Allbritton NL. Building a Thick Mucus Hydrogel Layer to Improve the Physiological Relevance of In Vitro Primary Colonic Epithelial Models. *Cell Mol Gastroenterol Hepatol.* 2019.
- 51) Wu X, Conlin VS, Morampudi V, Ryz NR, Nasser Y, Bhinder G, Bergstrom KS, Yu HB, Waterhouse CC, Buchan AM, Popescu OE, Gibson WT, Waschek JA, Vallance BA, Jacobson K. Vasoactive intestinal polypeptide promotes intestinal barrier homeostasis and protection against colitis in mice. *PLoS one.* 2015; 10(5): e0125225.

CHAPTER 7 – SEX DIFFERENCE IN NEURONAL MEDIATION OF ILEAL PANETH CELL RESPONSE TO LIPOPOLYSACCHARIDE

Overview:

Information on neuronal peptide regulation of gut mucosal epithelial function is sparse, but likely important for maintaining a healthy gut barrier. Previously, we have shown that vasoactive intestinal peptide may play a role in regulating production of mouse ileal goblet cells, a type of specialized epithelium. In the present study, data show vasoactive intestinal peptide immunoreactive neuronal fibers coursing intimately with UEA-1 lectin reactive Paneth cells in the base of mouse ileal crypts, with no difference observed between tissue from males and females. A sex difference in the fluorescent intensity of UEA-1 reactive Paneth cells was observed, regardless of treatment, with slices from female ileum having more fluorescently intense Paneth cells. When challenged with lipopolysaccharide, Paneth cells from male slices became as intense as Paneth cells in slices from females. Removal of the basal sex difference upon challenge with lipopolysaccharide was largely driven by a sharp decrease in intensity in Paneth cells in female derived slices treated with a VIP receptor antagonist, but not those treated with tetrodotoxin. This may point towards a VIP specific influence over Paneth cell function; however, further work is needed to correlate UEA-1 intensity more directly with secretion by Paneth cells in ileal crypts.

Introduction:

Neuronal fibers or glial projections to mucosal epithelia have been shown for goblet (1), tuft (2), and enteroendocrine (3, 4) cells. Functional roles of neural – epithelial connections are not well known. Much of the work in the field has been centered around enteroendocrine cell signaling with neuronal (3) and glial (5) fibers. Recent work demonstrated an influence of vasoactive intestinal peptide (VIP) over production of mouse ileal goblet cells (1). Better

anatomical understanding of neural – epithelial signaling pathway is needed to begin understanding potential functional influence of neural elements over barrier maintenance.

Situated at the base of intestinal crypts in the small and large intestine, Paneth cells secrete large amounts of anti-microbial molecules including alpha-defensins (6). Paneth cell secretions, including defensins, are thought to play roles in protection of closely localized crypt progenitor cells. Neural elements, along with Paneth and stem progenitor cells are included in the intestinal 'stem cell niche' (7), however, neural inputs to Paneth cells are not well characterized. In this study, we show anatomic localization of neuronal fibers and Paneth cells, a pathway potentially mediated by immune components like mast cells during pathogen invasion.

Numerous sex differences in various aspects of immunity have been demonstrated in recent years, with females often showing a baseline level of inflammation and more adaptive immune cells (8). While sex differences are known in enteric immune cell populations (9), data is needed on potential sexual differences in Paneth cell quantities, secretory capacity, and anatomic localization with neural elements.

The present study uses organotypic intestinal slices of mouse ileum which can be challenged with lipopolysaccharide (LPS), a component of bacterial cell walls. In this study, we use this system to build off previous work that showed a different epithelial subset, goblet cells, being regulated in their production by VIP (1). Paneth cells stand as the logical next target for investigation of VIP regulation of gut epithelial populations, particularly when concerned with bacterial challenge, as they are first line defenders that produce anti-microbial products.

Materials & Methods:

Animals:

Male and female mice aged between 8-12 wk old were used for all experiments. Mice were housed at Colorado State University in cages with aspen bedding (Sani-chips; Harlan Teklad, Madison, WI) with ad libitum access to water and food (No. 8649; Harlan Teklad) under a standard 14:10 hour light-dark cycle. Mice were on the C57BL/6 background and expressed a yellow fluorescent protein (YFP) driven by a promoter that is neuronally selective (Thy-1; (10)). YFP fluorescence was used to ascertain base levels of tissue/neuronal health ex vivo. Colorado State University's IACUC approved work under protocol #1021.

Organotypic slice preparation:

Preparation of intestinal slices has been previously described at length (1, 11), and was performed similarly here. In short, mice were deeply anesthetized with isoflurane prior to decapitation. Gastrointestinal tract was removed from duodenum to the ileo-cecal junction, and tissue was placed in 4°C 1X Krebs buffer prior to dissection of mesentery and separation of ileum. Small pieces (2-4mm) of ileum was blocked in 8% low melt point agarose (Gold Biotechnology, St. Louis, MO) and allowed to polymerize prior to slicing at 250 µm thick on a vibrating microtome (VT1000S; Leica Microsystems, Wetzlar, Germany). Slices were adhered to culture dishes using a thin layer of collagen solution [vol/vol: 10.4% 10X MEM (Minimal Essential Medium, Sigma-Aldrich, St. Louis, MO), 4.2% sodium bicarbonate, and 83.5% collagen (PureCol; Inamed, Fremont, CA)]. Slices were cultured in CTS Neurobasal-A Media (ANB; Life Technologies) with 5% B-27 supplement (B-27; Life Technologies, Carlsbad, CA) and maintained in an incubator at 37°C under 5% CO₂, and 1% O₂ gas.

Drug Treatments:

Slices of mouse ileum were treated in accordance with Table 3 at 24 h ex vivo for a subsequent 24 h. For those challenged with LPS, slices were treated at 0 h ex vivo prior to LPS at 24 h ex vivo for a subsequent 4 h.

Table 3. Drug treatments used throughout experiments

Treatment	Concentration	Source
Vasoactive Intestinal Peptide (VIP)	10 μ M	ABBIOTEC (Escondido, CA)
[D-p-Cl-Phe ⁶ ,Leu ¹⁷]-VIP (VPACa)	10 μ M	Bio-Techne Coproration (Minneapolis, MN)
Tetrodotoxin (TTX)	10 μ M	Abcam (Cambridge, MA)
TLR-grade Lipopolysaccharide (LPS)	10 μ g/ml	Enzo Life Sciences, Inc. (Farmingdale, NY)

Immunohistochemistry:

To improve visualization of cellular elements, 250 μ m slices were re-sectioned at 50 μ m prior to immunohistochemistry (IHC) as previously described (1). IHCs were performed as previously described (1, 11). Briefly, 50 μ m re-sectioned ileum sections were placed in 0.1M glycine made in 0.05M PBS for 30 min prior to three PBS washes before 15 min in 0.5% sodium borohydride in PBS. Sections were washed twice in PBS before blocking in 5% NGS, 0.5% Tx and 1% H₂O₂ in PBS for 30 min. Sections received anti-VIP (Immunostar, Inc., Hudson, WI) at 1:8000 dilution in PBS with 1% BSA and 0.3% Tx simultaneous with *Ulex europaeus* agglutinin – 1 (UEA-1; Vector Laboratories, Burlingame, CA) conjugate to fluorescein with 5% CaCl₂, 2% polyvinylpyrrolodine-40, and 0.125% Tween-20 in PBS prior to incubation for ~72 h. After incubation with primary, sections were washed four times in 1% NGS in PBS for 1 h before addition of a Cy-3 conjugated donkey anti-rabbit secondary at a 1:500 dilution for 1 h (Jackson Immuno Research Laboratories, Inc. West Grove, PA). After secondary, sections were washed in PBS before mounting with Aqua-Poly/Mount (Polysciences, Inc., Warrington, PA) prior to imaging.

Tissue Imaging and Analysis:

All tissues were imaged on a Zeiss LSM 880 confocal microscope with an Axiocam 503 mono camera (Carl Zeiss, Inc., Thornton, NY). 50 μm Z-stacks were acquired in 1 μm intervals prior to a max intensity Z-projection through the center 30 μm of each stack using FIJI (v1.0; NIH). Individual Paneth cells were used to define regions of interest that were manually drawn by a researcher blinded to treatment. Cells and neuronal fiber appositions were counted using FIJI.

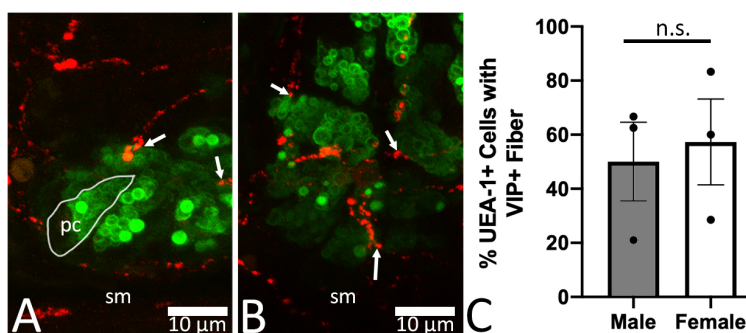


Figure 30. Paneth cells reactive to UEA-1 (green) are intimately associated with VIP immunoreactive fibers (red), regardless of sex. (A) is a representative image from a male ileal crypt, with an exemplary Paneth cells outlined in white and denoted 'pc'. Arrows point towards areas of VIP-immunoreactive fibers and UEA-1 reactive Paneth cell association. (B) is representative from a female ileum. Quantification is shown in (C). 'sm' denotes submucosa. $n = 3$ males, 3 females. Scale bars are 10 μm in (A) and (B).

Statistics:

Statistical analyses were performed in Prism 9 (Graphpad, San Diego, CA). Analyses were performed using either a one-way ANOVA (Figure 28) or two-way ANOVA (Figure 29-30) looking at cell counts across sex, and treatments. All ANOVAs had a Tukey's multi comparison's post-hoc test performed. All data are means \pm standard error of the mean.

Results:

Paneth cells were closely opposed by VIP-immunoreactive neuronal fibers in both fixative perfused and ex vivo cultured mouse distal ileal tissues. In slices from male and female

mice, Paneth cells had VIP-IR fibers within 1 μm (Figure 30A&B) with male ileal tissue showing 50.1 \pm 14.6 % and female 57.3 \pm 15.86 % of UEA-1+ cells within 1 μm of a VIP-IR Fiber (Figure 30C). The differences in VIP apposition of UEA-1 cells across sex was not significant as measured by a one-way ANOVA ($[F(2,2) = 1.187]$ $p > 0.5$). Quantification of images from slices cultured ex vivo showed that treatment with vehicle, VIP, VPACa, or TTX, did not impact the percentage of UEA-1+ cells within 1 μm of a VIP-IR fiber, regardless of sex (Figure 31A-D; $[F(3,23) = 0.5]$ $p > 0.5$). Challenge with LPS alongside either vehicle, VIP, VPACa, or TTX, did not impact the percentage of UEA-1+ cells near a VIP-IR fiber, again independent of sex (Figure 31E-H; $[F(3,23) = 0.07]$ $p > 0.5$).

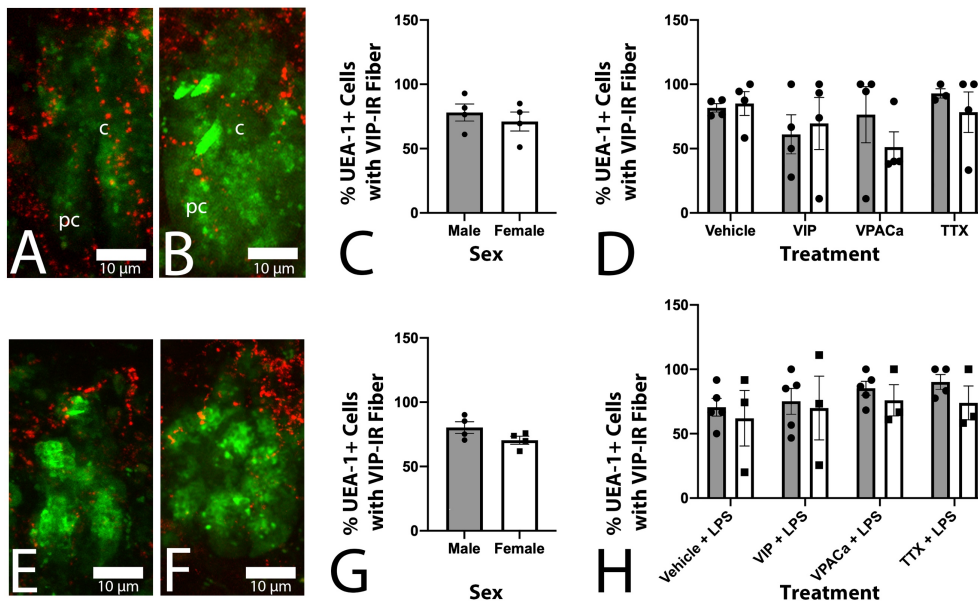


Figure 31. No sex differences were observed in the percentage of UEA-1 reactive Paneth cells (green) associated within 1 μm of a VIP-immunoreactive neuronal fiber (red). (A) and (B) are representative images from male and female ileums respectively. (C) and (D) are quantification of a group effect (C), and a treatment effect by sex (D) with grey bars representing males and white bars females. (E) and (F) are representative images from males and females respectively, with quantification in (G) and (H). 'c' represents a ileal crypt region, and 'pc' a Paneth cell. $n = 4$ males, 4 females for A-D and 5 males, 5 females for E-H. Scale bars in (A,B,E,F) are all 10 μm .

Fluorescent intensity of UEA-1 was observed to be higher in slices of ileum from female than male mice, regardless of treatment with vehicle, VIP, VPACa, or TTX (Figure 32A-D; $[F(1,23) =$

6.2] $p < 0.05$). When challenged with LPS there was a general increase in UEA-1 intensities with a significant decrease in female UEA-1 intensity in VPACa + LPS treated slices (Figure 32E-H; $[F(1,23) = 1.8] p > 0.5$). This change eliminated the sex difference.

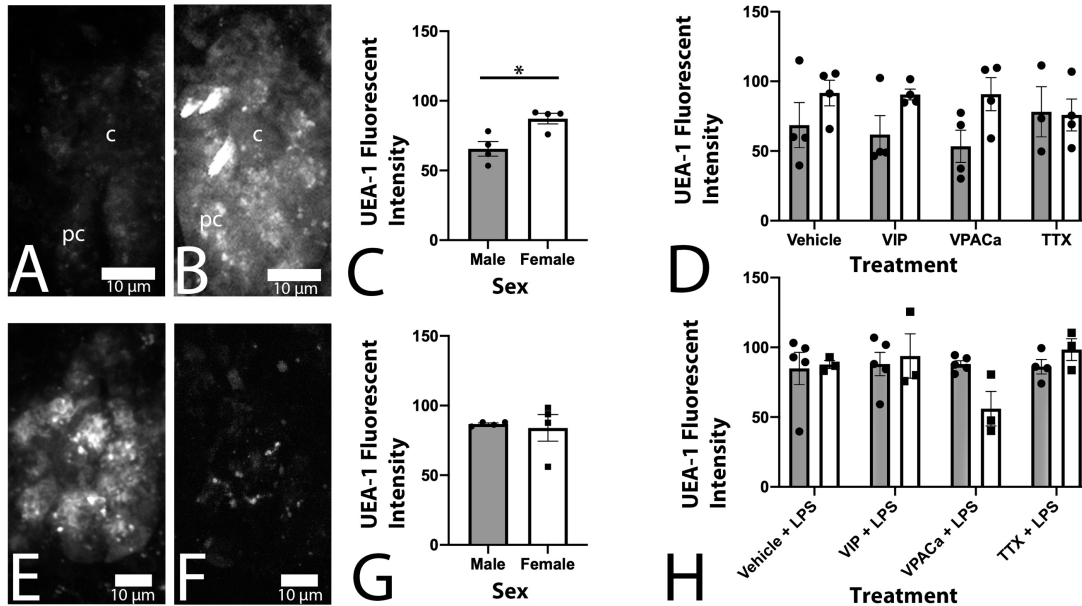


Figure 32. Paneth cells from female slices had more fluorescently intense Paneth cells, regardless of treatment. (A,E) and (B,F) are representative images of male and female Paneth cells, respectively. Quantification of mean fluorescent intensity is shown in treated (C-D) and treated + LPS challenged (G-H) slices. 'c' represents a ileal crypt region, and 'pc' a Paneth cell. $n = 4$ males, 4 females for A-D and 5 males, 5 females for E-H. Scale bars in (A,B,E,F) are all 10 μm .

Discussion:

Regulation of the intestinal epithelial and mucus barrier is critical for maintaining a healthy gut wall and host. Previous demonstrations of neural peptide influence over epithelial function concerning the barrier have been shown, with goblet cell production being regulated by VIP (1). In cases of pathogen invasion, acute inflammation, and other barrier compromising events, epithelial secretions by Paneth cells play a critical role in protecting host cells by producing numerous anti-microbial compounds like alpha-defensins and lysozyme (6). Data in the present study demonstrate a close association of Paneth cells with VIP+ neuronal fibers, and define a sex difference in Paneth cell intensity that is eliminated post LPS challenge.

Together, the data highlight the need to consider sex as a relevant variable when investigating Paneth cells and their functional roles during bacterial challenge.

The present study shows VIP-IR fibers coursing intimately with Paneth cells in the base of ileal crypts. There were no sex differences observed in the percentage of Paneth cells near a VIP-IR fiber, regardless of treatment or challenge with LPS. There was a substantial sex difference in the fluorescent intensity of ileal Paneth cells, with females having more intense cells across all treatments. After challenge with LPS, Paneth cell intensities from male slices caught up to females. This effect was largely driven by a substantial decrease in Paneth cell intensities in slices from females treated with VPACa. This could potentially point towards a VIP regulation of observed sex differences in fluorescent intensities, however, substantially more investigation is required to clarify the significance of this data.

Fluorescent intensity of UEA-1 was used in this study as an indirect marker of Paneth cell activity, as it is not a direct secretory product. It is possible that more fluorescently intense Paneth cells have larger stores of cellular cargo (12), ready to secrete contents like alpha-defensins (6). Conversely, it is possible that less fluorescently intense Paneth cells have recently secreted their contents. Defined measurements of Paneth cell secretion products like alpha-defensins will be needed to define the role of VIP and neuronal signaling in regulating Paneth cell function during healthy and bacterial challenged states.

In conclusion, Paneth cells are closely associated with VIP neuronal fibers, which potentially play a role in regulation of their secretion. Other measures of Paneth cell function are needed to ascertain the mechanistic role of VIP in regulating Paneth cell secretion, particularly in bacterially challenged tissues. Harnessing neural regulation of anti-bacterial secretion by

Paneth cells could serve as a novel pathway for treating acute infections in the long term, however, design of such therapeutics must include analysis of sex as a variable.

References:

- 1) Schwerdtfeger LA, Tobet SA. Vasoactive Intestinal Peptide Regulates Ileal Goblet Cell Production in Mice. *Physiological reports*. 2020; **8**(3).
- 2) Cheng X, Voss U, Ekblad E. Tuft cells: Distribution and connections with nerves and endocrine cells in mouse intestine. *Experimental cell research*. 2018; **369**(1): 105-11.
- 3) Bohorquez DV, Shahid RA, Erdmann A, Kreger AM, Wang Y, Calakos N, Wang F, Liddle RA. Neuroepithelial circuit formed by innervation of sensory enteroendocrine cells. *The Journal of clinical investigation*. 2015; **125**(2): 782-6.
- 4) Kaelberer MM, Buchanan KL, Klein ME, Barth BB, Montoya MM, Shen X, Bohorquez DV. A gut-brain neural circuit for nutrient sensory transduction. *Science*. 2018; **361**(6408).
- 5) Bohorquez DV, Samsa LA, Roholt A, Medicetty S, Chandra R, Liddle RA. An enteroendocrine cell-enteric glia connection revealed by 3D electron microscopy. *PloS one*. 2014; **9**(2): e89881.
- 6) Ayabe T, Satchell DP, Wilson CL, Parks WC, Selsted ME, Ouellette AJ. Secretion of microbicidal alpha-defensins by intestinal Paneth cells in response to bacteria. *Nat Immunol*. 2000; **1**(2): 113-8.
- 7) Meran L, Baulies A, Li VSW. Intestinal Stem Cell Niche: The Extracellular Matrix and Cellular Components. *Stem Cells Int*. 2017; **2017**7970385.
- 8) Klein SL, Flanagan KL. Sex differences in immune responses. *Nature reviews Immunology*. 2016; **16**(10): 626-38.
- 9) Lovell RM, Ford AC. Global prevalence of and risk factors for irritable bowel syndrome: a meta-analysis. *Clin Gastroenterol Hepatol*. 2012; **10**(7): 712-21 e4.

- 10) Feng G, Mellor RH, Bernstein M, Keller-Peck C, Nguyen QT, Wallace M, Nerbonne JM, Lichtman JW, Sanes JR. Imaging neuronal subsets in transgenic mice expressing multiple spectral variants of GFP. *Neuron*. 2000; **28**(1): 41-51.
- 11) Schwerdtfeger LA, Ryan EP, Tobet SA. An organotypic slice model for ex vivo study of neural, immune, and microbial interactions of mouse intestine. *American journal of physiology Gastrointestinal and liver physiology*. 2016; **310**(4): G240-8.

CHAPTER 8 – SEX DIFFERENCES IN ANATOMIC PLASTICITY OF GUT NEURONAL – MAST CELL INTERACTIONS

Overview:

Background: Mast cells are anatomically situated in close proximity to myriad enteric neuronal fibers in the gut mucosa, however, roles of specific neuropeptides in modulating function of immune components like mast cells in response to challenge with bacterial components are relatively unknown. The present study compared responses between tissues derived from male and female mice to examine neural – immune signaling in the gut wall after selected treatments.

Methods: An organotypic slice model was used to maintain cellular diversity in the gut wall ex vivo. Mouse ileum slices were treated with selected pharmacological reagents that block neuronal function (e.g., tetrodotoxin) or VIP receptors prior to challenge with lipopolysaccharide (LPS) to assess their influence on anatomic plasticity of VIP-IR fibers and activation of mast cells.

Results: Sex differences were observed in the number of mucosal mast cells (c-kit/ACK2 immunoreactive) at baseline, regardless of treatment, with female ileum tissue having 46% more ACK2-IR mast cells than males. After challenge with LPS, male mast cell counts rose to female levels. Further sex differences were observed in the percentage of ACK2-IR cells within 1 μm of a vasoactive intestinal peptide (VIP) neuronal fiber, as well as the size of mast cells, a metric previously tied to activation, with females having larger basal mast cell sizes. Male mast cell sizes reached female levels after LPS challenge.

Conclusions: This study suggests sex differences in neural-immune plasticity and in mast cell activation both basally and in response to challenge with LPS. These sex differences could potentially impact functional neuro-immune response to pathogens. Additional data is needed to

test the hypothesis that VIP has a functional role in regulating mast cell secretion in pathogen challenged states.

Introduction:

Neural regulation of immune components throughout the gut wall has gained increased attention. Mucosal immune cells, like mast cells among others, express neuropeptide receptors for vasoactive intestinal peptide (VIP; Keita et al., 2013), calcitonin gene related peptide (CGRP), substance P, and many others (Forsythe & Bienenstock, 2012). Mast cells are a multi-functional population of immune cells anatomically situated in close proximity to myriad enteric neuronal fibers in the gut mucosa (Stead et al., 1989). Neural stimuli can trigger the release of histamine from cultured mast cells (Piotrowski & Foreman, 1985) among other functions (Jacobson et al., 2021). Roles of specific enteric neuronal populations in regulating bi-directional communication with heterogenous mast cell subsets are important for understanding the neuro-immune axes of the gut.

VIP and pituitary adenylate cyclase activating polypeptide (PACAP) are vasoactive peptides transcribed and translated from different genes, but with significant sequence homology (Sikora et al., 1984) and are secreted by enteric neurons (Furness & Costa, 1979) and mucosal mast cells (Cutz et al., 1978). More than half of submucosal enteric neuronal fibers projecting throughout the mucosa of the small intestine are VIP-immunoreactive (VIP-IR; Fantaguzzi et al., 2009). VIP-IR neuronal fibers have been shown in close proximity to mast cells more regularly in rats with inflammatory bowel disease (Casado-Bedmar et al., 2019). VIP signaling has also been shown to regulate gut smooth muscle contraction (Katsoulis et al., 1993), and enteric goblet cell production (Schwerdtfeger & Tobet, 2020) among other functions. VIP and PACAP bind VPAC receptors 1 and 2 at slightly different affinities (Vaudry et al., 2009) and both are immunoreactive to most antisera targeting VIP. Therefore 'VIP' shall refer to VIP and PACAP

immunoreactivity and activity throughout this paper. VPAC receptors can be blocked using a receptor antagonist ([D-p-Cl- Phe⁶,Leu¹⁷]-VIP (Pandol et al.,1986), and will be referred to as “VPACa”.

Mucosal mast cells are bone marrow progenitor derived immune cells that play roles in the gut ranging from inflammatory events via histamine release, to innate immune responses to pathogenic bacteria (Albert-Bayo et al., 2019). Mucosal mast cells mature from mast cell precursors resident in blood and the gut wall, both of which express c-kit/CD117 (Liu et al., 2010) which can be labeled immunohistochemically with an anti-CD117 antibody (ACK2). Mucosal mast cells have been shown to sense and respond to bacteria and their wall components like lipopolysaccharide (LPS) during barrier breach of the gut wall (Malaviya et al., 1996; Piliponsky & Romani, 2018). Mast cells are also capable of producing and releasing VIP in response to LPS stimulation (Martinez et al., 1999). Neural regulation of the mast cell responses to pathogen challenge is largely unknown, partially due to the requirement of culture methods that maintain all three cellular components in proper anatomic arrangements.

A number of immunological sex differences have been reported, with females tending towards more adaptive immune cell expression and basal levels of inflammation in healthy states (Klein & Flanagan, 2016). Females are more likely to have gut pathologies such as irritable bowel syndrome (Lovell & Ford, 2012), and mucosal mast cell counts are increased in certain pathologies in females compared to males (Lee et al., 2016; Cremon et al., 2009). However, presence of basal sex differences in immune components, including mast cells, have not been well studied in intestinal cell populations. Neuronal modulation of mast cell production and secretion pathways is an unexplored target for better understanding of the effect sex plays in neuroimmune communications in the gut wall in healthy and perturbed states.

This study harnesses an organotypic intestinal slice model that has previously been shown to maintain slices of mouse intestine with neural, immune, epithelial, and bacterial components *ex vivo* (Schwerdtfeger et al., 2016), and can be challenged with bacterial antigens like LPS (Schwerdtfeger & Tobet, 2020). Organotypic gut slices were recently used to show the dense apposition of goblet cells by neuronal fibers in the mouse ileum, with VIP antagonism inhibiting production of new goblet cells (Schwerdtfeger & Tobet, 2020). These results pointed towards the importance of VIP in gut epithelial functional regulation. The immune system is a critical component of gut wall function, and was investigated in the context of VIP neuronal regulation of mast cell activation and function with respect to sex, and post challenge with LPS.

Materials and Methods:

Animals:

Mice aged between 8-12 wk old, of both sexes were used for all experiments. Animals were housed at Colorado State University under the care of Laboratory Animal Resources. Mice were housed in cages with aspen bedding (autoclaved Sani-chips; Harlan Teklad, Madison, WI) with *ad libitum* access to food (No. 8649; Harlan Teklad) and water under a 14:10 – h light-dark cycle. All slices were generated from mice (C57BL/6 background) expressing yellow fluorescent protein (YFP) driven by a neuronally selective promoter (Thy-1) as previously described (Thy-1 YFP; Feng et al., 2000). Animal studies were approved by the Colorado State University IACUC under protocol #1021.

Organotypic slice preparation:

Preparation of intestinal slices has been previously described at length (Schwerdtfeger et al., 2016; Schwerdtfeger & Tobet, 2020), and was performed similarly in the current study. Briefly, mice were deeply anesthetized with isoflurane and killed via decapitation. The small intestine was removed from the pylorus-duodenal junction, to the ileo-cecal junction. Tissue was

immediately placed into 4°C 1X Krebs buffer and the ileum was separated and cut into pieces roughly 2-4-mm in length. Tissue was blocked in 8%, low melting point agarose (Gold Biotechnology, St. Louis, MO) until polymerization prior to cutting on a vibrating microtome (VT1000S; Leica Microsystems, Wetzlar, Germany) at 250 µm thick. Slices were transferred into a 60 mm plastic-bottom dish (Corning Inc., Corning, NY) containing 5 ml of Hibernate Media (Life Technologies, Grand Island, NY). Slices spent 15 min at 4°C in Hibernate media prior to removal of hibernate and addition of 5 ml of CTS Neurobasal-A Media (ANB; Life Technologies) with 5% B-27 supplement (B-27; Life Technologies, Carlsbad, CA) where they spent 35 min at 37°C. Samples were plated on 35 mm plastic bottom dishes (MatTek, Ashland, MA) and covered by a thin layer of collagen solution [vol/vol: 10.4% 10X MEM (Minimal Essential Medium, Sigma-Aldrich, St. Louis, MO), 4.2% sodium bicarbonate, and 83.5% collagen (PureCol; Inamed, Fremond, CA)] until polymerized before a final addition of 1 ml of ANB + B-27. Tissue was left in a 37°C, 5% CO₂, and 1% O₂ incubator until experiments were performed.

Drug Treatments:

Slices of mouse ileum were treated in accordance with Table 4. Slices were treated at 24 h ex vivo for a subsequent 24 h. Treatments were added to LPS challenged slices prophylactically at 0 h ex vivo prior to addition of LPS at 24 h ex vivo for 4 h followed by fixation.

Table 4. Drug treatments used throughout experiments

Treatment	Concentration	Source
Vasoactive Intestinal Peptide (VIP)	10 µM	ABBIOTEC (Escondido, CA)
[D-p-Cl-Phe ₆ ,Leu ₁₇]-VIP (VPACa)	10 µM	Bio-Techne Coproration (Minneapolis, MN)
Tetrodotoxin (TTX)	10 µM	Abcam (Cambridge, MA)
TLR-grade Lipopolysaccharide (LPS)	10 µg/ml	Enzo Life Sciences, Inc. (Farmingdale, NY)

Re-sectioning of Slices:

To improve visualization of cellular elements, 250 µm slices were re-sectioned at 50 µm as previously described (Schwerdtfeger & Tobet, 2020). Briefly, slices were fixed in 4% formaldehyde prior to blocking in 4% agarose solution (w/v; Fisher Scientific, Pittsburgh, PA) and subsequently put in a 4°C fridge for 4 min to allow for agarose polymerization. Ileum slices were then re-sectioned on a vibrating microtome (VT1000S; Leica Microsystems, Wetzlar, Germany) at 50 µm thick prior to processing for immunohistochemistry.

Immunohistochemistry:

Immunohistochemistry (IHC) was performed as previously described (Schwerdtfeger et al., 2016; Schwerdtfeger & Tobet, 2020). Briefly, 50 µm re-sectioned tissue sections received 0.1M glycine made in 0.05M PBS for 30 min prior to three PBS washes before 15 min in 0.5% sodium borohydride in PBS. Sections were subsequently washed twice in PBS prior to blocking for 30 min in 5% NGS, 0.5% Tx, and 1% H₂O₂ in PBS. Sections then received 2.0 µg/ml of anti-c-kit 2 (ACK2; Novus Biologicals, Centennial, CO) primary antibody in PBS with 1% BSA and 0.3% Tx. After incubation in the first primary, tissue sections were washed with 1% NGS in PBS four times for a total of 1 h. Next, a biotinylated donkey anti-rat secondary made with 1% NGS and 0.5% Tx in PBS was added for 2 h at room temperature. Secondary antibody was washed out with four 15 min washes composed of 0.02% Tx in PBS. Sections were next incubated with Alexa Fluor 555 – streptavidin (Invitrogen, Waltham MA) conjugated tertiary with solution composed of 0.32% Tx in PBS for 1 h. Sections then received three PBS washes prior to the addition of the secondary primary antisera composed of anti-VIP (Immunostar, Inc., Hudson, WI) at 1:8000 dilution in PBS with 1% BSA and 0.3% Tx. Post primary incubation, tissue sections were washed four times for a total of 1 h in PBS with 1% NGS prior to the addition of an Alexa Fluor 488 conjugated goat-anti-rabbit secondary (Invitrogen, Waltham, MA) for 1 h.

After secondary antibody, sections were washed three times in PBS before mounting on slides with Aqua-Poly/Mount (Polysciences, Inc., Warrington, PA) and subsequent imaging.

Tissue Imaging and Analysis:

Randomly selected ex vivo slices were imaged on a Nikon TE2000-U inverted microscope using a 10X Plan-Fluor objective and a UniBlitz shutter system (incent Associates, Rochester, NY) to visualize Thy-1 YFP fluorescence to confirm presence of fluorescent neurons and neuronal fibers as a rudimentary marker for tissue health. Tissues perfused and sectioned at 50 μm , and re-sectioned slice tissue were imaged after mounting on a Zeiss LSM 880 confocal microscope with an AxioCam 503 mono camera (Carl Zeiss, Inc., Thornton, NY). Z-stacks were acquired in 1 μm intervals through all 50 μm of each tissue section prior to a max intensity Z-projection being performed through the center 30 μm of each stack using FIJI (v1.0; NIH). Regions of interest around individual mast cells were manually drawn by a researcher blinded to treatment. Cells and neuronal fiber appositions were counted using FIJI.

Statistics:

Statistical analyses were performed in Prism 9 (Graphpad, San Diego, CA). Comparisons of ACK2-IR cell counts and the percentage of ACK2-IR cells with a VIP-IR Fiber in Figure 1 were both performed using one-way ANOVA. Data in Figure 2E, which looked at ACK2-IR cell counts across sex, treatment, and LPS challenge, were analyzed via 3-way ANOVA with a post-hoc Tukey's multiple comparison test to compare individual means. Data in Figure 2F also used a 3-way ANOVA with a Tukey's post-hoc test. Data in Figures 3, 4, and 5 compared means using a 2-way ANOVA by sex and treatments. All data are presented as means \pm standard error of the mean (SEM).

Results:

In fixative perfused ileum sections, mucosal mast cells were regularly opposed by VIP-IR neuronal fibers in mouse distal ileum. Tissue from females had significantly more mast cells per crypt-villus axis (CVA) than male Figure 33A,B / 1A',B') (Figure 33C; [F(1,10) = 23.0], $p < 0.01$). ACK2-IR cells from female ileum sections were also significantly larger than males (Figure 33D; [F(1,10) = 5.1], $p < 0.05$). Immunoreactivity to ACK2 was used to localize mast cells, and dual labeling with VIP showed large amounts of fiber appositions on ACK2-IR mast cells throughout the lamina propria of male (Figure 33A/A') and female (Figure 33B/B') ileal tissue. There were no notable differences in the percentage of ACK2-IR cells within 1 μm of a VIP-IR neuronal fiber in perfused ileum sections (Figure 33E).

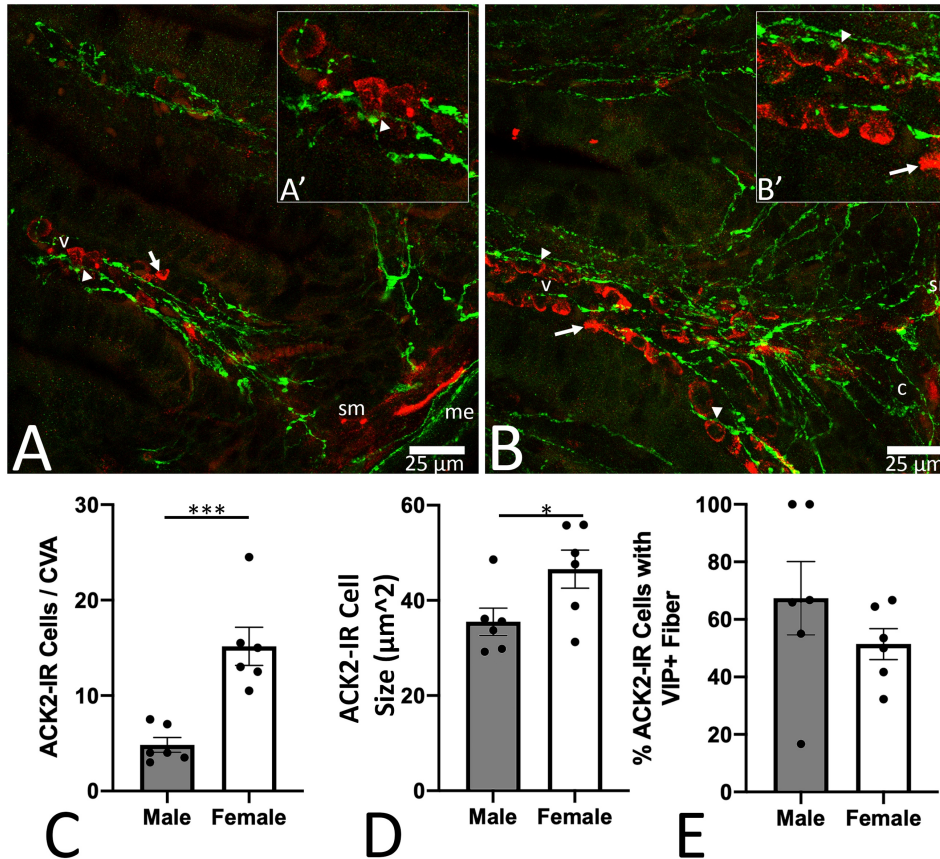


Figure 33. Basal sex difference in mast cell count per crypt-villus axis (CVA) and mean ACK2 cell size were observed. Representative images from male (A) and female (B) ileum samples with arrows denoting representative ACK2 immunoreactive (IR) cells (red) not near a VIP-immunoreactive fiber (green), while arrow heads point to exemplary ACK2-IR cells within 1 μm of a VIP-immunoreactive fiber. Cropped images in (A') and (B') show zoomed views of ACK2 cell proximity with VIP neuronal fibers. (C) quantification of ACK2 cell counts per CVA. (D) quantification of the percentage of ACK2-IR cells within 1 μm of a VIP-IR fiber. $n = 6$ males, 6 females. 'sm' denotes submucosa, 'c' crypt, and 'me' muscularis externa. Scale bars in (A) and (B) are both 25 μm .

Sex and LPS effects were observed in ACK2-IR cell counts per CVA regardless of treatment.

Representative images show male (Figure 34A/B) and female (Figure 34C/D) ileal villi with immunofluorescent ACK2 (red) and immunofluorescent VIP (green) closely localized.

Quantification of image sets from slices cultured *ex vivo* showed that treatment with vehicle, VIP, VPACa, or TTX, did not impact ACK2-IR cell counts per CVA ($[F(3,55) = 0.4]$ $p > 0.4$), however, sex ($[F(1,55) = 7.8]$ $p < 0.01$) and LPS challenge ($[F(1,55) = 8.2]$ $p < 0.01$) both

significantly influenced the ACK2-IR cell counts per CVA. Female tissues had more ACK2-IR

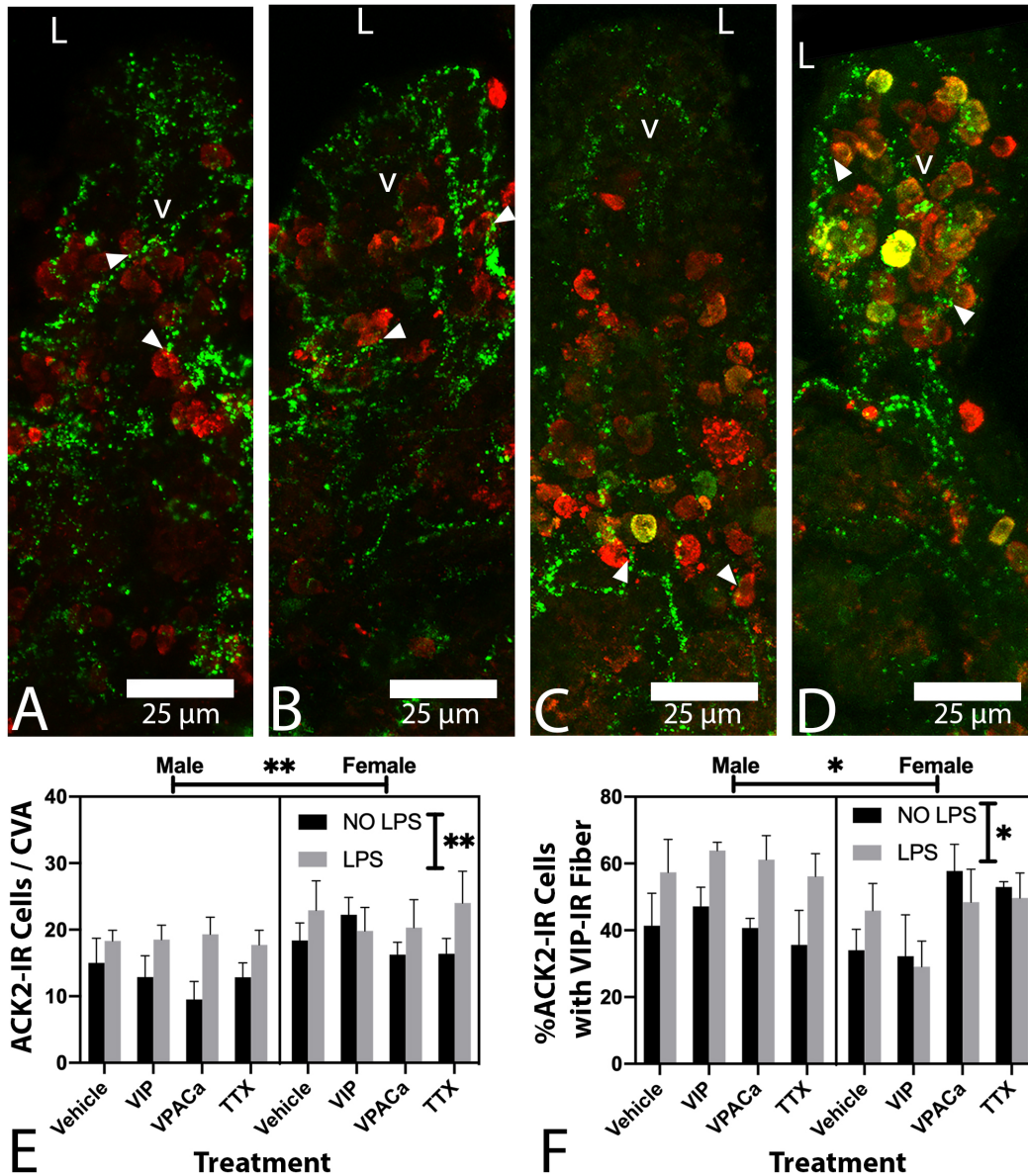


Figure 34. Sex and LPS effects were observed in ACK2-IR cell counts per CVA regardless of treatment, and in the percentage of ACK2-IR cells within 1 μ m of a fiber. (A-D) representative images from a male ileum treated with VIP (A) and TTX + LPS (B) showing ACK2-IR cells (red) and VIP-IR fibers (green). Representative images from female ileum treated with VIP (C) or Vehicle + LPS (D). (E) is a 3-way ANOVA quantitation showing effects of sex and LPS treatment on ACK2 cell counts. (F) is a 3-way ANOVA quantitation showing effects of sex and LPS treatment on the percentage of ACK2-IR cells within 1 μ m of a VIP-IR fiber. n = 4 male, 4 female in 'NO LPS' groups, and n = 5 male, 5 female in 'LPS' groups. Arrow heads in (A-D) point towards exemplary ACK2-IR cells within 1 μ m of a VIP-IR fiber. 'v' denotes a villus, 'L' lumen. Scale bars are 25 μ m in A-D. '*' denotes a p < 0.05, and '**' a p < 0.01.

cells than males, and LPS treatment increased ACK2-IR counts, regardless of sex, as there was no interaction between sex and LPS challenge (Figure 34E; [F(1,55) = 0.5] $p > 0.4$). In addition, the percentage of ACK2-IR cells within 1 μm of a VIP-IR fiber was not significantly different between sexes ([F(1,55) = 2.8] $p = 0.10$), but was altered by challenge with LPS ([F(1,55) = 4.8] $p < 0.05$). There was an interaction between sex and LPS challenge ([F(1,55) = 5.9] $p = 0.018$) and between sex and treatment ([F(3,55) = 2.9] $p < 0.05$). This effect was partially driven by VIP treatment in females, which had the lowest levels of % ACK2-IR within 1 μm of a VIP-IR fiber regardless of LPS challenge (Figure 34F).

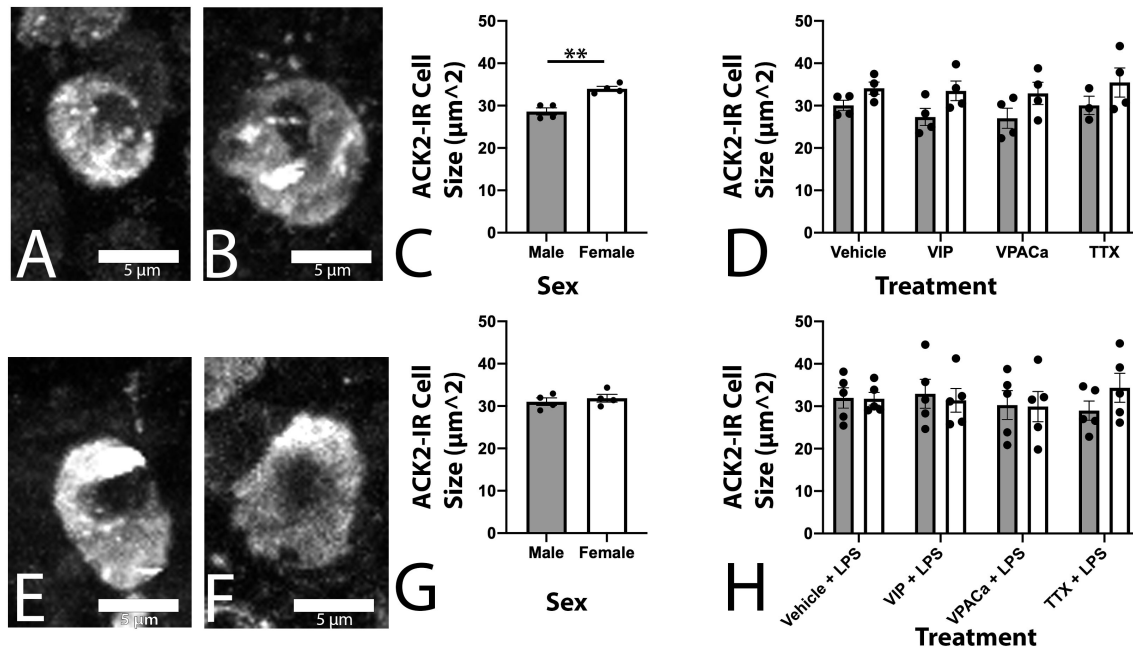


Figure 35: Female ACK2-IR cells were larger than males, an effect lost when slices were challenged with LPS. (A/E) and (B/F) are representative images of ACK2-immunoreactive cells from a male and female ileum slices respectively. (C) and (D) are quantification of mean ACK2-IR cell size across treatments. (G) and (H) are quantification of mean ACK2-IR cell size in slices challenged with LPS ex vivo. $n = 4$ male, 4 female in 'NO LPS' groups, and $n = 5$ male, 5 female in 'LPS' groups. Scale bars in (A/E) and (B/F) are all 5 μm .

Mast cell size was sex dependent, with ACK2-IR cell sizes larger in females than males. ACK2 area of immunoreactivity (μm^2) was smaller in male slices (Figure 35A) than it was in female (Figure 33B), regardless of treatment (Figure 33C-D; [F(1,23) = 10] $p < 0.01$). When challenged with LPS, ACK2-IR cell sizes from male mice (Figure 35E) were similar to those in females

(Figure 35F), independent of treatment (Figure 35G-H; $[F(1,32) = 0.1]$ $p > 0.50$). ACK2-IR cells within 1 μm of a VIP-IR neuronal fiber (Figure 35A/E) were larger than those not within 1 μm of a VIP fiber (Figure 34 B/F), regardless of treatment (Figure 36C/D; $[F(1,54) = 10.8]$ $p < 0.01$). When challenged with LPS, those ACK2-IR cells within 1 μm of a VIP-IR fiber were still larger than those not near a fiber, regardless of treatment (Figure 36G/H; $[F(1,72) = 5.43]$ $p < 0.05$; for all groups in Figure 36).

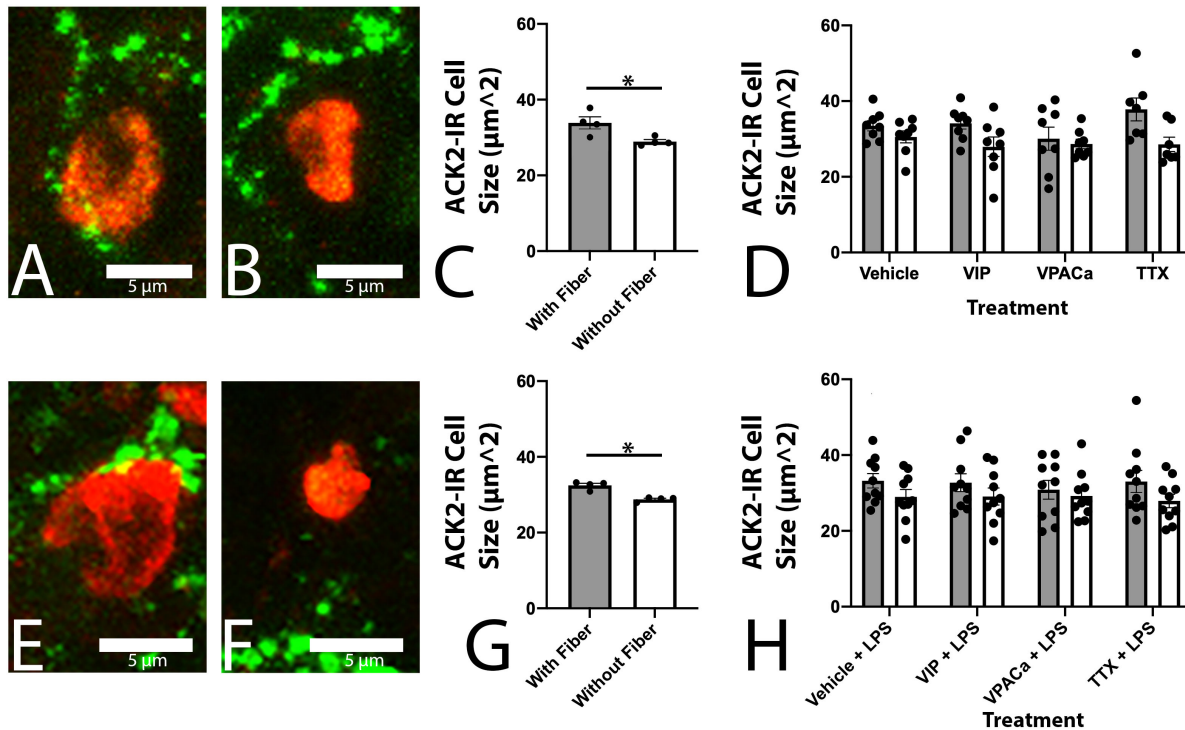


Figure 36. ACK2-IR cells within 1 μm of a VIP-IR neuronal fiber were larger than those not within 1 μm of a VIP-IR fiber, regardless of treatment or challenge with LPS. (A/E) and (B/F) are representative images of ACK2-immunoreactive cells (red) and VIP-immunoreactive fibers (green) from a cell < 1 μm from a VIP fiber or > 1 μm from a fiber, respectively. Quantification in (C) and (D) of the mean ACK2 cell size in μm^2 by treatment. (G) and (H) are quantification in the same fashion as (C/D) but in slices challenged with LPS. $n = 8$ animals Scale bars in (A/E) and (B/F) are all 5 μm .

There was a sex difference in the number of ACK2-IR cells that were also heavily immunoreactive for VIP was observed, but only in response to LPS challenge. Ileal tissue from males (Figure 37A/E) had an equivalent percentage of ACK2 cells also reactive for VIP per villus as females (Figure 37B/F), regardless of treatment (Figure 37C/D; $[F(1,23) = 0.06]$ $p >$

0.40). When challenged with LPS, the percentage of ACK2-IR cells heavily immunoreactive for VIP in male tissue remained largely unchanged, while females increased significantly, regardless of treatment (Figure 37G/H; $[F(1,32) = 5.03]$ $p < 0.05$).

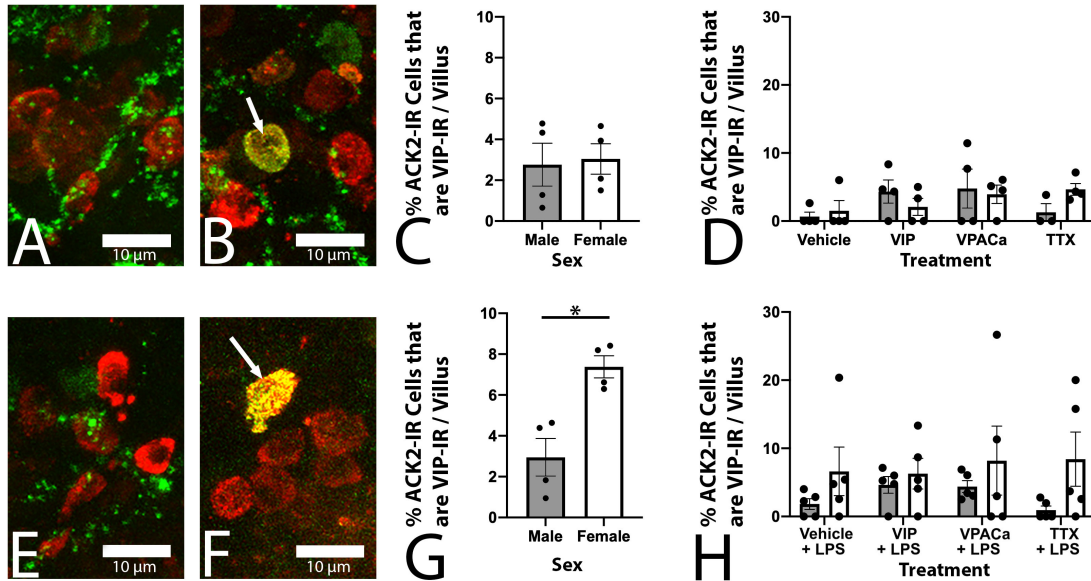


Figure 37: Slices from female ileums had more ACK2-IR cells also immunoreactive to VIP in response to LPS challenge than males. (A/E) and (B/F) are representative images of ACK2 immunoreactivity (red) and VIP immunoreactivity (green) with arrows pointing towards exemplary cells immunoreactive to both ACK2 and VIP. (C) and (D) are quantifications of the percentage of ACK2-IR cells that were greater than 20% of their area immunoreactive for VIP. (G) and (H) are quantifications the same as in (C/D) but in slices challenged with LPS. $n = 4$ male, 4 female in 'NO LPS' groups, and $n = 5$ male, 5 female in 'LPS' groups. Scale bars in (A/E) and (B/F) are all 10 μm .

Discussion:

Complex and diverse cellular elements in the intestinal wall must work in concert to maintain a healthy epithelial and mucus barrier, prevent pathogen invasion, and immunologically fight foreign antigens and pathogens if they breach the barrier. The extent to which enteric neuronal peptides are determinant, or modulatory players among gut wall signaling circuits is not well understood. Intestinal mucosal mast cells have been known to sit in close anatomic proximity to enteric neuronal fibers (Stead et al., 1989) and are capable of themselves producing a host of classical 'neuro' peptides like VIP (Cutz et al., 1978). Mucosal

mast cells also express VIP receptors (Keita et al., 2013), and produce VIP once exposed to LPS (Martinez et al., 1999). Data in this study documents a sex difference in anatomic arrangement, cell size, and VIP production capacity of enteric mast cells. Many of the observed sex differences were eliminated upon challenge with LPS, potentially indicating differences in basal compared to activated immunological states of the gut mucosa of males and females. Together, these data highlight the need to consider sex as a relevant variable when investigating enteric mast cell functional interactions with the rest of the gut wall.

Sex differences in immune components are relatively common, with female immune systems often being thought of as more 'active' than those in males (Klein & Flanagan, 2016). Additionally, differential levels of mast cell quantities and activation states during various gut pathologies across sexes has previously been shown (Lee et al., 2016; Cremon et al., 2009). In the current study, there was a sex difference in mast cell counts (ACK2-IR cells) at baseline in perfused ileum tissues, with females having higher cell counts. In ex vivo cultured slices, mast cell counts were higher at baseline in samples from female mice. Challenging with LPS reduced the observed sex difference in mast cell quantities, with males 'catching up' to female levels. The observed sex dependent response to challenge with LPS points towards a cohort of mast cells in female ileums that are either less likely to respond to a bacterial antigen or are already at capacity in their quantities in the gut wall. Conversely, male mast cells increased their quantities within 24 h, pointing towards a potentially more active mast cell population in male ileums. Preliminary data shows that ileums from a male animal had more proliferative mast cells in their villi lamina propria than female ileums, as measured by incorporation of 5-ethynyl-2'-deoxyuridine. This points towards the increase in male mast cell counts being potentially driven by proliferation at a local level, as these slices are removed from the body during culture and there is no external lymph node supply to shuttle lymphocytes.

Sex differences in mast cell sizes are not commonly reported, however, mast cell size has been correlated with activation, and secretory capacity, with mast cells being activated in vitro being larger in size (Levi-Shaffer et al., 2000). Larger mast cells could provide increased cytoplasmic area for packaging and storing secretory granules. This principle is in-line with a larger, potentially more 'active' female mast cell at basal state observed in this study, compared to a smaller, less 'active' male mast cell. When challenged with LPS, female mast cells did not change size, however, male mast cells increased in size compared to non-LPS dosed slices and became equivalent with female mast cell sizes. This points towards a potentially basal state activation of female mast cells in murine ileum, a sex difference in mast cell activation state only rectified in males when bacterial antigens like LPS are presented to mast cells.

Measurements of anatomic plasticity can be useful indicators of potential cell – cell signaling pathways like neuronal – immune networks. Proximity of mucosal mast cells to neuronal fibers has been tied to visceral pain levels in human irritable bowel syndrome patients (Barbara et al., 2004). This study also points toward mast cells in close proximity to neuronal fibers being more activated than those not near a fiber. In the present study, those mast cells that were within 1 μm of a VIP neuronal fiber were larger than those 1 μm of further away from a fiber, regardless of treatment. These data suggest a subset of more activated mast cells in close proximity to VIP neuronal fibers, echoing the human data from Barbara et al., 2004, while extending the hypothesis by specifying one specific neuronal fiber type potentially involved in activated mast cell interactions with neuronal fibers.

Mucosal mast cells are capable of producing numerous classical neuropeptides, including VIP, however, sex differences in this peptide production have not been shown. While baseline levels of VIP production have been observed in mast cells, the quantities are relatively minimal (Cutz et al., 1978) and we did not observe VIP-IR mast cells in perfusion fixed ileum sections in the

present work. Challenging mast cells with LPS was shown previously to trigger production and subsequent release of VIP (Martinez et al., 1999). In this study, we did not observe sex differences, irrespective of treatment, in the percentage of mast cells 'producing' VIP as indicated by VIP-IR in ex vivo slices. However, when challenged with LPS, there was an increase in the percentage of VIP-IR mast cells in female tissues only. This sex difference indicates that female mucosal mast cells are potentially more readily able to produce VIP in response to bacterial antigens like LPS, however, the downstream function of mast cell produced VIP after LPS challenge needs further investigation.

In conclusion, the results of this study illuminate a sex difference in the anatomical localization and plasticity of neuronal – mast cell interactions, and in mast cell size and capacity to produce the neuropeptide VIP. Female neuro – immune signaling seems to be in a more activated basal state, however, dosing with VIP or its antagonists did not substantially alter female or male mast cell numbers or size or VIP – mast cell anatomic relations or interactions. Not until LPS challenge did males recover from their decreased mast cell counts, sizes, and activation levels. Together, these data offer a different perspective on neuronal – mast cell signaling, suggesting sex differences in gut mucosal immunology and pointing towards the need to consider sex as a relevant variable when investigating mucosal neural – immune signaling pathways.

References:

- 1) Furness JB, Costa M. Projections of intestinal neurons showing immunoreactivity for vasoactive intestinal polypeptide are consistent with these neurons being the enteric inhibitory neurons. *Neurosci Lett.* 1979;15(2-3):199-204.
- 2) Malaviya R, Ikeda T, Ross E, Abraham SN. Mast cell modulation of neutrophil influx and bacterial clearance at sites of infection through TNF-alpha. *Nature.* 1996;381(6577):77-80.
- 3) Piotrowski W, Foreman JC. On the actions of substance P, somatostatin, and vasoactive intestinal polypeptide on rat peritoneal mast cells and in human skin. *Naunyn-Schmiedeberg's archives of pharmacology.* 1985;331:364-8.
- 4) Albert-Bayo M, Paracuellos I, Gonzalez-Castro AM, Rodriguez-Urrutia A, Rodriguez-Lagunas MJ, Alonso-Cotoner C, Santos J, Vicario M. Intestinal Mucosal Mast Cells: Key Modulators of Barrier Function and Homeostasis. *Cells.* 2019;8(2).
- 5) Barbara G, Stanghellini V, De Giorgio R, Cremon C, Cottrell GS, Santini D, Pasquinelli G, Morselli-Labate AM, Grady EF, Bunnett NW, Collins SM, Corinaldesi R. Activated mast cells in proximity to colonic nerves correlate with abdominal pain in irritable bowel syndrome. *Gastroenterology.* 2004;126(3):693-702.
- 6) Casado-Bedmar M, Heil SDS, Myreid P, Soderholm JD, Keita AV. Upregulation of intestinal mucosal mast cells expressing VPAC1 in close proximity to vasoactive intestinal polypeptide in inflammatory bowel disease and murine colitis. *Neurogastroenterology and motility : the official journal of the European Gastrointestinal Motility Society.* 2019;31(3):e13503.
- 7) Cremon C, Gargano L, Morselli-Labate AM, Santini D, Cogliandro RF, De Giorgio R, Stanghellini V, Corinaldesi R, Barbara G. Mucosal immune activation in irritable bowel syndrome: gender-dependence and association with digestive symptoms. *Am J Gastroenterol.* 2009;104(2):392-400.

- 8) Cutz E, Chan W, Track NS, Goth A, Said SI. Release of vasoactive intestinal polypeptide in mast cells by histamine liberators. *Nature*. 1978;275(5681):661-2.
- 9) Mongardi Fantaguzzi C, Thacker M, Chiocchetti R, Furness JB. Identification of neuron types in the submucosal ganglia of the mouse ileum. *Cell and tissue research*. 2009;336(2):179-89.
- 10) Feng G, Mellor R, Bernstein M, Keller-Peck C, Nguyen Q, Nerbonne J, Lichtman J, Sanes J. Imaging Neuronal Subsets in Transgenic Mice Expressing Multiple Spectral Variants of GFP. *Neuron*. 2000;28(1):41-51.
- 11) Forsythe P, Bienenstock J. The mast cell-nerve functional unit: a key component of physiologic and pathophysiologic responses. *Chem Immunol Allergy*. 2012;98:196-221.
- 12) Jacobson A, Yang D, Vella M, Chiu IM. The intestinal neuro-immune axis: crosstalk between neurons, immune cells, and microbes. *Mucosal immunology*. 2021.
- 13) Katsoulis S, Clemens A, Schworer H, Creutzfeldt W, Schmidt WE. Pacap Is a Stimulator of Neurogenic Contraction in Guinea-Pig Ileum. *American Journal of Physiology*. 1993;265(2):G295-G302.
- 14) Keita AV, Carlsson AH, Cigehn M, Ericson AC, McKay DM, Soderholm JD. Vasoactive intestinal polypeptide regulates barrier function via mast cells in human intestinal follicle-associated epithelium and during stress in rats. *Neurogastroenterology and motility : the official journal of the European Gastrointestinal Motility Society*. 2013;25(6):e406-17.
- 15) Klein SL, Flanagan KL. Sex differences in immune responses. *Nature reviews Immunology*. 2016;16(10):626-38.
- 16) Lee JY, Kim N, Kim YS, Nam RH, Ham MH, Lee HS, Jo W, Shim Y, Choi YJ, Yoon H, Shin CM, Lee DH. Repeated Water Avoidance Stress Alters Mucosal Mast Cell Counts, Interleukin-1beta Levels with Sex Differences in the Distal Colon of Wistar Rats. *J Neurogastroenterol Motil*. 2016;22(4):694-704.

- 17)** Levi-Schaffer F, Slovik D, Armetti L, Pickholtz D, Touitou E. Activation and inhibition of mast cells degranulation affect their morphometric parameters. *Life Sci.* 2000;66(21):PL283-90.
- 18)** Lovell RM, Ford AC. Global prevalence of and risk factors for irritable bowel syndrome: a meta-analysis. *Clin Gastroenterol Hepatol.* 2012;10(7):712-21 e4.
- 19)** Martinez C, Delgado M, Abad C, Gomariz RP, Ganea D, Leceta J. Regulation of VIP production and secretion by murine lymphocytes. *J Neuroimmunol.* 1999;93(1-2):126-38.
- 20)** Pandol SJ, Dharmasathaphorn K, Schoeffield MS, Vale W, Rivier J. Vasoactive intestinal peptide receptor antagonist [4Cl-D-Phe⁶, Leu¹⁷] VIP. *Am J Physiol.* 1986;250(4 Pt 1):G553-7.
- 21)** Piliponsky AM, Romani L. The contribution of mast cells to bacterial and fungal infection immunity. *Immunol Rev.* 2018;282(1):188-97.
- 22)** Schwerdtfeger LA, Nealon NJ, Ryan EP, Tobet SA. Human colon function ex vivo: Dependence on oxygen and sensitivity to antibiotic. *PloS one.* 2019;14(5):e0217170..
- 23)** Schwerdtfeger LA, Ryan EP, Tobet SA. An organotypic slice model for ex vivo study of neural, immune, and microbial interactions of mouse intestine. *American journal of physiology Gastrointestinal and liver physiology.* 2016;310(4):G240-8.
- 24)** Schwerdtfeger LA, Tobet SA. Vasoactive Intestinal Peptide Regulates Ileal Goblet Cell Production in Mice. *Physiological reports.* 2020;8(3).
- 25)** Sikora LKJ, Buchan AMJ, Levy JG, Mcintosh CHS, Brown JC. VIP-Innervation of Rate Intestine: A Developmental Study with Monoclonal Antibodies. *Peptides.* 1984;5:231-7.
- 26)** Stead RH, Dixon MF, Bramwell NH, Riddell RH, Bienenstock J. Mast Cells Are Closely Apposed to Nerves in the Human Gastrointestinal Mucosa. *Gastroenterology.* 1989;97:575-85.
- 27)** Vaudry D, Falluel-Morel A, Bourgault S, Basille M, Burel D, Wurtz O, Fournier A, Chow BK, Hashimoto H, Galas L, Vaudry H. Pituitary adenylate cyclase-activating polypeptide

and its receptors: 20 years after the discovery. *Pharmacological reviews*.
2009;61(3):283-357.

DISCUSSION

Methods to the madness:

Attempting to culture the >25 cell types found in a gut explant individually in a dish would seem akin to the labors of Hercules. Fortunately, because these numerous cell types subside together and work synergistically in vivo, letting nature 'do the engineering' means we can simply remove the organ from the body, slice it relatively thin using a microtome, and then proceed with culturing while having the anatomical arrangement of the diverse cellular components in their proper positions. Developing our lab's method for gut organotypic slices took large amounts of trial and error (Schwerdtfeger et al., 2016). However, lessons learned during that development process allowed for an easier time creating the human colon biopsy slice model contained in Section 2, Chapter 5 (Schwerdtfeger et al., 2019). Tissue garnered from human colons during routine colonoscopy allowed a more translational model to be used for investigation of the influence of antibiotics and oxygen concentration on gut wall health. The set of experiments that went into this manuscript served numerous purposes. They validated the use of our previously developed murine gut slice method in human colon biopsy samples. Additionally, the experiments demonstrated the critical role of oxygen in regulating gut epithelial proliferation, an effect compounded in non-antibiotic treated slices. This pointed towards the microbiome as playing a key role in regulating cellular proliferation in the human colon ex vivo. Probing with salmonella in these experiments offered a validation of the method for use in pathogen challenge studies and showed a local proliferation of T-lymphocytes, independent of lymph nodes as would be seen in vivo.

The principal downside of the organotypic slice methods is their inability to recapitulate the intestinal barrier ex vivo, something that is accomplished with microfluidic systems including

the Microfluidic Organotypic Device (MOD) described in Section 2, Chapter 4 of this dissertation (McLean et al., 2018; Richardson et al., 2020). Using mouse gut explants as a partition between two media flow channels allows the MOD to recapitulate the in vivo barrier observed between the lumen and its contents and the gut wall. Experiments conducted in the manuscript were designed to validate the MOD system as a means for maintaining mouse intestinal explants ex vivo, with a barrier present and an in vivo – like oxygen gradient imposed upon the tissue using nearly anoxic media in the luminal channel. With the MOD system validated, design modifications are planned to make it more amenable to higher throughput analyses of intestinal explants ex vivo. Further iterations currently in development in the laboratory include a larger device for maintenance of pig, and eventually human, intestinal explants. Additionally, sensor work is ongoing to create on-chip and in-line sensor modules for analysis of glucose, lactate, pH, and metabolites among other molecules.

Anatomy and Function:

It would be valuable to learn the biochemical languages that neurons and glia use to communicate directly with gut wall epithelia and immune components. Neural – epithelial signaling is a developing field, with main focuses being on neuronal signaling with Tuft (Cheng et al., 2018) or enteroendocrine cells (Bohorquez et al., 2014; 2015). Mechanisms with other epithelia cell types are less well known. As a first step in that direction in our lab, a notable interaction between two cell types, enteric submucosal neurons/fibers and a specialized epithelia called goblet cells, was noted in Section 3, Chapter 6 of this dissertation (Schwerdtfeger & Tobet, 2020). The roles of neuronal peptides in regulating epithelial function in the gut have been postulated. We demonstrated that goblet cells, a subset of epithelia, are intimately associated with submucosal neuronal fibers. This anatomical arrangement is plastic, and significantly increased when treated with a VIP antagonist ex vivo. Notably, the production

of new goblet cells was substantially decreased when VIP receptors were inhibited, potentially pointing towards a functional role of a specific neuronal peptide on epithelial production. Further work is needed to flesh out direct mechanism(s) of neuropeptide signaling with enteric goblet cells or their stem precursors to ascertain what influences these pathways have on gut wall maintenance in healthy and diseased intestines.

Paneth cells in the base of intestinal crypts are a unique epithelial population because they secrete anti-microbial products, protecting the stem cell niche from pathogens. Neural regulation of Paneth cell function is not well understood, and baseline investigations into neuronal fiber anatomic pathways for potential signaling with Paneth cells was needed. Section 3, Chapter 7 lays out the anatomical foundation of VIP neuronal fibers coursing intimately with ileal Paneth cells. This chapter also contains data demonstrating a sex difference in Paneth cell fluorescent intensity, with females having more intense Paneth cells than males, with male intensities rising to female Paneth cell levels post challenge with LPS. These data are preliminary but provide a starting off point for future work into neural regulation of Paneth cell function in response to bacterial challenge, while taking into account sex as a relevant variable.

Results in Chapter 6 pointed towards VIP as being potentially critical in maintenance of gut epithelial populations. However, immune components regulating neuronal and epithelial function have also been demonstrated. Coupling this with the fact that VIP signals bi-directionally with enteric mast cells, first line defenders against foreign bacterial invasion of the gut wall, the potential for neural – immune – epithelial anatomic and functional communication could not be ignored. Chapter 8 of this dissertation dives into the spatial relationships of VIP neuronal fibers with a bone marrow derived immune population called mast cells. Importantly, these experiments yielded data showing sex differences in the anatomic arrangements of VIP fibers with mast cells and larger and more abundant mast cell populations in females compared

to males. These differences were responsive to challenge with a component of bacterial cell walls, lipopolysaccharide, in a sex dependent manner, with male ileal mast cells showing large changes in all measures, while female mast cells did not change. These data add to a growing body of literature that shows female intestinal walls have more active immune populations at basal state than males (Klein & Flanagan, 2016). Sex differences are a critical aspect of human physiology that cannot be ignored in the intestinal wall, particularly when investigating immunological mechanisms. Future work in this arena should focus on the functional roles of VIP and other neuropeptides in regulating mast and epithelial cell secretions and anatomic plasticity in response to bacterial pathogens.

In conclusion, the data contained within this dissertation provide guidelines for generating culture methods for maintenance of intestinal tissue outside the body (Schwerdtfeger & Tobet, 2019; Schwerdtfeger & Tobet; 2020b). Further, it provides details of two methods for culturing mouse, human, and porcine intestinal tissues *ex vivo* (Schwerdtfeger et al., 2019; Richardson et al., 2020). Finally, the methodologies outlined are put to work to investigate neural – immune and neural – epithelial signaling pathways and anatomic plasticity with respect to sex in the mouse intestine (Schwerdtfeger & Tobet 2020a). These data, derived using organotypic culture methodologies, lay a foundation for studying neural – immune – epithelial signaling in the gut wall, with sex as a relevant variable. Important mechanisms of mast cell signaling, mediated by enteric neural elements, are being shown in arenas ranging from infection to neurodegenerative diseases, and neural – epithelial regulation of the gut barrier is seemingly more critical every day. Designing the next generation of treatments for bacterial and viral infections, drugs that modulate the immune reservoir in the intestine, among many others, requires using physiologically relevant culture systems, while not ignoring the critical variable of sex. Hopefully, these data will prove informative for future students and investigators when

designing and implementing organotypic culture methods for study of morbidities afflicting the intestinal tract and drug discovery for treatment of these complex diseases.

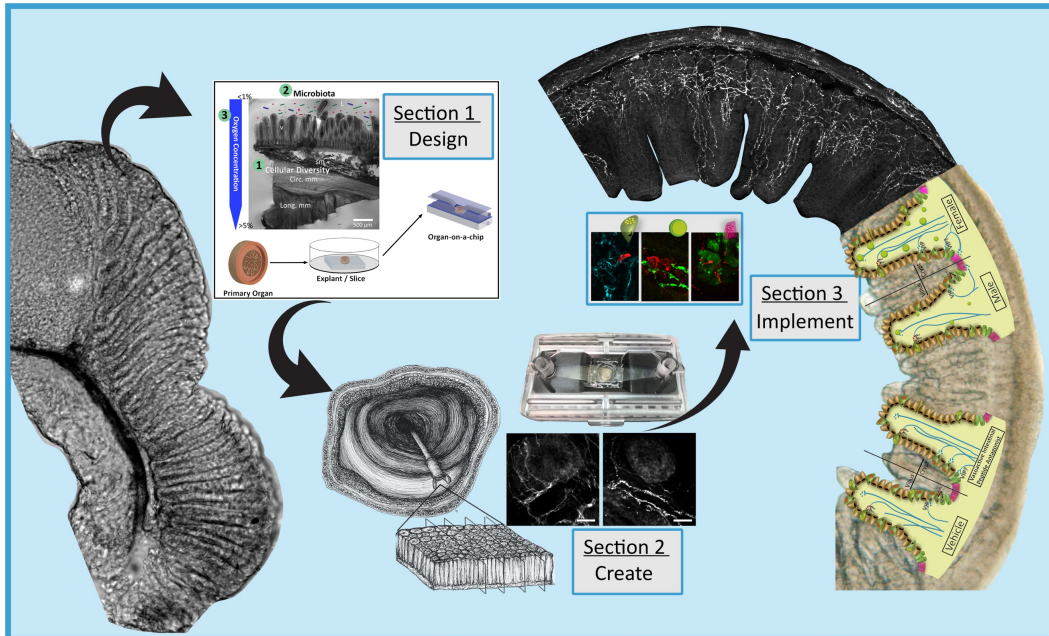


Figure 36. Graphical illustration of the dissertation project.

References:

- 1) Schwerdtfeger LA, Ryan EP, Tobet SA. An organotypic slice model for ex vivo study of neural, immune, and microbial interactions of mouse intestine. *American journal of physiology Gastrointestinal and liver physiology*. 2016;310(4):G240-8.
- 2) Schwerdtfeger LA, Nealon NJ, Ryan EP, Tobet SA. Human colon function ex vivo: Dependence on oxygen and sensitivity to antibiotic. *PloS one*. 2019;14(5):e0217170.
- 3) McLean IC, Schwerdtfeger LA, Tobet SA, Henry CS. Powering ex vivo tissue models in microfluidic systems. *Lab Chip*. 2018;18(10):1399-1410.
- 4) Richardson A, Schwerdtfeger LA, Eaton D, McLean I, Henry CS, Tobet SA. A microfluidic organotypic device for culture of mammalian intestines ex vivo. *Analytical Methods*. 2020;12:297-303.
- 5) Cheng X, Voss U, and Ekblad E. Tuft cells: Distribution and connections with nerves and endocrine cells in mouse intestine. *Experimental cell research* 369: 105-111, 2018.
- 6) Bohorquez DV, Shahid RA, Erdmann A, et al. Neuroepithelial circuit formed by innervation of sensory enteroendocrine cells. *J Clin Invest*. 2015;125(2):782-786.
- 7) Bohorquez DV, Samsa LA, Roholt A, Medicetty S, Chandra R, Liddle RA. An enteroendocrine cell-enteric glia connection revealed by 3D electron microscopy. *PloS one*. 2014;9(2):e89881.
- 8) Schwerdtfeger LA, Tobet SA. Vasoactive Intestinal Peptide Regulates Ileal Goblet Cell Production in Mice. *Physiological reports*. 2020;8(3).
- 9) Klein SL, Flanagan KL. Sex differences in immune responses. *Nature reviews Immunology*. 2016;16(10):626-38.
- 10) Schwerdtfeger LA, Tobet SA. From organotypic culture to body-on-a-chip: A neuroendocrine perspective. *J Neuroendocrinol*. 2019;31(3):e12650.

11) Schwerdtfeger LA & Tobet SA. Designing multicellular intestinal systems. In Precision Medicine for Investigators, Practitioners and Providers, ed., J Faintuch and S Faintauch, Elsevier Publishing, January, 2020.

APPENDIX

- A. Permission to reproduce manuscript entitled “From organotypic culture to body-on-a-chip: A neuroendocrine perspective”
- B. Permission to reproduce book chapter entitled “Designing Multicellular Intestinal Systems”
- C. Permission to reproduce manuscript entitled “Powering *ex vivo* tissue models in microfluidic systems”
- D. Permission to reproduce manuscript entitled “A microfluidic organotypic device for culture of mammalian intestines *ex vivo*”
- E. Permission to reproduce manuscript entitled “Human Colon Function Ex Vivo: Dependence on Oxygen and Sensitivity to Antibiotic”
- F. Permission to reproduce manuscript entitled “Vasoactive Intestinal Peptide Regulates Ileal Goblet Cell Production in Mice”

A. Permission to reproduce manuscript entitled “From organotypic culture to body-on-a-chip: A neuroendocrine perspective”

JOHN WILEY AND SONS LICENSE
TERMS AND CONDITIONS

Jun 09, 2020

This Agreement between Colorado State University -- Luke Schwerdtfeger ("You") and John Wiley and Sons ("John Wiley and Sons") consists of your license details and the terms and conditions provided by John Wiley and Sons and Copyright Clearance Center.

License Number	4844790143433
License date	Jun 09, 2020
Licensed Content Publisher	John Wiley and Sons
Licensed Content Publication	Journal of Neuroendocrinology
Licensed Content Title	From organotypic culture to body-on-a-chip: A neuroendocrine perspective
Licensed Content Author	Luke A. Schwerdtfeger, Stuart A. Tobet
Licensed Content Date	Nov 7, 2018
Licensed Content Volume	31
Licensed Content Issue	3
Licensed Content	

Pages	12
Type of use	Dissertation/Thesis
Requestor type	Author of this Wiley article
Format	Print and electronic
Portion	Full article
Will you be translating?	No
Title	NEURAL – EPITHELIAL SIGNALING AS A QUASI – IMMUNE PATHWAY IN THE GUT
Institution name	Colorado State University
Expected presentation date	Jun 2021
Order reference number	1234
Requestor Location	Colorado State University 1617 Campus Delivery Anatomy/Zoology W223 FORT COLLINS, CO 80523 United States Attn: Colorado State University
Publisher Tax ID	EU826007151
Total	0.00 USD
Terms and Conditions	

TERMS AND CONDITIONS

This copyrighted material is owned by or exclusively licensed to John Wiley & Sons, Inc. or one of its group companies (each a "Wiley Company") or handled on behalf of a society with which a Wiley Company has exclusive publishing rights in relation to a particular work (collectively "WILEY"). By clicking "accept" in connection with completing this licensing transaction, you agree that the following terms and conditions apply to this transaction (along with the billing and payment terms and conditions established by the Copyright Clearance Center Inc., ("CCC's Billing and Payment terms and conditions"), at the time that you opened your RightsLink account (these are available at any time at <http://myaccount.copyright.com>).

Terms and Conditions

- The materials you have requested permission to reproduce or reuse (the "Wiley Materials") are protected by copyright.
- You are hereby granted a personal, non-exclusive, non-sub licensable (on a stand-alone basis), non-transferable, worldwide, limited license to reproduce the Wiley Materials for the purpose specified in the licensing process. This license, **and any CONTENT (PDF or image file) purchased as part of your order**, is for a one-time use only and limited to any maximum distribution number specified in the license. The first instance of republication or reuse granted by this license must be completed within two years of the date of the grant of this license (although copies prepared before the end date may be distributed thereafter). The Wiley Materials shall not be used in any other manner or for any other purpose, beyond what is granted in the license. Permission is granted subject to an appropriate acknowledgement given to the author, title of the material/book/journal and the publisher. You shall also duplicate the copyright notice that appears in the Wiley publication in your use of the Wiley Material. Permission is also granted on the understanding that nowhere in the text is a previously published source acknowledged for all or part of this Wiley Material. Any third party content is expressly excluded from this permission.
- With respect to the Wiley Materials, all rights are reserved. Except as expressly granted by the terms of the license, no part of the Wiley Materials may be copied, modified, adapted (except for minor reformatting required by the new Publication), translated, reproduced, transferred or distributed, in any form or by any means, and no derivative works may be made based on the Wiley Materials without the prior permission of the respective copyright owner. **For STM Signatory Publishers clearing permission under the terms of the [STM Permissions Guidelines](#) only, the terms of the license are extended to include subsequent editions and for editions in other languages, provided such editions are for the work as a whole in situ and does not involve the separate exploitation of the permitted figures or extracts**, You may not alter, remove or suppress in any manner any copyright, trademark or other notices displayed by the Wiley Materials. You may not license, rent, sell, loan, lease, pledge, offer as security, transfer or assign the Wiley Materials on a stand-alone basis, or any of the rights granted to you hereunder to any other person.

- The Wiley Materials and all of the intellectual property rights therein shall at all times remain the exclusive property of John Wiley & Sons Inc, the Wiley Companies, or their respective licensors, and your interest therein is only that of having possession of and the right to reproduce the Wiley Materials pursuant to Section 2 herein during the continuance of this Agreement. You agree that you own no right, title or interest in or to the Wiley Materials or any of the intellectual property rights therein. You shall have no rights hereunder other than the license as provided for above in Section 2. No right, license or interest to any trademark, trade name, service mark or other branding ("Marks") of WILEY or its licensors is granted hereunder, and you agree that you shall not assert any such right, license or interest with respect thereto
- NEITHER WILEY NOR ITS LICENSORS MAKES ANY WARRANTY OR REPRESENTATION OF ANY KIND TO YOU OR ANY THIRD PARTY, EXPRESS, IMPLIED OR STATUTORY, WITH RESPECT TO THE MATERIALS OR THE ACCURACY OF ANY INFORMATION CONTAINED IN THE MATERIALS, INCLUDING, WITHOUT LIMITATION, ANY IMPLIED WARRANTY OF MERCHANTABILITY, ACCURACY, SATISFACTORY QUALITY, FITNESS FOR A PARTICULAR PURPOSE, USABILITY, INTEGRATION OR NON-INFRINGEMENT AND ALL SUCH WARRANTIES ARE HEREBY EXCLUDED BY WILEY AND ITS LICENSORS AND WAIVED BY YOU.
- WILEY shall have the right to terminate this Agreement immediately upon breach of this Agreement by you.
- You shall indemnify, defend and hold harmless WILEY, its Licensors and their respective directors, officers, agents and employees, from and against any actual or threatened claims, demands, causes of action or proceedings arising from any breach of this Agreement by you.
- IN NO EVENT SHALL WILEY OR ITS LICENSORS BE LIABLE TO YOU OR ANY OTHER PARTY OR ANY OTHER PERSON OR ENTITY FOR ANY SPECIAL, CONSEQUENTIAL, INCIDENTAL, INDIRECT, EXEMPLARY OR PUNITIVE DAMAGES, HOWEVER CAUSED, ARISING OUT OF OR IN CONNECTION WITH THE DOWNLOADING, PROVISIONING, VIEWING OR USE OF THE MATERIALS REGARDLESS OF THE FORM OF ACTION, WHETHER FOR BREACH OF CONTRACT, BREACH OF WARRANTY, TORT, NEGLIGENCE, INFRINGEMENT OR OTHERWISE (INCLUDING, WITHOUT LIMITATION, DAMAGES BASED ON LOSS OF PROFITS, DATA, FILES, USE, BUSINESS OPPORTUNITY OR CLAIMS OF THIRD PARTIES), AND WHETHER OR NOT THE PARTY HAS BEEN ADVISED OF THE POSSIBILITY OF SUCH DAMAGES. THIS LIMITATION SHALL APPLY NOTWITHSTANDING ANY FAILURE OF ESSENTIAL PURPOSE OF ANY LIMITED REMEDY PROVIDED HEREIN.
- Should any provision of this Agreement be held by a court of competent jurisdiction to be illegal, invalid, or unenforceable, that provision shall be deemed amended to achieve as nearly as possible the same economic effect as the original provision, and the legality, validity and enforceability of the remaining provisions of this Agreement shall not be affected or impaired thereby.

- The failure of either party to enforce any term or condition of this Agreement shall not constitute a waiver of either party's right to enforce each and every term and condition of this Agreement. No breach under this agreement shall be deemed waived or excused by either party unless such waiver or consent is in writing signed by the party granting such waiver or consent. The waiver by or consent of a party to a breach of any provision of this Agreement shall not operate or be construed as a waiver of or consent to any other or subsequent breach by such other party.
- This Agreement may not be assigned (including by operation of law or otherwise) by you without WILEY's prior written consent.
- Any fee required for this permission shall be non-refundable after thirty (30) days from receipt by the CCC.
- These terms and conditions together with CCC's Billing and Payment terms and conditions (which are incorporated herein) form the entire agreement between you and WILEY concerning this licensing transaction and (in the absence of fraud) supersedes all prior agreements and representations of the parties, oral or written. This Agreement may not be amended except in writing signed by both parties. This Agreement shall be binding upon and inure to the benefit of the parties' successors, legal representatives, and authorized assigns.
- In the event of any conflict between your obligations established by these terms and conditions and those established by CCC's Billing and Payment terms and conditions, these terms and conditions shall prevail.
- WILEY expressly reserves all rights not specifically granted in the combination of (i) the license details provided by you and accepted in the course of this licensing transaction, (ii) these terms and conditions and (iii) CCC's Billing and Payment terms and conditions.
- This Agreement will be void if the Type of Use, Format, Circulation, or Requestor Type was misrepresented during the licensing process.
- This Agreement shall be governed by and construed in accordance with the laws of the State of New York, USA, without regards to such state's conflict of law rules. Any legal action, suit or proceeding arising out of or relating to these Terms and Conditions or the breach thereof shall be instituted in a court of competent jurisdiction in New York County in the State of New York in the United States of America and each party hereby consents and submits to the personal jurisdiction of such court, waives any objection to venue in such court and consents to service of process by registered or certified mail, return receipt requested, at the last known address of such party.

WILEY OPEN ACCESS TERMS AND CONDITIONS

Wiley Publishes Open Access Articles in fully Open Access Journals and in Subscription journals offering Online Open. Although most of the fully Open Access journals publish open access articles under the terms of the Creative Commons Attribution (CC BY) License only, the subscription journals and a few of the Open Access Journals offer a choice of

B. Permission to reproduce book chapter entitled “Designing Multicellular Intestinal Systems”

Permissions were obtained via e-mail, attached below:

Rights and Permissions (ELS) Inbox - Exchange Yesterday at 2:36 PM 

Re: Obtain permission request - Book (1065555) [201006-015341]
To: luke.schwerdtfeger@colostate.edu,
Reply-To: Rights and Permissions (ELS)

Dear Luke Schwerdtfeger

We hereby grant you permission to reprint the material below at no charge in your thesis subject to the following conditions:

RE:

1. If any part of the material to be used (for example, figures) has appeared in our publication with credit or acknowledgement to another source, permission must also be sought from that source. If such permission is not obtained then that material may not be included in your publication/copies.
2. Suitable acknowledgment to the source must be made, either as a footnote or in a reference list at the end of your publication, as follows:
"This article was published in Publication title, Vol number, Author(s), Title of article, Page Nos, Copyright Elsevier (or appropriate Society name) (Year)."
3. Your thesis may be submitted to your institution in either print or electronic form.
4. Reproduction of this material is confined to the purpose for which permission is hereby given.
5. This permission is granted for non-exclusive world English rights only. For other languages please reapply separately for each one required. Permission excludes use in an electronic form other than submission. Should you have a specific electronic project in mind please reapply for permission.
6. As long as the article is embedded in your thesis, you can post/share your thesis in the University repository.
7. Should your thesis be published commercially, please reapply for permission.

This includes permission for the Library and Archives of Canada to supply single copies, on demand, of the complete thesis. Should your thesis be published commercially, please reapply for permission.

This includes permission for UMI to supply single copies, on demand, of the complete thesis. Should your thesis be published commercially, please reapply for permission.
8. Posting of the full article/ chapter online is not permitted. You may post an abstract with a link to the Elsevier website www.elsevier.com, or to the article on ScienceDirect if it is available on that platform.

Regards,
Akshaya

C. Permission to reproduce manuscript entitled “Powering *ex vivo* tissue models in microfluidic systems”

Per the Royal Society of Chemistry: <https://www.rsc.org/journals-books-databases/journal-authors-reviewers/licences-copyright-permissions/#reuse-permission-requests>

You do not need to request permission to reuse your own figures, diagrams, etc., that were originally published in a Royal Society of Chemistry publication. However, permission should be requested for use of the whole article or chapter except if reusing it in a thesis. If you are including an article or book chapter published by us in your thesis please ensure that your co-authors are aware of this.

All authors have been notified via email, and appropriate citations are included in the footer for the chapter where this manuscript appears.

D. Permission to reproduce manuscript entitled “A microfluidic organotypic device for culture of mammalian intestines *ex vivo*”

Per the Royal Society of Chemistry: <https://www.rsc.org/journals-books-databases/journal-authors-reviewers/licences-copyright-permissions/#reuse-permission-requests>

You do not need to request permission to reuse your own figures, diagrams, etc., that were originally published in a Royal Society of Chemistry publication. However, permission should be requested for use of the whole article or chapter except if reusing it in a thesis. If you are including an article or book chapter published by us in your thesis please ensure that your co-authors are aware of this.

All authors have been notified via email, and appropriate citations are included in the footer for the chapter where this manuscript appears.

E. Permission to reproduce manuscript entitled “Human Colon Function Ex Vivo: Dependence on Oxygen and Sensitivity to Antibiotic”

This is an open access article distributed under the terms of the Creative Commons Attribution License, which permits unrestricted use, distribution, and reproduction in any medium, provided the original author and source are credited. © 2019 Schwerdtfeger et al.

**F. Permission to reproduce manuscript entitled “Vasoactive Intestinal Peptide
Regulates Ileal Goblet Cell Production in Mice”**

This is an open access article under the terms of the Creative Commons Attribution License, which permits use, distribution and reproduction in any medium, provided the original work is properly cited. © 2020 Schwerdtfeger & Tobet.